

**Charles University
Faculty of Science**

Microbiology



Mgr. Vojtěch Tláškal

Bacteria associated with decomposing deadwood

Bakterie asociované s rozkládajícím se dřevem

Doctoral thesis

Supervisor:
doc. RNDr. Petr Baldrian, Ph.D.
Institute of Microbiology
Czech Academy of Sciences

Prague, 2021

Declaration

I declare that I prepared the thesis independently and that I cited all the information and publications used. This work, or substantial part of it, was not previously used to obtain the same or another academic title.

Prague, 12. 8. 2021

Vojtěch Tláškal

Table of Contents

<u>Acknowledgements.....</u>	<u>1</u>
<u>Abstract.....</u>	<u>3</u>
<u>Abstrakt.....</u>	<u>4</u>
<u>List of Abbreviations.....</u>	<u>5</u>
<u>1. Introduction.....</u>	<u>7</u>
<u>2. List of Publications.....</u>	<u>17</u>
<u>3. Methods.....</u>	<u>26</u>
<u>4. Discussion.....</u>	<u>27</u>
<u>5. Conclusions.....</u>	<u>31</u>
<u>6. References.....</u>	<u>33</u>

Acknowledgements

I am grateful to my supervisor doc. RNDr. Petr Baldrian Ph.D., who has guided me since early university studies and taught me critical skills related to science – reading, learning, thinking, analysing and finally writing. Always with patient support and enthusiasm.

I thank the laboratory members, friends, and colleagues from the Institute of Microbiology whom I met from 2012 to 2021 and beyond. They all shared a common interest in microbiology, yet the diversity of personalities, approaches, and cultural backgrounds was a source of help and inspiration. I believe that without each individual person from this “community” the thesis would be different.

I thank my family who initially allowed me to choose the subject myself and later, when challenging but happy family-related moments arose, supported me in completing my studies.

This work was carried out in the Laboratory of Environmental Microbiology, Institute of Microbiology of the Czech Academy of Sciences, v. v. i. and it was supported by the Charles University (GAUK 950217) and by the Czech Science Foundation (17-20110S and 21-09334J).

This thesis is about small entities and subtle processes with ingenious order and functioning. People acknowledged here allowed me to see and imagine them.

Abstract

Deadwood is a hotspot of microbial diversity and its decomposition contributes to carbon and nitrogen cycling in temperate forests. The historically recognized importance of fungi in the decomposition of deadwood has recently been complemented by the description of bacterial functions thanks to the rapid progress of culture-independent methods based on the analysis of nucleic acids. To study different aspects of deadwood decomposition, a temperate mixed forest in Zofinsky prales National Nature Reserve was selected as a site with rich historical forestry data where deadwood decomposition represents an important process in wood turnover. The aim of this thesis is to describe role of bacteria in deadwood decomposition at fine scale resolution with respect to community composition, enzyme transcription, and metabolic potential of dominant species. Effects of deadwood age together with pH and water content on the bacterial community composition proved to be more important than tree species identity. Bacteria showed distinct composition between early and late community in decomposing deadwood. The bacterial community was also under a significant influence of fungal community composition. Despite being in a close contact, bacterial and fungal communities differed significantly between deadwood and the underlying soil horizons. Bacteria in deadwood contributed to the nitrogen (N) cycling with an important role in N₂ fixation. Bacterial utilization of carbon (C) via degradation of recalcitrant polymers was present, but less important than fungal degradation. The decomposition potential of abundant bacterial taxa in deadwood can be delineated from the presence of carbohydrate active enzyme (CAZy) set which was found to be rich in *Acidobacteria*, *Bacteroidetes*, and *Actinobacteria* in contrast to less CAZy-equipped *Alphaproteobacteria* and *Gammaproteobacteria*. The latter taxa depended on mycophagy, low-molecular-mass C sources and were able to perform several N-cycling steps including N₂ fixation. Deadwood is a unique habitat with interkingdom interactions among prokaryotic and eukaryotic microorganisms and in which individual bacterial groups show adaptations to specific habitat conditions characterized by high C:N ratio, recalcitrant C sources, extracellular activity of degradative enzymes, and substrate impermeability.

Abstrakt

Odumřelé dřevo představuje významný habitat z hlediska biodiverzity a jeho rozklad v lesích mírného pásma přispívá k cyklům uhlíku a dusíku. Historicky doložený význam hub při rozkladu odumřelého dřeva byl v posledních letech doplněn o poznatky o roli bakterií v tomto procesu díky rychlému rozvoji metod založených na analýze nukleových kyselin. Pro studium procesu rozkladu dřeva byl vybrán smíšený temperátní les v Národní přírodní rezervaci Žofínský prales, ke kterému existuje bohatý historickým lesnický záznam o množství dřeva a kde rozklad odumřelého dřeva představuje důležitou součást celkového obratu rostlinné biomasy. Cílem této práce je detailně popsat roli bakterií v procesu rozkladu dřeva vzhledem ke složení bakteriálního společenstva, transkripce enzymů a metabolického potenciálu dominantních bakteriálních zástupců. Vliv stáří odumřelého dřeva spolu s pH a obsahem vody byl pro ovlivnění struktury bakteriálního společenstva důležitější než vliv druhu dřeva. Bakteriální společenstvo na počátku rozkladu se lišilo od pozdní fáze rozkladu. Složení houbového společenstva také významně ovlivňovalo složení bakterií. I přes přímý kontakt dřeva s půdou se bakterie a houby v těchto dvou habitatech lišily. Bakterie ve dřevě přispívaly k cyklu dusíku zejména fixací N_2 . Dále byly schopné využít uhlík skrze rozklad odolných polymerů dřeva, ale tento bakteriální rozklad byl méně významný než houbový. U nejzastoupenějších bakteriálních skupin bylo možné odvodit jejich potenciál k rozkladu na základě přítomnosti glykosidhydroláz (CAZy), které byly ve zvýšené míře nalezeny u kmenů *Acidobacteria*, *Bacteroidetes* a *Actinobacteria*. Naopak výskyt genů pro tyto enzymy byl nižší u tříd *Alphaproteobacteria* a *Gammaproteobacteria*. Tyto třídy byly závislé na degradaci houbové biomasy, na nízkomolekulárních zdrojích uhlíku a byly schopné vykonávat jednotlivé části cyklu dusíku včetně fixace N_2 . Odumřelé dřevo je unikátní habitat, ve kterém intenzivně interagují prokaryotní a eukaryotní organizmy a ve kterém jsou jednotlivé bakteriální skupiny adaptovány na specifické podmínky, jako je vysoký poměr obsahu uhlíku a dusíku, těžko rozložitelné zdroje uhlíku, extracelulární aktivita enzymů a stížená prostupnost substrátu.

List of Abbreviations

C – carbon

N – nitrogen

P – phosphorus

DNA – deoxyribonucleic acid

RNA – ribonucleic acid

mRNA – messenger RNA

rRNA – ribosomal RNA

CAZyme – carbohydrate active enzyme

MAG – metagenome-assembled genome

SIP – stable isotope probing

ATP – adenosine triphosphate

DNRA – dissimilatory reduction of nitrate to ammonium

1. Introduction

Temperate forests represent significant global sink of carbon (C, -3.6 ± 48 gigatonne of CO_2 equivalent yr^{-1} , Harris et al., 2021). Portion of this C is sequestered into living tree tissues and after tree senescence, wood is subject to decomposition accompanied by a CO_2 efflux back to the atmosphere. Amount of C stored in deadwood is estimated to be 8% of the total forest C stock (Pan et al., 2011). This C pool is represented by plant structural compounds such as cellulose, hemicellulose, lignin and by other, labile compounds (pectin, starch). After the death of the tree, wood components serve as a nutrient source for saprotrophs which colonized the tree before its death or which live nearby, further saprotrophs are transported to the site of decomposing wood by insect vectors or stochastically by anemochory. Dead tree trunk thus becomes a unique habitat offering multiple niches, releasing nutrients into surrounding soil, representing source of concentrated though recalcitrant C. As decomposition proceeds, initially rigid trunk structure (Figure 1) becomes fragile, trunk changes its dimensions, becomes soft and its ratio of C to N decreases due to microbial activity which enables faster decomposition (Weedon et al., 2009). The rate of decomposition is further positively correlated with humidity of the site and negatively correlated with site sun exposure. Full contact with ground enables faster saprotrophic colonization and thus leads to faster decomposition. Eventually, at the end of tree trunk decomposition period which may take 40–110 years in temperate forests (Přívětivý et al., 2018), deadwood components are incorporated into soil (Figure 2). At this point, the initially high amount of concentrated C was utilized by saprotrophs to form their own bodies, was released as CO_2 , or it was sequestered into surrounding soil in form of soil organic matter. Single tree trunk thus significantly affects its surroundings and releases CO_2 .



Figure 1: Example of recently fallen beech tree with ID 104117 downed between years 2012 and 2016. Rigid structure of the stem and bark cover are signs of initial decomposition. The picture was taken in October 2019.

Despite intensive forest management, which has negative effect on forest biodiversity (Halme et al., 2013) and which accounts for 99% of tree cover loss in Europe (Curtis et al., 2018), there are still areas with restricted forms of management or no management at all (worldwide list of protected areas available at IUCN & UNEP, 2018). Such forests may contain significant stock of dead tree trunks and represent hotspots of diversity (Seibold et al., 2015; Lepinay et al., 2021). Estimates of deadwood volume for mixed temperate forest in Zofinsky prales report 201.6 t ha⁻¹ which represents 22.3% of total stand volume (Král et al., 2010). Large deadwood stocks in natural forests create diverse opportunities for niche colonization while releasing high volumes of C which is leached either to soil or released to atmosphere. Estimates of C flux from deadwood vary: 0.11–2.45 Mg C ha⁻¹ yr⁻¹ is an area-related flux which is dependent on the forest type (Bond-Lamberty et al., 2002; Forrester et al., 2012). Wood mass-related estimate shows decomposition rate to reach up to 2.4 g CO₂ kg⁻¹ d⁻¹ and annual C flux to be 117 g C kg⁻¹ yr⁻¹ (Rinne-Garmston et al., 2019). Deadwood in natural forests thus represents significant source of greenhouse gas CO₂ and as such, is usually included in global estimates of C turnover (Luyssaert et al., 2008; Pugh et al., 2019).



Figure 2: Fragment of the spruce stem with ID 16875 downed between forestry surveys in 1975 and 1997. Signs of advanced decomposition are well visible – collapsed shape, gradual incorporation into the surrounding litter and soil matrix, major colonization by brown-rot fungi with smaller area decomposed by white-rot fungi on the right side of the fragment. The picture was taken in October 2019.

The main organisms with a potential to degrade wood structure and utilize recalcitrant forms of C are fungi and bacteria (Eastwood et al., 2011). Genomes of these microorganisms contain genes for extracellular enzymes glycoside hydrolases which employ hydrolytic mechanism, act on target substrates like polysaccharides (cellulose, hemicellulose, chitin, starch) and release oligomers or monomers. In addition to hydrolysis, aerobically favoured oxidative degradation by metalloenzymes such as lytic polysaccharide monoxygenases contributes to deconstruction of these biopolymers as well (Bomble et al., 2017). Another group of enzymes called oxidases is responsible for delignification.

The fact that produced enzymes are (mostly) extracellular further diversifies microbial life-strategies to acquire nutrients. More specifically, there are microorganisms that invest into production of enzymes which, however, can not be controlled once they are transported out of the microbial cell. Cleavage outcome which is not controlled by enzyme producer gives chance to opportunistic neighbours who might benefit from degradation products (i.e., “public goods”) without the need to invest into the release of enzymes (Allison, 2005). Such social cheating strategy is widespread among bacteria and it can even

increase resource utilization efficiency and total population yields (García-Contreras and Loarca, 2021). Majority of bacterial genomes was shown to contain genes for utilization of simple compounds like cellobiose (Berlemont and Martiny, 2013).

In deadwood context, bacteria are indeed responsible for quantitatively lower rates of C release in comparison with fungi. This can be explained by restricted motility and unicellular growth – the characteristics which cause limited ability of bacteria to penetrate the substrate. Bacteria are not able to degrade lignin efficiently, at least not for the C utilization, which also results in lower possibility to penetrate wood. In contrast, hyphal growth allows fungi to colonize large patches of deadwood. Specific bacterial taxa benefit from the strong habitat shaping by fungi (Valášková et al., 2009; Hervé et al., 2013). Some of them are able to move along fungal hyphae through the substrate (Warmink et al., 2011), other utilize byproducts of fungal metabolism, for example degrade compounds such as oxalic acid (Bravo et al., 2013; Nazir et al., 2013).

Another specialized metabolism of bacteria relies on environmentally relevant gas methane. Aerobic methanotrophs such as *Gammaproteobacteria*, *Alphaproteobacteria* or *Verrucomicrobia* express *mmo* genes and synthesize monooxygenases for oxidation of methane liberated by fungal esterases (Lenhart et al., 2012) or by methanogenic Archaea (Rinta-Kanto et al., 2016). Monooxygenases can serve also for oxidation of other low-molecular-mass compounds as shown in *Betaproteobacteria* (Rochman et al., 2020). Methylotrophic *Proteobacteria* use *mxoF* gene to synthesize methanol oxygenase and utilize methanol which is released during lignin demethylation by brown-rot fungi (Filley et al., 2002). Tetrahydromethanopterin branch of the Wood-Ljungdahl pathway is later used to detoxify formaldehyde emerging from methanol oxidation (Adam et al., 2019). Methanotrophy and methylotrophy are reported to be further combined with potential for N₂ fixation in some taxa (Vorob'ev et al., 2009; Mäkipää et al., 2018).

Abundant fungal biomass represents further C-rich substrate available in deadwood. Specific mycophagous bacterial taxa such as *Collimonas* (Leveau et al., 2010), *Pedobacter*, *Variovorax* (Brabcová et al., 2016) and *Granulicella* (López-Mondéjar et al., 2018) were shown to be enriched on fungal biomass utilizing chitin as a C source. Further, *Burkholderiales* are being repeatedly detected in the presence of fungi (Warmink et al., 2011; Hervé et al., 2013, 2016b).

Chitin, cellulose, hemicellulose and other plant and microbial biopolymers are targeted by carbohydrate active enzymes (CAZymes) which are separated into families and subfamilies based on their structure (Cantarel et al., 2009; Garron and Henrissat, 2019). The diversity of characterized enzyme families follows natural diversity of carbohydrates, families are grouped based on the similarity of protein domains. Individual families might have narrow substrate specificity as well as broad range of activities on different substrates. Thus we can identify chitinases (e.g. GH18, GH19), cellulases (e.g. GH6, GH9), enzymes targeting cellobiose or xylobiose, wide group of enzymes targeting hemicellulose etc. Identification of CAZyme genes is allowed by genome and metagenome sequencing, gene prediction and CAZy annotation based on comparison with Hidden Markov Models which provides high specificity of the CAZy assignment (Rossi et al., 2017). Presence of the CAZymes in microbial genomes might suggest potential utilization of a given substrate (Berlemont and Martiny, 2015). It was shown that the diversity of extracellular enzymes varies at fine taxonomical scale and it is non-randomly distributed among taxonomical

groups of prokaryotes (Zimmerman et al., 2013). Despite occurrence of other C-rich compounds in deadwood such as proteins, carbohydrates are dominant C source and thus CAZy analysis provides insight into important targets of microbial degradation.

Bacterial importance in ecosystem functioning becomes obvious when it comes to the pathways which are unique to bacteria due to their metabolic versatility. Such pathways are dissimilatory and assimilatory oxidation and reduction of several compounds including anorganic ions. Namely non-symbiotic N₂ fixation by diazotrophic bacterial community was being stressed in connection with deadwood (Brunner and Kimmins, 2003; Hoppe et al., 2014; Rinne et al., 2017). The metalloenzyme nitrogenase is responsible for the reduction of N₂ to NH₃ while using 16 molecules of ATP (Hoffman et al., 2014) – the step is thus energetically costly and it must be advantageous for bacteria to fix N₂. One of the reasons for investment in N₂ fixation is the high C:N ratio in deadwood. C represents on average 48.5% of deadwood dry mass (Martin et al., 2021) while N accounts for 0.5–2% of dry mass depending on several factors such as tree species (Weedon et al., 2009; Kahl et al., 2017; Moll et al., 2018). N₂ fixation may reduce N limitation in deadwood and probably occurs in anaerobic, high-moisture containing patches of wood substrate. Phosphorus (P) is another factor influencing the N₂ fixation rate as it is key element for microbial growth and biosynthesis of ATP. Studies from soil and litter confirm the importance of C:N, C:N:P stoichiometry and high C content/quality of substrate in sustaining high N₂ fixation rates (Vitousek and Hobbie, 2000; Zheng et al., 2020). Quantification of N₂ fixation and extrapolation of this process to the ecosystem level show importance of areas with large stocks of deadwood (Brunner and Kimmins, 2003). Other steps of nitrogen cycle in deadwood such as nitrification or denitrification have not been assessed before and their rate is unknown. Despite these gaps in the knowledge, it is clear that forests react to ongoing climate change (Hoffmann et al., 2019) and to antropogenic impact by the changes in processes related to C and N cycling (Rinne-Garmston et al., 2019). For example increase in C storage in European forests is expected due to high N and P depositions (Wang et al., 2017). Subsequently, such change in the overall budget of key nutrients will have impact on dominant deadwood microbial taxa and their functions (Lepinay et al., 2021).

Considering that deadwood substrate undergoes chemical and physical changes through its lifetime, logical question is whether bacterial community follows some sort of successional development as well. Although studies focusing several years of decomposition are experimentally challenging, some experiments showed initial phase of bacterial succession to be very dynamic and somehow influenced by those organisms who colonized substrate earlier and thus got the temporal advantage (Hiscox et al., 2015). So called *priority effect* thus drives initial composition of microbial community during which the remaining labile C sources are being utilized, directing the community into intermediate stages of decomposition where ability of cellulose decomposition or chitin utilization provide further advantage. Among the factors influencing community composition, the most important are pH, C:N ratio and water content (Folman et al., 2008; Hoppe et al., 2015; Moll et al., 2018; Mieszkina et al., 2021). Beside changes in composition, bacterial abundance (Rinta-Kanto et al., 2016) as well as diversity (Kielak et al., 2016; Rinta-Kanto et al., 2016) were occasionally reported to increase with progressing decomposition.

Despite known and mentioned examples of metabolic interactions between fungi and bacteria, the description of fungal-bacterial co-occurrence in deadwood is difficult due to

micro-scale level at which interactions among them happen. Attempts to overcome this limitation include co-cultivation tests of selected microorganisms on plates or in manipulated field experiments (Christofides et al., 2019; Johnston et al., 2019). Further, vast diversity of fungi and bacteria occupying deadwood habitat and showing myriads of possible combinations makes assessment of inter-microbial relationships more difficult. One possibility is to apply statistical co-occurrence networks to resolve prevailing relationship (Hoppe et al., 2014; Gómez-Brandón et al., 2020; Moll et al., 2021), although such networks might be biased by the presumption that taxa correlate in their abundance while, in fact, they are unrelated and just react to the same environmental factor. With the advance in the field of statistics and computation it is now possible to apply approaches like joint species distribution modeling to predict biotic interactions and differentiate them from shared environmental responses which is usually difficult in observational, non-manipulative studies (Warton et al., 2015; Tikhonov et al., 2020).

When analyzing bacteria at the level of individual species it is possible to screen culture collection of isolates obtained from particular habitat for those abundant in 16S rRNA data and by this approach select dominant bacterial species that best represent the studied environment (Hervé et al., 2016b; Lladó et al., 2016). Dominant taxa can be further retrieved by longer cultivation (Sait et al., 2002) and growth on low-nutrient media selecting for bacteria used to compete under oligotrophic conditions (VanInsberghe et al., 2013). As community dominants are often responsible for the key ecological traits such approach may lead to identification of important functions and link them with specific taxa (Lladó et al., 2019). Cultivation may provide complete genotypic data (Figure 3) and extensive phenotypic data about isolated strains (Madin et al., 2020).

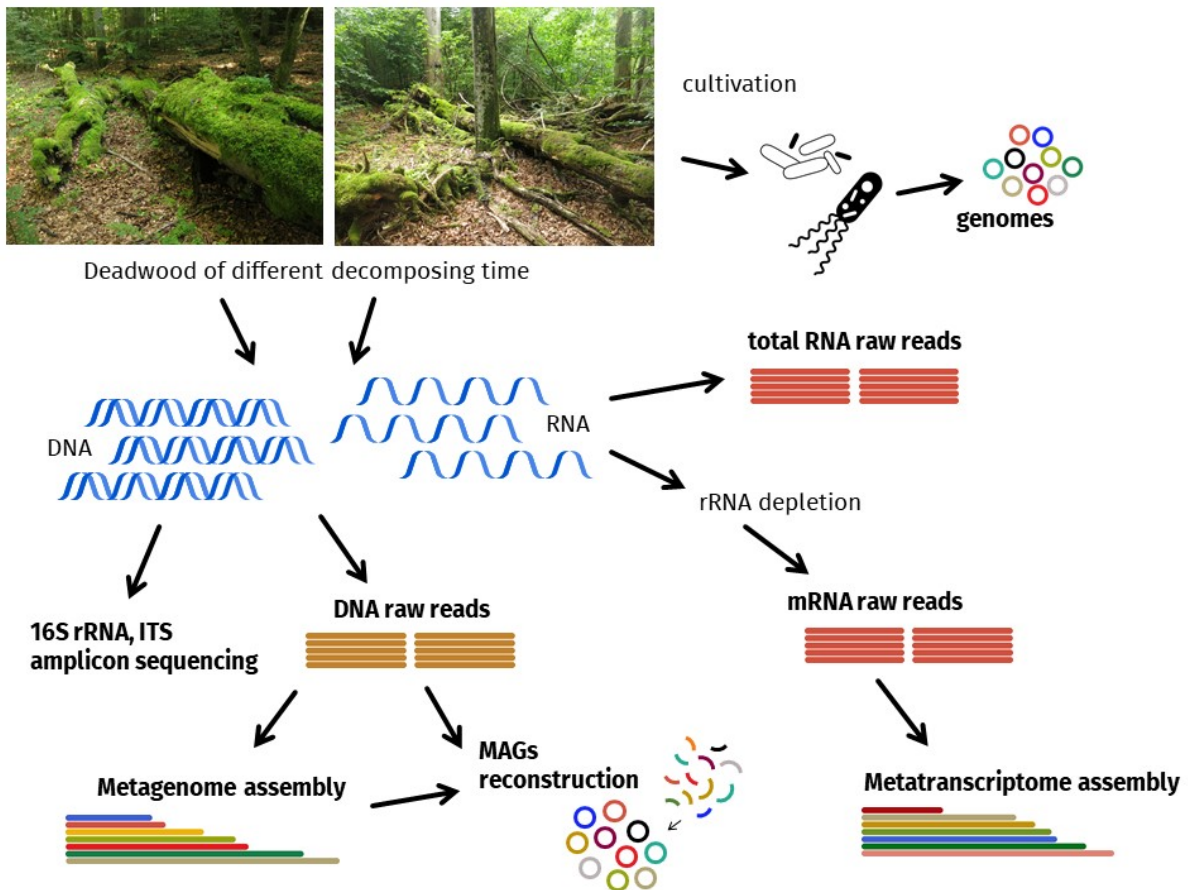


Figure 3: Conceptual scheme of approaches used to study deadwood microorganisms which includes cultivation-dependent as well as cultivation-independent methods. Sequencing of nucleic acids is used to infer taxonomy and function of the community members. Bold descriptions represent datasets presented in this thesis.

In contrast, culture independent approaches offer the theoretical possibility to reconstruct large fractions of individual genomes by binning of DNA contigs obtained by shotgun metagenome sequencing and thus predict potential of individual metagenome-assembled genomes (MAGs, Figure 3, Lemos et al., 2021) without the need for their potentially difficult cultivation (Steen et al., 2019). Depending on the amount of input data, MAGs resolving may provide vast number of uncultivated taxa and can unveil novel metabolic pathways (Parks et al., 2017; Woodcroft et al., 2018; Bay et al., 2021; Nayfach et al., 2021), however with the threat of obtaining composite or incomplete genomes (Shaiber and Eren, 2019) and without the guarantee to capture dominant taxa. For this reason, community-established metrics are used to evaluate quality of the resolving results (Bowers et al., 2017; Chen et al., 2020). Notably, description of eukaryotic MAGs is somewhat lagging behind bacterial and archaeal ones – due to complex genome architecture of eukaryotes their resolving still represents computational challenge (West et al., 2018).

Beside MAG reconstruction, metagenomes offer evaluation of functional potential at the level of total bacterial and archaeal community (Figure 3, Woodcroft et al., 2018). Application of metagenomes in characterization of eukaryotic potential is limited because of insufficient representativeness of often highly fragmented eukaryotic contigs in metagenome assembly based on short-read sequencing (Levy Karin et al., 2020). With the global increase of environmental metagenomic data (Figure 4) there is a growing need for structured lists of available studies (Corrêa et al., 2020) and for unified workflows for

metagenome analysis. The latter is represented by metagenome repositories such as MG-RAST (Meyer et al., 2008), IMG/M (Markowitz et al., 2007) or standalone tools such as eggNOG-mapper (Cantalapiedra et al., 2021) which provide taxonomic and functional profiling of predicted genes found in metagenomes.

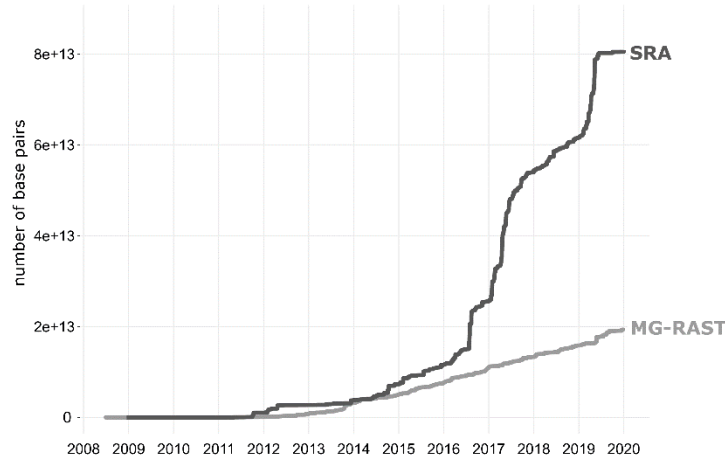


Figure 4: Cumulative sum of the base pairs in the MG-RAST and SRA databases used as proxy to visualize increase in availability of metagenomes between years 2008 and 2020. Data show sequences from terrestrial metagenomes only, data source: TerrestrialMetagenomeDB, Corrêa et al., 2020.

In contrast to metagenomes, metatranscriptomic approach (Figure 3) allows identification of functions which are expressed at the community level. Approximate taxonomical assignment of individual genes and identification of their function is done via mapping to one of the existing classifications – e.g. COG (Clusters of Orthologous Genes, Galperin et al., 2018), KEGG (Kyoto Encyclopedia of Genes and Genomes, Kanehisa and Goto, 2000) or Pfam (Protein families, Mistry et al., 2021). Metatranscriptomics is being successfully applied to study microbial expression in soils (Hultman et al., 2015; Žifčáková et al., 2016, 2017). The challenging RNA extraction from wood material has prevented proper analysis of wood metatranscriptomes so far. Critical step in a workflow to obtain profile of expressed genes is mRNA enrichment in the sample through rRNA depletion. Without the depletion, sequencing data obtain almost exclusively sequences of rRNA (Figure 3) and are useful for taxonomical identification of metabolically active organisms with much higher specificity than in the case of metatranscriptome (Geisen et al., 2015).

To study described microbial processes during deadwood decomposition by aforementioned methods, Zofinsky prales National Nature Reserve (48.668N, 14.707E) was selected as a model site of an unmanaged temperate forest consisting of European beech (*Fagus sylvatica*), European silver fir (*Abies alba*) and Norway spruce (*Picea abies*). The forest is protected since 1838 (Andreska, 2006) and is included in a global network ForestGEO (Anderson-Teixeira et al., 2015; Davies et al., 2021) with regular censuses of the deadwood volume and turnover (Přívětivý et al., 2016). The database containing geolocated tree records (Figure 5) can be used to retrieve tree species with its dimensions and to estimate approximate length of decomposition as well as other important metadata for each individual decomposing tree trunk with diameter >10 cm.

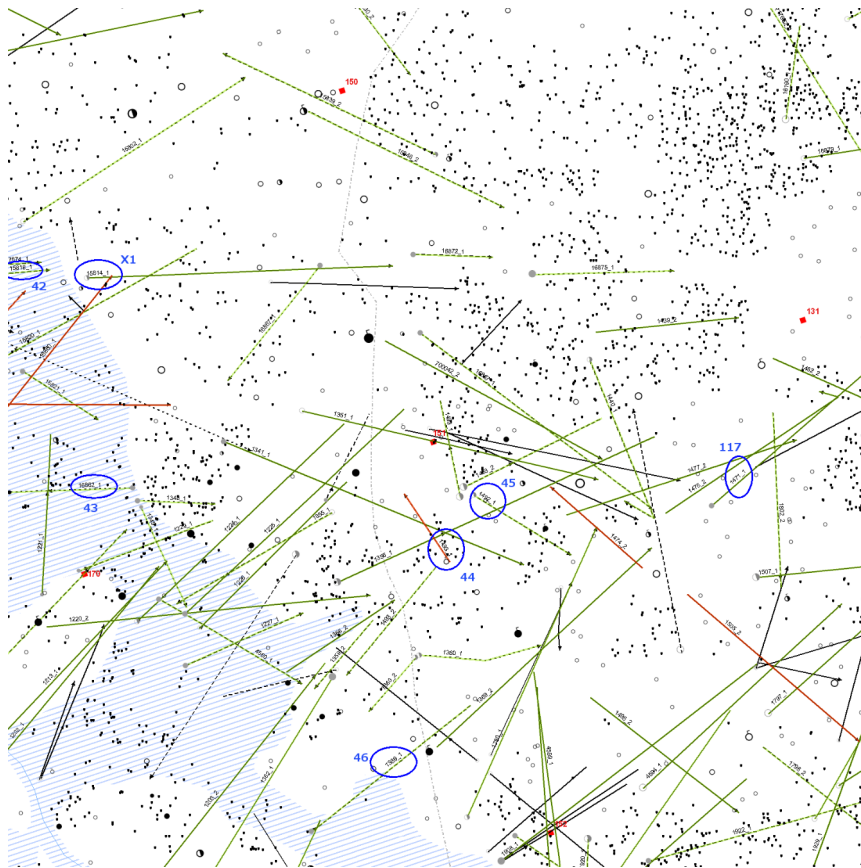


Figure 5: Example square from the Zofin forestry map with the edge of 100 metres and detailed records of fallen stems (green, black and red lines), standing trees (individual circles), tree species (circle colour), young trees (black dots). Red points are intersections of the grid marked by wooden sticks across the forest, blue circles denote trees which were sampled to study fungal and bacterial community.

The research presented in this thesis includes 8 papers with the intention to describe bacterial role in the process of deadwood decomposition with the following specific aims.

- To analyze temporal changes in bacterial community composition and shifts in dominant taxa over time.
Publication I, VI
- To compare microbial communities in relevant habitats: deadwood, underlying soil and control soil with emphasis on the effect of chemical factors in each habitat.
Publication II
- To analyze inter-kingdom relationship of fungi and bacteria with the focus on who influences whom.
Publication III
- To focus on difference between the roles of bacteria and fungi in C and N cycle. To analyze expressed genes in deadwood with the aim to identify prevailing microbial functions.
Publication IV
- To describe uncultured bacterial taxa which are abundant in metagenomes, with emphasis on their gene potential and taxonomy.
Publication IV, V, VIII
- To analyze bacteria at the species-level and describe abundant cultured bacterial representatives together with their decomposition potential, taxonomy and growth preferences.
Publication VI, VII

2. List of Publications

This thesis consists of the following papers:

- I. **Tláskal V**, Zrůstová P, Vrška T, Baldrian P (2017). Bacteria associated with decomposing dead wood in a natural temperate forest. *FEMS Microbiology Ecology* 93, fix157. doi:10.1093/femsec/fix157
- II. Šamonil P, Daněk P, Baldrian P, **Tláskal V**, Tejnecký V, Drábek O (2020). Convergence, divergence or chaos? Consequences of tree trunk decay for pedogenesis and the soil microbiome in a temperate natural forest. *Geoderma* 376, 114499. doi:10.1016/j.geoderma.2020.114499
- III. Odriozola I, Abrego N, **Tláskal V**, Zrůstová P, Morais D, Větrovský T, Ovaskainen O, Baldrian P (2021). Fungal communities are important determinants of bacterial community composition in deadwood. *mSystems* 6, e01017-20. doi:10.1128/mSystems.01017-20
- IV. **Tláskal V**, Brabcová V, Větrovský T, Jomura M, López-Mondéjar R, Monteiro L M O, Saraiva J P, Human Z R, Cajthaml T, da Rocha U N, Baldrian P (2021). Complementary roles of wood-inhabiting fungi and bacteria facilitate deadwood decomposition. *mSystems* 6, e01078-20. doi:10.1128/mSystems.01078-20
- V. **Tláskal V**, Brabcová V, Větrovský T, López-Mondéjar R, Monteiro L M O, Saraiva J P, da Rocha U N, Baldrian P (2021). Metagenomes, metatranscriptomes and microbiomes of naturally decomposing deadwood. *Scientific Data* 8, 198. doi:10.1038/s41597-021-00987-8
- VI. **Tláskal V**, Baldrian P (2021). Deadwood-inhabiting bacteria show adaptations to changing carbon and nitrogen availability during decomposition. *Frontiers in Microbiology* 12, 685303. doi:10.3389/fmicb.2021.685303
- VII. **Tláskal V**, Pylro V S, Žifčáková L, Baldrian P (2021). Ecological divergence within the enterobacterial genus *Sodalis*: From insect symbionts to inhabitants of decomposing deadwood. *Frontiers in Microbiology* 12, 668644. doi:10.3389/fmicb.2021.668644
- VIII. Kyselková M, **Tláskal V**, Morais D K, Michalčíková L, Hollá S A, Větrovský T, Baldrian P (2021). Taxonomy assignment of bacterial genes in a metagenome: assessment of accuracy and recommendations for reporting. *submitted*

Vojtěch Tláskal ORCID: 0000-0002-2924-9470

Publication I

Tláskal V, Zrůstová P, Vrška T, Baldrian P (2017). Bacteria associated with decomposing dead wood in a natural temperate forest. *FEMS Microbiology Ecology* 93, fix157. doi:10.1093/femsec/fix157

Dead wood represents an important pool of organic matter in forests and is one of the sources of soil formation. It has been shown to harbour diverse communities of bacteria, but their roles in this habitat are still poorly understood. Here, we describe the bacterial communities in the dead wood of *Abies alba*, *Picea abies* and *Fagus sylvatica* in a temperate natural forest in Central Europe. An analysis of environmental factors showed that decomposing time along with pH and water content was the strongest drivers of community composition. Bacterial biomass positively correlated with N content and increased with decomposition along with the concurrent decrease in the fungal/bacterial biomass ratio. *Rhizobiales* and *Acidobacteriales* were abundant bacterial orders throughout the whole decay process, but many bacterial taxa were specific either for young (< 15 years) or old dead wood. During early decomposition, bacterial genera able to fix N₂ and to use simple C1 compounds (e.g. *Yersinia* and *Methylomonas*) were frequent, while wood in advanced decay was rich in taxa typical of forest soils (e.g. *Bradyrhizobium* and *Rhodoplanes*). Although the bacterial contribution to dead wood turnover remains unclear, the community composition appears to reflect the changing conditions of the substrate and suggests broad metabolic capacities of its members.

Publication II

Šamonil P, Daněk P, Baldrian P, **Tláškal V**, Tejnecký V, Drábek O (2020). Convergence, divergence or chaos? Consequences of tree trunk decay for pedogenesis and the soil microbiome in a temperate natural forest. *Geoderma* 376, 114499. doi:10.1016/j.geoderma.2020.114499

The biochemical effects of trees may significantly influence local pedogenesis as well as pedocomplexity, bio-diversity and forest dynamics on both stand and landscape scales. One such effect is the decay of tree trunks, which is driven by organisms, and especially by the microbiome. Decomposition modifies soil formation, which due to the existence of many feedbacks affects the composition of the decomposer community. We aimed to uncover general trends in the evolution of Entic Podzols as well as individual trajectories of soil properties below decaying beech trunks in an old-growth mountain forest. In particular, we used mathematical models to distinguish soil convergence, divergence and chaotic behaviour to enhance a general theory of pedogenesis. We further aimed to calculate the depth and time of convergence if this scenario is prevailing in the study plot. Pedogenetic pathways were assessed regarding the changing composition of fungal and bacterial communities in soils to obtain a complex picture of the decaying trunk-soil microbiome system. We sampled the decaying wood layer under 24 lying beech trunks and corresponding organic horizons on adjacent control microsites occupied by decaying beech leaves. At the same time we sampled underlying mineral soil horizons at both microsites (wood vs. leaves), all on Entic Podzols and granite (in total 192 soil samples). Individual trunk fall events were dated using precise dendrochronology, with the resulting chronosequence covering trunks lying for 8 – 52 years. We analysed decomposition processes (with a wide spectra of organic acids and ions analysed), soil chemistry (28 additional soil properties assessed), and the microbiome composition in both decaying organic matter and soils (relative abundances of the 200 most common bacterial and fungal OTUs analysed). During the first stage of trunk decay, underlying Entic Podzols responded with a significant increase of nutrients, pH, and CEC, and the maximal divergence compared to control sites was reached between 12 and 60 years after the trunk fall. Subsequently, a majority of soil properties slowly converged over a few decades to match the soil properties of control sites. The modelled convergence point occurred at ages between 39 (SO_4^{2-}) and 229 (Al_w) years, with a median convergence time of 53 years. The majority of soil properties converged within 20 cm below the trunk, but mathematical models predicted footprints of some soil properties down to depths of ca 60 cm. In addition, 11 soil properties did not converge at any depth, and for some properties the models even diverged. Differences in bacterial and fungal communities between below-trunk and control positions were relatively minor. Pechochemical drivers of fungal and bacterial communities (nutrients content, N_{tot} , C_{ox} , Al, Fe, Mn forms) changed significantly in the mineral soil below trunks, and the microbiome partly reflected these depth-related changes. However, we propose that there is a threshold between organic and mineral soil horizons limiting the impacts of trunk decay and pedogenesis in changes to the microbiome.

Publication III

Odriozola I, Abrego N, **Tláškal V**, Zrůstová P, Morais D, Větrovský T, Ovaskainen O, Baldrian P (2021). Fungal communities are important determinants of bacterial community composition in deadwood. *mSystems* 6, e01017-20. doi:10.1128/mSystems.01017-20

Fungal-bacterial interactions play a key role in the functioning of many ecosystems. Thus, understanding their interactive dynamics is of central importance for gaining predictive knowledge on ecosystem functioning. However, it is challenging to disentangle the mechanisms behind species associations from observed co-occurrence patterns, and little is known about the directionality of such interactions. Here, we applied joint species distribution modeling to high-throughput sequencing data on co-occurring fungal and bacterial communities in deadwood to ask whether fungal and bacterial co-occurrences result from shared habitat use (i.e., deadwood's properties) or whether there are fungal-bacterial interactive associations after habitat characteristics are taken into account. Moreover, we tested the hypothesis that the interactions are mainly modulated through fungal communities influencing bacterial communities. For that, we quantified how much the predictive power of the joint species distribution models for bacterial and fungal community improved when accounting for the other community. Our results show that fungi and bacteria form tight association networks (i.e., some species pairs co-occur more frequently and other species pairs co-occur less frequently than expected by chance) in deadwood that include common (or opposite) responses to the environment as well as (potentially) biotic interactions. Additionally, we show that information about the fungal occurrences and abundances increased the power to predict the bacterial abundances substantially, whereas information about the bacterial occurrences and abundances increased the power to predict the fungal abundances much less. Our results suggest that fungal communities may mainly affect bacteria in deadwood.

Publication IV

Tláškal V, Brabcová V, Větrovský T, Jomura M, López-Mondéjar R, Monteiro L M O, Saraiva J P, Human Z R, Cajthaml T, da Rocha U N, Baldrian P (2021). Complementary roles of wood-inhabiting fungi and bacteria facilitate deadwood decomposition. *mSystems* 6, e01078-20. doi:10.1128/mSystems.01078-20

Forests accumulate and store large amounts of carbon (C), and a substantial fraction of this stock is contained in deadwood. This transient pool is subject to decomposition by deadwood-associated organisms, and in this process it contributes to CO₂ emissions. Although fungi and bacteria are known to colonize deadwood, little is known about the microbial processes that mediate carbon and nitrogen (N) cycling in deadwood. In this study, using a combination of metagenomics, metatranscriptomics, and nutrient flux measurements, we demonstrate that the decomposition of deadwood reflects the complementary roles played by fungi and bacteria. Fungi were found to dominate the decomposition of deadwood and particularly its recalcitrant fractions, while several bacterial taxa participate in N accumulation in deadwood through N fixation, being dependent on fungal activity with respect to deadwood colonization and C supply. Conversely, bacterial N fixation helps to decrease the constraints of deadwood decomposition for fungi. Both the CO₂ efflux and N accumulation that are a result of a joint action of deadwood bacteria and fungi may be significant for nutrient cycling at ecosystem levels. Especially in boreal forests with low N stocks, deadwood retention may help to improve the nutritional status and fertility of soils.

Publication V

Tláškal V, Brabcová V, Větrovský T, López-Mondéjar R, Monteiro L M O, Saraiva J P, da Rocha U N, Baldrian P (2021). Metagenomes, metatranscriptomes and microbiomes of naturally decomposing deadwood. *Scientific Data* 8, 198. doi:10.1038/s41597-021-00987-8

Deadwood represents significant carbon (C) stock in temperate forests. Its decomposition and C mobilization is accomplished by decomposer microorganisms – fungi and bacteria – who also supply the foodweb of commensalist microbes. Due to the ecosystem-level importance of deadwood habitat as a C and nutrient stock with significant nitrogen fixation, the deadwood microbiome composition and function are critical to understanding the microbial processes related to its decomposition. We present a comprehensive suite of data packages obtained through environmental DNA and RNA sequencing from natural deadwood. Data provide a complex picture of the composition and function of microbiome on decomposing trunks of European beech (*Fagus sylvatica* L.) in a natural forest. Packages include deadwood metagenomes, metatranscriptomes, sequences of total RNA, bacterial genomes resolved from metagenomic data and the 16S rRNA gene and ITS2 metabarcoding markers to characterize the bacterial and fungal communities. This project will be of use to microbiologists, environmental biologists and biogeochemists interested in the microbial processes associated with the transformation of recalcitrant plant biomass.

Publication VI

Tláskal V, Baldrian P (2021). Deadwood-inhabiting bacteria show adaptations to changing carbon and nitrogen availability during decomposition. *Frontiers in Microbiology* 12, 685303. doi:10.3389/fmicb.2021.685303

Deadwood decomposition is responsible for a significant amount of carbon (C) turnover in natural forests. While fresh deadwood contains mainly plant compounds and is extremely low in nitrogen (N), fungal biomass and N content increase during decomposition. Here, we examined 18 genome-sequenced bacterial strains representing the dominant deadwood taxa to assess their adaptations to C and N utilization in deadwood. Diverse gene sets for the efficient decomposition of plant and fungal cell wall biopolymers were found in *Acidobacteria*, *Bacteroidetes*, and *Actinobacteria*. In contrast to these groups, *Alphaproteobacteria* and *Gammaproteobacteria* contained fewer carbohydrate-active enzymes and depended either on low-molecular-mass C sources or on mycophagy. This group, however, showed rich gene complements for N₂ fixation and nitrate/nitrite reduction—key assimilatory and dissimilatory steps in the deadwood N cycle. We show that N₂ fixers can obtain C independently from either plant biopolymers or fungal biomass. The succession of bacteria on decomposing deadwood reflects their ability to cope with the changing quality of C-containing compounds and increasing N content.

Publication VII

Tláskal V, Pylro V S, Žifčáková L, Baldrian P (2021). Ecological divergence within the enterobacterial genus *Sodalis*: From insect symbionts to inhabitants of decomposing deadwood. *Frontiers in Microbiology* 12, 668644. doi:10.3389/fmicb.2021.668644

The bacterial genus *Sodalis* is represented by insect endosymbionts as well as free-living species. While the former have been studied frequently, the distribution of the latter is not yet clear. Here, we present a description of a free-living strain, *Sodalis ligni* sp. nov., originating from decomposing deadwood. The favored occurrence of *S. ligni* in deadwood is confirmed by both 16S rRNA gene distribution and metagenome data. Pangenome analysis of available *Sodalis* genomes shows at least three groups within the *Sodalis* genus: deadwood-associated strains, tsetse fly endosymbionts and endosymbionts of other insects. This differentiation is consistent in terms of the gene frequency level, genome similarity and carbohydrate-active enzyme composition of the genomes. Deadwood-associated strains contain genes for active decomposition of biopolymers of plant and fungal origin and can utilize more diverse carbon sources than their symbiotic relatives. Deadwood-associated strains, but not other *Sodalis* strains, have the genetic potential to fix N₂, and the corresponding genes are expressed in deadwood. Nitrogenase genes are located within the genomes of *Sodalis*, including *S. ligni*, at multiple loci represented by more gene variants. We show decomposing wood to be a previously undescribed habitat of the genus *Sodalis* that appears to show striking ecological divergence.

Publication VIII

Kyselková M, **Tláškal V**, Morais D K, Michalčíková L, Hollá S A, Větrovský T, Baldrian P (2021). Taxonomy assignment of bacterial genes in a metagenome: assessment of accuracy and recommendations for reporting. *submitted*

Correct taxonomic assignments of metagenome and metatranscriptome sequences are indispensable for linking predicted functions to the responsible members of environmental microbiomes as well as for assessing the relative representation of microbial taxa. End-users of annotation tools can use alignment reliability scores such as the bit score or e-value to improve the accuracy of the taxonomic assignment of called genes, but the use of these scores is limited by the fact that their accuracy thresholds have not been reported to date. In this study, we tested the accuracy of taxonomic assignments using a mock soil metagenome consisting of 82 bacterial genomes to assess the accuracy of taxonomic classifications across various e-value cutoffs and to make recommendations for reporting taxonomic information for metagenomes and metatranscriptomes. The accuracy of the taxonomic assignments of the called genes from our mock soil metagenome was highly dependent on both the e-value threshold used for data filtering and the chosen taxonomic rank. We showed that the mean rate of more than 95% of correct annotations was achievable at all e-value cutoffs for all ranks up to family level, and at e-value cutoff of $1E-90$ (bit score 276) for genus level. Though, the accuracy of taxonomic assignments substantially varied among bacterial genomes of various taxonomic placements and more stringent criteria such as assignments to only family level with e-value cutoff of $1E-40$ (bit score 146) should be applied to reach the 95% accuracy with 75% of the present genomes. Concluding, reporting highly accurate results from metagenomes and metatranscriptomes at low bacterial ranks is currently possible, but necessitates applying stringent e-value/bit score thresholds.

3. Methods

List of methods and linked publications

Deadwood and soil sampling: I, II, IV, VI, VII

Extracellular enzyme assay: I, II, VI

16S rRNA and ITS sequencing, I, II, III, V, VI

Biomass quantification: I, II, IV

Metagenomics: IV, V, VII, VIII

Metatranscriptomics: IV, V, VII

Gas flux measurement: IV

Bacterial strain isolation: VI, VII

Sanger sequencing: VI, VII

Bacterial genomics: VI, VII, VIII

Co-occurrence modelling: III

Multivariate statistics: I, II, III, IV

4. Discussion

Deadwood decomposition attracted focus of researchers since the early days of environmental microbiology (Rayner and Boddy, 1988; bacteria reviewed in Clausen, 1996). Nowadays, there is a solid body of evidence that decomposition of individual wood components is an interplay between fungi and bacteria – the two microbial groups sharing the ability to synthesize degradation enzymes and exploit recalcitrant substances directly for C uptake. Bacteria associated with decomposing wood are influenced by a combination of physical factors (length of decomposition, tree species, tree diameter), chemical factors (moisture, pH, C:N ratio, lignin content, nutrient availability etc.), and also influenced by fungi. These factors shape community composition, diversity and amount of bacterial biomass with changing intensity during the process of decomposition. Several studies assign decisive role in community structuring to pH, C:N ratio and water content (Folman et al., 2008; Hoppe et al., 2015; Moll et al., 2018; Mieszkin et al., 2021). In addition to that, length of decomposition was shown to be more important than tree species (Tláškal et al., 2017 – I.). As a consequence we see distinct bacterial community composition in the fresh and old deadwood (Tláškal et al., 2017 – I.). This distinction is accompanied by an increase in bacterial biomass (and the decrease in fungal:bacterial rDNA copy ratio) but not necessarily by increase in bacterial diversity which was not observed in the studied ecosystem (Tláškal et al., 2017 – I.) in contrast to other experiments (Kielak et al., 2016; Rinta-Kanto et al., 2016). Initial community of bacteria consists of degrader taxa with potentially endophytic origin focused on utilization of diverse substrates. This community is replaced by opportunistic groups which rely on fungal C release, mycophagy and low-molecular-mass C sources (Tláškal and Baldrian, 2021 – VI.). Similar pattern was observed during leaf litter decomposition (Tláškal et al., 2016). Deadwood habitat itself has potential to host increasing biomass of microorganisms, while alpha diversity increase strongly depends on ability for niche differentiation and competitive exclusion of individual taxa. The rate of microbial succession in deadwood is probably slower than primary succession observed in other ecosystems (Harantová et al., 2017). Advanced decay is characterized by bacterial community clustered closely in multivariate ordination which suggests that inter-sample similarity of bacteria is higher at advanced decomposition than in early decay trees (Tláškal et al., 2017 – I.). Bacteria from late decomposition are also similar to those from the forest litter layer (Tláškal et al., 2017 – I.; Probst et al., 2018; Šamonil et al., 2020 – II.).

When analyzing fungal-bacterial interactions of communities by joint species distribution modelling (Warton et al., 2015; Ovaskainen et al., 2017) applied to amplicon sequencing data, many fungal and bacterial taxa co-occurred more or less frequently than expected by chance, showing potential interactions among species. Fungal occurrences and abundances increased the power to predict the bacterial community composition, whereas the power to predict fungal communities with bacterial data was less strong indicating that deadwood fungi determine bacterial communities and not vice versa (Odriozola et al., 2021 – III.). This is a consequence of mycophagous lifestyle of particular taxa, utilization of fungal hyphae for transport by some bacterial groups and specialization to utilize fungal metabolism by-products. Chemical factors of deadwood were shown to have stronger effect on variance of bacterial structure than physical factors (Odriozola et al., 2021 – III.).

Although deadwood nutrients are limited, deadwood is not a closed system. Nutrients are expected to be actively enriched, transported and deposited from a habitat surrounding. Physical contact of forest soil and decomposing stems supports colonization by microorganisms which thus do not have to rely only on passive and stochastic (spore) deposition. Nutrient flux by soil-foraging fungi between deadwood and underlying soil was shown during microcosm experiment (Philpott et al., 2014) and N translocation by ectomycorrhizal fungi dominating spruce deadwood was reported (Mäkipää et al., 2017). Such transport might represent source of valuable N in addition to N₂ fixation (Rinne et al., 2017). Despite that, we did not observe significant similarity of deadwood and soil fungal community in these two habitats (Šamonil et al., 2020 – II.), indicating that the system of active transport of soil nutrients to deadwood is not likely.

One of the ecosystem-relevant consequences of deadwood decomposition is the release of CO₂ caused by respiration of microorganisms during decomposition. CO₂ flux from deadwood in Zofin was experimentally recorded to be 1.21–1.43 g CO₂ kg⁻¹ day⁻¹ considering deadwood dry mass which shows that this habitat is an important CO₂ source (Rinne-Garmston et al., 2019; Tláskal et al., 2021a – IV.). Another relevant process occurring in deadwood is N₂ fixation. Activity of a diazotrophic community in deadwood was predicted in the early study of Cowling and Merrill (1966). Growth of N₂-fixers was indeed recorded in Zofin deadwood. Apart from the methylotrophic *Alphaproteobacterium* which has been isolated during incubation of beech blocks (Vorob'ev et al., 2009), isolation of N₂-fixers shown here represents successful retrieval from naturally decomposing trees after almost 40 years (Seidler et al., 1972; Spano et al., 1982). In addition to the two alphaproteobacterial N₂-fixing taxa (Tláskal and Baldrian, 2021 – VI.), deadwood-isolated strain from the enterobacterial genus *Sodalis* was obtained and shown to actively transcribe nitrogenase – the feature that is not shared by its closely related insect endosymbionts. This bacterium represents the type strain for the *Sodalis ligni* sp. nov. (dw23^T = LMG 32208^T = CECT 30299^T) (Tláskal et al., 2021c – VII.). Further activity of N₂-fixers was confirmed by strong expression of nitrogenase genes in metatranscriptome data and by indirect N₂ fixation quantification which showed N input rate to be 37–297 µg N₂ kg⁻¹ day⁻¹. Total per-area input thus results in 0.49 g N m⁻² year⁻¹ (Tláskal et al., 2021a – IV.) which is in the range of values published previously (Roskoski, 1980; Rinne et al., 2017). Intensive asymbiotic N₂ fixation reveals the importance of deadwood as a hotspot of N enrichment with impact on the nutrient status of the soil. From the taxonomical perspective, *Proteobacteria*, *Firmicutes*, *Chlorobi*, *Verrucomicrobia*, and *Bacteroidetes* were shown to express nitrogenase genes (Tláskal et al., 2021a – IV.).

As seen in a gene potential of individual isolates and metatranscriptome data, bacteria are performing further important steps within N cycle. In addition to N₂ fixation, nitrate and nitrite dissimilatory reduction leading to ammonium steps were identified in the data (Tláskal and Baldrian, 2021 – VI.). Notably, denitrification rate in metatranscriptome was very low and no isolates with genes for final denitrifying steps were obtained showing that loss of N via leaching to atmosphere is prevented by preference of dissimilatory nitrate reduction to ammonium (known as DNRA) rather than denitrification (Nelson et al., 2016). Similarly to denitrification, ammonia-oxidation genes were limited in metatranscriptome or bacterial genomes suggesting that ammonium does not serve for dissimilatory steps in nitrification and is rather used for amino acid synthesis (Tláskal and Baldrian, 2021 – VI.;

Tláskal et al., 2021a – IV.). Described steps and their intensity is driven by the main factor which is a limited N availability.

According to the metatranscriptome analysis, fungi played the decisive role in degradation of deadwood C sources (like cellulose, cello/xylobiose, pectin and lignin) in the studied system (Tláskal et al., 2021a – IV.). Particularly white-rot basidiomycetes show diverse enzyme sets and high enzyme production, their metabolic activity is connected with significant substrate acidification which might further negatively influence bacteria (Folman et al., 2008; de Boer et al., 2010). However, the acidification effect may not always be antibacterial (Valášková et al., 2009). Basidiomycota were the most abundant group when looking at either total gene expression or only at ribosomal protein transcription or at taxonomy of small subunit of rRNA (Tláskal et al., 2021a – IV.). Interestingly, exceptions showing dominance of Ascomycota together with relative increase of bacterial transcripts and lower overall CAZyme expression were observed in a few samples. This supports observation of dominance by highly heterogenous fungal taxa in individual tree trunks (Baldrian et al., 2016).

High potential for cellulose and hemicellulose degradation was displayed in the bacterial phyla *Acidobacteria* and *Bacteroidetes* (Lladó et al., 2019; Tláskal and Baldrian, 2021 – VI.) and cellulolytic activity was observed in several genera from these phyla (Štursová et al., 2012). Interestingly, selected N₂-fixing strains showed presence of genes for cellulases as well, hinting that they might be independent in C release from recalcitrant sources (Tláskal and Baldrian, 2021 – VI.). As the most readily available plant biopolymers are gradually depleted during decomposition, those bacteria with genes for chitin degradation might switch to utilize C from the fungal biomass and their abundance might increase with ongoing decomposition and fungal biomass development (Tláskal and Baldrian, 2021 – VI.). Chitin as one of the main structural polymers of the fungal cell wall represents relatively easily accessible source of C and N. Mycophagous gene expression was detected in the phyla *Bacteroidetes*, *Acidobacteria* and *Proteobacteria* (Tláskal et al., 2021a – IV.). In accordance, isolates with genes for chitin targeting were retrieved from the genera *Mucilaginibacter*, *Granulicella*, *Edaphobacter*, *Luteibacter*, *Pseudomonas*, *Variovorax*, and *Caballeronia* (Tláskal and Baldrian, 2021 – VI.). *Burkholderiales* (*Variovorax* and *Caballeronia*) were shown earlier to be enriched on fungal mycelium substrate (Valášková et al., 2009; Hervé et al., 2016a; Brabcová et al., 2018; Starke et al., 2020). The genus *Luteibacter* shows mycolytic as well as cellulolytic activity (López-Mondéjar et al., 2016; Lasa et al., 2019; Mieszkin et al., 2021). *Acidobacteria* are found among abundant taxa in deadwood in many studies (Valášková et al., 2009; Kielak et al., 2016; Rinta-Kanto et al., 2016; Tláskal et al., 2017 – I.; Probst et al., 2021) and multiple chitinases were found in the genomes of *Granulicella* and *Edaphobacter* suggesting their ability to utilize fungal biomass (Tláskal and Baldrian, 2021 – VI.).

As a complement to the isolation, 58 high-quality bacterial MAGs were resolved from deadwood metagenome (Tláskal et al., 2021b – V.). The advantage of the MAG approach over isolation is that MAGs often come from organisms which are distantly related to any isolated species which can bring information about new genes and pathways. Indeed, deadwood MAGs included often uncultivated phyla such as *Patescibacteria*, *Verrucomicrobia*, *Planctomycetes*. Despite the potential of MAGs to assess the features of rare and cryptic microbial groups, cultivation represents an approach which provides more

reliable genomic information and gives the opportunity for phenotype screening (Tláskal and Baldrian, 2021 – VI.). As shown by comparison of MAGs and isolates, even nearly complete MAGs with quality based on single copy genes missed 25% from core and 50% from variable genes in microbial population (Meziti et al., 2021). Accuracy of MAGs can be, however, further improved by manual curation and long-read sequencing (Arumugam et al., 2019) thus showing cultivation and genome resolving to be two complementary approaches. Their selection depends on the model habitat and goal of the study.

Metagenomics further allows to study population genetics of microorganisms by quantification of heterogeneity of strains/MAGs at the subspecies level. This heterogeneity is represented by differences in single-nucleotide variants in their genomes (Reveillaud et al., 2019; Van Rossum et al., 2020). Further, comparison of gene content of strains/MAGs serves for identification of core pangenome (portion of genes shared by taxonomically related genomes, Vos and Eyre-Walker, 2017). Both these methods – population genomics and pangenome analysis helped to demonstrate that genomically homogenous population of *Sodalis ligni* in deadwood shares essential genome functions with other *Sodalis* strains while several accessory genes like those for carbohydrate utilization are shared only among free-living strains (Tláskal et al., 2021c – VII.).

The use of metagenome data to characterize overall microbial potential when genes are not binned to genomes (e.g., Mackelprang et al., 2018) is hampered by the uncertainty connected with taxonomy of identified genes. To identify error rate of such taxonomic assignment, genes in a simulated mock community metagenome were compared by homology-based alignment with RefSeq database (Kyselková et al., 2021 – VIII.). Comparison showed that filtering of the database hits should be included during results analysis. This means application of arbitrary thresholds for e-value or bit-score before analysis of taxonomic composition. To reach certain degree of taxonomic correctness (i.e., 95%) at the genus level, higher confidence threshold filtering (e-value 1E-90) at the cost of decrease of annotated gene counts is necessary (Kyselková et al., 2021 – VIII.). Such assignments should be still taken with cautions because they only reflect the content of used databases that are heavily biased to easily culturable taxa from the most studied environments.

Despite the limitations of databases, metastudies collecting and re-analyzing large datasets are getting increased importance (Thompson et al., 2017; Větrovský et al., 2020; Nayfach et al., 2021). Such efforts expect data and associated metadata to be well-annotated and publicly accessible. In order to facilitate the reuse of generated datasets, data included in the presented thesis were deposited in annotated forms to the NCBI, ENA, MG-RAST or FigShare and key parts of the processing scripts were deposited to GitHub (Tláskal, 2021; Tláskal et al., 2021b – V.).

5. Conclusions

With the research presented in this thesis, I was able to answer several main questions specified in deadwood-devoted review by Johnston et al. (2016) and challenges mentioned by Mieszkin et al. (2021). This includes questions about:

- Temporal aspect of community during decomposition
- Determinants of the bacterial community
- Fungal-bacterial interactions
- Bacterial metabolism

I described successive changes of bacterial community during the lifetime of decomposing trees which enabled to identify bacterial groups specific for early and late decomposition. The length of decomposition was recorded to be stronger predictor of community than tree species.

Fungi were unequivocally showed to influence bacterial community structure and several abundant bacterial taxa dependent on utilization of fungal mycelia were cultivated. I demonstrated unequal roles of fungi and bacteria in deadwood biomass decomposition so that fungi dominate carbohydrate utilization while bacteria perform activities which are allowed by their metabolic adaptations namely N_2 fixation and other steps in N cycle, methanotrophy and methylotrophy. Strains containing genes for these traits are cultivable and represent high proportion of bacterial community.

I showed that N_2 -fixation in deadwood is important for replenishing the N budget at the ecosystem level. Cultivation of free-living N_2 -fixing *Sodalis* strains unveiled unexpected deadwood preference and thus broad ecological niche of otherwise insect-associated genus.

The potential of bacteria for degradation of plant-derived compounds is variable and taxonomy-dependent as confirmed by both cultivation-dependent and cultivation-independent genomic techniques. The latter applied approach represents the first effort to tackle uncultured bacterial diversity in deadwood at the genome level.

In the light of these findings, deadwood is seen as a hotspot of nutrient exchange and recycling which is enabled by interplay of inhabiting microorganisms.

6. References

- Adam, P. S., Borrel, G., and Gribaldo, S. (2019). An archaeal origin of the Wood–Ljungdahl H₄MPT branch and the emergence of bacterial methylophily. *Nat. Microbiol.* 4, 2155–2163. doi:10.1038/s41564-019-0534-2.
- Allison, S. D. (2005). Cheaters, diffusion and nutrients constrain decomposition by microbial enzymes in spatially structured environments. *Ecol. Lett.* 8, 626–635. doi:10.1111/j.1461-0248.2005.00756.x.
- Anderson-Teixeira, K. J., Davies, S. J., Bennett, A. C., Muller-landau, H. C., and Wright, S. J. (2015). CTFS-ForestGEO: a worldwide network monitoring forests in an era of global change. *Glob. Chang. Biol.* 21, 528–549. doi:10.1111/gcb.12712.
- Andreska, J. (2006). K dějinám Národní přírodní rezervace Žofínský prales. *Živa* 5, 214–216.
- Arumugam, K., Bağcı, C., Bessarab, I., Beier, S., Buchfink, B., Górska, A., et al. (2019). Annotated bacterial chromosomes from frame-shift-corrected long-read metagenomic data. *Microbiome* 7, 61. doi:10.1186/s40168-019-0665-y.
- Baldrian, P., Zrůstová, P., Tláskal, V., Davidová, A., Merhautová, V., and Vrška, T. (2016). Fungi associated with decomposing deadwood in a natural beech-dominated forest. *Fungal Ecol.* 23, 109–122. doi:10.1016/j.funeco.2016.07.001.
- Bay, S. K., Dong, X., Bradley, J. A., Leung, P. M., Grinter, R., Jirapanjawan, T., et al. (2021). Trace gas oxidizers are widespread and active members of soil microbial communities. *Nat. Microbiol.* 6, 246–256. doi:10.1038/s41564-020-00811-w.
- Berlemont, R., and Martiny, A. C. (2013). Phylogenetic distribution of potential cellulases in bacteria. *Appl. Environ. Microbiol.* 79, 1545–1554. doi:10.1128/AEM.03305-12.
- Berlemont, R., and Martiny, A. C. (2015). Genomic potential for polysaccharide deconstruction in Bacteria. *Appl. Environ. Microbiol.* 81, 1513–1519. doi:10.1128/AEM.03718-14.
- Bomble, Y. J., Lin, C. Y., Amore, A., Wei, H., Holwerda, E. K., Ciesielski, P. N., et al. (2017). Lignocellulose deconstruction in the biosphere. *Curr. Opin. Chem. Biol.* 41, 61–70. doi:10.1016/j.cbpa.2017.10.013.
- Bond-Lamberty, B., Wang, C., and Gower, S. T. (2002). Annual carbon flux from woody debris for a boreal black spruce fire chronosequence. *J. Geophys. Res. Atmos.* 108, 8220. doi:10.1029/2001JD000839.
- Bowers, R. M., Kyrpides, N. C., Stepanauskas, R., Harmon-Smith, M., Doud, D., Reddy, T. B. K., et al. (2017). Minimum information about a single amplified genome (MISAG) and a metagenome-assembled genome (MIMAG) of bacteria and archaea. *Nat. Biotechnol.* 35, 725–731. doi:10.1038/nbt.3893.
- Brabcová, V., Nováková, M., Davidová, A., and Baldrian, P. (2016). Dead fungal mycelium in forest soil represents a decomposition hotspot and a habitat for a specific microbial community. *New Phytol.* 210, 1369–1381. doi:10.1111/nph.13849.
- Brabcová, V., Štursová, M., and Baldrian, P. (2018). Nutrient content affects the turnover of fungal biomass in forest topsoil and the composition of associated microbial communities. *Soil Biol. Biochem.* 118, 187–198. doi:10.1016/j.soilbio.2017.12.012.
- Bravo, D., Cailleau, G., Bindschedler, S., Simon, A., Job, D., Verrecchia, E., et al. (2013). Isolation of oxalotrophic bacteria able to disperse on fungal mycelium. *FEMS Microbiol. Lett.* 348, 157–166. doi:10.1111/1574-6968.12287.
- Brunner, A., and Kimmins, J. P. (2003). Nitrogen fixation in coarse woody debris of *Thuja plicata* and *Tsuga heterophylla* forests on northern Vancouver Island. *Can. J. For. Res.* 33, 1670–1682. doi:10.1139/x03-085.
- Cantalapiedra, C. P., Hernández-plaza, A., Letunic, I., and Bork, P. (2021). eggNOG-mapper v2: Functional annotation, orthology assignments, and domain prediction at the

- metagenomic scale. *bioRxiv*. doi:10.1101/2021.06.03.446934.
- Cantarel, B. L., Coutinho, P. M., Rancurel, C., Bernard, T., Lombard, V., and Henrissat, B. (2009). The Carbohydrate-Active EnZymes database (CAZy): an expert resource for Glycogenomics. *Nucleic Acids Res.* 37, D233-238. doi:10.1093/nar/gkn663.
- Chen, L. X., Anantharaman, K., Shaiber, A., Murat Eren, A., and Banfield, J. F. (2020). Accurate and complete genomes from metagenomes. *Genome Res.* 30, 315–333. doi:10.1101/gr.258640.119.
- Christofides, S. R., Hiscox, J., Savoury, M., Boddy, L., and Weightman, A. J. (2019). Fungal control of early-stage bacterial community development in decomposing wood. *Fungal Ecol.* 42, 100868. doi:10.1016/j.funeco.2019.100868.
- Clausen, C. A. (1996). Bacterial associations with decaying wood: a review. *Int. Biodeterior. Biodegradation* 37, 101–107. doi:10.1016/0964-8305(95)00109-3.
- Corrêa, F. B., Saraiva, J. P., Stadler, P. F., and da Rocha, U. N. (2020). TerrestrialMetagenomeDB: a public repository of curated and standardized metadata for terrestrial metagenomes. *Nucleic Acids Res.* 48, 626–632. doi:10.1093/nar/gkz994.
- Cowling, E. B., and Merrill, W. (1966). Nitrogen in wood and its role in wood deterioration. *Can. J. Bot.* 44, 1539–1554. doi:10.1139/b66-167.
- Curtis, P. G., Slay, C. M., Harris, N. L., Tyukavina, A., and Hansen, M. C. (2018). Classifying drivers of global forest loss. *Science* 361, 1108–1111. doi:10.1126/science.aau3445.
- Davies, S. J., Abiem, I., Abu Salim, K., Aguilar, S., Allen, D., Alonso, A., et al. (2021). ForestGEO: Understanding forest diversity and dynamics through a global observatory network. *Biol. Conserv.* 253, 108907. doi:10.1016/j.biocon.2020.108907.
- de Boer, W., Folman, L. B., Klein Gunnewiek, P. J. A., Svensson, T., Bastviken, D., Öberg, G., et al. (2010). Mechanism of antibacterial activity of the white-rot fungus *Hypholoma fasciculare* colonizing wood. *Can. J. Microbiol.* 56, 380–388. doi:10.1139/W10-023.
- Eastwood, D. C., Floudas, D., Binder, M., Majcherczyk, A., Schneider, P., Aerts, A., et al. (2011). The plant cell wall-decomposing machinery underlies the functional diversity of forest fungi. *Science* 333, 762–765. doi:10.1126/science.1205411.
- Filley, T. R., Cody, G. D., Goodell, B., Jellison, J., Noser, C., and Ostrofsky, A. (2002). Lignin demethylation and polysaccharide decomposition in spruce sapwood degraded by brown rot fungi. *Org. Geochem.* 33, 111–124. doi:10.1016/S0146-6380(01)00144-9.
- Folman, L. B., Gunnewiek, P. J. A. K., Boddy, L., and de Boer, W. (2008). Impact of white-rot fungi on numbers and community composition of bacteria colonizing beech wood from forest soil. *FEMS Microbiol. Ecol.* 63, 181–191. doi:10.1111/j.1574-6941.2007.00425.x.
- Forrester, J. A., Mladenoff, D. J., Gower, S. T., and Stoffel, J. L. (2012). Interactions of temperature and moisture with respiration from coarse woody debris in experimental forest canopy gaps. *For. Ecol. Manage.* 265, 124–132. doi:10.1016/j.foreco.2011.10.038.
- Galperin, M. Y., Kristensen, D. M., Makarova, K. S., Wolf, Y. I., and Koonin, E. V. (2018). Microbial genome analysis: The COG approach. *Brief. Bioinform.* 20, 1063–1070. doi:10.1093/bib/bbx117.
- García-Contreras, R., and Loarca, D. (2021). The bright side of social cheaters: Potential beneficial roles of “social cheaters” in microbial communities. *FEMS Microbiol. Ecol.* 97, fiae239. doi:10.1093/femsec/fiae239.
- Garron, M., and Henrissat, B. (2019). The continuing expansion of CAZymes and their families. *Curr. Opin. Chem. Biol.* 53. doi:10.1016/j.cbpa.2019.08.004.
- Geisen, S., Tveit, A. T., Clark, I. M., Richter, A., Svenning, M. M., Bonkowski, M., et al. (2015). Metatranscriptomic census of active protists in soils. *ISME J.* 9, 2178–2190. doi:10.1038/ismej.2015.30.
- Gómez-Brandón, M., Probst, M., Siles, J. A., Peintner, U., Bardelli, T., Egli, M., et al. (2020). Fungal communities and their association with nitrogen-fixing bacteria affect early decomposition of Norway spruce deadwood. *Sci. Rep.* 10, 8025. doi:10.1038/s41598-020-64808-5.

- Halme, P., Allen, K. A., Auniņš, A., Bradshaw, R. H. W., Brūmelis, G., Čada, V., et al. (2013). Challenges of ecological restoration: Lessons from forests in northern Europe. *Biol. Conserv.* 167, 248–256. doi:10.1016/j.biocon.2013.08.029.
- Harantová, L., Mudrák, O., Kohout, P., Elhottová, D., Frouz, J., and Baldrian, P. (2017). Development of microbial community during primary succession in areas degraded by mining activities. *L. Degrad. Dev.* 28, 2574–2584. doi:10.1002/ldr.2817.
- Harris, N. L., Gibbs, D. A., Baccini, A., Birdsey, R. A., de Bruin, S., Farina, M., et al. (2021). Global maps of twenty-first century forest carbon fluxes. *Nat. Clim. Chang.* 11, 234–240. doi:10.1038/s41558-020-00976-6.
- Hervé, V., Junier, T., Bindschedler, S., Verrecchia, E., and Junier, P. (2016a). Diversity and ecology of oxalotrophic bacteria. *World J. Microbiol. Biotechnol.* 32, 28. doi:10.1007/s11274-015-1982-3.
- Hervé, V., Ketter, E., Pierrat, J.-C., Gelhaye, E., and Frey-Klett, P. (2016b). Impact of *Phanerochaete chrysosporium* on the functional diversity of bacterial communities associated with decaying wood. *PLoS One* 11, e0147100. doi:10.1371/journal.pone.0147100.
- Hervé, V., Roux, X. Le, Uroz, S., Gelhaye, E., and Frey-Klett, P. (2013). Diversity and structure of bacterial communities associated with *Phanerochaete chrysosporium* during wood decay. *Environ. Microbiol.* 16, 2238–2252. doi:10.1111/1462-2920.12347.
- Hiscox, J., Savoury, M., Müller, C. T., Lindahl, B. D., Rogers, H. J., and Boddy, L. (2015). Priority effects during fungal community establishment in beech wood. *ISME J.* 9, 2246–2260. doi:10.1038/ismej.2015.38.
- Hoffman, B. M., Lukoyanov, D., Yang, Z.-Y., Dean, D. R., and Seefeldt, L. C. (2014). Mechanism of nitrogen fixation by nitrogenase: The next stage. *Chem. Rev.* 114, 4041–4062. doi:dx.doi.org/10.1021/cr400641x.
- Hoffmann, S., Irl, S. D. H., and Beierkuhnlein, C. (2019). Predicted climate shifts within terrestrial protected areas worldwide. *Nat. Commun.* 10, 4787. doi:10.1038/s41467-019-12603-w.
- Hoppe, B., Kahl, T., Karasch, P., Wubet, T., Bauhus, J., Buscot, F., et al. (2014). Network analysis reveals ecological links between N-fixing bacteria and wood-decaying fungi. *PLoS One* 9, e88141. doi:10.1371/journal.pone.0088141.
- Hoppe, B., Krüger, D., Kahl, T., Arnstadt, T., Buscot, F., Bauhus, J., et al. (2015). A pyrosequencing insight into sprawling bacterial diversity and community dynamics in decaying deadwood logs of *Fagus sylvatica* and *Picea abies*. *Sci. Rep.* 5, 9456. doi:10.1038/srep09456.
- Hultman, J., Waldrop, M. P., Mackelprang, R., David, M. M., Mcfarland, J., Blazewicz, S. J., et al. (2015). Multi-omics of permafrost, active layer and thermokarst bog soil microbiomes. *Nature* 521, 208–212. doi:10.1038/nature14238.
- IUCN & UNEP (2018). The World Database on Protected Areas (WDPA). Available at: www.protectedplanet.net.
- Johnston, S. R., Boddy, L., and Weightman, A. J. (2016). Bacteria in decomposing wood and their interactions with wood-decay fungi. *FEMS Microbiol. Ecol.* 92, fiw179. doi:10.1093/femsec/fiw179.
- Johnston, S. R., Hiscox, J., Savoury, M., Boddy, L., and Weightman, A. J. (2019). Highly competitive fungi manipulate bacterial communities in decomposing beech wood (*Fagus sylvatica*). *FEMS Microbiol. Ecol.* 95, fiy225. doi:10.1093/femsec/fiy225.
- Kahl, T., Arnstadt, T., Baber, K., Bässler, C., Bauhus, J., Borken, W., et al. (2017). Wood decay rates of 13 temperate tree species in relation to wood properties, enzyme activities and organismic diversities. *For. Ecol. Manage.* 391, 86–95. doi:10.1016/j.foreco.2017.02.012.
- Kanehisa, M., and Goto, S. (2000). KEGG: Kyoto Encyclopedia of Genes and Genomes. *Nucleic Acids Res.* 28, 27–30. doi:10.1093/nar/28.1.27.
- Kielak, A. M., Scheublin, T. R., Mendes, L. W., van Veen, J. A., and Kuramae, E. E. (2016).

- Bacterial community succession in pine-wood decomposition. *Front. Microbiol.* 7, 231. doi:10.3389/fmicb.2016.00231.
- Král, K., Janík, D., Vrška, T., Adam, D., Hort, L., Unar, P., et al. (2010). Local variability of stand structural features in beech dominated natural forests of Central Europe: Implications for sampling. *For. Ecol. Manage.* 260, 2196–2203. doi:10.1016/j.foreco.2010.09.020.
- Kyselková, M., Tláskal, V., Morais, D. K., Michalčíková, L., Hollá, S. A., Větrovský, T., et al. (2021). Taxonomy assignment of bacterial genes in a metagenome: assessment of accuracy and recommendations for reporting. *submitted*.
- Lasa, A. V., Mašínová, T., Baldrian, P., and Fernández-López, M. (2019). Bacteria from the endosphere and rhizosphere of *Quercus* spp. use mainly cell wall-associated enzymes to decompose organic matter. *PLoS One* 14, e0214422. doi:10.1371/journal.pone.0214422.
- Lemos, L. N., Mendes, L. W., Baldrian, P., and Pylro, V. S. (2021). Genome-resolved metagenomics is essential for unlocking the microbial black box of the soil. *Trends Microbiol.* 29, 279–282. doi:10.1016/j.tim.2021.01.013.
- Lenhart, K., Bunge, M., Ratering, S., Neu, T. R., Schüttmann, I., Greule, M., et al. (2012). Evidence for methane production by saprotrophic fungi. *Nat. Commun.* 3, 1046. doi:10.1038/ncomms2049.
- Lepinay, C., Jirásková, L., Tláskal, V., Brabcová, V., Vrška, T., and Baldrian, P. (2021). Successional development of fungal communities associated with decomposing deadwood in a natural mixed temperate forest. *J. Fungi* 7, 412. doi:10.3390/jof7060412.
- Leveau, J. H. J., Uroz, S., and de Boer, W. (2010). The bacterial genus *Collimonas*: Mycophagy, weathering and other adaptive solutions to life in oligotrophic soil environments. *Environ. Microbiol.* 12, 281–292. doi:10.1111/j.1462-2920.2009.02010.x.
- Levy Karin, E., Mirdita, M., and Söding, J. (2020). MetaEuk-sensitive, high-throughput gene discovery, and annotation for large-scale eukaryotic metagenomics. *Microbiome* 8, 48. doi:10.1186/s40168-020-00808-x.
- Lladó, S. F., Větrovský, T., and Baldrian, P. (2019). Tracking of the activity of individual bacteria in temperate forest soils shows guild-specific responses to seasonality. *Soil Biol. Biochem.* 135, 275–282. doi:10.1016/j.soilbio.2019.05.010.
- Lladó, S. F., Žifčáková, L., Větrovský, T., Eichlerová, I., and Baldrian, P. (2016). Functional screening of abundant bacteria from acidic forest soil indicates the metabolic potential of Acidobacteria subdivision 1 for polysaccharide decomposition. *Biol. Fertil. Soils* 52, 251–260. doi:10.1007/s00374-015-1072-6.
- López-Mondéjar, R., Brabcová, V., Štursová, M., Davidová, A., Jansa, J., Cajthaml, T., et al. (2018). Decomposer food web in a deciduous forest shows high share of generalist microorganisms and importance of microbial biomass recycling. *ISME J.* 12, 1768–1778. doi:10.1038/s41396-018-0084-2.
- López-Mondéjar, R., Zühlke, D., Větrovský, T., Becher, D., Riedel, K., and Baldrian, P. (2016). Decoding the complete arsenal for cellulose and hemicellulose deconstruction in the highly efficient cellulose decomposer *Paenibacillus* O199. *Biotechnol. Biofuels* 9, 104. doi:10.1186/s13068-016-0518-x.
- Luyssaert, S., Schulze, E. D., Börner, A., Knohl, A., Hessenmöller, D., Law, B. E., et al. (2008). Old-growth forests as global carbon sinks. *Nature* 455, 213–215. doi:10.1038/nature07276.
- Mackelprang, R., Grube, A. M., Lamendella, R., Jesus, E. da C., Copeland, A., Liang, C., et al. (2018). Microbial community structure and functional potential in cultivated and native tallgrass prairie soils of the Midwestern United States. *Front. Microbiol.* 9, 1775. doi:10.3389/fmicb.2018.01775.
- Madin, J. S., Nielsen, D. A., Brbic, M., Corkrey, R., Danko, D., Edwards, K., et al. (2020). A synthesis of bacterial and archaeal phenotypic trait data. *Sci. Data* 7, 170. doi:10.1038/s41597-020-0497-4.

- Mäkipää, R., Leppänen, S. M., Sanz Munoz, S., Smolander, A., Tirola, M., Tuomivirta, T., et al. (2018). Methanotrophs are core members of the diazotroph community in decaying Norway spruce logs. *Soil Biol. Biochem.* 120, 230–232. doi:10.1016/j.soilbio.2018.02.012.
- Mäkipää, R., Rajala, T., Schigel, D., Rinne, K. T., Pennanen, T., Abrego, N., et al. (2017). Interactions between soil- and dead wood-inhabiting fungal communities during the decay of Norway spruce logs. *ISME J.* 11, 1964–1974. doi:10.1038/ismej.2017.57.
- Markowitz, V. M., Ivanova, N. N., Szeto, E., Palaniappan, K., Chu, K., Dalevi, D., et al. (2007). IMG/M: A data management and analysis system for metagenomes. *Nucleic Acids Res.* 36, 534–538. doi:10.1093/nar/gkm869.
- Martin, A. R., Domke, G. M., Doraisami, M., and Thomas, S. C. (2021). Carbon fractions in the world's dead wood. *Nat. Commun.* 12, 889. doi:10.1038/s41467-021-21149-9.
- Meyer, F., Paarmann, D., D'Souza, M., Olson, R., Glass, E., Kubal, M., et al. (2008). The metagenomics RAST server – a public resource for the automatic phylogenetic and functional analysis of metagenomes. *BMC Bioinformatics* 9, 386. doi:10.1186/1471-2105-9-386.
- Meziti, A., Rodriguez-R, L. M., Hatt, J. K., Peña-Gonzalez, A., Levy, K., and Konstantinidis, K. T. (2021). How reliably do metagenome-assembled genomes (MAGs) represent natural populations? Insights from comparing MAGs against isolate genomes derived from the same fecal sample. *Appl. Environ. Microbiol.* 89, e02593-20. doi:10.1128/aem.02593-20.
- Mieszkin, S., Richet, P., Bach, C., Lambrot, C., Augusto, L., Buée, M., et al. (2021). Oak decaying wood harbors taxonomically and functionally different bacterial communities in sapwood and heartwood. *Soil Biol. Biochem.* 155, 108160. doi:10.1016/j.soilbio.2021.108160.
- Mistry, J., Chuguransky, S., Williams, L., Qureshi, M., Salazar, G. A., Sonnhammer, E. L. L., et al. (2021). Pfam: The protein families database in 2021. *Nucleic Acids Res.* 49, D412–D419. doi:10.1093/nar/gkaa913.
- Moll, J., Heintz-Buschart, A., Bässler, C., Hofrichter, M., Kellner, H., Buscot, F., et al. (2021). Amplicon sequencing-based bipartite network analysis confirms a high degree of specialization and modularity for fungi and prokaryotes in deadwood. *mSphere* 6, e00856-20. doi:10.1128/mSphere.00856-20.
- Moll, J., Kellner, H., Leonhardt, S., Stengel, E., Dahl, A., Bässler, C., et al. (2018). Bacteria inhabiting deadwood of 13 tree species reveal great heterogeneous distribution between sapwood and heartwood. *Environ. Microbiol.* 20, 3744–3756. doi:10.1111/1462-2920.14376.
- Nayfach, S., Roux, S., Seshadri, R., Udwaray, D., Varghese, N., Schulz, F., et al. (2021). A genomic catalog of Earth's microbiomes. *Nat. Biotechnol.* 39, 499–509. doi:10.1038/s41587-020-0718-6.
- Nazir, R., Warmink, J. A., Voordes, D. C., van de Bovenkamp, H. H., and van Elsas, J. D. (2013). Inhibition of mushroom formation and induction of glycerol release - ecological strategies of *Burkholderia terrae* BS001 to create a hospitable niche at the fungus *Lyophyllum* sp. strain Karsten. *Microb. Ecol.* 65, 245–254. doi:10.1007/s00248-012-0100-4.
- Nelson, M. B., Martiny, A. C., and Martiny, J. B. H. (2016). Global biogeography of microbial nitrogen-cycling traits in soil. *Proc. Natl. Acad. Sci. U. S. A.* 113, 8033–8040. doi:10.1073/pnas.1601070113.
- Odriozola, I., Abrego, N., Tláskal, V., Zrůstová, P., Morais, D., Větrovský, T., et al. (2021). Fungal communities are important determinants of bacterial community composition in deadwood. *mSystems* 6, e01017-20. doi:10.1128/mSystems.01017-20.
- Ovaskainen, O., Tikhonov, G., Norberg, A., Guillaume Blanchet, F., Duan, L., Dunson, D., et al. (2017). How to make more out of community data? A conceptual framework and its implementation as models and software. *Ecol. Lett.* 20, 561–576. doi:10.1111/ele.12757.
- Pan, Y., Birdsey, R. A., Fang, J., Houghton, R., Kauppi, P. E., Kurz, W. A., et al. (2011). A large

- and persistent carbon sink in the world's forests. *Science* 333, 988–993. doi:10.1126/science.1201609.
- Parks, D. H., Rinke, C., Chuvochina, M., Chaumeil, P.-A., Woodcroft, B. J., Evans, P. N., et al. (2017). Recovery of nearly 8,000 metagenome-assembled genomes substantially expands the tree of life. *Nat. Microbiol.* 2, 1533–1542. doi:10.1038/s41564-017-0012-7.
- Philpott, T. J., Prescott, C. E., Chapman, W. K., and Grayston, S. J. (2014). Nitrogen translocation and accumulation by a cord-forming fungus (*Hypholoma fasciculare*) into simulated woody debris. *For. Ecol. Manage.* 315, 121–128. doi:10.1016/j.foreco.2013.12.034.
- Přívětivý, T., Adam, D., and Vrška, T. (2018). Decay dynamics of *Abies alba* and *Picea abies* deadwood in relation to environmental conditions. *For. Ecol. Manage.* 427, 250–259. doi:10.1016/j.foreco.2018.06.008.
- Přívětivý, T., Janík, D., Unar, P., Adam, D., Král, K., and Vrška, T. (2016). How do environmental conditions affect the deadwood decomposition of European beech (*Fagus sylvatica* L.)? *For. Ecol. Manage.* 381, 177–187. doi:10.1016/j.foreco.2016.09.033.
- Probst, M., Ascher-Jenull, J., Insam, H., and Gómez-Brandón, M. (2021). The molecular information about deadwood bacteriomes partly depends on the targeted environmental DNA. *Front. Microbiol.* 12, 640386. doi:10.3389/fmicb.2021.640386.
- Probst, M., Gómez-Brandón, M., Bardelli, T., Egli, M., Insam, H., and Ascher-Jenull, J. (2018). Bacterial communities of decaying Norway spruce follow distinct slope exposure and time-dependent trajectories. *Environ. Microbiol.* 20, 3657–3670. doi:10.1111/1462-2920.14359.
- Pugh, T. A. M., Lindeskog, M., Smith, B., Poulter, B., Arneth, A., Haverd, V., et al. (2019). Role of forest regrowth in global carbon sink dynamics. *Proc. Natl. Acad. Sci. U. S. A.* 116, 4382–4387. doi:10.1073/pnas.1810512116.
- Rayner, A. D., and Boddy, L. (1988). *Fungal decomposition of wood. Its biology and ecology.* John Wiley & Sons Ltd.
- Reveillaud, J., Bordenstein, S. R., Cruaud, C., Shaiber, A., Esen, Ö. C., Weill, M., et al. (2019). The *Wolbachia* mobilome in *Culex pipiens* includes a putative plasmid. *Nat. Commun.* 10, 1051. doi:10.1038/s41467-019-08973-w.
- Rinne-Garmston, K. T., Peltoniemi, K., Chen, J., Peltoniemi, M., Fritze, H., and Mäkipää, R. (2019). Carbon flux from decomposing wood and its dependency on temperature, wood N₂ fixation rate, moisture and fungal composition in a Norway spruce forest. *Glob. Chang. Biol.* 25, 1852–1867. doi:10.1111/gcb.14594.
- Rinne, K. T., Rajala, T., Peltoniemi, K., Chen, J., Smolander, A., and Mäkipää, R. (2017). Accumulation rates and sources of external nitrogen in decaying wood in a Norway spruce dominated forest. *Funct. Ecol.* 31, 530–541. doi:10.1111/1365-2435.12734.
- Rinta-Kanto, J. M., Sinkko, H., Rajala, T., Al-Soud, W. A., Sørensen, S. J., Tamminen, M. V., et al. (2016). Natural decay process affects the abundance and community structure of Bacteria and Archaea in *Picea abies* logs. *FEMS Microbiol. Ecol.* 92, fiw087. doi:10.1093/femsec/fiw087.
- Rochman, F. F., Kwon, M., Khadka, R., Tamas, I., Lopez-Jauregui, A. A., Sheremet, A., et al. (2020). Novel copper-containing membrane monooxygenases (CuMMOs) encoded by alkane-utilizing *Betaproteobacteria*. *ISME J.* 14, 714–726. doi:10.1038/s41396-019-0561-2.
- Roskoski, J. P. (1980). Nitrogen fixation in hardwood forests of the northeastern United States. *Plant Soil* 54, 33–44. doi:10.1007/BF02181997.
- Rossi, M. F., Mello, B., and Schrago, C. G. (2017). Performance of Hidden Markov Models in recovering the standard classification of glycoside hydrolases. *Evol. Bioinforma.* 13, 1–5. doi:10.1177/1176934317703401.
- Sait, M., Hugenholtz, P., and Janssen, P. H. (2002). Cultivation of globally distributed soil bacteria from phylogenetic lineages previously only detected in cultivation-independent surveys. *Environ. Microbiol.* 4, 654–666. doi:10.1046/j.1462-

2920.2002.00352.x.

- Šamonil, P., Daněk, P., Baldrian, P., Tláškal, V., Tejnecký, V., and Drábek, O. (2020). Convergence, divergence or chaos? Consequences of tree trunk decay for pedogenesis and the soil microbiome in a temperate natural forest. *Geoderma* 376, 114499. doi:10.1016/j.geoderma.2020.114499.
- Seibold, S., Bäessler, C., Brandl, R., Gossner, M. C., Thorn, S., Ulyshen, M. D., et al. (2015). Experimental studies of dead-wood biodiversity — A review identifying global gaps in knowledge. *Biol. Conserv.* 191, 139–149. doi:10.1016/j.biocon.2015.06.006.
- Seidler, R. J., Aho, P. E., Raju, P. N., and Evans, H. J. (1972). Nitrogen fixation by bacterial isolates from decay in living white fir trees [*Abies concolor* (Gord. and Glend.) Lindl.]. *J. Gen. Microbiol.* 73, 413–416. doi:10.1099/00221287-73-2-413.
- Shaiber, A., and Eren, A. M. (2019). Composite metagenome-assembled genomes reduce the quality of public genome repositories. *mBio* 10, e00725-19. doi:10.1128/mBio.00725-19.
- Spano, S. D., Jurgensen, M. F., Larsen, M. J., and Harvey, A. E. (1982). Nitrogen-fixing bacteria in Douglas-fir residue decayed by *Fomitopsis pinicola*. *Plant Soil* 68, 117–123. doi:10.1007/BF02374731.
- Starke, R., Morais, D., Větrovský, T., Mondéjar, R. L., Baldrian, P., and Brabcová, V. (2020). Feeding on fungi: Genomic and proteomic analysis of the enzymatic machinery of bacteria decomposing fungal biomass. *Environ. Microbiol.* 22, 4604–4619. doi:10.1111/1462-2920.15183.
- Steen, A. D., Crits-Christoph, A., Carini, P., DeAngelis, K. M., Fierer, N., Lloyd, K. G., et al. (2019). High proportions of bacteria and archaea across most biomes remain uncultured. *ISME J.* 13, 3126–3130. doi:10.1038/s41396-019-0484-y.
- Štursová, M., Žifčáková, L., Leigh, M. B., Burgess, R., and Baldrian, P. (2012). Cellulose utilization in forest litter and soil: identification of bacterial and fungal decomposers. *FEMS Microbiol. Ecol.* 80, 735–746. doi:10.1111/j.1574-6941.2012.01343.x.
- Thompson, L. R., Sanders, J. G., McDonald, D., Amir, A., Ladau, J., Locey, K. J., et al. (2017). A communal catalogue reveals Earth’s multiscale microbial diversity. *Nature* 551, 457–463. doi:10.1038/nature24621.
- Tikhonov, G., Opedal, Ø. H., Abrego, N., Lehikoinen, A., de Jonge, M. M. J., Oksanen, J., et al. (2020). Joint species distribution modelling with the R-package Hmsc. *Methods Ecol. Evol.* 11, 442–447. doi:10.1111/2041-210X.13345.
- Tláškal, V. (2021). GitHub profile. Available at: <https://github.com/TlaskalV>.
- Tláškal, V., and Baldrian, P. (2021). Deadwood-inhabiting bacteria show adaptations to changing carbon and nitrogen availability during decomposition. *Front. Microbiol.* 12, 685303. doi:10.3389/fmicb.2021.685303.
- Tláškal, V., Brabcová, V., Větrovský, T., Jomura, M., López-Mondéjar, R., Monteiro, L. M. O., et al. (2021a). Complementary roles of wood-inhabiting fungi and bacteria facilitate deadwood decomposition. *mSystems* 6, e01078-20. doi:10.1128/mSystems.01078-20.
- Tláškal, V., Brabcová, V., Větrovský, T., López-Mondéjar, R., Monteiro, L. M. O., Saraiva, J. P., et al. (2021b). Metagenomes, metatranscriptomes and microbiomes of naturally decomposing deadwood. *Sci. Data* 8, 198. doi:10.1038/s41597-021-00987-8.
- Tláškal, V., Pyro, V. S., Žifčáková, L., and Baldrian, P. (2021c). Ecological divergence within the enterobacterial genus *Sodalis*: From insect symbionts to inhabitants of decomposing deadwood. *Front. Microbiol.* 12, 668644. doi:10.3389/fmicb.2021.668644.
- Tláškal, V., Voříšková, J., and Baldrian, P. (2016). Bacterial succession on decomposing leaf litter exhibits a specific occurrence pattern of cellulolytic taxa and decomposers of fungal mycelia. *FEMS Microbiol. Ecol.* 92, fiw177. doi:10.1093/femsec/fiw177.
- Tláškal, V., Zrůstová, P., Vrška, T., and Baldrian, P. (2017). Bacteria associated with decomposing dead wood in a natural temperate forest. *FEMS Microbiol. Ecol.* 93, fix157. doi:10.1093/femsec/fix157.
- Valášková, V., de Boer, W., Gunnewiek, P. J. A. K., Pospíšek, M., and Baldrian, P. (2009).

- Phylogenetic composition and properties of bacteria coexisting with the fungus *Hypholoma fasciculare* in decaying wood. *ISME J.* 3, 1218–1221. doi:10.1038/ismej.2009.64.
- Van Rossum, T., Ferretti, P., Maistrenko, O. M., and Bork, P. (2020). Diversity within species: interpreting strains in microbiomes. *Nat. Rev. Microbiol.* 18, 491–506. doi:10.1038/s41579-020-0368-1.
- VanInsberghe, D., Hartmann, M., Stewart, G. R., and Mohn, W. W. (2013). Isolation of a substantial proportion of forest soil bacterial communities detected via pyrotag sequencing. *Appl. Environ. Microbiol.* 79, 2096–2098. doi:10.1128/AEM.03112-12.
- Větrovský, T., Morais, D., Kohout, P., Lepinay, C., Algora, C., Hollá, S. A., et al. (2020). GlobalFungi, a global database of fungal occurrences from high-throughput-sequencing metabarcoding studies. *Sci. Data* 7. doi:10.1038/s41597-020-0567-7.
- Vitousek, P. M., and Hobbie, S. (2000). Heterotrophic nitrogen fixation in decomposing litter: Patterns and regulation. *Ecology* 81, 2366–2376. doi:10.1890/0012-9658(2000)081[2366:HNFIDL]2.0.CO;2.
- Vorob'ev, A. V., de Boer, W., Folman, L. B., Bodelier, P. L. E., Doronina, N. V., Suzina, N. E., et al. (2009). *Methylovirgula ligni* gen. nov., sp. nov., an obligately acidophilic, facultatively methylotrophic bacterium with a highly divergent *mxoF* gene. *Int. J. Syst. Evol. Microbiol.* 59, 2538–2545. doi:10.1099/ijs.0.010074-0.
- Vos, M., and Eyre-Walker, A. (2017). Are pangenomes adaptive or not? *Nat. Microbiol.* 2, 1576. doi:10.1038/s41564-017-0067-5.
- Wang, R., Goll, D., Balkanski, Y., Hauglustaine, D., Boucher, O., Ciais, P., et al. (2017). Global forest carbon uptake due to nitrogen and phosphorus deposition from 1850 to 2100. *Glob. Chang. Biol.* 23, 4854–4872. doi:10.1111/gcb.13766.
- Warmink, J. A., Nazir, R., Corten, B., and van Elsas, J. D. (2011). Hitchhikers on the fungal highway: The helper effect for bacterial migration via fungal hyphae. *Soil Biol. Biochem.* 43, 760–765. doi:10.1016/j.soilbio.2010.12.009.
- Warton, D. I., Blanchet, F. G., O'Hara, R. B., Ovaskainen, O., Taskinen, S., Walker, S. C., et al. (2015). So many variables: Joint modeling in community ecology. *Trends Ecol. Evol.* 30, 766–779. doi:10.1016/j.tree.2015.09.007.
- Weedon, J. T., Cornwell, W. K., Cornelissen, J. H. C., Zanne, A. E., Wirth, C., and Coomes, D. A. (2009). Global meta-analysis of wood decomposition rates: A role for trait variation among tree species? *Ecol. Lett.* 12, 45–56. doi:10.1111/j.1461-0248.2008.01259.x.
- West, P. T., Probst, A. J., Grigoriev, I. V., Thomas, B. C., and Banfield, J. F. (2018). Genome-reconstruction for eukaryotes from complex natural microbial communities. *Genome Res.* 28, 569–580. doi:10.1101/gr.228429.117.
- Woodcroft, B. J., Singleton, C. M., Boyd, J. A., Evans, P. N., Emerson, J. B., Zayed, A. A. F., et al. (2018). Genome-centric view of carbon processing in thawing permafrost. *Nature* 560, 49–54. doi:10.1038/s41586-018-0338-1.
- Zheng, M., Chen, H., Li, D., Luo, Y., and Mo, J. (2020). Substrate stoichiometry determines nitrogen fixation throughout succession in southern Chinese forests. *Ecol. Lett.* 23, 336–347. doi:10.1111/ele.13437.
- Žifčáková, L., Větrovský, T., Howe, A., and Baldrian, P. (2016). Microbial activity in forest soil reflects the changes in ecosystem properties between summer and winter. *Environ. Microbiol.* 18, 288–301. doi:10.1111/1462-2920.13026.
- Žifčáková, L., Větrovský, T., Lombard, V., Henrissat, B., Howe, A., and Baldrian, P. (2017). Feed in summer, rest in winter: microbial carbon utilization in forest topsoil. *Microbiome* 5, 122. doi:10.1186/s40168-017-0340-0.
- Zimmerman, A. E., Martiny, A. C., and Allison, S. D. (2013). Microdiversity of extracellular enzyme genes among sequenced prokaryotic genomes. *ISME J.* 7, 1187–1199. doi:10.1038/ismej.2012.176.

RESEARCH ARTICLE

Bacteria associated with decomposing dead wood in a natural temperate forest

Vojtěch Tláškal^{1,*}, Petra Zrůstová¹, Tomáš Vrška² and Petr Baldrian¹

¹Laboratory of Environmental Microbiology, Institute of Microbiology of the CAS, Vídeňská 1083, 14220 Praha 4, Czech Republic and ²Silva Tarouca Research Institute for Landscape and Ornamental Gardening, Lidická 25/27, Brno 60200, Czech Republic

*Corresponding author: Laboratory of Environmental Microbiology, Institute of Microbiology of the CAS, Vídeňská 1083, 14220 Praha 4, Czech Republic. Tel: +420 732466591; Fax: +420 241062384; E-mail: tlaskal@biomed.cas.cz

One sentence summary: Bacterial community composition is influenced by the chemistry of the dead wood, bacterial biomass is correlated with accumulated N and the occurrence of taxa with specific ecological traits can be detected as decomposition advances.

Editor: Max Haggblom

[†]Vojtěch Tláškal, <http://orcid.org/0000-0002-2924-9470>

ABSTRACT

Dead wood represents an important pool of organic matter in forests and is one of the sources of soil formation. It has been shown to harbour diverse communities of bacteria, but their roles in this habitat are still poorly understood. Here, we describe the bacterial communities in the dead wood of *Abies alba*, *Picea abies* and *Fagus sylvatica* in a temperate natural forest in Central Europe. An analysis of environmental factors showed that decomposing time along with pH and water content was the strongest drivers of community composition. Bacterial biomass positively correlated with N content and increased with decomposition along with the concurrent decrease in the fungal/bacterial biomass ratio. *Rhizobiales* and *Acidobacteriales* were abundant bacterial orders throughout the whole decay process, but many bacterial taxa were specific either for young (<15 years) or old dead wood. During early decomposition, bacterial genera able to fix N₂ and to use simple C1 compounds (e.g. *Yersinia* and *Methylomonas*) were frequent, while wood in advanced decay was rich in taxa typical of forest soils (e.g. *Bradyrhizobium* and *Rhodoplanes*). Although the bacterial contribution to dead wood turnover remains unclear, the community composition appears to reflect the changing conditions of the substrate and suggests broad metabolic capacities of its members.

Keywords: bacteria; dead wood; decomposition; cellulose; nitrogen; natural forest

INTRODUCTION

Temperate forests represent a globally important stock of carbon (C), and a significant portion of this pool is formed by recalcitrant plant polymers, mainly cellulose, hemicelluloses and lignin. Wood represents the largest pool of plant biopolymers: while the wood of living trees has important structural and functional roles and is largely protected against microbial breakdown, dead wood represents an important source of C, energy and other nutrients. Despite the high variation in stock across

forests (Baldrian 2017a), the global amount of coarse woody debris (CWD) is estimated at as much as 36–72 Pg of C (Magnússon et al. 2016), and its importance for global nutrient cycling is obvious. The dead wood stock within forests has its own temporal dynamics, including accumulation caused by windthrows, beetle outbreaks, fire or other processes followed by subsequent decay when the dead wood material is partly mineralised and partly transformed, contributing to the formation of soil organic matter (Přívětivý et al. 2016). Tree dieback allows for stand replacement, and dead wood supports the existence of complex

Received: 21 September 2017; Accepted: 7 November 2017

© FEMS 2017. All rights reserved. For permissions, please e-mail: journals.permissions@oup.com

saproxyllic food webs and soil formation. The stock of dead wood in temperate Europe is especially high in natural, unmanaged forests where it typically reaches several hundreds of $\text{m}^3 \text{ha}^{-1}$ (Hahn and Christensen 2004) and reaches up to $1200 \text{m}^3 \text{ha}^{-1}$, an amount comparable to the stock of living trees (Stokland, Siitonen and Jonsson 2012).

Due to the high amount of organic C, dead wood represents a potentially rich resource for microbial decomposers; however, it is also a highly specific habitat. Compared to litter or soil, dead wood is much more unevenly distributed and possesses specific characteristics, especially in the initial stages of decomposition, such as a low amount of N and being physically impermeable, which both negatively affect the decomposition rate (Baldrian 2017a). Due to the properties of dead wood, decomposition has always been assumed to be dominated by saprotrophic fungi that are favoured due to their filamentous growth, lower demand of N compared to bacteria and ability to translocate nutrients and produce multiple classes of enzymes that decompose wood biopolymers (van der Wal et al. 2007; Rajala et al. 2011; Kubartová et al. 2012; Eichlerová et al. 2015). This assumption is supported by the observed abundance of fungal biomass in decomposing wood (Baldrian et al. 2016; Rinta-Kanto et al. 2016). Although the presence of bacteria in dead wood was noticed relatively early (reviewed in Clausen 1996), it was only the arrival of the high throughput sequencing of nucleic acids that allowed surveys of bacterial communities in dead wood at an increased depth and with finer taxonomic resolution and provided the tools to analyse the genes and genomes of these bacteria (Johnston, Boddy and Weightman 2016).

The first few reports on bacteria associated with dead wood indicated some candidate drivers of their community composition including water and N content, pH and density (Lladó, López-Mondéjar and Baldrian 2017). Bacterial communities were reported to be influenced by the succession stage of the decaying wood, as well as by the relative moisture, pH and the C/N ratio. Furthermore, community composition and dynamics were reported to be tree species-specific; *Actinobacteria* and *Firmicutes* decreased with time in *Fagus sylvatica* and *Picea abies*, *Bacteroidetes* decreased only in *P. abies* and *Gamma*proteobacteria decreased in *F. sylvatica* (Hoppe et al. 2015). As decomposition proceeds, the dead wood density decreases, while the bacterial diversity and abundance in *Pinus sylvestris* and *P. abies* were reported to increase (Kielak et al. 2016; Rinta-Kanto et al. 2016). Similar successional patterns towards advanced decay of plant biomass with increasing bacterial dominance were also observed during leaf litter decomposition (Tláskal, Voříšková and Baldrian 2016). It should be noted that both in litter and dead wood, bacteria are under the influence of fungi whose community also undergoes profound changes in composition and abundance (Voříšková and Baldrian 2013; Baldrian et al. 2016).

Due to the direct contact of fallen dead wood and soil, these forest habitats influence each other, and this interaction affects the dead wood decomposition rates (Přívětivý et al. 2016) and the transfer of wood derivatives into the underlying forest floor (Stutz et al. 2017). The soil also represents a source of microbial inoculum for dead wood (van der Wal et al. 2007; Sun et al. 2014; Mäkipää et al. 2017). This is highly important if we consider the fact that the forest topsoil is rich in bacterial decomposers of plant biopolymers and fungal mycelia (Brabcová et al. 2016; López-Mondéjar et al. 2016; Lladó, López-Mondéjar and Baldrian 2017).

The initial C/N ratio in dead wood is high but decreases with time (Rajala et al. 2011; Hoppe et al. 2015; Baldrian et al. 2016). Recently, it was demonstrated that the increase of N (as either

relative or absolute content) is a result of multiple processes, including C mineralisation and loss, translocation of N from the soil by fungi and, importantly, the activity of bacteria that fix atmospheric N_2 (Rinne et al. 2017). Some of the N-fixing bacteria are also mycotrophs (Folman et al. 2008; Vorob'ev et al. 2009), and this combination of traits proves specifically useful in dead wood where methanol and methane occur as products of wood decomposition. The ability to use these C1 compounds, which are otherwise rare, represents a clear competitive advantage (Lenhart et al. 2012).

Due to their high abundance in dead wood, the mycelia of fungi represent an important nutrient pool that is attractive for bacteria because of its lower recalcitrance and higher N content compared to lignocellulose (Brabcová et al. 2016). The fact that one of the major components of the fungal cell wall, chitin, contains both C and N in a stoichiometric ratio close to that of the bacterial biomass makes it a convenient resource (de Boer et al. 2004; Rudnick, van Veen and de Boer 2015). Soil bacteria from a wide range of phylogenetic groups are able to utilise the fungal biomass in forest topsoil (Brabcová et al. 2016), and they would be expected to find suitable conditions in dead wood as well. Close coexistence of certain bacteria with living fungi in dead wood may also be expected. For example, the bacterial family *Burkholderiaceae* was repeatedly described in association with wood-decay fungi (Folman et al. 2008; Valášková et al. 2009; Hervé et al. 2013; Prewitt et al. 2014; Sun et al. 2014). Bacteria can thrive as commensals by using hyphal exudates or products of wood decomposition performed by fungi (Hervé et al. 2016b), by utilizing organic acids produced by fungi (Daniel, Pilsel and Drake 2007; Hervé et al. 2016a), or simply by benefiting from the competitive advantage given to them by wood acidification, as is the case for the *Acidobacteria* recorded in acidic dead wood colonised by fungi (Valášková et al. 2009).

The aim of this study was to describe the bacterial community in dead wood in a natural temperate forest, identify its drivers and follow its development during dead wood decomposition. The study was aided by the fact that historical surveys of the study site allowed the dating of individual CWDs. Within the decomposing dead wood, the presence of bacterial taxa with traits relevant to the utilisation of certain classes of resources may indicate their potential ecological or nutritional strategies, such as the ability to utilise cellulose or the fungal biomass or to fix N_2 .

MATERIALS AND METHODS

Study area and dead wood data collection

The study area was located in the Novohradské Hory mountains, specifically in the 25-ha Zofin ForestGEO[®] Dynamics Plot (www.forestgeo.si.edu), which is part of the 42-ha core zone of the Žofínský prales National Nature Reserve in the Czech Republic (48°39'57"N, 14°42'24"E). This core zone of the forest reserve was never managed and has stood under protection since 1838. It thus represents a rare fragment of virgin forest. The reserve is situated along an altitudinal gradient of 735–830 m a.s.l.; gentle NW slopes predominate. The bedrock is almost homogeneous and consists of fine to medium-grained porphyritic and biotite granite. Annual average rainfall is 866 mm, and annual average temperature is 6.2°C (Anderson-Teixeira et al. 2015). At present, the reserve is covered by a mixed forest. *Fagus sylvatica* predominates in all diameter classes (51.5% of the total living wood volume), followed by *P. abies* (42.8%). *Abies alba* represents 4.8% of the standing volume, and the remaining tree species

(*Ulmus glabra*, *Acer pseudoplatanus*, *Acer platanoides*, *Sorbus aucuparia*) together represent 1% of the standing volume. The living tree volume is calculated at 690 m³ ha⁻¹ (Král et al. 2014). Dead wood CWD represents 6–41% of total wood volume, ranging from 102 to 310 m³ ha⁻¹ in volume with an average volume of 208 m³ ha⁻¹ (Král et al. 2010; Šamonil et al. 2013). The representation of *F. sylvatica*, *P. abies* and *A. alba* is much more even in the dead wood population, in which they represent 23.6%, 43.7% and 31.4% of the total volume, respectively (Král et al. 2014).

The positions of all trees with diameter at breast height (DBH) values ≥10 cm and selected tree parameters (tree species, DBH, tree status—live/dead, standing/lying, snag, breakage, windthrow, stump, etc.) were recorded repeatedly in 1975, 1997, 2008 and 2013, and a stem-position (including lying dead wood) map resulted from each census (Král et al. 2010). The information on dead wood and the records about the corresponding trees when alive allowed us to track the fate of individual CWD and to randomly select debris with appropriate properties.

Tree selection and sampling of dead wood

Preselection of trees and sampling was done in the context of a previous study that focused on fungal communities in the same CWD (Baldrian et al. 2016). Briefly, CWD of three species (*F. sylvatica*, *P. abies* and *A. alba*) with DBH values between 30 and 100 cm in the year when the tree was first recorded as dead and lying (1975, 1997, 2008 or 2013) were evenly chosen to cover all diameter classes and all decay lengths (also referred to as age classes). Trees decomposing as standing snags were omitted to exclude CWD with unclear decay lengths. The CWD types were designated beech, fir or spruce, indicating the CWD tree species (CWD species) and as having a decay length of <5, 5–15, 16–38 or >38 years. The distance between the closest sampled logs typically ranged in the tens of metres.

Four CWD samples were obtained from each selected log in October 2013 using an electric drill with a bit diameter of 8 mm. The length of each CWD (or the sum of the lengths of its fragments) was measured, and samples were collected at 1/5, 2/5, 3/5 and 4/5 of the CWD length. Drilling was performed vertically from the middle of the upper surface to a depth of 40 cm. The drill bit was sterilised between drillings, and sawdust was collected in batches from two adjacent drill holes in sterile plastic bags and frozen within a few hours after drilling.

Sample processing, chemical and enzyme analyses

Dead wood samples were processed as described previously (Baldrian et al. 2016). Briefly, the sawdust material was weighed, freeze-dried and milled using an Ultra Centrifugal Mill ZM 200 (Retsch, Germany). The resulting fine sawdust was used for subsequent analyses. The dry mass content was measured as a loss of mass during freeze drying, and the pH was measured in distilled water (1:10). The wood C and N contents were measured in an external laboratory. Total ergosterol was extracted using 10% KOH in methanol and was analysed by HPLC (Šnajdr et al. 2008). Klason lignin content was measured as dry weight of solids after hydrolysis with 72% (w/w) H₂SO₄ (Kirk and Obst 1988). Enzyme activities of endocellulase, cellobiohydrolase (exocellulase), β-glucosidase, endoxylanase, β-xylosidase, β-galactosidase, α-glucosidase, N-acetylglucosaminidase, phosphomonoesterase (phosphatase), esterase (lipase), laccase and Mn-peroxidase were measured in a previously published study (Baldrian et al. 2016).

DNA extraction and amplification

Total genomic DNA was extracted from 200 mg of pooled material from two adjacent drill holes using the NucleoSpin Soil Kit (Macherey-Nagel, Düren, Germany) in the procedure of the previous study (Baldrian et al. 2016). This extracted DNA was then used as a template for the amplification of the hypervariable region V4 of the 16S rRNA gene using the bar-coded primers 515F (5'-GTGCCAGCMGCCGCGGTAA) and 806R (5'-GGACTACHVGGGTWTCTAAT) (Caporaso et al. 2011). PCR amplification was performed as described previously (Žižňáková et al. 2016). Triplicate PCR reactions contained 2.5 μL of 10×buffer for DyNAzyme DNA Polymerase; 0.75 μL DyNAzyme II DNA polymerase (2 u μL⁻¹); 1.5 μL of BSA (10 mg mL⁻¹); 0.5 μL of PCR Nucleotide Mix (10 mM); 0.5 μL of primer 515F (10 μM); 0.5 μL of primer 806R (10 μM); 1.0 μL of template DNA (concentration approximately 5–50 ng μL⁻¹) and sterile ddH₂O up to 25 μL. Conditions for amplification started at 94°C for 4 min followed by 35 cycles of 94°C for 45 s, 50°C for 60 s, 72°C for 75 s and finished with a final setting of 72°C for 10 min. Amplicons were purified, pooled and sequenced on the Illumina MiSeq to obtain pair-end sequences of 2 × 250 bp.

Bacterial and fungal rRNA gene copies were quantified by qPCR using the 1108f and 1132r primers for bacteria (Wilmotte, Van der Auwera and De Wachter 1993; Amann, Ludwig and Schleifer 1995) and FR1 and FF390 primers for fungi (Prévost-Bouré et al. 2011). The fungal/bacterial rRNA gene ratio (F/B) was calculated by dividing rRNA gene copy numbers.

Bioinformatic workflow and statistical analyses

The sequencing data were processed using SEED v 2.0.3 (Větrovský and Baldrian 2013a). Briefly, pair-end reads were merged using fastq-join (Aronesty 2013). Sequences with ambiguous bases were omitted, as well as sequences with a mean quality score below 30. Chimeric sequences were detected using UCHIME implementation in USEARCH 7.0.1090 (Edgar et al. 2011) and were deleted, and sequences shorter than 200 bp were removed. Filtered sequences were clustered using the UPARSE algorithm implemented in USEARCH 7.0.1090 (Edgar 2013) at a 97% similarity level. Consensus sequences were constructed for each cluster using MAFFT 7.130 (Katoh et al. 2005), and the closest hits at a genus or species level were identified using BLASTn 2.5.0 against the Ribosomal Database Project (Cole et al. 2014) and GenBank databases (database versions from January 2016). Sequences identified either as no hits or as nonbacterial were discarded. From the 16S rRNA in the DNA, bacterial genome count estimates were calculated based on the 16S rRNA gene copy numbers in the closest available sequenced genome as described previously (Větrovský and Baldrian 2013b). Adjustment was based on RDP 16S rRNA database training set 16 (Cole et al. 2014). Sequence data have been deposited into the MG-RAST public database (Meyer et al. 2008; dataset number mgp82275).

Diversity estimates, such as the Shannon–Wiener index, the Chao-1 and the Evenness index were calculated for a data set containing 3000 randomly chosen sequences per sample to eliminate the effect of sampling effort. Ordination of bacterial taxa in the context of time and environmental factors were visualised using nonmetric multidimensional scaling (NMDS) using *vegan* package 2.4–3 (Oksanen et al. 2017) in R 3.4.0 (R Core Team 2017). Ordination was based on the Bray–Curtis dissimilarity of the relative abundances of the 145 most abundant bacterial OTUs with abundances >0.5% in more than five samples. Correlations between community composition and enzyme

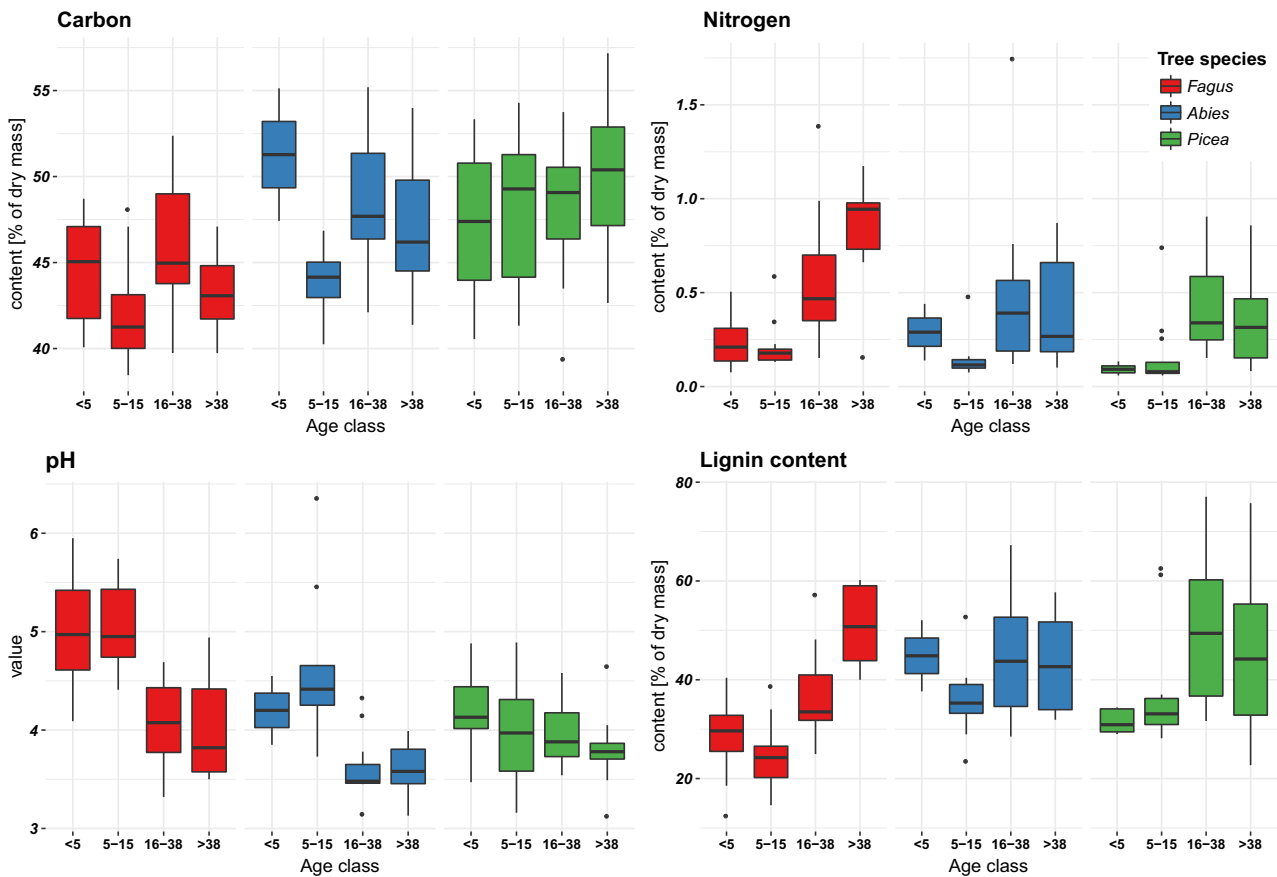


Figure 1. Chemistry of the CWD of *Fagus sylvatica*, *Abies alba* and *Picea abies* in the Žofin natural forest. Data on C and N content and pH are from (Baldrian et al. 2016).

activities were analysed using the Mantel test (*vegan* package) using the Bray–Curtis dissimilarity for Hellinger-transformed OTU abundances and Euclidean distances for enzyme activities. Variation partitioning (*vegan* package) was used to infer the influence of environmental factors on Hellinger-transformed dominant OTU abundances. PERMANOVA with 9999 permutations (*vegan* package) was used to infer significant influences of environmental factors on Hellinger-transformed OTU abundances. Transformation was done in order to lower the influence of extreme values. Indicator species analysis was performed using the *indicspecies* package 1.7.6 (De Cáceres and Legendre 2009). The Kruskal–Wallis rank sum test with Bonferroni corrected *P*-values from the *agricolae* package 1.2–4 (de Mendiburu 2016) was used to test for significant differences among observed abundances. Pearson correlation coefficients from the same package were used to test for correlations between environmental factors. Differences at $P < 0.05$ were regarded as statistically significant.

RESULTS

The content of N ($P < 0.0001$) and the content of fungal biomass (i.e. ergosterol content, $P < 0.005$) increased with CWD age, while the pH decreased ($P < 0.0001$); in addition, the dead wood of coniferous trees exhibited significantly lower pH values than that of beech CWD ($P < 0.0001$) (Baldrian et al. 2016). The content of Klason lignin increased significantly with CWD age ($P < 0.0001$) from 31% to 33% in the <5 and 5–15 age classes to 44–46% in the 16–38 and >38 classes. Beech CWD showed

consistently lower lignin contents (mean of 33.0%) than fir and spruce CWD (means of 40.9% and 41.4%, respectively, $P < 0.005$, Fig. 1). The water content was significantly higher in CWD from the two older age classes ($P < 0.0001$).

The median F/B ratio was approximately 1 in the two younger classes but dropped in the two older classes to 0.5–0.6. When comparing tree species, the highest F/B ratio of 1.2 was recorded in fir CWD, compared to 0.7 and 0.6 in spruce and beech CWD, respectively. Occasionally, very high F/B ratios were recorded in certain samples: in seven CWD samples this ratio was even higher than 10, showing high variability in the composition of the microbial biomass in dead wood. Importantly, the copy numbers of bacterial gene for 16S rRNA showed a highly significant positive correlation with N content ($R = 0.246$, $P < 0.01$).

In total, 669,260 bacterial sequences were obtained and clustered into 21,260 OTUs. The most abundant bacterial taxa, irrespective of tree species and age class, were *Acidobacteria*, *Alphaproteobacteria*, *Actinobacteria* and *Gammaproteobacteria*, followed by *Verrucomicrobia*, *Bacteroidetes*, *Betaproteobacteria* and *Firmicutes* (Fig. 2A). The distribution of dominant bacteria among trees and age classes was fairly even: at least 25% of the total bacterial communities across tree species and age classes were composed of genera that exhibited a high abundance of >3% in >15 samples (except for the age class 5–15 from beech CWD, in which the abundance of dominant genera was 20.7%). Relative abundances of several dominant genera showed significant associations with certain sample classes; *Cellulomonas* (*Actinobacteria*) exhibited higher abundances in the two younger age classes ($P < 0.0001$). *Rhodococcus* (*Actinobacteria*), *Sphingomonas* (*Alphaproteobacteria*), *Terriglobus* (*Acidobacteria*) and

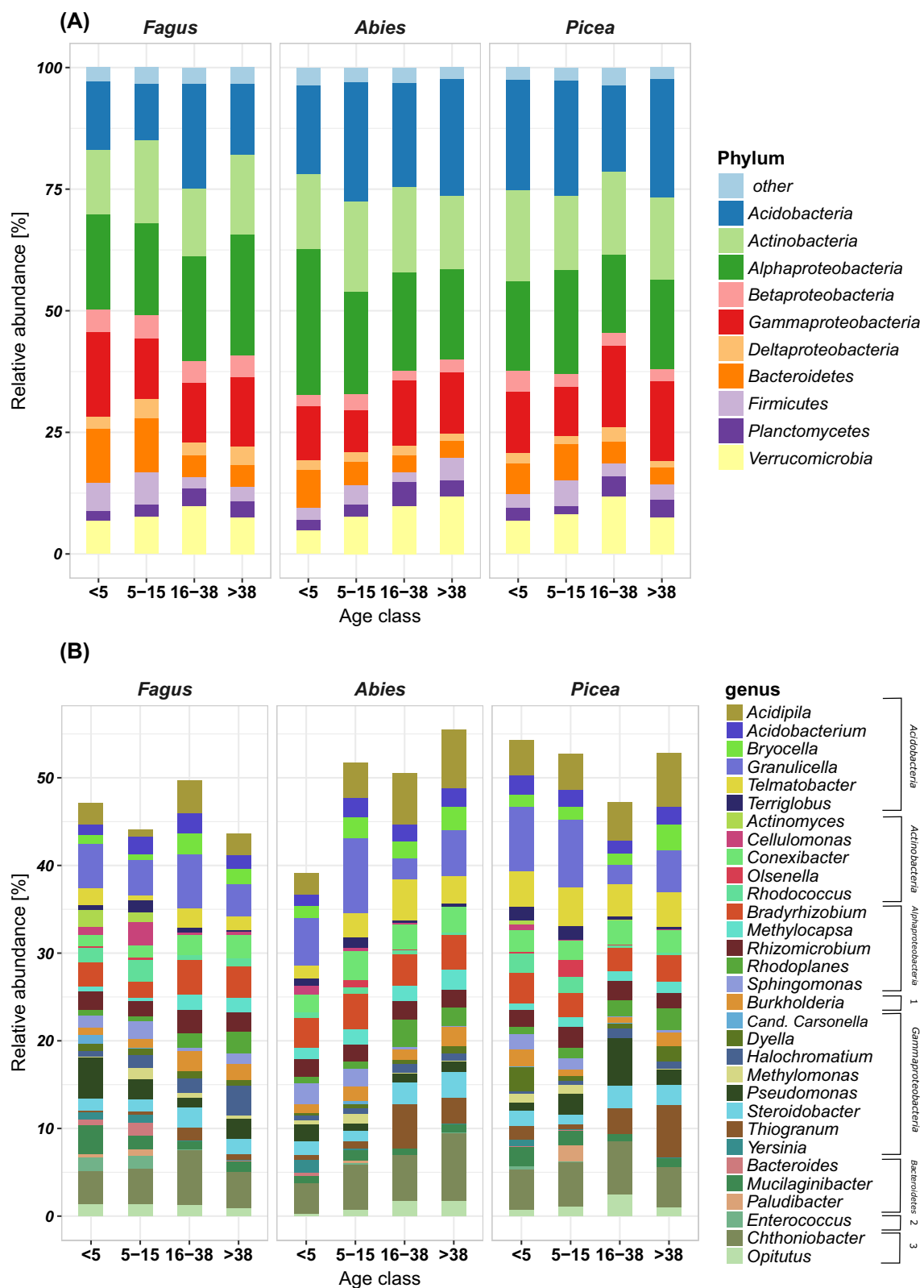


Figure 2. Relative abundances of (A) major bacterial phyla (classes of Proteobacteria) and (B) genera in the CWD of *Fagus sylvatica*, *Abies alba* and *Picea abies* in the Žofín natural forest. Only genera with abundances of >5% in more than 1 sample are displayed. (Phylum assignment of the genera: 1—Betaproteobacteria, 2—Firmicutes and 3—Verrucomicrobia)

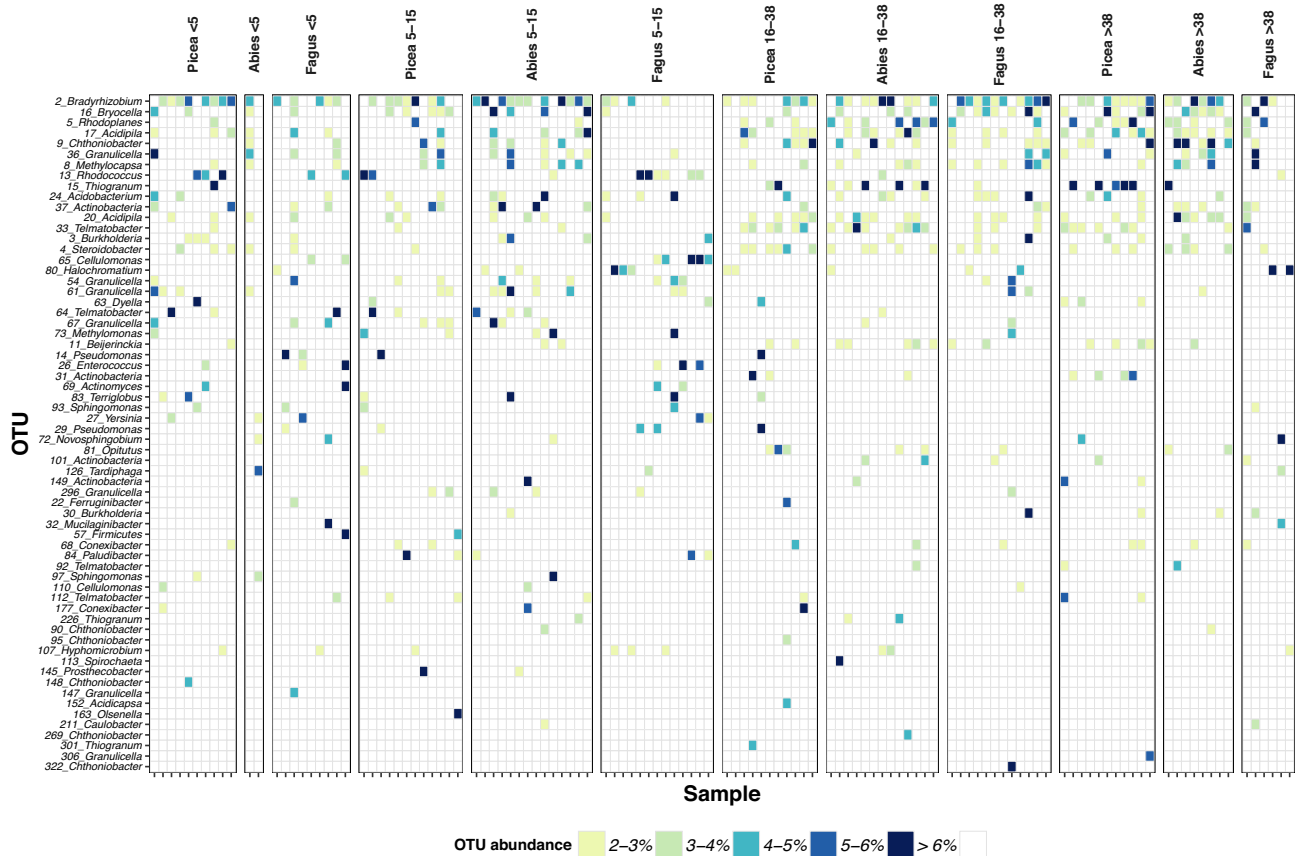


Figure 3. Distribution of abundant OTUs in individual CWD of *Fagus sylvatica*, *Abies alba* and *Picea abies* in the Žofin natural forest. Colours of points indicate the relative abundances of each OTU in each CWD sample (x axis). OTUs are specified by their number and the genus of the best hit on the y axis.

Yersinia (Gammaproteobacteria) were also more abundant in younger dead wood ($P < 0.001$ in all cases). On the other hand, *Rhodoplanes* (Alphaproteobacteria) and *Thiogranum* (Gammaproteobacteria) were more abundant in the two older age classes ($P < 0.0001$ in both cases). *Thiogranum* further prevailed in conifers over beech CWD ($P < 0.01$) as did the two acidobacterial genera *Acidipila* and *Telmatobacter* ($P < 0.0001$ in both cases), while the opposite was true for *Cellulomonas* ($P < 0.01$; Fig. 2B).

No significant differences in diversity or community evenness were observed among trees and dead wood age classes. The average number of those OTUs with relative abundances $\geq 3\%$ of the detected sequences per sample was 3.6 (Fig. 3). The core OTUs that were present at a basal threshold in the majority of the samples throughout all age classes belonged to the orders Rhizobiales (*Bradyrhizobium*, *Beijerinckia*, *Methylocapsa*) and Acidobacteriales (*Acidipila*, *Bryocella*, *Acidobacterium*). Several OTUs were significantly associated with distinct age classes of CWD as indicated by their presence as a high proportion of findings for such CWD (fidelity, according to indicator species analysis) and simultaneous absence in CWD of other age classes (specificity; Table 1). OTUs with the closest association with the age class <5 were assigned to *Yersinia* (Gammaproteobacteria) and *Variovorax* (Betaproteobacteria). *Methylomonas* (Gammaproteobacteria) and *Prosthecoibacter* (Verrucomicrobia) were the best indicators of the 5–15 years age class, while *Opitutus* (Verrucomicrobia), *Telmatobacter* (Acidobacteria) and other genera of Acidobacteria were the best indicators of the 16–38 years age class. The oldest logs were characterised by the presence of *Aquisphaera* (Planctomycetes), *Steroidobacter* (Gammaproteobacteria) and *Rhodoplanes* (Alphaproteobacteria). The quantitatively dominant

OTUs in individual logs were often among the indicators for a particular age class and often reached high levels of dominance in particular CWD (Fig. 3; Fig. S1, Supporting Information). For example, this was the case for OTUs from the genera *Telmatobacter* (up to 26.9% in single <5 CWD), *Dyella* (up to 19.9% in <5 CWD), *Sphingomonas* (up to 16.7% in 5–15 CWD), *Cellulomonas* (10.4% and 8.9% in two 5–15 CWD), *Opitutus* (up to 5.4% in 16–38 CWD), and *Thiogranum* and *Rhodoplanes* (up to 22.5% and 8.2% in >38 CWD, respectively).

Visualisation of samples in the ordination space according to NMDS reflected the successional development of bacterial communities in CWD (Fig. 4A). While bacterial communities in CWD younger and older than 15 years were separated, the younger two and older two age classes of CWD showed high levels of overlap. While the CWD age and pH separated the samples along the first axis, the N content, ergosterol content and F/B ratio correlated significantly with the second axis. NMDS ordination of abundant OTUs confirmed the differences in the composition of bacterial communities among age classes younger and older than 15 years (Fig. 4B). According to PERMANOVA, age class was the strongest recorded driver of bacterial community composition (adjusted $R^2 = 0.060$, $P < 0.0001$) followed by pH (adjusted $R^2 = 0.028$, $P < 0.0001$) and water content ($P = 0.0007$). Significant effects were also found for the F/B ratio ($P = 0.0165$) and the lignin content ($P = 0.0319$), while the effects of tree species and N were not significant. Variation partitioning showed that wood chemistry (pH, water content, carbon, nitrogen and lignin content) is a significant driver of community composition, and explains 5.1% of total variation. Additional variation was explained the most by wood chemistry combined with age class

Table 1. Bacterial indicator OTUs associated with CWD age classes in a natural beech-dominated forest. Abundance values are means for particular age class.

Age class	OTU	Best hit	Specificity	Fidelity	P value	Abundance (%)			
						<5	5–15	16–38	>38
<5	27	<i>Yersinia</i> (Gammaproteobacteria)	0.62	0.86	0.0013**	0.79	0.43	0.01	0.05
	63	<i>Dyella</i> (Gammaproteobacteria)	0.54	0.90	0.0155*	1.21	0.35	0.17	0.47
	64	<i>Telmatobacter</i> (Acidobacteria)	0.64	0.76	0.0108*	1.98	0.86	0.20	0.06
	52	<i>Variovorax</i> (Betaproteobacteria)	0.46	1.00	0.0006***	0.67	0.48	0.14	0.17
	13	<i>Rhodococcus</i> (Actinobacteria)	0.42	1.00	0.0306*	1.84	1.67	0.46	0.42
	333	<i>Beijerinckia</i> (Alphaproteobacteria)	0.50	0.81	0.0022**	0.18	0.16	0.01	0.01
	93	<i>Sphingomonas</i> (Alphaproteobacteria)	0.45	0.90	0.0416*	0.48	0.39	0.02	0.17
	167	<i>Mycobacterium</i> (Actinobacteria)	0.45	0.90	0.0203*	0.53	0.39	0.09	0.17
	126	<i>Tardiphaga</i> (Alphaproteobacteria)	0.44	0.90	0.0371*	0.49	0.38	0.05	0.19
	205	<i>Sphingomonas</i> (Alphaproteobacteria)	0.46	0.81	0.0171*	0.27	0.23	0.02	0.05
	419	<i>Candidatus Xiphinematobacter</i> (Verrucomicrobia)	0.60	0.57	0.0043**	0.29	0.15	0.03	0.01
	188	<i>Opitutus</i> (Verrucomicrobia)	0.45	0.62	0.0456*	0.44	0.26	0.13	0.13
	57	unclassified (Firmicutes)	0.68	0.38	0.0213*	0.53	0.25	0.00	0.00
	5–15	97	<i>Sphingomonas</i> (Alphaproteobacteria)	0.57	0.87	0.0312*	0.43	0.73	0.02
73		<i>Methylomonas</i> (Gammaproteobacteria)	0.58	0.77	0.0025**	0.42	0.85	0.13	0.06
326		<i>Prostheco bacter</i> (Verrucomicrobia)	0.69	0.64	0.0004***	0.08	0.26	0.02	0.02
251		<i>Methylomonas</i> (Gammaproteobacteria)	0.63	0.69	0.0032**	0.09	0.24	0.04	0.02
162		<i>Methylorosula</i> (Alphaproteobacteria)	0.47	0.87	0.0249*	0.13	0.26	0.07	0.10
296		<i>Granulicella</i> (Acidobacteria)	0.61	0.67	0.0033**	0.17	0.47	0.11	0.03
83		<i>Terriglobus</i> (Acidobacteria)	0.45	0.90	0.0454*	0.78	0.89	0.19	0.11
179		<i>Rhodospirillum</i> (Alphaproteobacteria)	0.47	0.85	0.0314*	0.18	0.21	0.03	0.04
71		<i>Jatrophihabitans</i> (Actinobacteria)	0.38	0.97	0.0421*	0.52	0.54	0.16	0.17
65		<i>Cellulomonas</i> (Actinobacteria)	0.56	0.67	0.0401*	0.58	0.89	0.02	0.10
84		<i>Paludibacter</i> (Bacteroidetes)	0.96	0.38	0.0023**	0.03	0.81	0.00	0.00
399		<i>Edaphobacter</i> (Acidobacteria)	0.49	0.72	0.0165*	0.18	0.22	0.03	0.03
450		<i>Conexibacter</i> (Actinobacteria)	0.46	0.56	0.0324*	0.06	0.15	0.04	0.07
163		<i>Olsenella</i> (Actinobacteria)	0.79	0.31	0.0096**	0.15	0.56	0.00	0.00
16–38	81	<i>Opitutus</i> (Verrucomicrobia)	0.53	0.92	0.0007***	0.13	0.21	0.95	0.50
	102	<i>Phycisphaera</i> (Planctomycetes)	0.54	0.86	0.0004***	0.09	0.05	0.53	0.30
	166	<i>Thiogramnum</i> (Gammaproteobacteria)	0.56	0.83	0.0001***	0.08	0.05	0.33	0.13
	92	<i>Telmatobacter</i> (Acidobacteria)	0.51	0.92	0.0002***	0.10	0.12	0.77	0.69
	269	<i>Chthoniobacter</i> (Verrucomicrobia)	0.59	0.78	0.0027**	0.06	0.07	0.35	0.12
	119	unclass. genus (Actinobacteria)	0.52	0.86	0.0003***	0.05	0.05	0.41	0.26
	113	<i>Spirochaeta</i> (Spirochaetes)	0.50	0.89	0.0129*	0.22	0.09	0.54	0.23
	115	unclassified (Actinobacteria)	0.46	0.94	0.0002***	0.07	0.11	0.35	0.24
	266	<i>Luteolibacter</i> (Verrucomicrobia)	0.55	0.78	0.0002***	0.04	0.02	0.24	0.14
	33	<i>Telmatobacter</i> (Acidobacteria)	0.45	0.94	0.0006***	0.38	0.55	1.84	1.35
	31	unclassified (Actinobacteria)	0.45	0.92	0.0401*	0.12	0.17	1.04	0.94
	259	<i>Ruminococcus</i> (Firmicutes)	0.51	0.81	0.0008***	0.07	0.06	0.24	0.11
	142	<i>Iamia</i> (Actinobacteria)	0.49	0.83	0.0019**	0.07	0.06	0.34	0.22
	301	<i>Thiogramnum</i> (Gammaproteobacteria)	0.64	0.61	0.0144*	0.01	0.02	0.26	0.11
	151	unclassified (Actinobacteria)	0.42	0.92	0.0072**	0.15	0.09	0.46	0.39
	183	<i>Rhizomicrobium</i> (Alphaproteobacteria)	0.48	0.81	0.0058**	0.05	0.04	0.25	0.18
	172	<i>Prostheco bacter</i> (Verrucomicrobia)	0.41	0.94	0.0013**	0.09	0.11	0.27	0.19
	40	<i>Candidatus Solibacter</i> (Acidobacteria)	0.44	0.89	0.0063**	0.15	0.17	0.82	0.74
	94	unclass. genus (Actinobacteria)	0.45	0.86	0.0012**	0.11	0.19	0.71	0.57
	139	<i>Luteolibacter</i> (Verrucomicrobia)	0.45	0.83	0.006**	0.07	0.09	0.40	0.33
	216	<i>Prostheco bacter</i> (Verrucomicrobia)	0.47	0.78	0.0209*	0.05	0.04	0.26	0.20
	182	<i>Acidicapsa</i> (Acidobacteria)	0.40	0.92	0.0103*	0.13	0.18	0.36	0.25
	210	<i>Thiogramnum</i> (Gammaproteobacteria)	0.43	0.81	0.0057**	0.05	0.07	0.27	0.25
	4	<i>Steroidobacter</i> (Gammaproteobacteria)	0.34	1.00	0.009**	1.02	0.74	1.78	1.63
	231	unclass. genus (Actinobacteria)	0.40	0.86	0.0068**	0.11	0.09	0.27	0.21
	11	<i>Beijerinckia</i> (Alphaproteobacteria)	0.35	0.97	0.0136*	0.68	0.59	1.45	1.38
	249	<i>Candidatus Koribacter</i> (Acidobacteria)	0.37	0.89	0.014*	0.07	0.09	0.22	0.21
	277	<i>Pseudolabrys</i> (Alphaproteobacteria)	0.41	0.81	0.0089**	0.05	0.06	0.21	0.19
77	<i>Thiohalophilus</i> (Gammaproteobacteria)	0.32	1.00	0.0408*	0.25	0.21	0.38	0.35	
20	<i>Acidipila</i> (Acidobacteria)	0.33	0.97	0.0318*	0.90	0.83	1.71	2.01	
305	<i>Holophaga</i> (Acidobacteria)	0.48	0.67	0.0367*	0.04	0.13	0.21	0.06	
>38	15	<i>Thiogramnum</i> (Gammaproteobacteria)	0.53	0.83	0.0236*	0.57	0.23	1.80	2.85
	46	<i>Aquisphaera</i> (Planctomycetes)	0.42	1.00	0.0029**	0.11	0.13	0.50	0.53
	86	<i>Steroidobacter</i> (Gammaproteobacteria)	0.44	0.92	0.0035**	0.11	0.08	0.28	0.37

Table 1 – continued

Age class	OTU	Best hit	Specificity	Fidelity	P value	Abundance (%)			
						<5	5–15	16–38	>38
	5	<i>Rhodoplanes</i> (Alphaproteobacteria)	0.40	1.00	0.0098**	0.52	0.57	1.92	2.08
	111	<i>Halochromatium</i> (Gammaproteobacteria)	0.40	0.92	0.0116*	0.16	0.15	0.49	0.52
	116	<i>Dyella</i> (Gammaproteobacteria)	0.42	0.88	0.0275*	0.16	0.11	0.22	0.34
	196	<i>Bradyrhizobium</i> (Alphaproteobacteria)	0.37	0.96	0.0063**	0.07	0.09	0.24	0.26
	101	unclassified (Actinobacteria)	0.44	0.79	0.0264*	0.20	0.07	0.61	0.69
	23	<i>Pseudomonas</i> (Gammaproteobacteria)	0.37	0.96	0.0451*	0.31	0.29	0.74	0.80
	138	<i>Chitinophaga</i> (Bacteroidetes)	0.42	0.83	0.0334*	0.05	0.06	0.15	0.18
	95	<i>Chthoniobacter</i> (Verrucomicrobia)	0.36	0.96	0.0288*	0.27	0.35	0.68	0.72
	286	<i>Conexibacter</i> (Actinobacteria)	0.40	0.83	0.025*	0.06	0.09	0.22	0.26
	359	<i>Pseudolabrys</i> (Alphaproteobacteria)	0.43	0.63	0.0434*	0.05	0.02	0.15	0.16

Signif. codes: 0 '***' 0.001 '**' 0.01 '*'.

and tree species, which altogether accounted for an additional 13.3% of the explained variation. According to the Mantel test, there were no correlations between the activities of individual enzymes and the composition of the bacterial community, except for β -glucosidase activity ($R = 0.1$, $P < 0.05$).

DISCUSSION

Bacterial diversity did not change among CWD age classes, which was consistent with the results of a fungal community analysis (Baldrian et al. 2016) but different from the reports on bacterial community development in pine wood (Kielak et al. 2016; Rinta-Kanto et al. 2016). Even CWD from <5 years age class already hosted a heterogeneous and diverse bacterial community, and it is apparent that despite the physical impermeability of fresh dead wood, both fungi and bacteria are able to colonise dead wood rapidly. In comparing the composition of bacterial communities in the decomposing CWD of this study with the fungal composition (Baldrian et al. 2016), multiple substantial differences are observed. First, fungal communities are often highly specific for each individual log: as many as 57 different fungal species were found to be quantitatively the most dominant in at least one log, and in many cases, the sequences of the dominant fungus represented >40% of all sequences. In addition, many of these locally abundant species occurred on only a few CWDs (Baldrian et al. 2016). Bacterial communities did not show such a high dominance by individual OTUs, but in certain CWDs, the abundance of dominant bacterial OTUs was still high, often >10%, and dominant taxa encompassed members of the groups *Acidobacteria*, *Alphaproteobacteria*, *Gammaproteobacteria*, *Bacteroidetes* and *Verrucomicrobia* (Fig. S1, Supporting Information). This makes the dead wood habitat different from that of the soil or litter of temperate forests, in which the dominant bacterial OTUs typically represent <4% of the total community, and the community composition does not show high spatial variation (Baldrian et al. 2012; López-Mondéjar et al. 2015).

Unlike in fungal community, the most abundant bacterial OTUs were present in most CWDs. Of 30 dominant fungal and bacterial OTUs, each CWD contained on average 26 bacterial and 8 fungal OTUs (Fig. S2, Supporting Information). This result indicates a lower level of stochasticity in the bacterial community assembly compared to the fungal community assembly, which is in line with observations in forest litter and soil (Štursová et al. 2016).

The age of the CWD and pH was shown to affect the bacterial community most significantly. However, the factors of age and chemistry are not independent, and variation partitioning indicated that the direct effect on bacterial community composition was only significant for chemistry (modelled as the combined effect of pH, water content, carbon, nitrogen and lignin content). Neither the effect of N content alone nor that of CWD tree species that significantly shaped the composition of fungal communities (Baldrian et al. 2016), affected bacterial community composition. The stronger association of fungi with wood of different tree species in dead wood may indicate their higher nutritional dependence on substrates of a certain quality and thus their important role in decomposition (Baldrian 2017a).

Among the drivers of bacterial community composition, pH was the most important. This finding is not surprising since the same driver is also important for soil bacterial communities (Rousk et al. 2010). In dead wood, acidification is the result of fungal activity, especially that of white rot fungi, which were highly abundant in the CWDs of the study (Baldrian et al. 2016). Fungi need acidic conditions for optimal functioning of the lignocellulose degrading enzymes (Baldrian 2008) and acidify dead wood through the secretion of organic acids such as oxalate (Jarosz-Wilkolazka and Graz 2006). However, the bacterial relationship with fungi goes beyond modulation of pH. Several bacterial taxa are able to degrade either live or dead fungal mycelia as previously demonstrated in forest litter (Brabcová et al. 2016; Tláškal, Voříšková and Baldrian 2016). Here, the F/B ratio was a significant factor that affected the bacterial community composition in a different way than pH did (Fig. 4A), suggesting that there are multiple mechanisms by which fungi affect wood-associated bacteria. Some manipulative studies indicate that bacterial communities may be specific to certain fungal taxa (Folman et al. 2008; Hervé et al. 2016b). However, the co-occurrence patterns of fungi and bacteria in dead wood are still unexplored. While a specific bacterial community was reported in natural wood colonised by *Hypholoma fasciculare* (Valášková et al. 2009), our results indicate little difference in bacterial communities in CWD dominated by different fungi (Fig. S2, Supporting Information); thus, the specificity of associations between fungal and bacterial taxa appears limited.

Although N content was not significantly associated with the composition of the bacterial community, it was positively correlated with bacterial 16S rRNA gene copy numbers. This result supports the view that bacteria face N limitation, especially in fresh wood with a high C/N ratio (Hoppe et al. 2015). Together with N, the bacterial biomass increased and the F/B ratio

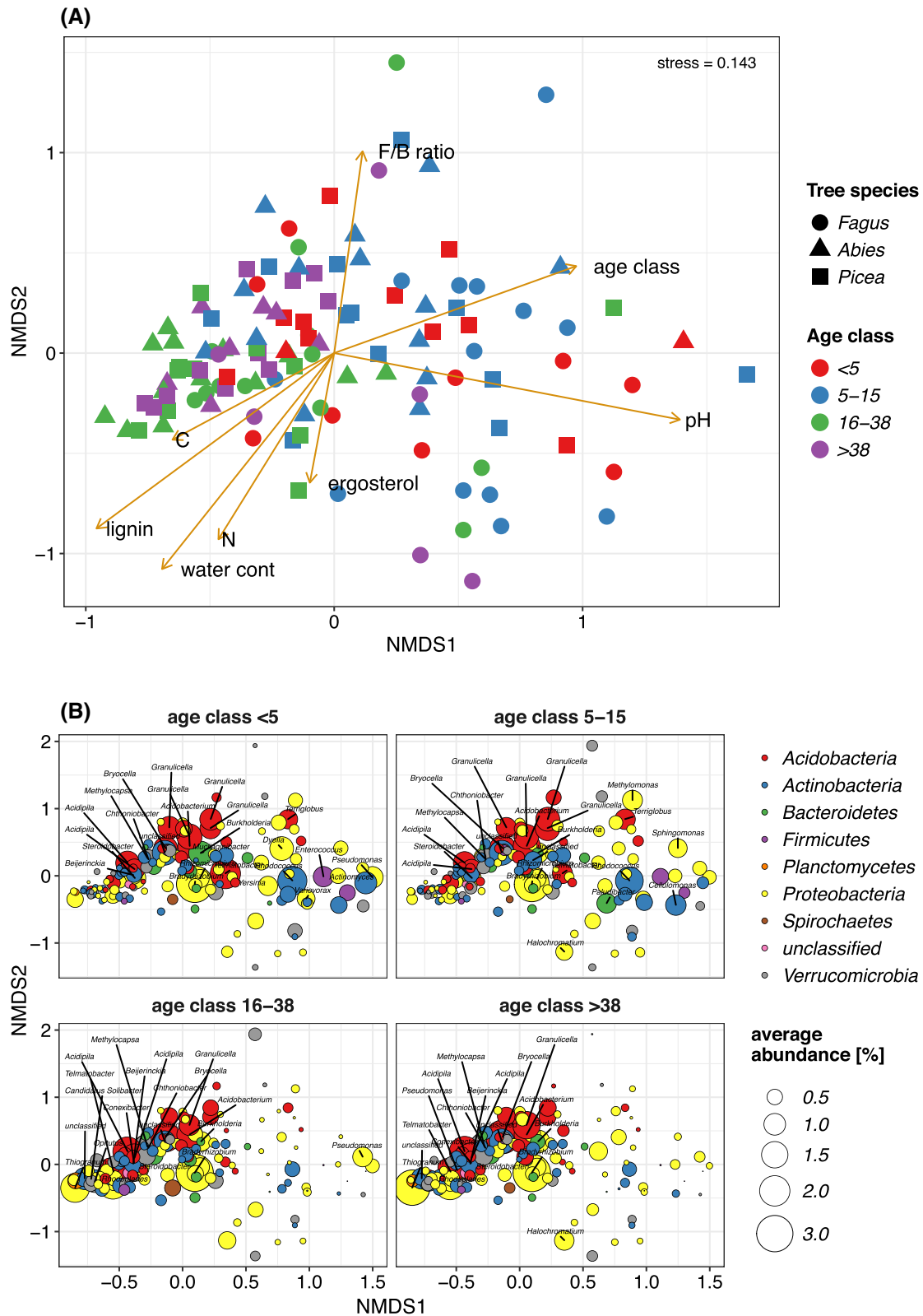


Figure 4. Non-metric multidimensional scaling of bacterial communities in the CWD of *Fagus sylvatica*, *Abies alba* and *Picea abies* in the Žofín natural forest. (A) Plot of individual CWD samples. Vectors of environmental variables are included. (B) Plot of dominant bacterial taxa and their average abundances (circle size) across CWD of various age classes.

decreased during CWD decomposition in a similar way as observed during litter decomposition, yet on a very different timescale (Šnajdr et al. 2011; Baldrian 2017b). Despite decreasing F/B ratio, increase in ergosterol content with decomposing time was recorded (Baldrian et al. 2016). The fact that the effects of ergosterol and F/B were divergent in multidimensional ordination may indicate that bacterial biomass increases more rapidly with time than fungal biomass and F/B thus decreases.

The bacterial community in dead wood showed a successional change that likely reflected the change in substrate chemistry. In contrast to the gradual succession observed for fungi, bacterial communities from the two younger and two older CWD age classes were rather similar, and the most important transition occurred after year 15 of CWD age.

At the beginning of decomposition, some bacteria are able to fix atmospheric N₂ as a consequence of N limitation (Hoppe et al. 2014). This process was shown to contribute to N enrichment, and the amount of N accumulated through fixation may be significant under certain conditions (Rinne et al. 2017). This may theoretically be the case for *Yersinia*, which represents an indicator OTU in CWD <5, since soil isolates from the same genus were able to fix N₂ (Elo et al. 2000). Methylophony is another adaptation to the conditions in dead wood (Lladó, López-Mondéjar and Baldrian 2017). The metabolism of C1 compounds enables bacteria to use by-products of wood decomposition as a carbon source (Folman et al. 2008) and is possibly connected with N-fixation (Zehr et al. 2003; Vorob'ev et al. 2009). Some taxa belonging to the core OTUs in our study (order *Rhizobiales*, genera *Bradyrhizobium*, *Beijerinckia*, *Methylocapsa*) were described as utilisers of C1 compounds with strategies such as facultative methylophony and obligate methanotrophy (Tamas et al. 2013; Morawe et al. 2017). The order *Rhizobiales* was consistently previously found to be associated with dead wood (Folman et al. 2008; Hoppe et al. 2015). Additionally, one of the indicator OTUs in the fresh CWDs belonged to the genus *Methylomonas*, known for its utilisation of C1 compounds (Radajewski et al. 2002). Another OTU specific for fresh CWD belonged to the genus *Luteibacter*, previously described as being associated with *P. chrysosporium* (Hervé et al. 2013) and already previously detected in fresh wood (Noll et al. 2010). Although neither N-fixation nor methylophony was described for this genus, a close association with fungi can be meaningful for the exchange of metabolites such as glycerol or oxalic acid (Bravo et al. 2013; Nazir et al. 2013) or may allow the bacterium to use wood degradation products such as cellobiose (Berlemont and Martiny 2013). However, *Luteibacter* was also described as cellulolytic (López-Mondéjar et al. 2016).

In older CWD, members of the phylum *Acidobacteria* (*Telmatobacter*, *Candidatus Solibacter*, *Acidicapsa* and *Acidipila*) appeared among the indicators of 16–38 CWD age class. One species of *Telmatobacter*, *T. bradus*, was described as a slow-growing species capable of degrading crystalline cellulose (Pankratov et al. 2012). Generally, members of *Acidobacteria* were abundant in this study, and some of them (*Acidipila*, *Bryocella*, *Acidobacterium*) belonged to the core OTUs. *Acidobacteria* were also described as abundant in dead wood from another temperate mixed forest (Hoppe et al. 2015). Moreover, *Acidobacteria* was shown to be a dominant and metabolically active group in soil (Žifčáková et al. 2016), which likely served as its reservoir. The fact that *Acidobacteria* exhibited by far the highest production of lignocellulose-decomposing enzymes among bacterial isolates from acidic soil (Lladó et al. 2016) suggests that *Acidobacteria* may contribute to the degradation of plant polysaccharides in dead wood.

The oldest age class of CWD after >38 years of decomposition hosted indicator OTUs assigned to the genus *Steroidbac-*

ter, typically present in high abundances in forest soils (Baldrian et al. 2012; Štursová et al. 2012) and detected in the mycorrhizosphere (Uroz et al. 2012). Another indicator taxon, *Bradyrhizobium*, is also a soil autotroph that possibly has the ability to fix nitrogen (Vaninsberghe et al. 2015). Another indicator of advanced decay, *Rhodoplanes*, is a phototrophic bacterium (Chakravarthy et al. 2012) that is also abundant in forest soil (Baldrian et al. 2012). The late phase of decomposition is characterised by significant disintegration of most logs (Fraver et al. 2013), which can result in the direct contact and mixing of dead wood with soil. This phenomenon, together with the appearance of ectomycorrhizal fungi in late wood decay, (Rajala et al. 2012) appears to be the reason why bacterial communities in old dead wood and soil overlap substantially.

Importantly, the unmanaged sampling site allowed us to focus on CWD in its natural conditions even long after the death of a tree. Our results show that several bacterial taxa are adapted to the dead wood habitat. In addition to taxa that are constantly present throughout decomposition, there are bacterial specialists for early and late decay, the former containing potential nitrogen fixers and methylophony and the latter including soil bacteria. Unlike fungi, bacteria are less stochastically distributed and have a more homogenous community composition that is influenced by substrate chemistry and is at least partly modulated by the presence of fungi. Bacterial biomass appears to be strongly influenced by N availability, suggesting that the high C/N ratio of fresh dead wood limits bacterial growth. Despite these findings, several questions remain open. These include what the contributions of bacteria to N accumulation in dead wood and to biopolymer decomposition are as well as what the importance of mycophagy is for the bacterial community. Further research on the traits of dominant bacterial taxa and their in situ activity will be needed to address these questions.

SUPPLEMENTARY DATA

Supplementary data are available at [FEMSEC](http://FEMSEC.org) online.

ACKNOWLEDGEMENTS

We would like to thank to our colleagues from the Laboratory of Environmental Microbiology who helped with the collection of samples.

FUNDING

This work was supported by the Czech Science Foundation [13-27454S].

Conflicts of interest. None declared.

REFERENCES

- Amann RI, Ludwig W, Schleifer KH. Phylogenetic identification and in situ detection of individual microbial cells without cultivation. *Microbiol Rev* 1995;59:143–69.
- Anderson-Teixeira KJ, Davies SJ, Bennett AC et al. CTFS-ForestGEO: a worldwide network monitoring forests in an era of global change. *Glob Chang Biol* 2015;21:528–49.
- Aronesty E. Comparison of sequencing utility programs. *Open Bioinforma J* 2013;7:1–8.

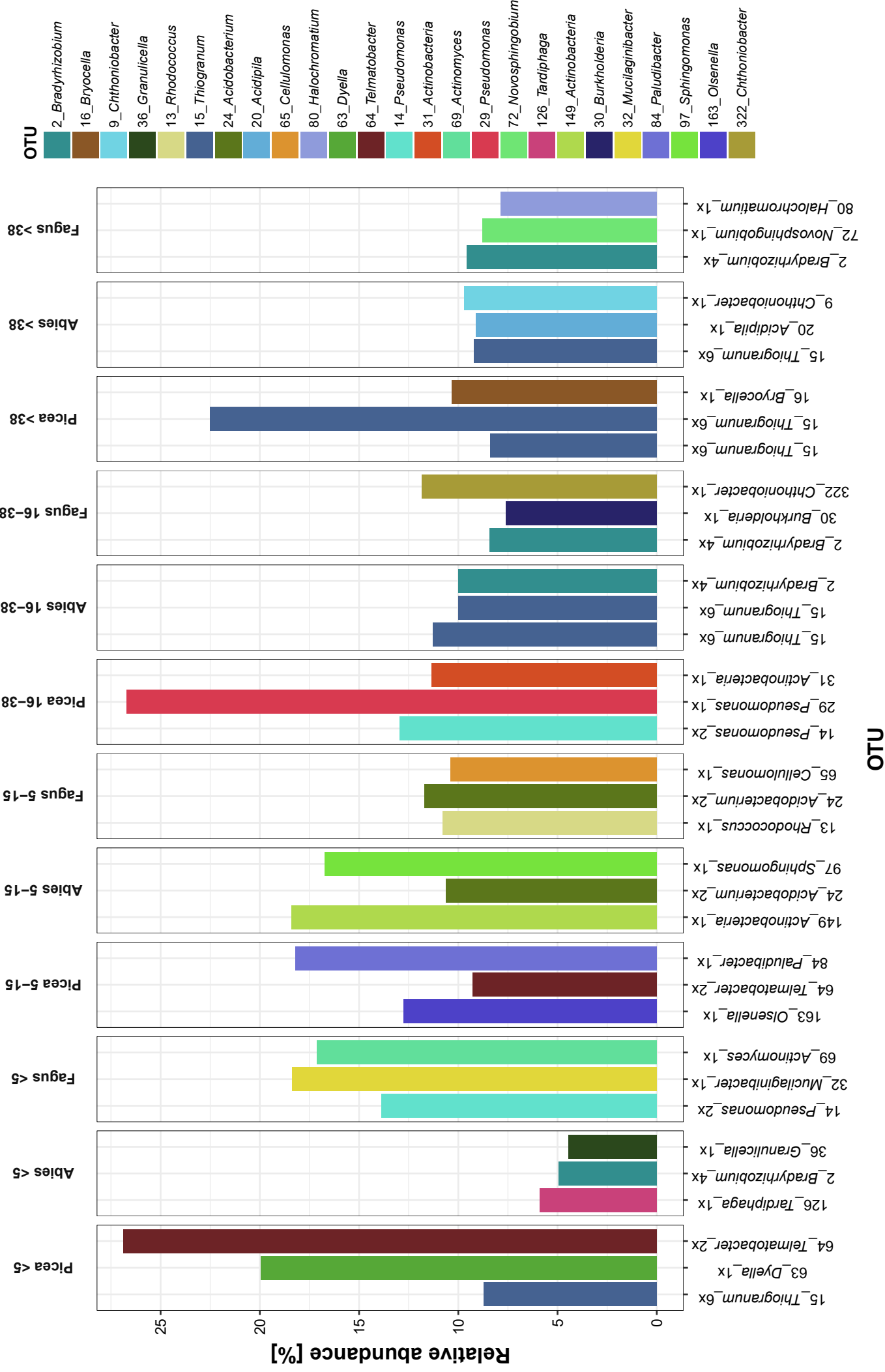
- Baldrian P. Enzymes of saprotrophic basidiomycetes. In: Boddy L, Frankland JC, van West P (eds). *Ecology of Saprotrophic Basidiomycetes*. Amsterdam: Academic Press, 2008, 19–41.
- Baldrian P. Forest microbiome: diversity, complexity and dynamics. *FEMS Microbiol Rev* 2017a;41:109–30.
- Baldrian P. Microbial activity and the dynamics of ecosystem processes in forest soils. *Curr Opin Microbiol* 2017b;37:128–34.
- Baldrian P, Kolařík M, Štursová M et al. Active and total microbial communities in forest soil are largely different and highly stratified during decomposition. *ISME J* 2012; 6:248–58.
- Baldrian P, Zrůstová P, Tláškal V et al. Fungi associated with decomposing deadwood in a natural beech-dominated forest. *Fungal Ecol* 2016;23:109–22.
- Berlemont R, Martiny AC. Phylogenetic distribution of potential cellulases in bacteria. *Appl Environ Microbiol* 2013;79:1545–54.
- Brabcová V, Nováková M, Davidová A et al. Dead fungal mycelium in forest soil represents a decomposition hotspot and a habitat for a specific microbial community. *New Phytol* 2016;210:1369–81.
- Bravo D, Cailleau G, Bindschedler S et al. Isolation of oxalotrophic bacteria able to disperse on fungal mycelium. *FEMS Microbiol Lett* 2013;348:157–66.
- Caporaso JG, Lauber CL, Walters WA et al. Global patterns of 16S rRNA diversity at a depth of millions of sequences per sample. *P Natl Acad Sci U S A* 2011;108:4516–22.
- Chakravarthy KS, Ramaprasad EV V, Shobha E et al. *Rhodoplanes piscinae* sp. nov. isolated from pond water. *Int J Syst Evol Microbiol* 2012;62:2828–34.
- Clausen CA. Bacterial associations with decaying wood: a review. *Int Biodeterior Biodegradation* 1996;37:101–7.
- Cole JR, Wang Q, Fish JA et al. Ribosomal database project: data and tools for high throughput rRNA analysis. *Nucleic Acids Res* 2014;42:1–10.
- Daniel SL, Pilsl C, Drake HL. Anaerobic oxalate consumption by microorganisms in forest soils. *Res Microbiol* 2007;158:303–9.
- de Boer W, Leveau JHJ, Kowalchuk GA. et al. *Collimonas fungivora* gen. nov., sp. nov., a chitinolytic soil bacterium with the ability to grow on living fungal hyphae. *Int J Syst Evol Microbiol* 2004;54:857–64.
- De Caceres M, Legendre P. Associations between species and groups of sites: indices and statistical inference. *Ecology* 2009;90:3566–74.
- de Mendiburu F. *Agricolae: statistical procedures for agricultural research*. R package version 1.2-4, 2016.
- Edgar RC. UPARSE: highly accurate OTU sequences from microbial amplicon reads. *Nat Methods* 2013;10:996–8.
- Edgar RC, Haas BJ, Clemente JC et al. UCHIME improves sensitivity and speed of chimera detection. *Bioinformatics* 2011;27:2194–200.
- Eichlerová I, Homolka L, Žifčáková L et al. Enzymatic systems involved in decomposition reflects the ecology and taxonomy of saprotrophic fungi. *Fungal Ecol* 2015;13:10–22.
- Elo S, Maunuksela L, Salkinoja-Salonen M et al. Humus bacteria of Norway spruce stands: plant growth promoting properties and birch, red fescue and alder colonizing capacity. *FEMS Microbiol Ecol* 2000;31:143–52.
- Folman LB, Gunnewiek PJA, Boddy L et al. Impact of white-rot fungi on numbers and community composition of bacteria colonizing beech wood from forest soil. *FEMS Microbiol Ecol* 2008;63:181–91.
- Fraver S, Milo AM, Bradford JB et al. Woody debris volume depletion through decay: implications for biomass and carbon accounting. *Ecosystems* 2013;16:1262–72.
- Hahn K, Christensen M. Dead wood in European forest reserves—a reference for forest management. *EFI Proc* 2004:181–91.
- Hervé V, Junier T, Bindschedler S et al. Diversity and ecology of oxalotrophic bacteria. *World J Microbiol Biotechnol* 2016a;32: 1–7.
- Hervé V, Ketter E, Pierrat J-C et al. Impact of *Phanerochaete chrysosporium* on the functional diversity of bacterial communities associated with decaying wood. *PLoS One* 2016b;11:e0147100.
- Hervé V, Roux X Le, Uroz S et al. Diversity and structure of bacterial communities associated with *Phanerochaete chrysosporium* during wood decay. *Environ Microbiol* 2013; 16:2238–52.
- Hoppe B, Kahl T, Karasch P et al. Network analysis reveals ecological links between N-fixing bacteria and wood-decaying fungi. *PLoS One* 2014;9:e88141.
- Hoppe B, Krüger D, Kahl T et al. A pyrosequencing insight into sprawling bacterial diversity and community dynamics in decaying deadwood logs of *Fagus sylvatica* and *Picea abies*. *Sci Rep* 2015;5:9456.
- Jarosz-Wilkolazka A, Graz M. Organic acids production by white rot Basidiomycetes in the presence of metallic oxides. *Can J Microbiol* 2006;52:779–85.
- Johnston SR, Boddy L, Weightman AJ. Bacteria in decomposing wood and their interactions with wood-decay fungi. *FEMS Microbiol Ecol* 2016;92:fiw179.
- Katoh K, Kuma K, Toh H et al. MAFFT version 5: improvement in accuracy of multiple sequence alignment. *Nucleic Acids Res* 2005;33:511–8.
- Kielak AM, Scheublin TR, Mendes LW et al. Bacterial community succession in pine-wood decomposition. *Front Microbiol* 2016;7:1–12.
- Kirk KT, Obst JR. Lignin determination. *Methods Enzymol* 1988;161:87–101.
- Král K, Janík D, Vrška T et al. Local variability of stand structural features in beech dominated natural forests of Central Europe: implications for sampling. *For Ecol Manage* 2010;260:2196–203.
- Král K, Valtera M, Janík D et al. Spatial variability of general stand characteristics in central European beech-dominated natural stands—effects of scale. *For Ecol Manage* 2014; 328:353–64.
- Kubartová A, Ottosson E, Dahlberg A et al. Patterns of fungal communities among and within decaying logs, revealed by 454 sequencing. *Mol Ecol* 2012;21:4514–32.
- Lenhart K, Bunge M, Ratering S et al. Evidence for methane production by saprotrophic fungi. *Nat Commun* 2012;3:1046.
- Lladó SF, López-Mondéjar R, Baldrian P. Forest soil bacteria: diversity, involvement in ecosystem processes, and response to global change. *Microbiol Mol Biol Rev* 2017;81:e00063–16.
- Lladó SF, Žifčáková L, Větrovský T et al. Functional screening of abundant bacteria from acidic forest soil indicates the metabolic potential of Acidobacteria subdivision 1 for polysaccharide decomposition. *Biol Fertil Soils* 2016;52:251–60.
- López-Mondéjar R, Voříšková J, Větrovský T et al. The bacterial community inhabiting temperate deciduous forests is vertically stratified and undergoes seasonal dynamics. *Soil Biol Biochem* 2015;87:43–50.
- López-Mondéjar R, Zühlke D, Becher D et al. Cellulose and hemicellulose decomposition by forest soil bacteria proceeds by the action of structurally variable enzymatic systems. *Sci Rep* 2016;6:25279.

- Magnússon Rí, Tietema A, Cornelissen JHC et al. Tamm review: sequestration of carbon from coarse woody debris in forest soils. *For Ecol Manage* 2016;**377**:1–15.
- Mäkipää R, Rajala T, Schigel D et al. Interactions between soil- and dead wood-inhabiting fungal communities during the decay of Norway spruce logs. *ISME J* 2017;**11**:1964–74.
- Meyer F, Paarmann D, D'Souza M et al. The metagenomics RAST server—a public resource for the automatic phylogenetic and functional analysis of metagenomes. *BMC Bioinformatics* 2008;**9**:386.
- Morawe M, Hoeke H, Wissenbach DK et al. Acidotolerant bacteria and fungi as a sink of methanol-derived carbon in a deciduous forest soil. *Front Microbiol* 2017;**8**:1–18.
- Nazir R, Warmink JA, Voordes DC et al. Inhibition of mushroom formation and induction of glycerol release-ecological strategies of *Burkholderia terrae* BS001 to create a hospitable niche at the fungus *Lyophyllum* sp. strain Karsten. *Microb Ecol* 2013;**65**:245–54.
- Noll M, Naumann A, Ferrero F et al. Exothermic processes in industrial-scale piles of chipped pine-wood are linked to shifts in gamma-, alphaproteobacterial and fungal ascomycete communities. *Int Biodeterior Biodegrad* 2010;**64**:629–37.
- Oksanen J, Blanchet FG, Kindt R et al. vegan: community ecology package. R package version 2.4-3, 2017.
- Pankratov TA, Kirsanova LA, Kaparullina EN et al. *Telmatobacter bradus* gen. nov., sp. nov., a cellulolytic facultative anaerobe from subdivision 1 of the Acidobacteria, and emended description of *Acidobacterium capsulatum* Kishimoto et al. 1991. *Int J Syst Evol Microbiol* 2012;**62**:430–7.
- Prévost-Bouré NC, Christen R, Dequiedt S et al. Validation and application of a PCR primer set to quantify fungal communities in the soil environment by real-time quantitative PCR. *PLoS One* 2011;**6**:e24166.
- Prewitt L, Kang Y, Kakumanu ML et al. Fungal and bacterial community succession differs for three wood types during decay in a forest soil. *Microb Ecol* 2014;**68**:212–21.
- Přivětivý T, Janík D, Unar P et al. How do environmental conditions affect the deadwood decomposition of European beech (*Fagus sylvatica* L.)? *For Ecol Manage* 2016;**381**:177–87.
- R Core Team. R: A language and environment for statistical computing. 2017.
- Radajewski S, Webster G, Reay DS et al. Identification of active methylotroph populations in an acidic forest soil by stable-isotope probing. *Microbiology* 2002;**148**:2331–42.
- Rajala T, Peltoniemi M, Hantula J et al. RNA reveals a succession of active fungi during the decay of Norway spruce logs. *Fungal Ecol* 2011;**4**:437–48.
- Rajala T, Peltoniemi M, Pennanen T et al. Fungal community dynamics in relation to substrate quality of decaying Norway spruce (*Picea abies* [L.] Karst.) logs in boreal forests. *FEMS Microbiol Ecol* 2012;**81**:494–505.
- Rinne KT, Rajala T, Peltoniemi K et al. Accumulation rates and sources of external nitrogen in decaying wood in a Norway spruce dominated forest. *Funct Ecol* 2017;**31**:530–41.
- Rinta-Kanto JM, Sinkko H, Rajala T et al. Natural decay process affects the abundance and community structure of Bacteria and Archaea in *Picea abies* logs. *FEMS Microbiol Ecol* 2016;**92**:fiw087.
- Rousk J, Bååth E, Brookes PC et al. Soil bacterial and fungal communities across a pH gradient in an arable soil. *ISME J* 2010;**4**:1340–51.
- Rudnick MB, van Veen JA, de Boer W. Oxalic acid: a signal molecule for fungus-feeding bacteria of the genus *Colimonas*? *Environ Microbiol Rep* 2015;**7**:709–14.
- Šamonil P, Doleželová P, Vašíčková I et al. Individual-based approach to the detection of disturbance history through spatial scales in a natural beech-dominated forest. *J Veg Sci* 2013;**24**:1167–84.
- Šnajdr J, Cajthaml T, Valášková V et al. Transformation of *Quercus petraea* litter: successive changes in litter chemistry are reflected in differential enzyme activity and changes in the microbial community composition. *FEMS Microbiol Ecol* 2011;**75**:291–303.
- Šnajdr J, Valášková V, Merhautová V et al. Spatial variability of enzyme activities and microbial biomass in the upper layers of *Quercus petraea* forest soil. *Soil Biol Biochem* 2008;**40**:2068–75.
- Stokland JN, Siitonen J, Jonsson BG. *Biodiversity in Dead Wood*. Cambridge: Cambridge University Press, 2012.
- Stutz KP, Dann D, Wambsganss J et al. Phenolic matter from deadwood can impact forest soil properties. *Geoderma* 2017;**288**:204–12.
- Štursová M, Bárta J, Šantrůčková H et al. Small-scale spatial heterogeneity of ecosystem properties, microbial community composition and microbial activities in a temperate mountain forest soil. *FEMS Microbiol Ecol* 2016;**92**:fiw185.
- Štursová M, Žižňáková L, Leigh MB et al. Cellulose utilization in forest litter and soil: identification of bacterial and fungal decomposers. *FEMS Microbiol Ecol* 2012;**80**:735–46.
- Sun H, Terhonen E, Kasanen R et al. Diversity and community structure of primary wood-inhabiting bacteria in boreal forest. *Geomicrobiol J* 2014;**31**:315–24.
- Tamas I, Smirnova AV, He Z et al. The (d)evolution of methanotrophy in the *Beijerinckiaceae*—a comparative genomics analysis. *ISME J* 2013;**8**:369–82.
- Tláškal V, Voříšková J, Baldrian P. Bacterial succession on decomposing leaf litter exhibits a specific occurrence pattern of cellulolytic taxa and decomposers of fungal mycelia. *FEMS Microbiol Ecol* 2016;**92**:fiw177.
- Uroz S, Oger P, Morin E et al. Distinct ectomycorrhizospheres share similar bacterial communities as revealed by pyrosequencing-based analysis of 16S rRNA genes. *Appl Environ Microbiol* 2012;**78**:3020–4.
- Valášková V, de Boer W, Gunnewiek PJA et al. Phylogenetic composition and properties of bacteria coexisting with the fungus *Hypholoma fasciculare* in decaying wood. *ISME J* 2009;**3**:1218–21.
- VanInsberghe D, Maas KR, Cardenas E et al. Non-symbiotic *Bradyrhizobium* ecotypes dominate North American forest soils. *ISME J* 2015;**9**:1–7.
- Větrovský T, Baldrian P. Analysis of soil fungal communities by amplicon pyrosequencing: current approaches to data analysis and the introduction of the pipeline SEED. *Biol Fertil Soils* 2013a;**49**:1027–37.
- Větrovský T, Baldrian P. The variability of the 16S rRNA gene in bacterial genomes and its consequences for bacterial community analyses. *PLoS One* 2013b;**8**:e57923.
- Vorob'ev AV, de Boer W, Folman LB et al. *Methylovirgula ligni* gen. nov., sp. nov., an obligately acidophilic, facultatively methylotrophic bacterium with a highly divergent *mxoF* gene. *Int J Syst Evol Microbiol* 2009;**59**:2538–45.
- Voříšková J, Baldrian P. Fungal community on decomposing leaf litter undergoes rapid successional changes. *ISME J* 2013;**7**:477–86.

- van der Wal A, de Boer W, Smant W et al. Initial decay of woody fragments in soil is influenced by size, vertical position, nitrogen availability and soil origin. *Plant Soil* 2007;**301**:189–201.
- Wilmotte A, Van der Auwera G, De Wachter R. Structure of the 16 S ribosomal RNA of the thermophilic cyanobacterium *Chlorogloeopsis* HTF (*Mastigocladus laminosus* HTF) strain PCC7518, and phylogenetic analysis. *FEBS Lett* 1993;**317**:96–100.
- Zehr JP, Jenkins BD, Short SM et al. Nitrogenase gene diversity and microbial community structure: a cross-system comparison. *Environ Microbiol* 2003;**5**:539–54.
- Žifčáková L, Větrovský T, Howe A et al. Microbial activity in forest soil reflects the changes in ecosystem properties between summer and winter. *Environ Microbiol* 2016;**18**:288–301.

Supplementary Figure 1

Relative abundances of dominant bacterial taxa in coarse woody debris. Three CWDs with the highest abundances of the dominant bacterial OTUs are depicted for each sample class together with OTU numbers and numbers of samples where this OTU is dominant.



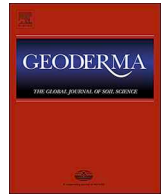




ELSEVIER

Contents lists available at ScienceDirect

Geoderma

journal homepage: www.elsevier.com/locate/geoderma

Convergence, divergence or chaos? Consequences of tree trunk decay for pedogenesis and the soil microbiome in a temperate natural forest

P. Šamonil^{a,b,*}, P. Daněk^{a,c}, P. Baldrian^d, V. Tláškal^d, V. Tejnecký^e, O. Drábek^e

^a Department of Forest Ecology, The Silva Tarouca Research Institute, 602 00 Brno, Czech Republic

^b Department of Forest Botany, Dendrology and Geobiocoenology, Faculty of Forestry and Wood Technology, Mendel University in Brno, Zemědělská 1, 613 00 Brno, Czech Republic

^c Department of Botany and Zoology, Faculty of Science, Masaryk University, Kotlářská 267/2, 611 37 Brno, Czech Republic

^d Laboratory of Environmental Microbiology, Institute of Microbiology of the Czech Academy of Sciences, v.v.i., Videnska 1083, 14220 Prague 4, Czech Republic

^e Department of Soil Science and Soil Protection, Faculty of Agrobiolgy, Food and Natural Resources, Czech University of Life Sciences Prague, Kamycka 129, 160 00 Prague, Czech Republic

ARTICLE INFO

Handling Editor: Alberto Agnelli

Keywords:

Soil evolution
Biochemical effects of trees
Podzolization
Tree-soil interactions
Soil microorganisms
Old-growth forest dynamics

ABSTRACT

The biochemical effects of trees may significantly influence local pedogenesis as well as pedocomplexity, biodiversity and forest dynamics on both stand and landscape scales. One such effect is the decay of tree trunks, which is driven by organisms, and especially by the microbiome. Decomposition modifies soil formation, which due to the existence of many feedbacks affects the composition of the decomposer community. We aimed to uncover general trends in the evolution of Entic Podzols as well as individual trajectories of soil properties below decaying beech trunks in an old-growth mountain forest. In particular, we used mathematical models to distinguish soil convergence, divergence and chaotic behaviour to enhance a general theory of pedogenesis. We further aimed to calculate the depth and time of convergence if this scenario is prevailing in the study plot. Pedogenetic pathways were assessed regarding the changing composition of fungal and bacterial communities in soils to obtain a complex picture of the decaying trunk-soil microbiome system.

We sampled the decaying wood layer under 24 lying beech trunks and corresponding organic horizons on adjacent control microsites occupied by decaying beech leaves. At the same time we sampled underlying mineral soil horizons at both microsites (wood vs. leaves), all on Entic Podzols and granite (in total 192 soil samples). Individual trunk fall events were dated using precise dendrochronology, with the resulting chronosequence covering trunks lying for 8–52 years. We analysed decomposition processes (with a wide spectra of organic acids and ions analysed), soil chemistry (28 additional soil properties assessed), and the microbiome composition in both decaying organic matter and soils (relative abundances of the 200 most common bacterial and fungal OTUs analysed).

During the first stage of trunk decay, underlying Entic Podzols responded with a significant increase of nutrients, pH, and CEC, and the maximal divergence compared to control sites was reached between 12 and 60 years after the trunk fall. Subsequently, a majority of soil properties slowly converged over a few decades to match the soil properties of control sites. The modelled convergence point occurred at ages between 39 (SO_4^{2-}) and 229 (Al_w) years, with a median convergence time of 53 years. The majority of soil properties converged within 20 cm below the trunk, but mathematical models predicted footprints of some soil properties down to depths of ca 60 cm. In addition, 11 soil properties did not converge at any depth, and for some properties the models even diverged. Differences in bacterial and fungal communities between below-trunk and control positions were relatively minor. Padochemical drivers of fungal and bacterial communities (nutrients content, N_{tot} , C_{ox} , Al, Fe, Mn forms) changed significantly in the mineral soil below trunks, and the microbiome partly reflected these depth-related changes. However, we propose that there is a threshold between organic and mineral soil horizons limiting the impacts of trunk decay and pedogenesis in changes to the microbiome.

* Corresponding author at: Department of Forest Ecology, The Silva Tarouca Research Institute, 602 00 Brno, Czech Republic.

E-mail address: pavel.samonil@vukoz.cz (P. Šamonil).

<https://doi.org/10.1016/j.geoderma.2020.114499>

Received 20 November 2019; Received in revised form 25 May 2020; Accepted 1 June 2020

0016-7061/ © 2020 Elsevier B.V. All rights reserved.

1. Introduction

Individual trees may locally accelerate, slow or redirect pedogenetic pathways. Trees affect soils via biomechanical processes such as root mounding (Hoffman and Anderson 2013), and biochemically through metabolism and body parts decay (Binkley and Giardina 1998). These are strong point impacts, but they can also be expressed at stand and landscape scales. Recent studies have suggested that tree influences may contribute to the exceptional but still weakly explained spatial pedocomplexity of some mountain forests (including the Žofínský Prales Reserve in the Czech Republic, where this study took place – Šamonil et al. 2014). The discovery of the significant effects of individual trees on soil evolution in landscapes has led to modifications of the evolutionary theory of pedogenesis (e.g. Phillips, 2001, 2009, Roering et al. 2010, Šamonil et al. 2014). Pedocomplexity is closely interconnected with disturbance regimes, land use, and biodiversity (Nachtergale et al., 2002; Daněk et al. 2016), issues extending beyond life sciences to the whole of human society.

The decomposition of lying trunks is one of the characteristic biochemical influences of trees in soils in old-growth forests, where they may potentially be a source of local non-linearity in soil evolution and spatial pedocomplexity. For example, lying trunks cover approximately 4% of the area in Central European old-growth forests (e.g. Průša 1985). Due to ongoing tree mortality and gradual lying trunk decomposition, the underlying soils are constantly changing. However, the information remains in the soil memory, potentially for long time periods. Soil properties do not necessarily homogenize in time and space. Examples of divergent or chaotic soil evolution have already been recognized (Phillips, 2001; Šamonil et al. 2015, see below). Moreover, soils locally affected by trees influence the new generation of trees (Simon et al., 2011). The complex system of decaying wood – i.e. the community of decomposers and soils, with many hidden feedbacks – has still not been sufficiently described and requires further attention.

Current publications generally agree on the significant impact of decomposing trunks on soils, but they differ in their evaluations of the outcome of these processes. While for example Kayahara et al. (1998) and Dhiedt et al. (2019) described the positive effects of decomposing trunks on nutrient contents and increases in soil CEC, Spears and Lajtha (2004) found the opposite. Hence, additional studies are needed to obtain a more general picture of the process in various ecosystems. Pedogenetic studies have generally ignored the potentially important role of soil organisms such as fungi and bacteria in pedogenesis under lying tree trunks. We aimed to expand on the traditional pedogenetic approach by studying changes of the microbial community during beech trunk decay (see Mäkipää et al., 2017, Peršoh and Borken, 2017) and a detailed analysis of the products of trunk decay affecting pedogenesis.

Both divergent soil development and deterministic chaos in soils (Phillips, 2001) are significant alternatives to the traditionally accentuated soil convergence. Divergence or chaotic behaviour can be very local processes that take place on a fine spatial scale due to the influence of an individual tree, against the background of a general soil convergence in the landscape. But many other scenarios are possible. Potentially, only some soil properties may diverge while others converge. Such non-linear pedogenesis and the coexistence of different directions in evolutionary soil trajectories have not yet been given much scientific attention, although they may have a significant impact on the spatial complexity of soils and the dynamics of the whole forest landscape.

In our study we focused on the influence of decaying *Fagus sylvatica* L. trunks in a region of enormous soil complexity, where Entic Podzols represent the main soil unit. The aims of the study were (i) to determine individual evolutionary trajectories of soil properties and the general trends in soils under decomposing *Fagus sylvatica* trunks, (ii) to find evidence pointing to the convergence, divergence, or chaos in soils influenced by a trunk, and (iii) to calculate the depth and time of

convergence if this process is predominant. Furthermore, we asked (iv) what is the composition of the soil microbiome along the gradient of trunk decay. The results should deepen our understanding of soil complexity sources in old-growth forests and, subsequently, a better understanding of the impacts of human forest management in mountain forest ecosystems when all trunks are removed.

2. Terminology

Within this study we refer to “convergent soil development” as the process where differences in studied soil properties decrease along a gradient of soil depth or along a gradient of time. We used a standard chronosequence approach, i.e. space-for-time substitution, to study the effect of age (e.g. Bockheim, 1980). “Divergent development” is the opposite process where differences in soil quality increase along depth or time gradients (see Phillips, 2001). Chaotic development represents a specific scenario of significantly increasing variance of a studied soil property without significant changes in its mean value (Phillips et al., 1996; Phillips, 2006).

3. Material and methods

3.1. Study area

The research was carried out in the Žofínský Prales Reserve in the Novohradské Mts. (hereinafter Zofin). The reserve is located along an altitudinal gradient ranging between 735 and 830 m a.s.l. Mild NW slopes predominate. The bedrock is nearly homogeneous and consists of porphyritic and biotite granite (CGS, 2019). Soils are characteristically podzolized, acidic, and sandy (Šamonil et al., 2011). Annual average temperature in Zofin is about 4.3 °C and annual average rainfall is about 704 mm (CHMU, 2019). Plant communities can be most often classified into the association *Galio odorati-Fagetum*. Long-term forest dynamics are driven by fine scale disturbances with infrequent occurrences of severe winds or biotic disturbances (Šamonil et al., 2013a). *Fagus sylvatica* dominates in Zofin (62% of the volume of living trees), followed by *Picea abies* (34%). *Abies alba* and sporadic broadleaves (e.g. *Acer pseudoplatanus*, *Ulmus glabra*) represent 3% and 1% of the living tree volume, respectively.

3.2. Data collection – trunk selection

We sampled organic and mineral soil horizons on positions of decaying beech trunks and adjacent control positions (we call these positions “microsites”). To select appropriate beech trunks we used two extensive datasets:

- In total 3020 dendrochronological cores had been taken by a regular randomized approach through the whole reserve between 2008 and 2012 for the purpose of studying disturbance history (see details in Šamonil et al., 2013a). Here we focused on precise dendrochronological dating of lying beeches according to methodology by Šamonil et al. (2013b).
- A detailed soil map, with soils classified in 5 replications on each of 353 square plots of area 1958 m² (see details in Šamonil et al., 2011). Based on a total of 1765 shallow profiles and penetrations by a soil borer, we assessed the occurrence of soil units. For the purposes of this paper, we selected areas with predominantly Entic Podzols and disregarded areas occupied by other soils (Haplic Cambisols, Dystric Cambisols, Albic Podzols, Glesols, Stagnosols, Histosols, Fluvisols, Leptosols, IUSS Working Group WRB, 2014)

These two data sources were interconnected by choosing a set of ca 50 beech trunks at different degrees of decomposition on the Entic Podzols, surrounded by cored trees. We dendrochronologically dated the death of each trunk with an accuracy of 1–5 years. Then, for soil and

microbiology data, we chose 24 trunks with the highest degree of certainty in dating accuracy, evenly covering a gradient of ages from 8 to 52 years. The time since the tree death roughly corresponded with a stage of trunk decomposition. Trunks lying for 8 years were still compact and solid (i.e. hard at a 3-level classification by Průša, 1985), while all trunks lying for more than 33 years occurred in final degree of decomposition (decayed according to Průša, 1985). Trunks lying between 8 and 33 years appeared characteristically intermediately decomposed (partly rotten). Selected trunks were randomly distributed within the ForestGEO plot of area 25 ha, and the distance between two adjacent trunks usually exceeded 40 m.

3.3. Data collection – Soil sampling

At distances $\frac{1}{4}$ and $\frac{3}{4}$ along their length, soil samples were taken under each of 24 lying trunks in autumn 2015. In shallow excavated profiles, all soil horizons present were described in terms of soil morphology (Schoeneberger et al., 1998) and soils were classified according to the IUSS Working Group WRB (2014). Samples were taken from just under the decomposing trunks, the upper mineral A horizon, and at depths of 5 and 10 cm below the A horizon base. We call these deepest samples as Bs-upper and Bs-lower. Corresponding samples from the 2 sampling points below each trunk were merged. As a result, under each of the 24 trunks chosen for soil and microbiology analyses, 4 mixed samples were taken along the gradient of soil depth (including one sample from organic horizon, i.e. decaying trunk). The boundaries between organic and mineral horizons as well as the lower boundary of upper mineral A horizon were deliberately taken into account, and these horizons were not mixed with others to best determine the potential course of podzolization, which is initiated just below the A horizon. The thickness of the A horizon was most often 5 cm of sampling depth, so modifications of sampling depth were minor. Samples associated with trunk microsite are denoted by the symbol W – wood.

Control profiles were excavated 2 m away from the soil profiles under trunks, i.e. two control points close to each trunk. The sampling strategy and subsequent mixture of correspond samples were the same as with trunk microsites, except that the organic horizons did not represent decomposed wood, but decomposing leaves, with litter, fermented, and humification horizons (see Klinka et al., 1997; Jabiol, 2013). Control samples are denoted by the symbol L – litter. A similar sampling scheme was used by Stutz et al. (2017). All samples were frozen immediately after sampling, and altogether 192 samples were taken for laboratory analysis. Bulk densities below the trunk were similar to those in control positions.

3.4. Laboratory analyses

3.4.1. Soil chemistry

The samples were dried at laboratory temperature and sieved through 2 mm sieves (except for analysis of low molecular mass organic acids, see below). Organic horizons were ground to this fraction. We focused on a wide spectrum of chemical soil characteristics: (i) First we were interested in characteristics associated with humification and the transformation of organic matter in soils. (ii) Second, we were interested in soil qualities expressing the degree of weathering and leaching processes, especially podzolization. (iii) Third, we determined soil properties suggesting the nutrition requirements of the organisms present.

Dry and homogenized samples were analysed according to the following procedures by Zbiral (2002, 2003) and Zbiral et al. (2004): active ($\text{pH}_{\text{H}_2\text{O}}$) and exchange (pH_{KCl}) soil reaction – 0.2 M KCl; total organic C (C_{ox}) – using a spectrophotometric approach after oxidation by $\text{H}_2\text{SO}_4 + \text{K}_2\text{Cr}_2\text{O}_7$; total N content according to Kjeldahl (Bremner, 1996); exchangeable base cations Ca^{2+} , Mg^{2+} , K^+ , Na^+ , effective cation exchange capacity (CEC), base saturation (BS), and exchangeable acidity ($\text{Al} + \text{H}$) – all according to Gillman and Sumpter (1986; BaCl_2 -

compulsive exchange procedure, native pH). Concentrations of elements in the various liquid extracts were subsequently measured using a Specol 221 UV/VIS spectrophotometer and an atomic absorption spectrophotometer (GBC 932 AB Plus).

All mineral samples were analysed in terms of the contents of amorphous, labile and organically bound Fe, Al, Mn and Si forms by extraction methods. Whereas extracted Fe and Al can be classified into these three forms relatively reliably (Courchesne and Turmel, 2008), for Si and Mn this division is less clear (Guest et al., 2002). Tejnecký et al. (2015) analysed the mineralogy of such extracts in detail using diffuse reflectance spectroscopy and voltammetry of microparticles. We used the approach of Drabek et al. (2003, 2005) to determine contents of reactive-exchangeable and weakly organics bond forms. The labile forms were extracted in 0.5 M KCl (37.27 g l^{-1}) (1:10, v/w), and are indicated by the subscript “k” (Fe_k , Al_k , Mn_k , Si_k). 0.2 M acid ammonium oxalate (according to Courchesne and Turmel, 2008 at a ratio of 0.25:10, w/v, pH 3) was used to detect the contents of the sum of exchangeable, organic and particularly amorphous forms. The amorphous forms are indicated by the subscript “ox” (Fe_{ox} , Al_{ox} , Mn_{ox} , Si_{ox}). Primarily organically bound forms were determined using extraction by $\text{Na}_4\text{P}_2\text{O}_7$ at pH 10 (Schnitzer et al. 1958); these are indicated by the subscript “p” (Fe_p , Al_p , Si_p , Mn_p).

Low molecular mass organic acids (LMMOA) in soils were analysed in samples that were thawed at laboratory temperature (25 °C) before water extraction for LMMOA analysis. Unfrozen samples represented a “fresh” state of actual soil moisture. These were subjected to a deionised water (conductivity $< 0.055 \mu\text{S cm}^{-1}$, Crystal Adrona and simultaneously $< 2 \text{ ng l}^{-1}$ TOC) extraction (ratio soil/water 1:10 w/v, 1 h extraction on a reciprocal shaker at a stable laboratory temperature 20 °C). The suspension was then centrifuged at 4000 rpm for 10 min, then extracts were filtered through a 0.45 μm nylon membrane filter (Cronus Membrane Filter Nylon, GB). In aqueous extracts, the following chemical parameters were analysed: contents of LMMOA, inorganic anions by means of ion chromatography (IC; see details below), and contents of selected elements (Al_w , Ca_w , Fe_w , K_w , Mn_w , Mg_w) using an inductively-coupled plasma-optical emission spectrometer (ICP-OES; iCAP 7000, Thermo Scientific, USA). All results were recalculated using soil moisture to soil dry mass ($\mu\text{mol kg}^{-1}$ and $\mu\text{eq kg}^{-1}$).

Major LMMOA (lactate, acetate, formate, malate, oxalate and citrate) and inorganic (NO_3^- , PO_4^{3-} and SO_4^{2-}) anions were determined by means of ion-exchange chromatography with suppressed conductivity using an ICS 1600 ion chromatograph (Dionex, USA) equipped with an IonPac AS11-HC (Dionex, USA) guard and analytical columns. The eluent composition was 1–35.2 mM KOH with a linear gradient 1–65 min ($0.55 \text{ mM KOH min}^{-1}$); flow rate was set to 1 ml min^{-1} . Detailed descriptions of IC analyses were described in Hubova et al. (2018).

To suppress eluent conductivity, an ASRS 300 – 4 mm suppressor (Dionex, USA), and Carbonate Removal Device 200 (Dionex, USA) were used. Chromatograms were processed and evaluated using the software Chromeleon 6.80 (Dionex, USA). Standards were prepared from 1 g l^{-1} anion concentrates (Analytika, CZ and Inorganic Ventures, USA) and deionised water (conductivity $< 0.055 \mu\text{S cm}^{-1}$; Crystal Adrona, Latvia) in the range of 0.1–40 mg l^{-1} . Limits of detection were calculated from the 3:1 signal-to-noise ratio (Shabir, 2003), and for determined organic acids the limits of detection were: 0.25 $\mu\text{mol l}^{-1}$ for lactate, 0.46 $\mu\text{mol l}^{-1}$ for acetate, 0.53 $\mu\text{mol l}^{-1}$ for propionate, 0.27 $\mu\text{mol l}^{-1}$ for formate, 0.55 $\mu\text{mol l}^{-1}$ for butyrate, 0.28 $\mu\text{mol l}^{-1}$ for malate, 0.23 $\mu\text{mol l}^{-1}$ for tartrate, 0.43 $\mu\text{mol l}^{-1}$ for maleate, 0.24 $\mu\text{mol l}^{-1}$ for oxalate and 0.34 $\mu\text{mol l}^{-1}$ for citrate.

3.4.2. DNA extraction and amplification

Organic and mineral samples were homogenized, weighed, freeze-dried and weighed again before DNA extraction. Total DNA was extracted in triplicates from 300 mg of sample material using a modified SK method (Sagova-Mareckova et al., 2008) and cleaned with a

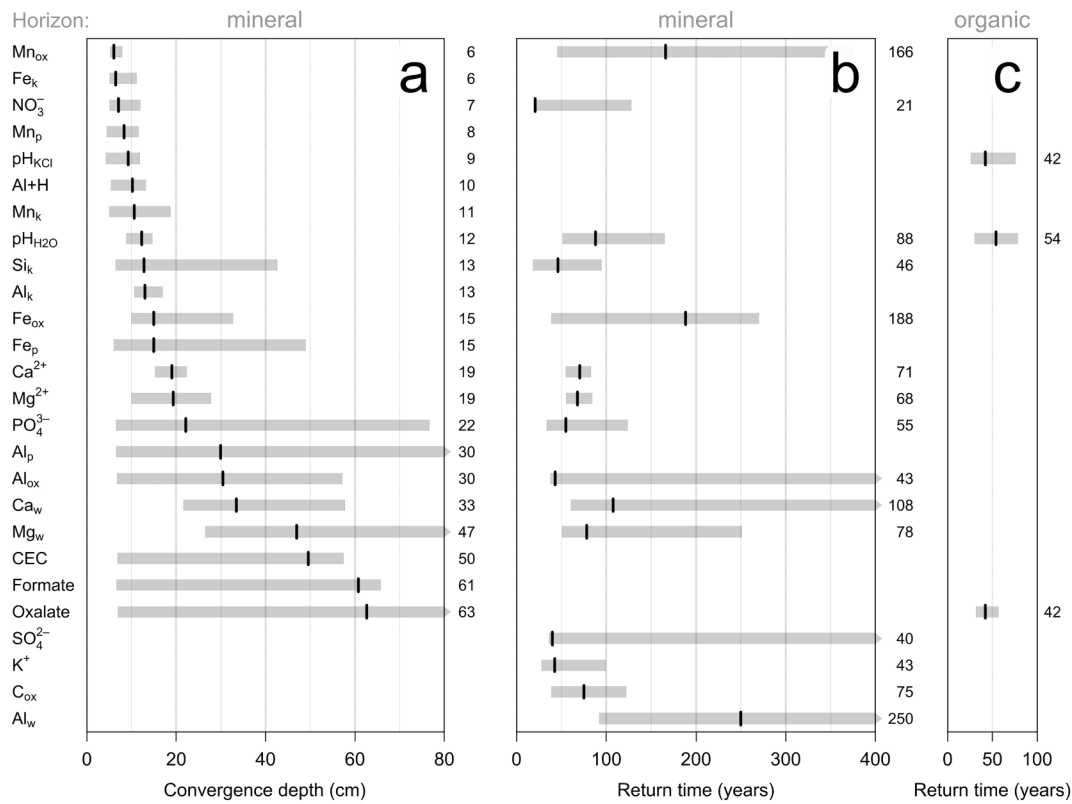


Fig. 3. Estimates of a) convergence depths (depth at which the difference in a measured soil characteristic between the soil under decaying trunks and control sites disappears) and return times (times after which values of a measured characteristic affected by decaying trunks return to the initial values) for b) mineral soil horizons and c) organic horizons. Vertical black bars show estimated mean values (displayed also numerically to the right of the plots) and horizontal grey bars give 95% confidence intervals.

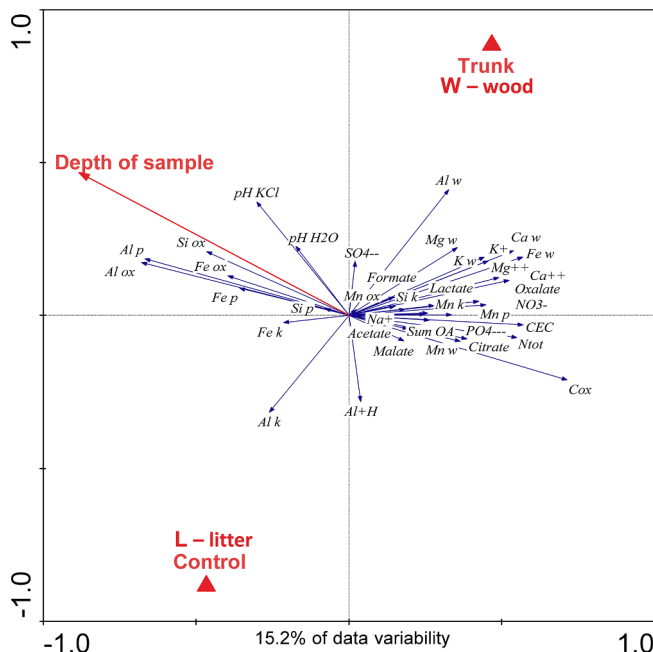


Fig. 4. The result of redundancy analysis focused on differences in mineral soils below decomposing trunks (W – wood) and control profiles (below leaf litter – L), and on the effect of sample depth in soil chemistry. Adjustment of analysis is visible in Tab. 1, coding of properties in Section 3.4.

criterion (AIC) of the model.

For models with the time variable included we considered two scenarios, convergence and a general trend. The convergent model

assumed that there was no difference between the microsites at time zero (the moment of trunk fall) and any impact of the lying dead wood disappeared after a certain time (convergence time). We defined two convergent models, which differed in the development of the difference between the microsites between time zero and the convergence time. The development was either unimodal (modelled by a quadratic curve) or more complicated (a cubic curve). Similar to convergence depth, convergence time was determined as that for which the model reached the lowest AIC (with the interval 5–1000 years). The model for the general trend included a quadratic term of depth, a quadratic term of time and their interaction as explanatory variables. For convergence models the time variable for control microsites was set to the value of the convergence time (i.e. the optimum value in case of the final model or the one currently tested during optimization) while for general trend model it was set to zero (see Appendix A for the derivation of convergence models).

Performance of the models was measured by their AIC, which was increased by 2 for convergence models as a penalization for estimation of the convergence parameter. We first identified the best model among those that did not include time. Generally, we chose the one with the lowest AIC, but prioritized the convergence model if it was not significantly worse than the best model (i.e. its AIC was not more than 4 units higher than that of the best model; Burnham and Anderson 2004). In other words, we selected the convergence model unless there was substantial evidence against it. The reason for this is because of the assumption that the influence of the decaying log is indeed likely depth-limited, and thus this model is likely more pedologically relevant. A time-specific model was considered only if it performed substantially better than the best depth-only model.

Confidence intervals (CI) for the convergence parameters (depth and time) were computed from 100 bootstrap resamples. For individual resampling units we took the complete data from each microsite pair

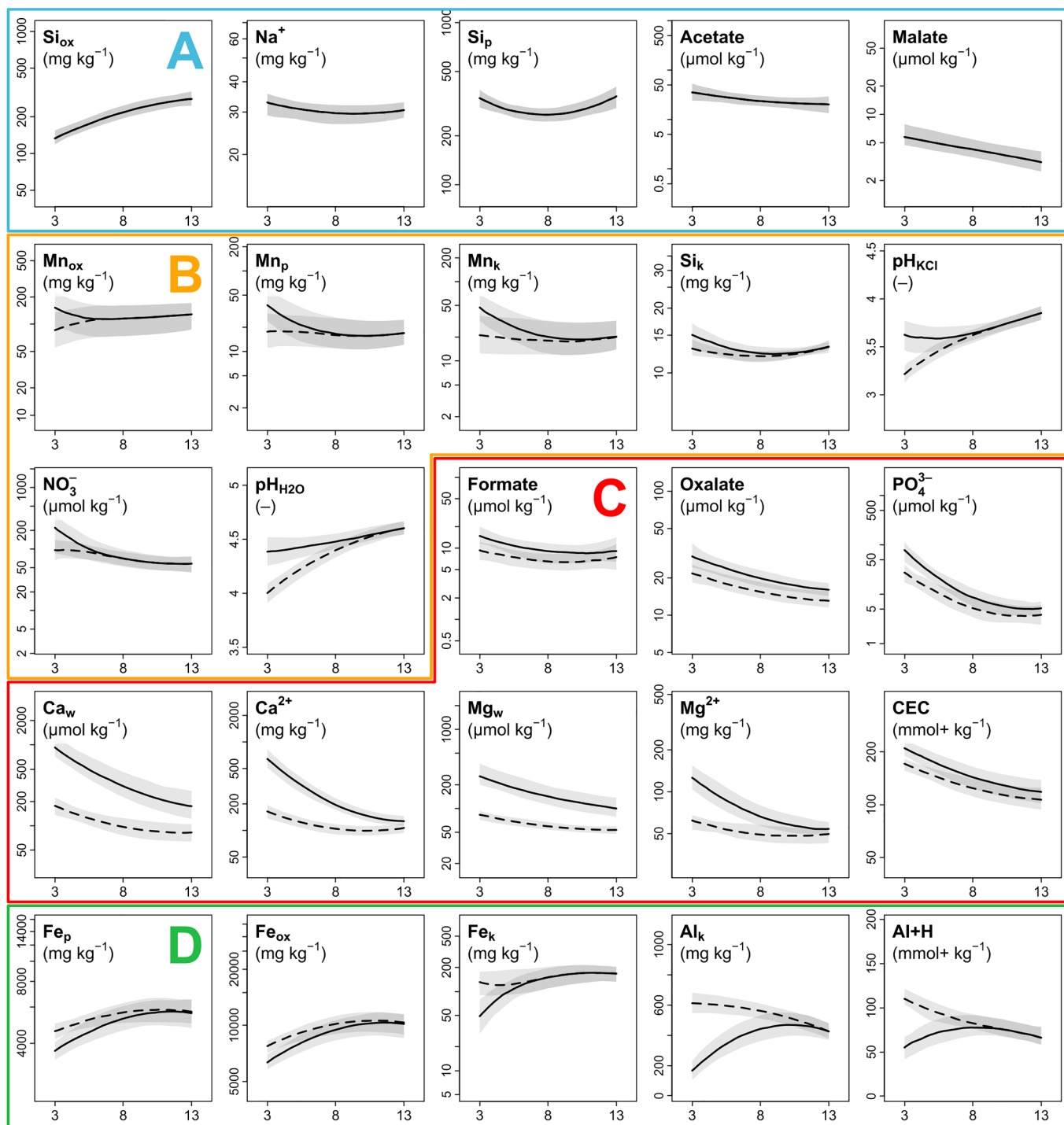


Fig. 5. Modelled values of soil characteristics with respect to soil depth. Lines of two types are shown if there were significantly different values under decaying trunks (solid line) and in control sites (dashed line). Grey areas surrounding the lines represent 95% confidence intervals.

(24 units in total). We report only those convergence parameters (and their confidence intervals) for which the optimization converged (a minimum AIC was found for some value within the target interval) and the optimum value was inside the confidence interval. These CIs can be interpreted independently from the overall comparison of model performance based on AIC. Particularly in the case of time-specific models, it may happen that although the time-convergence model did not perform significantly better than the depth-only models, the CI for its time-convergence parameter could have been narrow. This means that although there was not a universal pattern in the development of the soil after the decaying log started to influence it (the time variable itself was

not significant), the period after which the soil returns to its initial condition could still be estimated. The narrower the CI, the more useful this estimate is.

We considered chaotic behaviour to be the situation when the development of a property could take any direction. This results in no universal temporal trend in the development of the differences between the below-trunk sample and the control but rather a clear increase in variance of these differences with time. We searched for evidence of this behaviour separately in each of the three depths (3, 8 and 13 cm) for each studied soil property using generalized least squares (GLS) models. For each case we fitted four GLS models with the observed

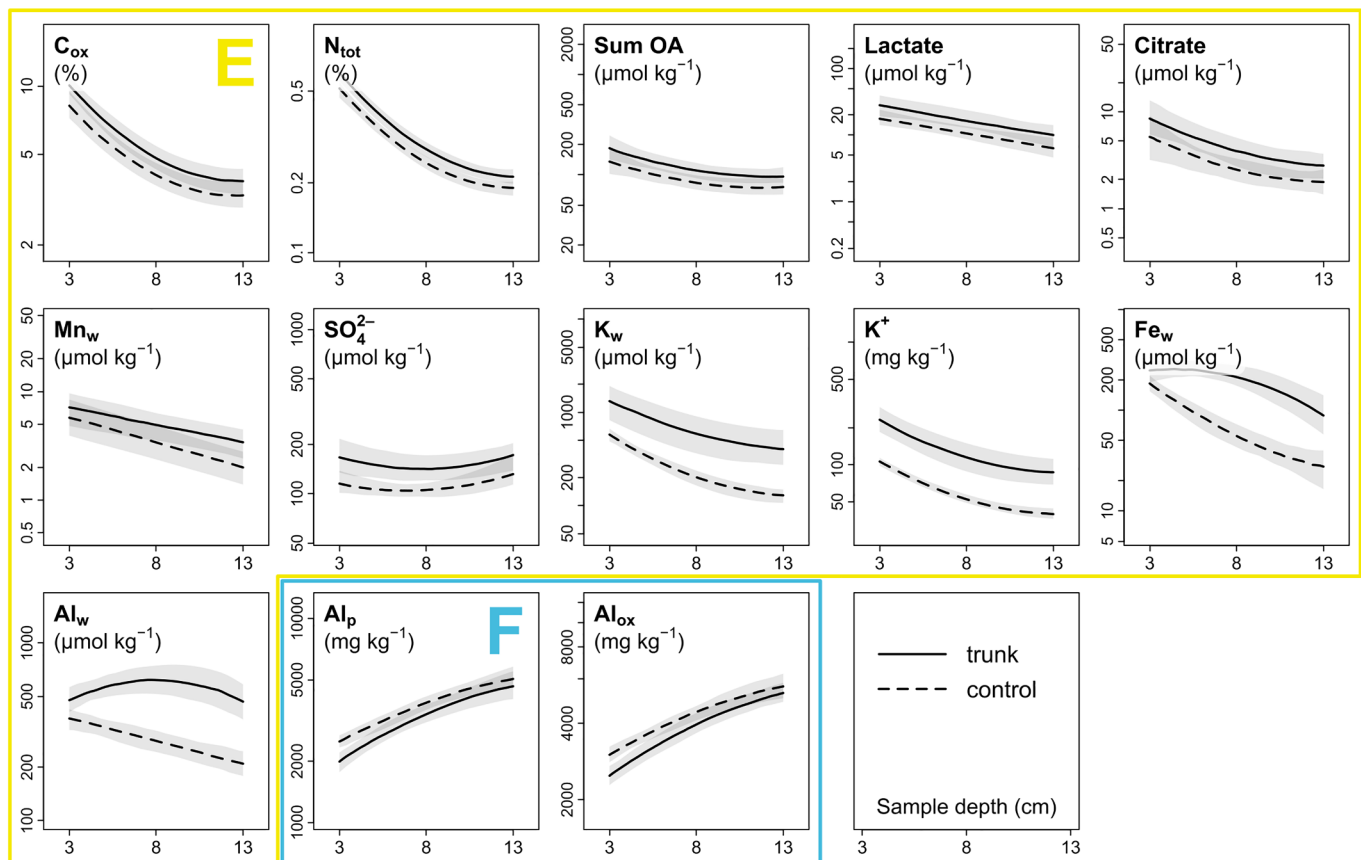


Fig. 5. (continued)

difference between the below-trunk and control values as the dependent variable: 1) a null (intercept-only) model, 2) a linear-trend model with trunk age as an explanatory variable, 3) a null model with variance modelled as a power function of trunk age, and 4) a linear-trend model with age both as an explanatory variable and a covariate for modelling variance (the same as in model 3). Among these four models, chaotic behaviour corresponds to model 3, and we considered it plausible if this model performed significantly better than models 1 and 2, was not significantly outperformed by model 4, and the estimated power exponent for variance was positive. Again, a model was considered significantly better performing if its AIC was at least 4 units lower than that of a competing model. For LMM and GLS fitting we used the nlme package (Pinheiro et al. 2019) in R (R Core Team, 2019).

3.5.2. Bioinformatic workflow and statistical analyses

The sequencing data were processed using SEED v 2.1.05 (Větrovský et al., 2018). Briefly, pair-end reads were merged using fastq-join (Aronesty 2013). Sequences with ambiguous bases were omitted, as were sequences with a mean quality score below 30. Chimeric sequences were detected using UCHIME implementation in USEARCH 8.1.1861 (Edgar 2010) and deleted, and sequences shorter than 200 bp were also removed. Filtered sequences were clustered using the UPARSE algorithm implemented in USEARCH 8.1.1861 (Edgar, 2013) at a 97% similarity level. OTU construction was done together with previously published (Baldrian et al., 2016; Tláškal et al., 2017) sequences obtained from wood samples of proximal trunks to enable comparisons between mineral soil and wood inhabiting taxa. The most abundant sequences were taken as representative for each OTU. To assign taxonomy, the closest hits at a genus or species level were identified using BLASTn 2.5.0 against the Ribosomal Database Project (Cole et al., 2014) and GenBank databases. Sequences identified either as no hits or as nonbacterial/nonfungal were discarded. To assign

putative ecological functions to fungal OTUs, fungal genera of the best hit were classified into ecophysiological categories (e.g., white-rot, brown-rot, saprotroph, yeast, ectomycorrhiza) based on the published literature. The definition of categories was the same as in (Tedersoo et al., 2014). Fungal OTUs not assigned to a genus with known ecophysiology and those assigned to genera with unclear ecophysiology remained unassigned. Sequence data have been deposited into the NCBI database under the accession number PRJNA558885.

Multivariate analysis of microbial abundance data with environmental variables was performed using *vegan* package 2.5–5 (Oksanen et al., 2019) in R 3.6.0 (R Core Team 2019). The function *adonis* was used to test for significant differences in community composition among compartments (WO – deadwood, LO – litter, WA – upper mineral A soil horizon below deadwood, LA – upper mineral A soil below the litter, WBS-upper – mineral soil 5 cm below A horizon in the deadwood microsite, LBS-upper – mineral soil 5 cm below the A horizon in litter microsite) based on the Hellinger distance of the datasets containing relative abundances of the 200 most abundant bacterial and fungal OTUs. Permutation in *adonis* was constrained to individual sites using the *strata* option to filter out possible spatial effects. Two-dimensional non-metric multidimensional scaling (NMDS) ordination analysis on Hellinger distances was performed in R with the package *vegan* and the function *metaMDS*. Environmental variables were fitted using the function *envfit* to the ordination diagram as vectors with 999 permutations. Square rooted values of variables with non-normal distribution were used for fitting. Only significant variables with high R^2 values were displayed in resulting plots. Differences at $P < 0.05$ were regarded as statistically significant. Microbial abundance (qPCR) was tested by a pairwise comparison of deadwood and litter at the corresponding site using a pairwise Wilcoxon test.

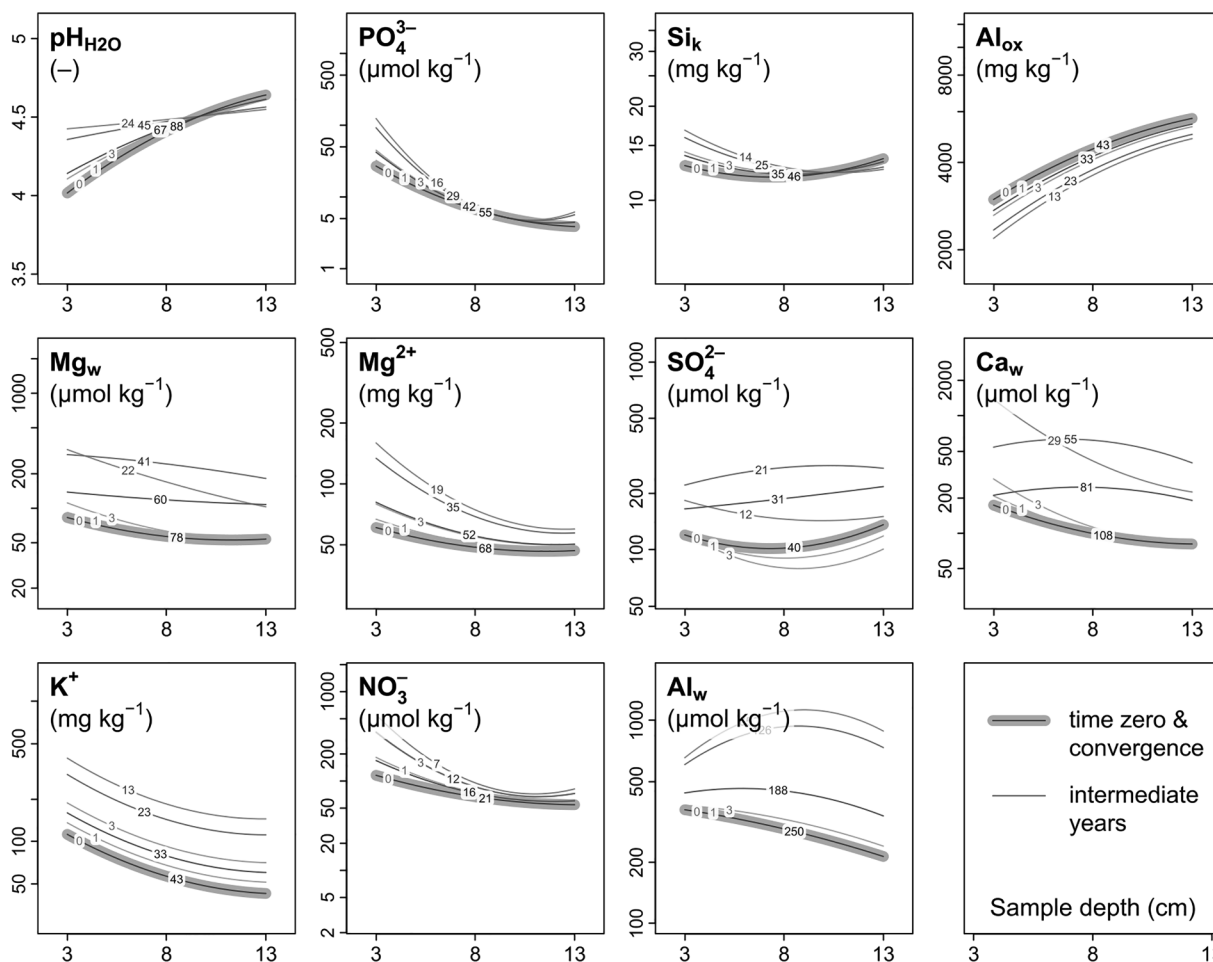


Fig. 6. Modelled values of soil characteristics with respect to soil depth and time of trunk decay. All models assume convergence, i.e. as the trunk decays the values start to change but eventually they return back to the state at time zero (thick line). The temporal progression of this process is depicted by thin lines marked with the time of decay (in years) to which they correspond.

4. Results

4.1. Relationship between soil properties

Mean values and standard deviations of 38 soil properties show a general picture of acidic podzolized soils with a predominance of amorphous and organically bound fractions of Al and particularly Fe (Fig. 1). Cation exchange capacity was highly variable, generally weak, and dependent on the amount of organic matter in soils. The amount of organic C was relatively high. The concentrations of nutrients were changeable and generally low, with Ca the most common. Many soil properties were naturally correlated with each other (Fig. 1). The highest correlation ($r = 0.98$) was found between concentrations of K in the water extract, which imitates the soil solution and easily available forms, and available K^+ based on Gillman’s approach. There was a correlation ($r = 0.96$) between active and exchangeable soil reaction values, but their large differences reflected a highly acidic soil environment. Many relations were statistically significant at $\alpha = 0.001$ (Fig. 1), and models of property behaviour in soil were also sometimes very similar (see below). As mentioned above, concentrations of base cations in the water extract (Ca_w , Mg_w , K_w) developed similarly as the concentrations of cations in standardized and the more powerful Gillman’s extract. Concentrations of active, organically bound and amorphous forms of metals and metalloids gradually increased with increasing powerful extraction, and their models resembled each other (maximal correlation coefficients between these forms of elements were 0.28–0.94). This suggests that there was a similar proportion of forms in

many samples. As expected there was a high correlation between C_{ox} and N_{tot} ($r = 0.92$) and between characteristics of the sorption complex.

4.2. Trunk decay

The multidirectional redundancy analysis revealed a significantly different chemical composition in decomposed trunks versus leaf material in the control profile (Tab. 1, Fig. 2). Trunks had a higher proportion of organic carbon but a lower proportion of total nitrogen; differences in the nitrogen anion NO_3^- were minor. We also found higher values of active and exchange soil reaction and simultaneously lower concentrations of water-extracted Al and Fe (Al_w , Fe_w) in woody material compared to leaves. Concentrations of organic acids were slightly higher in wood as well, while the concentration of PO_4^{3-} was slightly higher in leaf material. The mean time of convergence of the decaying trunk to the characteristics of the control profile was 40–50 years (Fig. 3c, see below).

4.3. General effects of microsite and sample depth in the mineral soil

The redundancy analysis (RDA) showed a significant role of microsite (wood versus litter) and sample depth in the mineral soil (Tab. 1, Fig. 4). The effect of microsite was significant in all horizons and depths, and slightly decreased along the gradient of sample depth. These results should be considered to be averages about the whole data set, and cannot be used to evaluate the detailed shape and range of

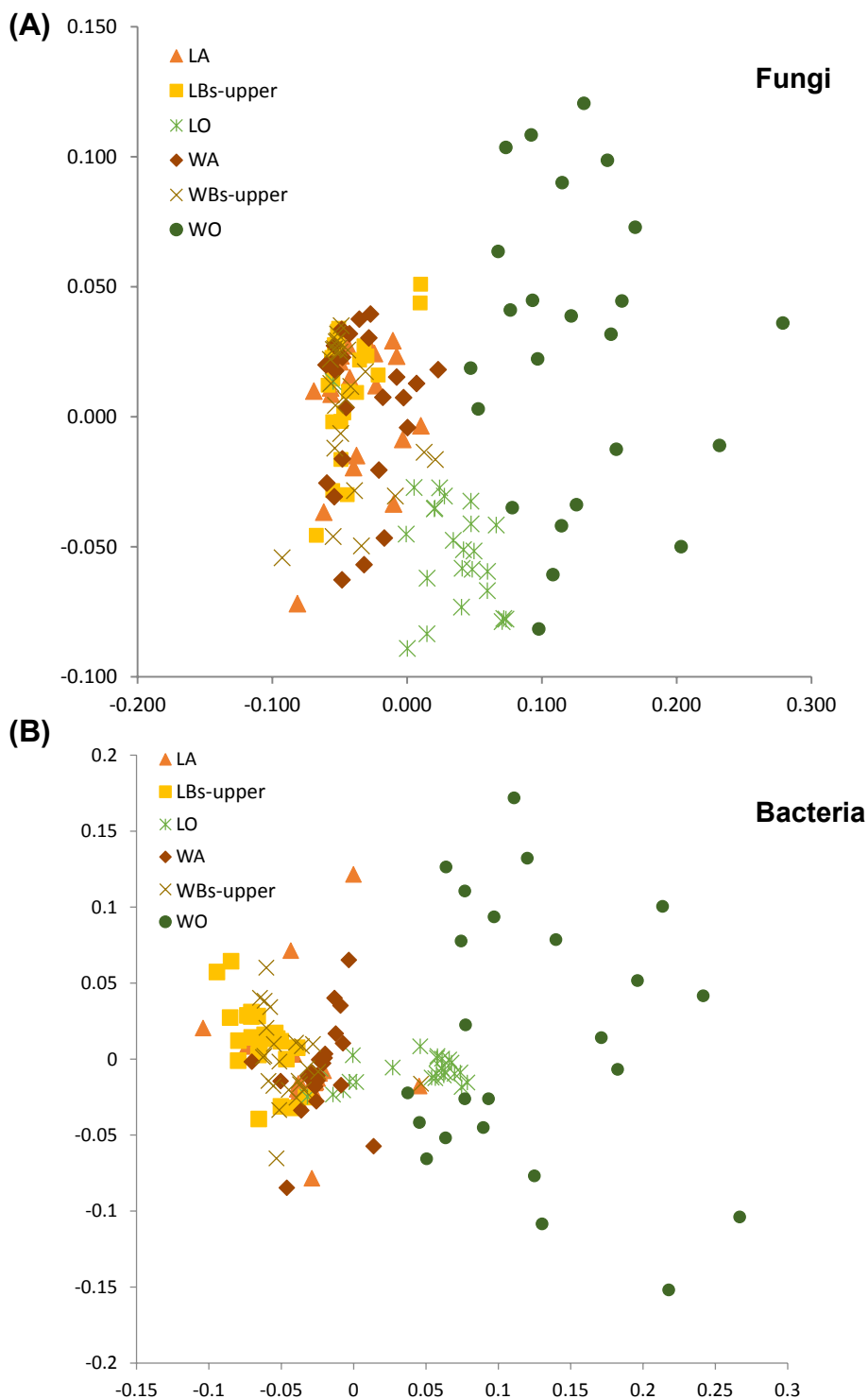


Fig. 7. Two-dimensional NMDS of fungal (A) and bacterial (B) communities in decomposing wood, litter and soil in Zofin. The dataset contained the top 200 OTUs of bacteria or fungi.

individual soil properties. For that purpose, we calculated individual models (see below).

In general, individual characteristics developed predictably along the depth gradient (Fig. 4), following the transitions between organic, upper mineral A, and deeper spodic horizons. Soil characteristics of biogenic origin (C_{ox} , N_{tot} , organic acids etc.) decreased with sample depth. On the other hand, characteristics of rather geogenous origin (e.g. amorphous forms of Si, Al, Fe) increased with increasing sample depth. Increased values of active and exchangeable pH with sample

depth was clearly related to a greater the decrease of exchangeable acidity, which was higher than the decrease in the concentration of basic cations bound to the low soil clay content, especially in organic matter. The cation exchange capacity decreased with the depth as well, which is in line with the decreasing concentrations of C_{ox} .

The mineral soil below the trunk generally had higher amounts of nutrients than control, especially very active forms found in the water extract (Fig. 4). The higher exchangeable acidity and higher concentration of Al in the KCl extract are naturally related. Soils affected by

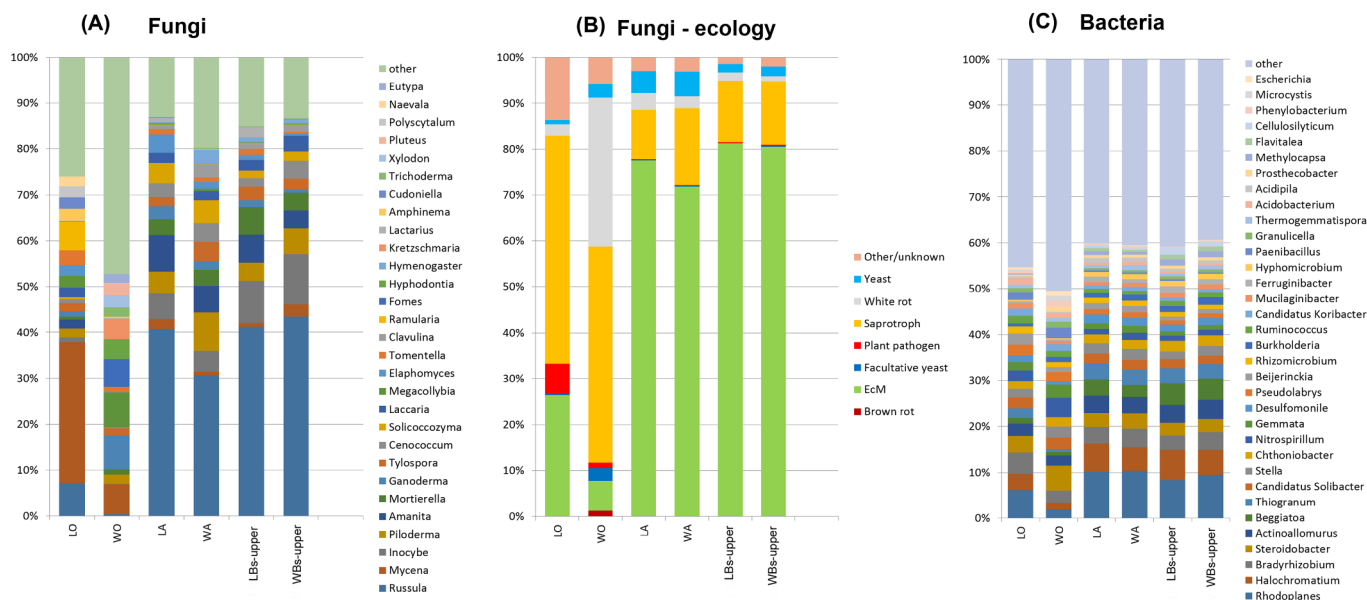


Fig. 8. Composition of fungal communities (A), fungal ecological groups (B) and bacterial communities (C) in decomposing wood, litter and soil in Zofin.

trunk decay also generally showed higher active and exchange soil reaction, cation exchange capacity, and concentrations of some organic acids (lactate, oxalate etc.).

4.4. Detailed pedogenetic pathways in the mineral soil

All 38 soil properties separately showed a significant relationship to the soil sample depth. The relation to microsite could be classified into 6 groups (Fig. 5). Only 5 soil properties showed no difference between the profile under the trunk and the control profile (group A in Fig. 5). These were amorphous and organically bound forms of Si, Na content and some organic acids. Some of these properties were found in very low concentrations across the entire dataset (Na, acetate, malate), and therefore it is not surprising that their models were insignificant. Concentrations of Si forms were not limiting, but more reflect geogenic factors and not the presence of lying trunks.

A total of 22 soil characteristics (58%) converged below the trunk at different depths towards the control values (groups B, C, D, F in Fig. 5). The model depths of convergence, along with the widths of the confidence intervals, are shown in Fig. 3a. For 7 chemical soil properties, values below the trunk were significantly higher than in the control and converged at a very low depth of about 10 cm (group B). These included the most active form of Si (Si_k), all evaluated forms of Mn, both types of soil reaction and NO_3^- . Below, at depths between 19 and 65 cm, 8 characteristics converged (group C). Most of these were basic anions or cations of nutrients, effective CEC, and oxalate concentrations. A total of 7 soil characteristics were higher in the control profile than under the trunk. Five of them converged just below the trunk (group D), and included organically bound and amorphous forms of Fe, active Al, as well as exchangeable acidity. With the exception of the active Fe_k , which already converged in the A horizon, the other characteristics converged within a maximum of 13 cm depth. Organically bound and amorphous forms of Al were significantly lower under the trunk than in the control profile, and converged only at considerable depth (group F).

Altogether, 11 soil properties did not converge at any depth, or the models even diverged. All of them were positively influenced by the presence of the trunk (group E in Fig. 5). These comprised organic C and N contents in soil, some organic acids as well as very mobile concentrations of nutrients (K) and metals (Fe_w , Al_w , Mn_w).

For 11 chemical soil properties, the age of the decomposing trunk was statistically significant, and it was possible to model the

pedogenetic soil pathways in detail along the age and depth gradients (Fig. 6). With the exception of amorphous Al, all properties were very dynamic (contents of nutrient cations and anions, extracts with weakly aggressive agents – H_2O , KCl). Most of these characteristics belonged to groups B, C and E in Fig. 5, i.e. convergence models predominated. With the decomposition of the trunk, these models showed a gradual deviation in the developmental trajectory from the control profile to stage of maximal divergence, and then usually convergence back to control values. The maximal divergence ranged between 12 and 60 years, averaging 25 years after the tree fall. The modelled convergence point back to the control values occurred at ages between 39 (SO_4^{2-}) and 229 (Al_w) years (Fig. 3b). This long-term response of water-extracted Al is quite surprising, considering the known seasonal variability of these forms. The median convergence time for analysed soil properties was 53 years.

We found only very limited evidence for chaotic behaviour in soil development. Only three property-depth combinations exhibited signs of chaotic development (Appendix B), and given that 114 tests were performed in total, these may have been just due to random results within the 5% Type I error rate. Furthermore, in all these three instances a well-fitting model with depth or age was found. Therefore, chaotic soil development under a decaying tree trunk does not appear to be a likely scenario.

4.5. Effects of deadwood on the microbiome composition

To explore the effects of changes in soil chemistry induced by deadwood decomposition, microbial communities were compared in decaying deadwood versus in leaf litter (i.e. two corresponding organic horizons), and in mineral soils under decomposing trunks versus under leaf litter. The communities of both fungi and bacteria in decaying leaves and wood were significantly different ($p < 0.0001$), with the wood community expressing a much higher composition variability than that in leaf litter (Fig. 7). Members of the bacterial order *Rhizobiales* genera *Rhodoplanes* and *Bradyrhizobium* were enriched in leaf litter (Fig. 8). The genera *Nitrospirillum* and *Steroidobacter* were abundant in wood.

Soil communities were dominated by Proteobacteria that represented around 50% of the whole community, followed by Actinobacteria, Firmicutes and Acidobacteria. The most abundant bacterial genera in soil were *Rhodoplanes* and *Halochromatium* (Fig. 8).

Another genera enriched in soil in comparison with litter were *Beggiatoa* and *Thioplanum*. Importantly, bacterial communities were significantly different between soil horizons ($p = 0.001$, $R^2 = 0.131$), and this was consistent below both the trunk (W-wood) and the leaves (L, Fig. 9B). This horizon effect was stronger for bacteria than for fungi (see below). The effect of decomposing wood (sites under trunks versus under leaves) on bacterial community in mineral soils was significant as well

($p = 0.004$, $R^2 = 0.034$), and likely resulted from higher C and N availability under wood than under litter (Fig. 9B). However, the interaction of horizon and position effect was not significant. *Gamma-proteobacteria* showed a preference for sites rich in Fe, while *Betaproteobacteria* occurred at higher pH at sites rich in Ca, Mg and Mn (Appendix C).

Fungal communities in decomposing wood and leaves were

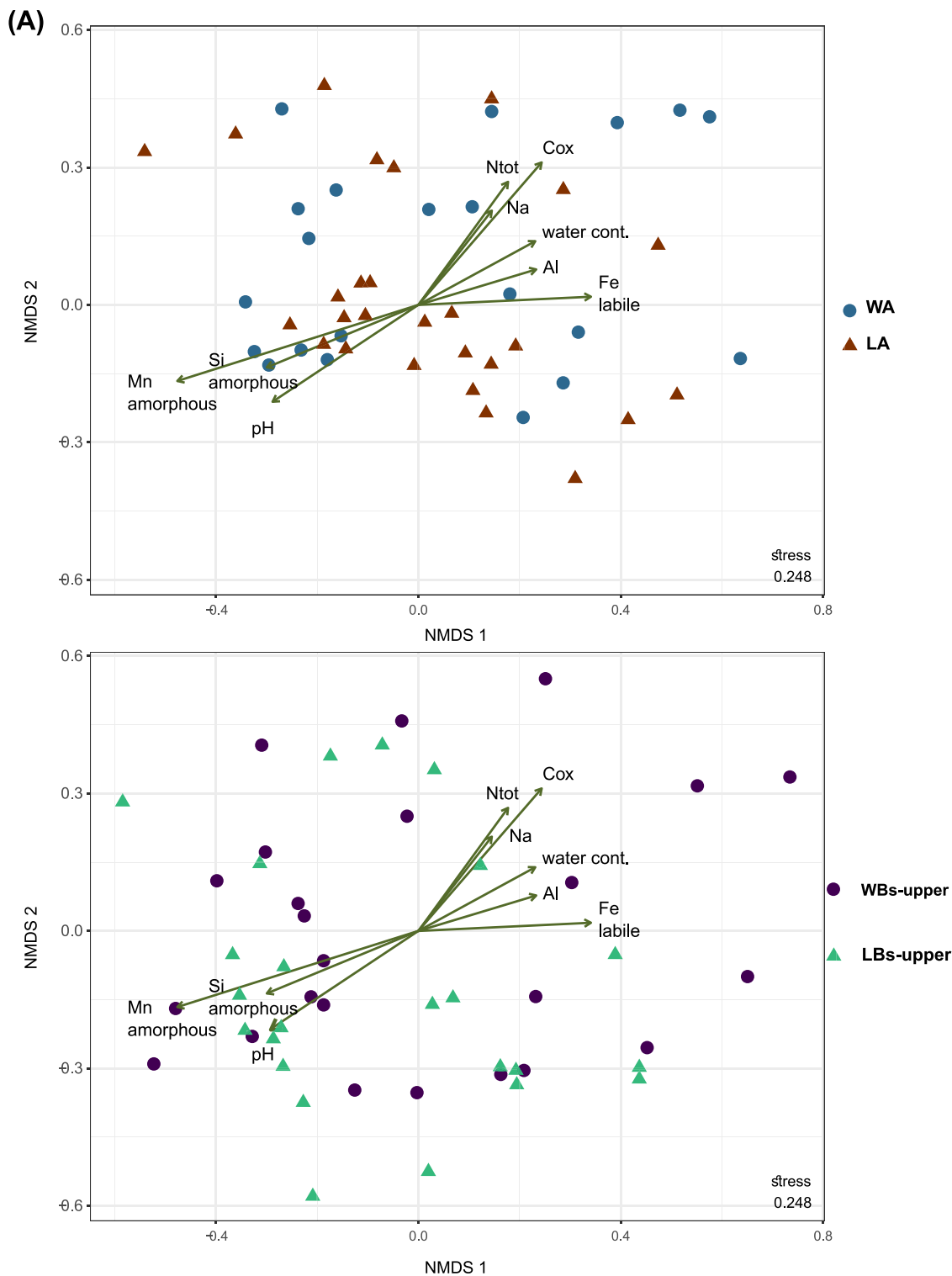


Fig. 9. Two-dimensional NMDS of microbial communities in soils of the A and Bs-upper horizons under litter and under wood in Zofin. The ordination of individual sites for fungi (A) and bacteria (B) are shown. The vectors show environmental variables with significant ordination to NMDS axes ($p < 0.05$) and high R^2 values. Samples from both horizons are shown in separate panels for clarity.

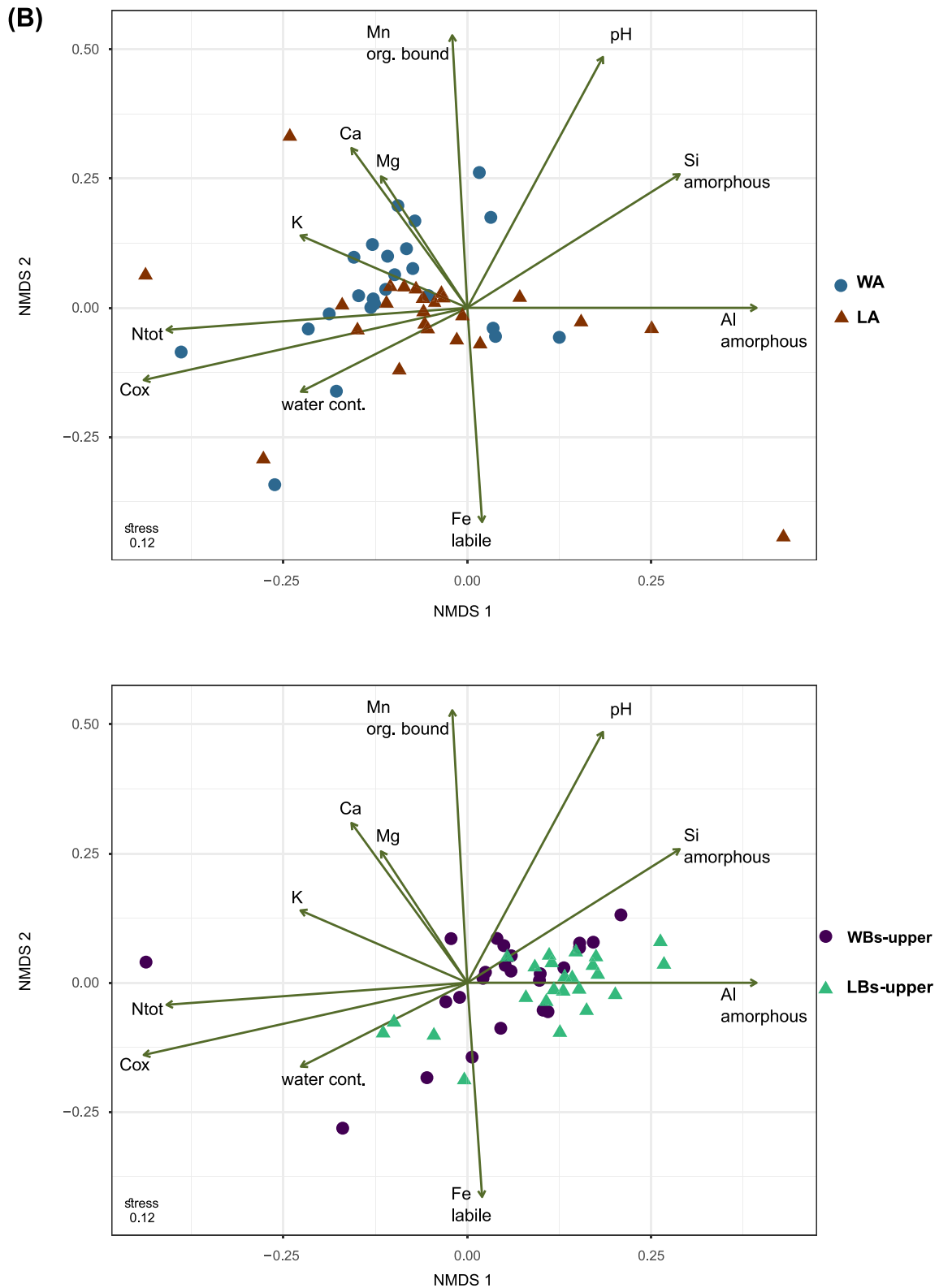


Fig. 9. (continued)

dominated by *Mycena*, *Megacollybia*, *Fomes*, *Hyphodontia*, *Ganoderma* and *Kretzschmaria*. Mineral soil horizons were rich in *Inocybe*, *Piloderma*, *Cenococcum* and *Amanita* (Fig. 8). In the soil below wood we did not find typical wood decomposers. Fungal communities in the A horizon and upper Bs horizon were significantly different (i.e. soil horizon effect, $p = 0.001$, $R^2 = 0.033$) as were those from the soil

below the wood and below the litter (i.e. decomposing wood effect, $p = 0.001$, $R^2 = 0.022$, Fig. 9A) where difference in C and N availability was a strong driver of the microbial community. At the class level, fungal taxa did not display a preference for sites with a higher content of some nutrient with the exception of *Eurotium* OTUs, which occurred preferentially at high pH sites rich in Si, Mn, C and N

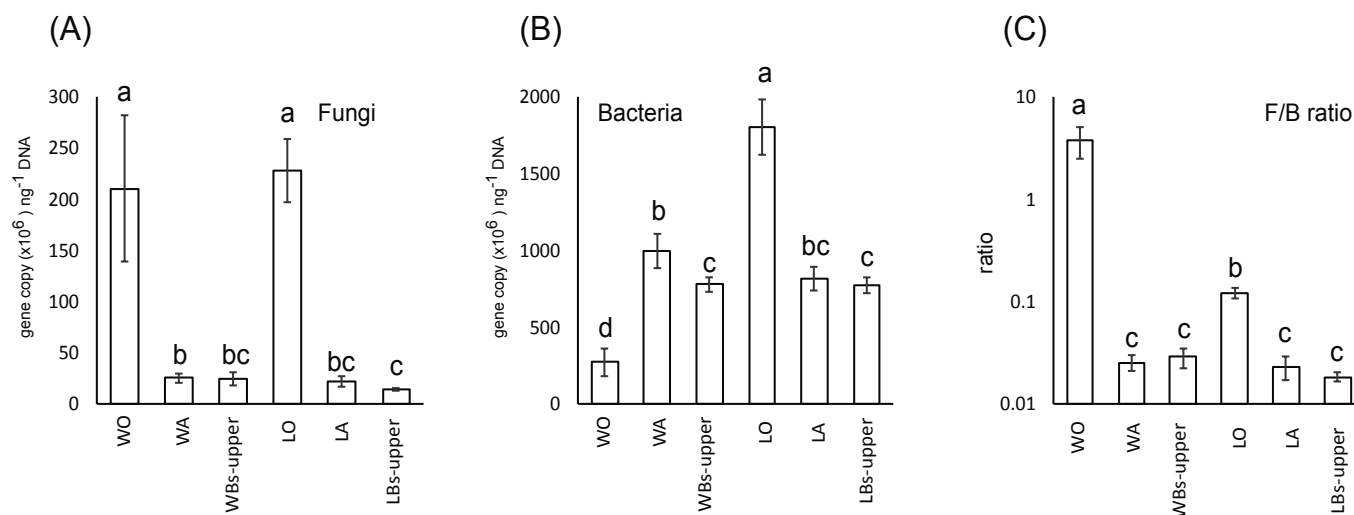


Fig. 10. Biomass content of A) fungi, B) bacteria and C) fungal/bacterial biomass ratio in decomposing wood, litter and soil in Zofin. The data show means and standard errors of counts ($\times 10^6$) of A) 18S rRNA B) 16S rRNA gene copies in 1 ng of DNA.

Table 1

Adjustment of multidirectional redundancy analyses (RDA) and their results.

Environmental data	Covariable data	Soil layer	Average depth of sample (cm)	No. samples	No. soil properties	Explained variability (%)	p-value	F-value
Sample depth (cm)	Microsite	All mineral	3–13	144	38	13.1	< 0.001	21.3
Microsite	Sample depth	All mineral	3–13	144	38	6.2	< 0.001	9.6
Microsite		0 horizon	0	48	20	12.1	< 0.001	6.4
Microsite		A horizon	3	48	38	15.4	< 0.001	8.0
Microsite		5 cm below A	8	48	38	8.5	< 0.001	4.3
Microsite		10 cm below A	13	48	38	6.7	0.004	3.3

(Appendix C).

According to fitted nutrient concentrations onto the microbial multidimensional ordination, the composition of fungal communities was generally most influenced by the content of nutrients, Cox and Ntot, but also by the concentrations of Mn, Al, Si, Fe and Na. Similarly, the composition of bacterial communities among individual microsites was driven by C_{ox} , N_{tot} , Mg^{2+} , Mn, K, Ca, Al, Fe, and Si (Fig. 9, Appendix D).

The content of fungal biomass was similar in wood and litter ($2.1 \times 10^8 \pm 0.3 \times 10^8$ of rDNA copies g^{-1} and $2.3 \times 10^8 \pm 0.8 \times 10^8$), and significantly higher than in soil where it ranged between $0.14 \times 10^8 \pm 0.02 \times 10^8$ and $0.26 \times 10^8 \pm 0.05 \times 10^8$; however, differences between A and Bs upper horizons and between soils under litter and wood were not significant (Fig. 10). In bacteria, litter was most rich with $18.0 \times 10^8 \pm 1.8 \times 10^8$ of rDNA copies g^{-1} , while the fewest bacteria were found in deadwood ($2.7 \times 10^8 \pm 0.9 \times 10^8$). Soils harboured between $7.7 \times 10^8 \pm 0.5 \times 10^8$ and $9.9 \times 10^8 \pm 1.0 \times 10^8$ rDNA copies g^{-1} , and the differences between soils under litter and wood were not significant; the ratio of fungi and bacteria in soils was between 0.018 and 0.028 (Table 1).

5. Discussion

Along a gradient of weathering and leaching on acidic rocks in the temperate zone, Entic Podzols occupy a special position. From the point of view of pedogenesis, these are Podzols, soils with spodic horizons formed through the chemical destruction of clay particles and the gradual illuviation of organo-metallic complexes (Buurman and Jongmans, 2005, Sauer et al., 2007). However, from the perspective of the ecological role of soils in forest dynamics, these soils can be considered rather initial Cambisols than Podzols. In other words, the ecological role of soils in forest dynamics does not follow their genetic (and

diagnostic) character in this case. Šamonil et al. (2015, 2018) found (during the research of biomechanical effects of trees due to tree uprooting) that Albic Podzols develop divergently after mechanical soil disturbances, but Haplic Cambisols develop convergently. From the viewpoint of typical genetic sequence of the soil evolution (with respect to more evolutionary trajectories, Huggett, 1998), Entic Podzols appear roughly between Albic Podzols and Haplic Cambisols, and may express most the interesting responses to local mechanical or chemical disturbances. This was demonstrated by our current research here, where the majority of chemical soil properties expressed soil convergence but a significant proportion of properties developed in different or even opposite trajectories. Such a picture of opposing trajectories of soil properties was also described by Šamonil et al. (2015) and (2018), who found podzolic horizon thicknesses exhibiting divergence in time, while chemical properties behaved convergently. These findings may supplement the traditional concept of soil evolution on the border between Cambisols and Podzols (see Schaeztl et al., 1994).

Using mathematical modelling we distinguished divergent, convergent and chaotic behaviours of individual soil properties. The majority converged by 25 cm below the decomposing trunk and during the first century after trunk fall. We expect that decreasing inputs of chemical compounds from gradually decomposing and shrinking beech trunk (potentially associated with changes in hydrological and microclimatological conditions, e.g. deadwood partly saturated by rain water) and a still sufficient cation exchange capacity in Entic Podzols allowing the capture of the components drive pedogenetic convergence under deadwood. Unfortunately, as far as we know, comparable studies including detailed models with predictions of soil development do not exist. We can only generally support the results of Kayahara (1998), who found a positive effect of coniferous decaying trunks in the amount of nutrients in mineral soils (cf. Kayahara et al. 1996). A similar finding was observed by Dhiedt et al. (2019) below beech trunks on Umbrisols and Retisols in Belgium. In Cambisols in Germany, Stutz et al. (2017)

found higher effective CEC, exchangeable Ca^{2+} , Mg^{2+} , and base saturation below beech trunks as well. The authors concluded that deadwood affects soil through the composition of added phenolic matter. We expect that beech deadwood produced more water extractable organic carbon (Stutz et al. 2019), and this DOC increased the mobility of Al and Fe. Also, higher contents of LMMOA under trunks consequently lead to lower contents of Al and Fe in soils (Hubová et al. 2018). These mentioned results are partly in contradiction with the conclusions of Spears and Lajtha (2004) concerning coniferous trunks on Andisols in Oregon, US. Similarly Goldin and Hutchinson (2013) described a rather acidifying effect of eucalyptus trunks on Regosols, Leptosols, Luvisols, and Solonetz in Australia. However, neither studied specific Entic Podzols below decaying *Fagus sylvatica* trunks. As suggested by Šamonil et al. (2018), it is likely that the resulting effect of a decomposing trunk is very dependent on the particular soil-forming process, notably the soil's ability to absorb the released nutrients and organic compounds. Entic Podzols in Zofin still retain this ability although continuing podzolization was evident. Entic Podzols are sensitive to biochemical tree influences, which may temporarily increase spatial soil complexity on local scales in forested landscapes.

The unimodal course of exchangeable acidity, Fe forms and active Al in the water extract, as well as the correlation between LMMOA and Fe forms (Fig. 1), may all indicate podzolization with an initiation of the illuviation of organo-metallic complexes under trunks. This process originates at the base of the A-horizon, in our case at an average depth of 8 cm. However, the evolution of the eluvial and illuvial horizons was not yet evident, because the dynamics of other soil properties did not follow this suggested trend. The soil was already podzolized but still had the ability to bind larger amounts of substances released during trunk decomposition. Nonetheless, the significant depths at which some characteristics converged to the control values (see below) as well as the non-convergent development of others (e.g. C_{ox}) strongly suggest that the ability of Entic Podzols to absorb released substances from trunks was relatively low. There was a clear movement of chemical compounds (e.g. LMMOA) produced by trunk decay to deeper soil horizons.

The biomass of both fungi and bacteria in soils was generally similar below the trunks and leaves, suggesting that leaching nutrients from decomposing wood does not support the growth of microorganisms to higher densities than in the surrounding soil. Despite the effects of decomposing trunks on soil properties, we found their effects on the microbial community composition to be minor. This is similar to that found in a comparison of fungi under litter and decomposing *Picea abies* trees in Finland, which were, however, distinctly different and showed soil colonization by wood-associated fungi (Mäkipää et al. 2017). While there were a few taxa with a preference for sites with higher concentrations of leached nutrients, most taxa did not show such preference. This is in contrast with the impact of living trees, which actively transfer exudates to underlying microbial communities and where fungi are determined by tree species and bacteria show a preference for particular rhizosphere habitats (Urbanová et al. 2015; Uroz et al. 2016). In our study, a higher abundance of fungi typically associated with decomposing wood was not observed in the soil under dead trees. In an experiment where the decomposing wood of multiple trees was incubated on top of *Picea abies* soil in the laboratory, both microbial biomass and community composition differed from controls and also among tree species (Peršoh and Borken, 2017). The most pronounced differences in composition were among different habitats – wood, leaf litter and soil. Wood and litter, as a C rich and N limited substrate, hosted fungal saprotrophic degraders specialized for C uptake from recalcitrant polymers and bacteria known for N fixation or from associations with fungal hyphae (Uroz et al., 2012; Mäkipää et al. 2018). On the other hand, several bacterial taxa enriched in soil were chemolithotrophs and dominant fungi are known from ectomycorrhizal association with plant roots (Bahnmann et al. 2018; Lladó et al. 2018). In our study, soil fungi and bacteria within individual microsites were

affected by soil chemistry that responded to trunk decomposition, with the most important being C_{ox} , N_{tot} , Mg^{2+} , Mn and Al. However, the wood-on-soil effects were weak, and for bacteria the wood influence was overridden by the influence of individual horizons. The minor response of the fungal community in this study is likely due to the high spatial variability of the community in decomposing wood, forest floor and upper mineral soil horizons, which is substantially higher than that of bacteria (Štursová et al. 2016, Baldrian et al., 2016; Tláškal et al., 2017).

6. Conclusion

The evolution of Entic Podzols below decaying *Fagus sylvatica* trunks was evaluated in an old-growth temperate mountain forest. Using extensive sampling and laboratory analyses, we obtained a detailed picture of the process of wood decay, pedogenetic pathways and the composition of fungal and bacterial communities in both organic matter and in underlying mineral soils. Soil convergence was the prevailing pedogenetic pathway, although some individual soil properties expressed chaotic or even divergent pointing.

Soils below the decaying trunk followed generally unimodal pedogenetic trajectory culminating about 25 years after trunk fall. After ca 53 years, soils typically converged to the characteristics of the control soil (i.e. below the leaves). The changes were marked especially in the uppermost soil horizons, but modelled wood decomposition footprints were found even at a depth of 60 cm for some soil properties. Changes in the composition of bacterial and fungal communities were greatly restricted to the litter layer and uppermost mineral horizon, despite the finding that many important chemical drivers differed significantly between the trunk and control sites, even in deeper soil horizons (CEC, Ca^{2+} , Mg^{2+} , Al_{ox}) or did not converge at all (C_{ox} , N_{tot}). There is likely an additional barrier preventing the deepening of the trunk effect in microbiome compositions in mineral soil. This is most likely associated with unmeasured physical properties of different environments and requires further attention.

Our results demonstrate the complexity of soil evolution, and highlight the necessity to study a wide spectrum of soil properties in detail. Using only a few properties, one might obtain a highly biased picture of pedogenesis. Biochemical effects of lying beech trunks certainly increase the spatial soil complexity but this effect is rather temporary. Human interventions preventing the presence of newly decaying logs, for example by trunk haulage, will thus most likely decrease the soil spatial complexity. The response of soil will be long-lasting and qualities may rejuvenate based on changed management practices.

Declaration of Competing Interest

The authors declare that they have no known competing financial interests or personal relationships that could have appeared to influence the work reported in this paper.

Acknowledgement

The authors would like to thank Ondřej Paták for help with data collection in Zofin. The project was supported by the Czech Science Foundation (project No. 19-09427S – attendance of Pavel Šamonil and Pavel Daněk in team; project No. 17-20110S – attendance of Petr Baldrian and Vojtěch Tláškal).

Appendix A. Supplementary data

Supplementary data to this article can be found online at <https://doi.org/10.1016/j.geoderma.2020.114499>.

References


- Amann, R.L., Ludwig, W., Schleifer, K.H., 1995. Phylogenetic Identification and in-Situ Detection of Individual Microbial-Cells without Cultivation. *Microbiological Rev.* 59, 143–169.
- Aronesty, E., 2013. Comparison of Sequencing Utility Programs. *Open Bioinformatics J.* 7, 1–8.
- Bahnmann, B., Mašínová, T., Halvorsen, R., Davey, M.L., Sedláč, P., Tomšovský, M., Baldrian, P., 2018. Effects of oak, beech and spruce on the distribution and community structure of fungi in litter and soils across a temperate forest. *Soil Biol. Biochem.* 119, 162–173.
- Baldrian, P., Zrůstová, P., Tláškal, V., Davidová, A., Merhautová, V., Vrška, T., 2016. Fungi associated with decomposing deadwood in a natural beech-dominated forest. *Fungal Ecol.* 23, 109–122.
- Binkley, C., Giardina, D., 1998. Why do tree species affect soils? The warp and woof of tree–soil interactions. *Biogeochem.* 42, 89–106.
- Bockheim, J.G., 1980. Solution and use of chronofunctions in studying soil development. *Geoderma* 24, 71–85.
- Bremner, J.M., 1996. Nitrogen-total. In: Sparks, et al. (Eds.), *Methods of Soil Analysis. Part 3. Chemical Methods. Number 5 in Soil Science Society of America Book Series.* Soil Science Society of America, Inc. and American Society of Agronomy, Madison, Wisconsin, pp. 1085–1121.
- Burnham, K.P., Anderson, D.R., 2004. Multimodel Inference: Understanding AIC and BIC in Model Selection. *Sociol. Method. Res.* 33, 261–304. <https://doi.org/10.1177/0049124104268644>.
- Buurman, P., Jongmans, A.G., 2005. Podzolisation and soil organic matter dynamics. *Geoderma* 125, 71–83.
- Caporaso, J.G., Lauber, C.L., Walters, W.A., Berg-Lyons, D., Huntley, J., Fierer, N., Owens, S.M., Betley, J., Fraser, L., Bauer, M., Gormley, N., Gilbert, J.A., Smith, G., Knight, R., 2012. Ultra-high-throughput microbial community analysis on the Illumina HiSeq and MiSeq platforms. *ISME J.* 6, 1621–1624.
- CGS, Geological map 1:50000, Czech Geological Survey, available at: www.geology.cz, last access: November 2019, 2019.
- CHMU, average annual rainfall in period 1961–1990, Czech Hydrometeorological Institute, available at: www.chmu.cz, last access: November 2019, 2019.
- Cole, J.R., Wang, Q., Fish, J.A., Chai, B.L., McGarrell, D.M., Sun, Y.N., Brown, C.T., Porras-Alfaro, A., Kuske, C.R., Tiedje, J.M., 2014. Ribosomal Database Project: data and tools for high throughput rRNA analysis. *Nucleic Acids Res.* 42, D633–D642.
- Courchesne, F., Turmel, M.C., 2008. Extractable Al, Fe, Mn and Si. In: Carter MR, Gregorich EG (eds) *Soil sampling and methods of analysis*. 2nd ed. Canadian Society of Soil Science. CRC Press, Boca Raton, pp 307–315.
- Daněk, P., Šamonil, P., Phillips, J.D., 2016. Geomorphic controls of soil spatial complexity in a primeval mountain forest in the Czech Republic. *Geomorphology* 273, 280–291.
- Dhiedt, E., De Keersmaeker, L., Vandekerckhove, K., Verheyen, K., 2019. Effects of decomposing beech (*Fagus sylvatica*) logs on the chemistry of acidified sand and loam soils in two forest reserves in Flanders (northern Belgium). *Forest Ecol. Manag.* 445, 70–81.
- Drábek, O., Borůvka, L., Mládková, L., Kočárek, M., 2003. Possible method of aluminium speciation in forest soils. *J. Inorganic Biochem.* 97, 8–15.
- Drábek, O., Mládková, L., Borůvka, L., Száková, J., Nikodem, A., Němeček, K., 2005. Comparison of water-soluble and exchangeable forms of Al in acid forest soils. *J. Inorganic Biochem.* 99, 1788–1795.
- Edgar, R.C., 2010. Search and clustering orders of magnitude faster than BLAST. *Bioinformatics* 26, 2460–2461.
- Edgar, R.C., 2013. UPARSE: highly accurate OTU sequences from microbial amplicon reads. *Nat. Methods* 10, 996–998.
- Gillman, G.P., Sumpter, M.E., 1986. Modification of the compulsive exchange method for measuring exchange characteristics of soils. *Aust. J. Soil Res.* 17, 61–66.
- Goldin, S.R., Hutchinson, M.F., 2013. Coarse woody debris modifies surface soils of degraded temperate eucalypt woodlands. *Plant Soil* 370, 461–469.
- Guest, C.A., Schulze, D.G., Thompson, I.A., Huber, D.M., 2002. Correlating manganese X-ray absorption near-edge structure spectra with extractable soil manganese. *Soil Sci. Soc. Am. J.* 66, 1172–1181.
- Hoffman, B.S.S., Anderson, R.S., 2013. Tree root mounds and their role in transporting soil on forested landscapes. *Earth Surf. Proc. Landf.* 39, 711–722.
- Hubova, P., Tejnecký, V., Ceskova, M., Borůvka, L., Němeček, K., Drábek, O., 2018. Behaviour of aluminium in forest soils with different lithology and herb vegetation cover. *J. Inorganic Biochem.* 181, 139–144.
- Huggett, R.J., 1998. Soil chronosequences, soil development, and soil evolution: a critical review. *Catena* 32, 155–172.
- Ihrmark, K., Bodeker, I.T.M., Cruz-Martinez, K., Friberg, H., Kubartova, A., Schenck, J., Strid, Y., Stenlid, J., Brandstrom-Durling, M., Clemmensen, K.E., Lindahl, B.D., 2012. New primers to amplify the fungal ITS2 region - evaluation by 454-sequencing of artificial and natural communities. *FEMS Microbiology Ecol.* 82, 666–677.
- IUSS Working Group WRB, 2014. World Reference Base for Soil Resources 2014. International soil classification system for naming soils and creating legends for soil maps. *World Soil Resources Reports No. 106.* FAO, Rome.
- Jabiol, B., et al., 2013. A proposal for including humus forms in the world reference base for soil resources (WRB-FAO). *Geoderma* 192, 286–294.
- Kayahara, G.J., 1998. Effect of Decaying Wood on the Weathering of Soils in Coastal British Columbia. Canada. *Northwest Sci.* 72, 74–76.
- Kayahara, G.J., Klinka, K., Lavkulich, L.M., 1996. Effects of decaying wood on eluviation, podzolization, acidification, and nutrition in soils with different moisture regimes. *Environ. Monit. Assess.* 39, 485–492. <https://doi.org/10.1007/BF00396163>.
- Klinka, K., Fons, J., Krestov, P., 1997. Towards a taxonomic classification of humus forms; third approximation. *Scientia Silvicæ, Extension Series No. 9.* Forestry Sciences Department, The University of British Columbia, Vancouver. On-line: .
- Lladó, S., López-Mondéjar, R., Baldrian, P., 2018. Drivers of microbial community structure in forest soils. *Appl. Microbiol. Biotechnol.* 102, 4331–4338.
- Mäkipää, R., Leppänen, S.M., Munoz, S.S., Smolander, A., Tiirola, M., Tuomivirta, T., Fritze, H., 2018. Methanotrophs are core members of the diazotroph community in decaying Norway spruce logs. *Soil Biol. Biochem.* 120, 230–232.
- Mäkipää, R., Rajala, T., Schigel, D., Rinne, K.T., Pennanen, T., Abrego, N., Ouskainen, O., 2017. Interactions between soil- and dead wood-inhabiting fungal communities during the decay of Norway spruce logs. *ISME J.* 11, 1964–1974.
- Nachtergale, L., Ghekiere, K., De Schrijver, A., Muys, B., Luysaert, S., Lust, N., 2002. Earthworm biomass and species diversity in windthrow sites of a temperate lowland forest. *Pedobiologia (Jena)* 46, 440–451.
- Oksanen, J., Blanchet, F.G., Kindt, R. et al. 2019. *vegan: Community ecology package.* R package version 2.5–5.
- Peršoh, D., Borken, W., 2017. Impact of woody debris of different tree species on the microbial activity and community of an underlying organic horizon. *Soil Biol. Biochem.* 115, 516–525.
- Phillips, J.D., 2001. Divergent evolution and the spatial structure of soil landscape variability. *Catena* 43, 101–113.
- Phillips, J.D., 2006. Deterministic chaos and historical geomorphology: A review and look forward. *Geomorphology* 76, 109–121.
- Phillips, J.D., 2009. Soils as extended composite phenotypes. *Geoderma* 149, 143–151.
- Phillips, J.D., Perry, D., Carey, K., Garbee, A.R., Stein, D., Morde, M.B., Sheehy, J., 1996. Deterministic uncertainty and complex pedogenesis in some Pleistocene dune soils. *Geoderma* 73, 147–164.
- Pinheiro, J., Bates, D., DebRoy, S., Sarkar, D., 2019. R Core Team 2019. *nlme: Linear and Nonlinear Mixed Effects Models.* R package version 3.1-140, < URL:<https://CRAN.R-project.org/package=nlme> > .
- Prévost-Bouré, N.C., Christen, R., Dequiedt, S., Mougél, C., Lelievre, M., Jolivet, C., Shahbazkia, H.R., Guillou, L., Arrouays, D., Ranjard, L., 2011. Validation and Application of a PCR Primer Set to Quantify Fungal Communities in the Soil Environment by Real-Time Quantitative PCR. *PLoS ONE* 6, e24166.
- Průša, E., 1985. Die böhmischen und mährischen Urwälder—ihre Struktur und Ökologie. *Vegetate ČSSR A15.* Academia, Praha.
- R Core Team, 2019. *A language and environment for statistical computing.*
- Roering, J.J., Marshall, J., Booth, A.M., Mort, M., Jin, Q., 2010. Evidence for biotic controls on topography and soil production. *Earth Planet. Sci. Lett.* 298, 183–190.
- Sagova-Mareckova, M., Cermak, L., Novotna, J., Phackova, K., Forstova, J., Kopecky, J., 2008. Innovative methods for soil DNA purification tested in soils with widely differing characteristics. *Appl. Environ. Microbiol.* 74, 2902–2907.
- Šamonil, P., Daněk, P., Schaetzl, R.J., Vašíčková, I., Valtera, M., 2015. Soil mixing and genesis as affected by tree uprooting in three temperate forests. *Eur. J. Soil Sci.* 66, 589–603.
- Šamonil, P., Doleželová, P., Vašíčková, I., Adam, D., Valtera, M., Král, K., Janík, D., Šebková, B., 2013. Individual-based approach to the detection of disturbance history through spatial scales in a natural beech-dominated forest. *J. Veg. Sci.* 24, 1167–1184.
- Šamonil, P., Valtera, M., Bek, S., Šebková, B., Vrška, T., Houška, J., 2011. Soil variability through spatial scales in a permanently disturbed natural spruce-fir-beech forest. *Eur. J. Forest Res.* 130, 1075–1091.
- Šamonil, P., Vašíčková, I., Daněk, P., Janík, D., Adam, D., 2014. Disturbances can control fine-scale pedodiversity in old-growth forest: Is the soil evolution theory disturbed as well? *Biogeosciences* 11, 5889–5905.
- Šamonil, P., Daněk, P., Schaetzl, R.J., Tejnecký, V., Drábek, O., 2018. Converse pathways of soil evolution caused by tree uprooting: A synthesis from three regions with varying soil formation processes. *Catena* 161, 122–136.
- Šamonil, P., Schaetzl, R.J., Valtera, M., Goliáš, V., Baldrian, P., Vašíčková, I., Adam, D., Janík, D., Hort, L., 2013. Crossdating of disturbances by tree uprooting: can tree-throw microtopography persist for 6,000 years? *For. Ecol. Manag.* 307, 123–135.
- Sauer, D., et al., 2007. Podzol: soil of the year 2007. A review on its genesis, occurrence, and functions. *J. Plant Nutr. Soil Sci.* 170, 581–597.
- Schaetzl, R.J., Barrett, L.R., Winkler, J.A., 1994. Choosing models for chronofunctions and fitting them to data. *Eur. J. Soil Sci.* 45, 219–232.
- Schnitzer, M., Wright, J.R., Desjardins, J.G., 1958. A comparison of the effectiveness of various extracts for organic matter from two horizons of a Podzol Profile. *Canadian J. Soil Sci.* 38, 49–53.
- Schoeneberger, P.J., Wyszicki, D.A., Benham, E.C., Broderson, W.D., 1998. *Field Book for Describing and Sampling Soils.* Natural Resources Conservation Service, USDA, National Soil Survey Center, Lincoln, NE.
- Shahab, G.A., 2003. Validation of high-performance liquid chromatography methods for pharmaceutical analysis: Understanding the differences and similarities between validation requirements of the US Food and Drug Administration, the US Pharmacopeia and the International Conference on Harmonization. *J. Chromatography A*, 987, 57–66.
- Simon, A., Gratzler, G., Sieghardt, M., 2011. The influence of windthrow microsites on tree regeneration and establishment in an old growth mountain forest. *Forest Ecol. Manag.* 262, 1289–1297.
- Spears, J.D.H., Lajtha, K., 2004. The imprint of coarse woody debris on soil chemistry in the western Oregon cascades. *Biogeochemistry* 71, 163–175.
- Štursová, M., Bárta, J., Šantrůčková, H., Baldrian, P., 2016. Small-scale spatial heterogeneity of ecosystem properties, microbial community composition and microbial activities in a temperate mountain forest soil. *FEMS Microbiol. Ecol.* 92, fiw185.
- Stutz, K.P., Dann, D., Wambsgans, J., Scherer-Lorenzen, M., Lang, F., 2017. Phenolic matter from deadwood can impact forest soil properties. *Geoderma* 288, 204–212.
- Stutz, K.P., Kaiser, K., Wambsgans, J., Santos, F., Berhe, A.A., Lang, F., 2019. Lignin from

- white-rotted European beech deadwood and soil functions. *Biogeochemistry* 145, 81–105.
- Tedersoo, L., Bahram, M., Polme, S., Koljal, U., Yorou, N.S., Wijesundera, R., Ruiz, L.V., Vasco-Palacios, A.M., Thu, P.Q., Suija, A., Smith, M.E., Sharp, C., Saluveer, E., Saitta, A., Rosas, M., Riit, T., Ratkowsky, D., Pritsch, K., Poldmaa, K., Piepenbring, M., Phosri, C., Peterson, M., Parts, K., Partel, K., Otsing, E., Nouhra, E., Njouonkou, A.L., Nilsson, R.H., Morgado, L.N., Mayor, J., May, T.W., Majuakim, L., Lodge, D.J., Lee, S.S., Larsson, K.H., Kohout, P., Hosaka, K., Hiiesalu, I., Henkel, T.W., Harend, H., Guo, L.D., Greslebin, A., Grelet, G., Geml, J., Gates, G., Dunstan, W., Dunk, C., Drenkhan, R., Dearnaley, J., De Kesel, A., Dang, T., Chen, X., Buegger, F., Brearley, F.Q., Bonito, G., Anslan, S., Abell, S., Abarenkov, K., 2014. Global diversity and geography of soil fungi. *Science* 346, 1256688.
- Tejnecký, V., Šamonil, P., Matys Grygar, T., Vašát, R., Ash, C., Drahot, P., Šebek, O., Němeček, K., Drábek, O., 2015. Transformation of iron forms during soil formation after tree uprooting in a natural beech-dominated forest. *Catena* 132, 12–20.
- Ter Braak, C.J.F., Šmilauer, P., 2002. CANOCO reference manual and CanoDraw for Windows User's guide: Software for canonical community ordination (version 4.5). Microcomputer Power, Ithaca.
- Tláškal, V., Zrůstová, P., Vrška, T., Baldrian, P., 2017. Bacteria associated with decomposing dead wood in a natural temperate forest. *FEMS Microbiol. Ecol.* 93, Fix157.
- Urbanová, M., Šnajdr, J., Baldrian, P., 2015. Composition of fungal and bacterial communities in forest litter and soil is largely determined by dominant trees. *Soil Biol. Biochem.* 84, 53–64.
- Uroz, S., Oger, P., Morin, E., 2012. Distinct ectomycorrhizospheres share similar bacterial communities as revealed by pyrosequencing-based analysis of 16S rRNA genes. *Appl. Environ. Microbiol.* 78, 3020–3024.
- Uroz, S., Oger, P., Tisserand, E., et al., 2016. Specific impacts of beech and Norway spruce on the structure and diversity of the rhizosphere and soil microbial communities. *Sci. Rep.* 6, 1–11.
- Větrovský, T., Baldrian, P., Morais, D., 2018. SEED 2: a user-friendly platform for amplicon high-throughput sequencing data analyses. *Bioinformatics* 34, 2292–2294.
- Wilimotte, A., Van der Auwera, G., De Wachter, R., 1993. Structure of the 16 S ribosomal RNA of the thermophilic cyanobacterium *Chlorogloeopsis HTF* ([*†*]mastigocladus laminosus HTF) strain PCC7518, and phylogenetic analysis. *FEBS Lett.* 317, 96–100.
- Zbiral, J., 2002. Analýza půd I. Ústřední kontrolní a zkušební ústav zemědělský, Brno. Czech Republic.
- Zbiral, J., 2003. Analýza půd II. Ústřední kontrolní a zkušební ústav zemědělský, Brno. Czech Republic.
- Zbiral, J., Honsa, I., Malý, S., Čížmár, D., 2004. Analýza půd III. Ústřední kontrolní a zkušební ústav zemědělský, Brno, Czech Republic.
- Žifčáková, L., Větrovský, T., Howe, A., Baldrian, P., 2016. Microbial activity in forest soil reflects the changes in ecosystem properties between summer and winter. *Environ. Microbiol.* 18, 288–301.





Fungal Communities Are Important Determinants of Bacterial Community Composition in Deadwood

 Iñaki Odriozola,^a Nerea Abrego,^b Vojtěch Tláškal,^a Petra Zrůstová,^a Daniel Morais,^a Tomáš Větrovský,^a Otso Ovaskainen,^c
 Petr Baldrian^a

^aLaboratory of Environmental Microbiology, Institute of Microbiology of the Czech Academy of Sciences, Prague, Czech Republic

^bDepartment of Agricultural Sciences, University of Helsinki, Helsinki, Finland

^cOrganismal and Evolutionary Biology Research Programme, University of Helsinki, Helsinki, Finland

ABSTRACT Fungal-bacterial interactions play a key role in the functioning of many ecosystems. Thus, understanding their interactive dynamics is of central importance for gaining predictive knowledge on ecosystem functioning. However, it is challenging to disentangle the mechanisms behind species associations from observed co-occurrence patterns, and little is known about the directionality of such interactions. Here, we applied joint species distribution modeling to high-throughput sequencing data on co-occurring fungal and bacterial communities in deadwood to ask whether fungal and bacterial co-occurrences result from shared habitat use (i.e., deadwood's properties) or whether there are fungal-bacterial interactive associations after habitat characteristics are taken into account. Moreover, we tested the hypothesis that the interactions are mainly modulated through fungal communities influencing bacterial communities. For that, we quantified how much the predictive power of the joint species distribution models for bacterial and fungal community improved when accounting for the other community. Our results show that fungi and bacteria form tight association networks (i.e., some species pairs co-occur more frequently and other species pairs co-occur less frequently than expected by chance) in deadwood that include common (or opposite) responses to the environment as well as (potentially) biotic interactions. Additionally, we show that information about the fungal occurrences and abundances increased the power to predict the bacterial abundances substantially, whereas information about the bacterial occurrences and abundances increased the power to predict the fungal abundances much less. Our results suggest that fungal communities may mainly affect bacteria in deadwood.

IMPORTANCE Understanding the interactive dynamics between fungal and bacterial communities is important to gain predictive knowledge on ecosystem functioning. However, little is known about the mechanisms behind fungal-bacterial associations and the directionality of species interactions. Applying joint species distribution modeling to high-throughput sequencing data on co-occurring fungal-bacterial communities in deadwood, we found evidence that nonrandom fungal-bacterial associations derive from shared habitat use as well as (potentially) biotic interactions. Importantly, the combination of cross-validations and conditional cross-validations helped us to answer the question about the directionality of the biotic interactions, providing evidence that suggests that fungal communities may mainly affect bacteria in deadwood. Our modeling approach may help gain insight into the directionality of interactions between different components of the microbiome in other environments.

KEYWORDS biotic interactions, co-occurrence, cross-validation, conditional cross-validation, fungal-bacterial interactions, HMSC, joint species distribution modeling


Citation Odriozola I, Abrego N, Tláškal V, Zrůstová P, Morais D, Větrovský T, Ovaskainen O, Baldrian P. 2021. Fungal communities are important determinants of bacterial community composition in deadwood. *mSystems* 6:e01017-20. <https://doi.org/10.1128/mSystems.01017-20>.

Editor Ashley Shade, Michigan State University
Ad Hoc Peer Reviewer Eleonora Egidi, Western Sydney University

The review history of this article can be read [here](#).

Copyright © 2021 Odriozola et al. This is an open-access article distributed under the terms of the [Creative Commons Attribution 4.0 International license](#).

Address correspondence to Iñaki Odriozola, inaki.odriozola@biomed.cas.cz.

 By applying JSDM to fungal and bacterial communities, we show that fungal communities may mainly affect bacteria in deadwood. Our approach may help exploring the directionality of interactions between the components of the microbiome in other environments.

Received 5 October 2020

Accepted 7 December 2020

Published 5 January 2021

Fungi and bacteria are core members of communities driving biogeochemical cycles, and interactions between the groups play a key role in the functioning of numerous ecosystems (1). Thus, understanding their interactive dynamics is of central importance for gaining predictive knowledge on ecosystem functioning. Biotic interactions are one of the main assembly processes and are expected to result in nonrandom co-occurrence patterns between species (2). Interactive relationships such as mutualism, parasitism, and facilitation are expected to lead to aggregated distributions between species and positive species-to-species associations, whereas competition can be expected to lead to segregated distributions and negative species-to-species associations (3). However, inferring biotic processes from co-occurrence patterns in observational studies is not trivial: nonrandom patterns may result from shared habitat use rather than from interactive effects (3), whereas opposite responses to simultaneous environmental constraints may result in random co-occurrence patterns (4). Although only a manipulative experiment could establish a causal relationship between observed patterns and underlying biotic processes, recent advances in joint species distribution modeling (JSDM) (5) have significantly advanced the research on biotic interactions in observational studies by decomposing species co-occurrence patterns into shared environmental responses and residual species associations (3, 6, 7).

Fungi are the main contributors to wood decomposition and deeply modify its physical structure (8); thus, deadwood decomposition in forest ecosystems has been traditionally attributed to wood-decaying fungi. Nevertheless, the role of bacteria, either directly or through interactions with fungi, is being increasingly recognized (8–10). There are innumerable mechanisms by which fungi can affect bacteria and bacteria can affect fungi during wood decomposition, and studying them separately completely neglects such interactive effects (11). Fungi can strongly modify the deadwood environment by modifying pH or translocating N and P from soil (12, 13), which, in turn, may impact bacterial community composition (14, 15). Similarly, bacterial activity may alter wood properties through, for example, the fixation of atmospheric N₂ (16). Moreover, fungal-bacterial interactions go beyond these effects through modulation of the environment. There is ample *in vitro* evidence of antagonistic effects in both directions (17–19). Bacteria are able to directly feed on fungal mycelia (20). Bacteria can act as commensalists by consuming fungal exudates and products of wood decomposition (21, 22). Mutualistic interactions have also been described, where fungi gain protection against fungicides and bacteria get increased access to resources (23).

The capacity of fungi to modify the spatial structure of deadwood makes them crucial drivers of microbial community composition and activity (24). Mycelia enable fungi to exploit and expand through the three-dimensional space of deadwood (1), making hyphae an effective dispersal vector also for the wood-inhabiting bacteria (25). In this line, in experimental setups, Johnston et al. (26) and Christofides et al. (27) demonstrated strong directional effects from fungi to bacteria: they inoculated wood pieces with known wood-decaying fungi and then observed that the development of succeeding bacterial communities highly depended on the identity of the inoculated fungi. Therefore, fungal-bacterial interactions might be mainly modulated through fungal communities influencing bacterial communities.

Recent studies have shown that fungi and bacteria co-occur nonrandomly in deadwood (10, 28–30). However, using raw co-occurrences, none of the studies could distinguish between associations derived from shared habitat use and interactive effects nor could they explore the directionality of the interactions. Therefore, it remains largely unknown which are the principal mechanisms behind the reciprocal effects between fungi and bacteria (11).

The first objective of the present paper was to assess whether fungal and bacterial co-occurrences result from shared habitat use (i.e., deadwood's properties) or whether there are fungal-bacterial interactive associations after habitat characteristics are taken into account. For this, we applied JSDM to high-throughput sequencing data on co-occurring fungi and bacteria. Fungal community composition has been reported to be

strongly influenced by host tree species and deadwood diameter and decay stage (31–33), variables which reflect different physical-chemical properties. Likewise, bacterial community composition in deadwood is influenced by variables such as water content, pH, or C/N ratio of deadwood (26, 34–36). Hence, a wide range of log physical and chemical characteristics were included as fixed effects in the models, and residual association networks were compared between the models that did versus those that did not account for the response of species to the environmental variables. Additionally, we hypothesized that the fungal-bacterial interactions are mainly modulated through fungal communities influencing bacterial communities. To test the effects of fungal communities on the bacterial communities and the effect of bacteria on fungi, we quantified how much the predictive power of the JSDM for bacterial community improved when accounting for fungal community data and, vice versa, how much predictive power increased for the fungal community when accounting for bacterial community composition.

RESULTS

Nonmetric multidimensional scaling (NMDS) ordinations show that the filters to remove rare operational taxonomic units (OTUs) altered overall community structure very little, and, similarly, the set of wood physical and chemical characteristics that significantly correlated with main trends in community structure also remained the same (Fig. 1). Fungal and bacterial species richness were uncorrelated (see also Fig. S1 in the supplemental material), whereas beta-diversity metrics of both domains were significantly correlated, regardless of the filtering criteria used (see Fig. S2). Therefore, we proceeded to hierarchical modeling of species communities (HMSC) using the community data sets filtered to bigger data sets (452 fungal and 570 bacterial OTUs) and smaller data sets (103 fungal and 51 bacterial OTUs).

From the species-to-species association matrices, there was evidence for both co-occurrences arising from shared habitat preferences and from interactive effects. The association matrix derived from the residuals of the null model was strongly structured both within and between fungi and bacteria, with several species co-occurring more and less often than expected by chance (Fig. 2A; Fig. S3A). In the residual association matrix of the full model (i.e., the associations remaining after the effects of environmental predictors were taken into account), several of those associations remained, but many others disappeared. This means that many of the species-to-species associations detected by the null model were the result of many species pairs responding in the same (or opposite) way to the characteristics of deadwood (Fig. 2B; Fig. S3B). Additionally, many other associations shifted from positive to negative or from negative to positive (changes in the direction of the associations are easiest to see in Fig. S3, since the association matrix involves a lower number of OTUs).

Variance partitioning community composition revealed that for bacteria, log-level random effects (i.e., the species-to-species association network) explained a greater fraction of the variance than those for fungi (Fig. 3; Fig. S4). The partitioning further showed that the fractions explained by log chemical characteristics in comparison to log physical characteristics were similar in both fungi and bacteria: chemistry explained more than double the variance than physical characteristics for both domains (Fig. 3; Fig. S4).

The models had generally somewhat greater predictive power for bacteria than for fungi, especially when the prediction was conditioned by the occurrences and abundances of fungi (Table 1; Table S1). For prediction of fungal occurrences (the binomial model), including the fixed effects (all environmental predictors) increased the predictive power by 0.031 area under the curve (AUC) points in comparison to the null model not including environmental predictors. Including also the information on bacterial occurrences and abundances increased the power an additional 0.014 AUC points (conditional predictive power of full model versus nonconditional predictive power of full model) (Table 1; Table S1). Bacterial community was nearly half as good a predictor of fungal occurrences than were the environmental predictors (i.e., log chemical and

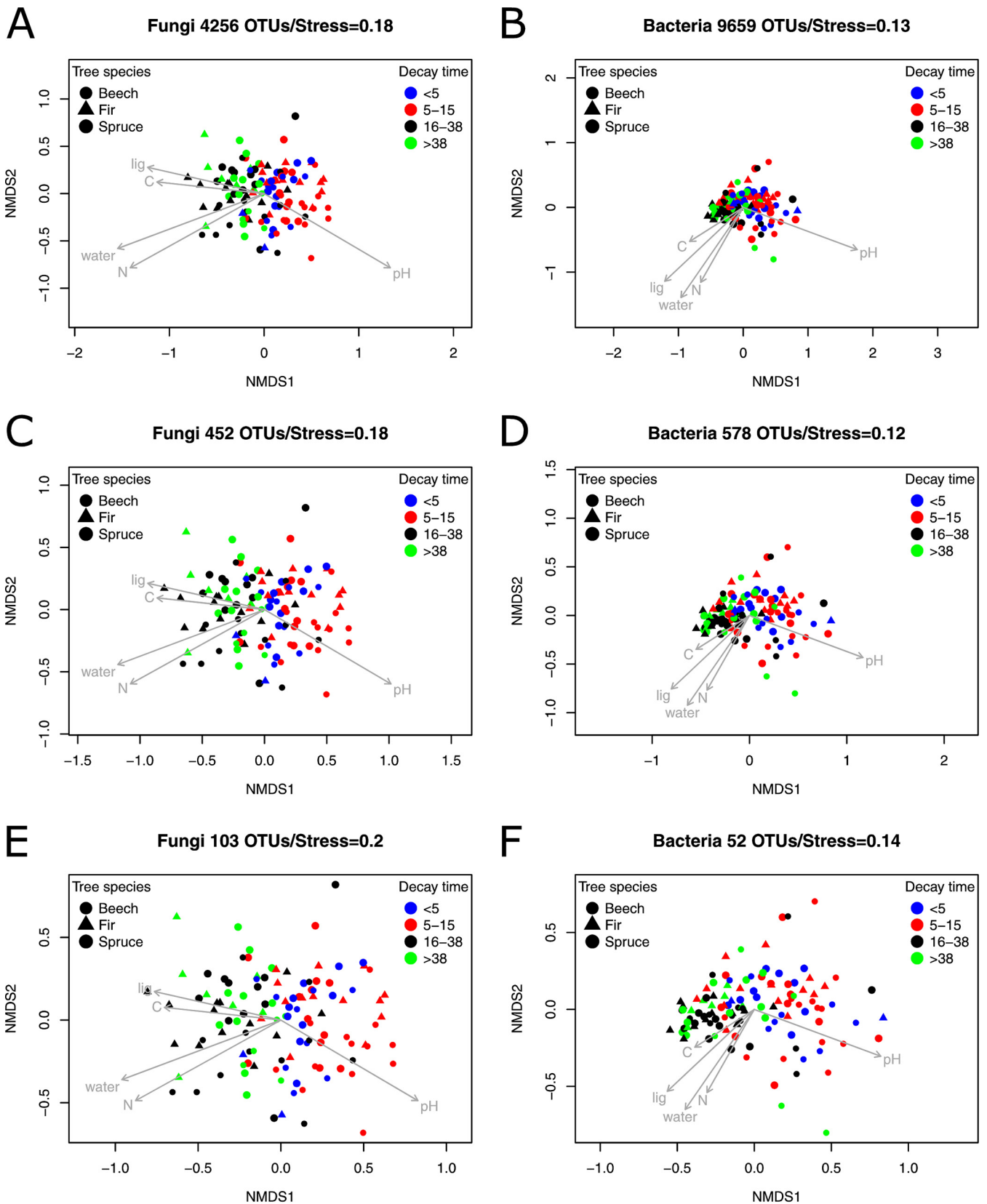


FIG 1 Fungal and bacterial community structures with the whole community and after filtering rare OTUs. NMDS ordination plots showing the main trends in fungal community structure including all OTUs (A), after applying the filter resulting in bigger data set (C), and after applying the filter resulting in smaller data set (E). Bacterial community structure including all OTUs (B), after applying the filter resulting in bigger data set (D), and after applying the filter resulting in smaller data set (F). Gray arrows depict the environmental variables significantly associated with the main trends in community structure.

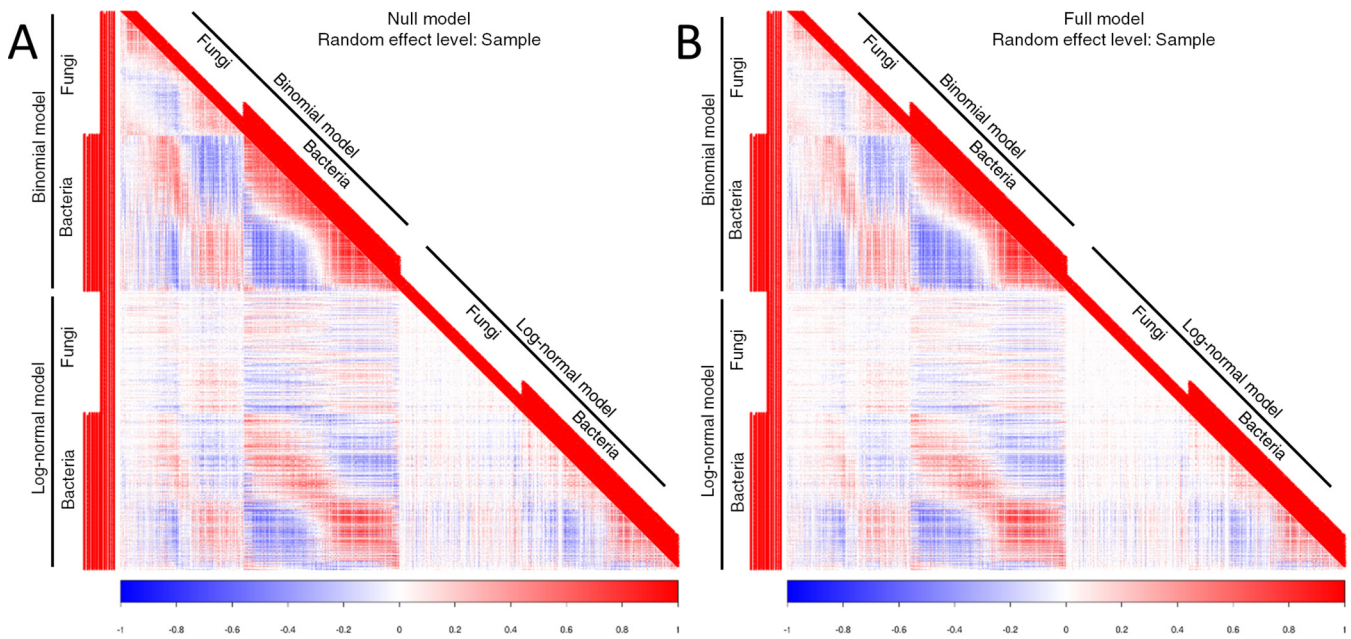


FIG 2 Species association networks. Species association networks derived from the log (i.e., sample)-level random effects of the JSDM. (A) The network derived from the null model (i.e., including only sequencing depths as explanatory variables) shows raw species co-occurrences. (B) The network derived from the full model (i.e., including all measured environmental predictors) shows co-occurrences once shared (or opposite) habitat use has been taken into account. Differences between networks of null and full models are more visible in Fig. S3 in the supplemental material, since the association matrix involves lower number of OTUs.

physical characteristics). When predicting bacterial occurrences, environmental predictors increased predictive power by 0.031 AUC points, and including fungal occurrences and abundances increased the power an additional 0.059 AUC points (Table 1; Table S1). For bacterial occurrences, fungal community was nearly twice as good a predictor as were the environmental predictors. Prediction of abundances (the log-normal models) was overall worse, but the trends were similar: information about the fungal occurrences and abundances increased the power to predict the bacterial abundances substantially, whereas information about the bacterial occurrences and abundances increased the power to predict the fungal abundances much less (Table 1; Table S1).

DISCUSSION

Fungal-bacterial interactions are ubiquitous in nature and play a key role in the function of many ecosystems (1). Here, we jointly studied fungal and bacterial communities in deadwood, and similar to other studies that reported nonrandom co-occurrence patterns between them (28–30), we observed that the species association network is strongly structured both within and between fungi and bacteria. Previous works have attributed the nonrandom associations between fungi and bacteria to modifications of wood chemistry by the fungal activity (26, 29); however, our results show that many significant associations remain after accounting for the effects of environmental predictors. This suggests that biotic interactions beyond the effects on and responses to environmental factors occur between fungi and bacteria.

In this study, we measured a wide range of environmental predictors, including both wood chemical and physical characteristics. Studies analyzing fungal communities in deadwood usually measure physical characteristics of wood, which, in turn, are correlated with chemistry (31–33), whereas wood chemical explanatory variables are more commonly included in studies involving the bacterial community (34–36). Here, addressing fungi and bacteria together, we show that both kinds of variables explained a similar fraction of variance in these domains: chemistry was twice as important as log physical characteristics. Since we lack temporal data, we could not distinguish whether fungi modified the wood chemistry first and bacteria responded to the modification or

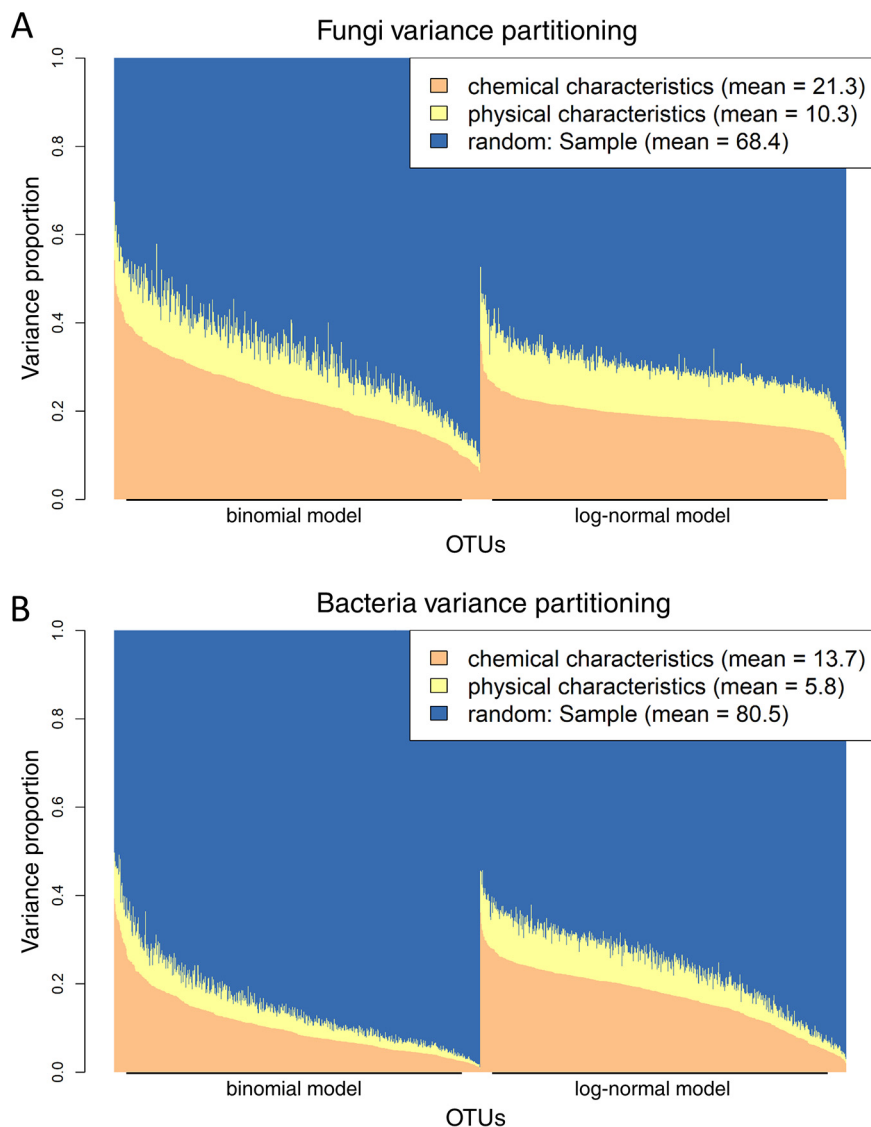


FIG 3 Variance partitioning of fungal and bacterial community compositions. Proportions of variance explained by log chemical (water, pH, C, N, and lignin) and physical characteristics (tree species identity, decay time, and DBH) and sample-level random effects (i.e., species-to-species association matrix) in fungi (A) and bacteria (B). Bar plots show the variance proportions species by species, whereas text boxes show proportions averaged over species and models (binomial versus log normal). Species are differently ordered in binomial and log-normal parts of the model, since they were separately ordered based on the effect size of chemical predictors. Note that only explained variance is depicted in the plot: the explanatory powers of binomial and log-normal models for fungi and bacteria are reported in the corresponding column of Table 1.

if both bacteria and fungi are responding to wood chemistry, which, in turn, depends on other log characteristics. The answer is probably complex, since dominant fungi may shape subsequent bacterial communities by lowering wood pH (13, 26), but different tree species may have specific chemical characteristics as well (33, 34).

Variance partitioning revealed a stronger effect of log-level random effects on bacterial community composition than on fungal community composition. Log-level random effects likely model interactive associations between species, since environmental predictors were included in the JSJM as fixed effects; however, they could also represent missing environmental covariates. In the same line, cross-validation results suggest directional interactive effects from fungi to bacteria: information on fungal occurrences

TABLE 1 Explanatory and predictive powers of the models^a

Category	Model	No. of species	Explanatory power	Unconditional predictive power	Conditional predictive power
Occurrence					
Fungi	Null	452	0.786	0.568	0.607
	Full	452	0.824	0.599	0.613
Bacteria	Null	570	0.876	0.556	0.665
	Full	570	0.894	0.587	0.646
Abundance					
Fungi	Null	452	0.315	−0.051	−0.016
	Full	452	0.425	−0.010	0.001
Bacteria	Null	570	0.398	−0.002	0.049
	Full	570	0.486	0.012	0.047

^aExplanatory and predictive powers of the models for fungal and bacterial occurrences (measured in terms of AUC of the binomial model) and abundances (measured in terms of R^2 of the log-normal model) were averaged over the species. Null models have sequencing depth as the sole explanatory variable, whereas full models include also the environmental predictors. Explanatory power is based on model fitted to all data, unconditional predictive power is based on 2-fold cross-validation, where values of environmental predictors are known, and conditional predictive power is based on 2-fold cross-validation where the occurrences and abundances of the nonfocal group (bacteria to predict fungi and fungi to predict bacteria) are also assumed to be known. Note that AUC index takes values between 0.5 and 1, whereas R^2 ranges between 0 and 1.

and abundances was twice as good a predictor of bacterial community composition than the environmental predictors altogether. However, this was not the case when using information on bacterial communities to predict fungi; in this case, environmental predictors had twice as good predictive power. Again, it might be argued that unmeasured explanatory variables rather than actual biotic interactions are responsible for residual associations between fungi and bacteria. We believe this to be unlikely, because a common response of fungi and bacteria to unmeasured variables would have resulted in symmetrical effects between fungi and bacteria, which is not the case in our study—fungi are a good predictor of bacteria, but the opposite is not true. The overall low predictive powers of the models are not surprising given the inherent stochasticity of microbial community development. There are many well-documented mechanisms affecting fungal and bacterial community assembly and altering their spatial distributions, such as drift, dispersal limitation, priority effects, or endpoint assembly cycles (37). Moreover, it is challenging predicting highly diverse communities with a relatively small data set.

The directional effect of fungi on bacteria is in line with other studies (26, 27, 29), which suggested that the modification of pH by fungi is an important underlying mechanism. Even if we cannot give any final answer on the involved mechanisms with this observational study, our results suggest that part of the effect of fungi on bacteria is uncorrelated with any chemical variable of the wood. There are alternative ways fungi might affect bacterial composition. Fungal hyphae are proficient in exploring the wood three-dimensional space, and they can be considered to constitute ideal transport paths and scaffolds for bacteria (1). In fact, bacteria have been reported to use fungal mycelia to disperse more efficiently in other substrates (23, 38).

The joint movement of bacteria with fungi (and hence, their interactions) might have deep consequences for deadwood decomposition and forest nutrient dynamics. Previous findings on co-occurrence patterns between wood-decaying fungi and N_2 -fixing bacteria suggest that deadwood decomposition might be an interactive process where bacteria may provide the N source and fungi provide the C source (10, 11, 28, 36). Similar interactions between fungi and bacteria have also been reported in the process of litter decomposition (38). Furthermore, implications of fungal-bacterial associations in ecosystem functions go well beyond plant matter decomposition (1). For instance, mycelium-based dispersal improves the movement of bacteria in heterogeneously polluted soils where movement of bacteria is otherwise impaired, thus stimulating contaminant biodegradation (39–41).

Finally, the JSDM approach that we applied does not model explicitly compositional data using a multinomial distribution. Extending the data models of JSDMs to include the multinomial distribution is one of the key challenges in the ongoing merging of multivariate methods developed separately for microbial ecology and for the community ecology of macroorganisms (3). Failing to account for the multinomial nature of the data could theoretically generate negative associations between species. This would certainly be the case if the data involve two species, as then the increase in sequence count of one species would directly decrease the sequence count of the other species. However, even for the case of two species, the presence-absence part of the model would be less problematic, as missing the occurrence of one species because the other species dominates the sequence data would be unlikely. Moreover, we believe that this is not a major problem for the abundance data either, since the community consists of a very large number of species, none of which dominates the data in terms of sequence abundance. Thus, the constraining effect of the total number of sequences is diluted through the whole community and is not likely to generate strong negative associations between any pair of species. Reflecting this, the associations we report are not predominantly negative (Fig. 2), but they contain a balanced set of associations that are positive, negative, or not statistically supported. Therefore, we consider our results robust even if the JSDM applied here does not include the multinomial data model.

In conclusion, our study shows that fungi and bacteria form tight association networks (i.e., they co-occur more or less frequently than expected by chance) in deadwood that include common (or opposite) responses to the environment, as well as (potentially) biotic interactions. Importantly, the combination of cross-validations and conditional cross-validations helped us to answer the question about the directionality of the biotic interactions, providing observational evidence suggesting that fungal-bacterial interactions may be modulated through fungal communities influencing bacterial communities. Our modeling approach may help gaining insight into the directionality of interactions between different components of the microbiome in other environments.

MATERIALS AND METHODS

Study area and sampling design. The study area was located in the 25-ha Zofin ForestGEO Dynamics plot in the Novohradské Hory mountains, Czech Republic (48°39'57''N, 14°42'24''E; www.forestgeo.si.edu). This area is part of the 42-ha core zone of the Žofínský prales National Nature Reserve (established 1838), which has never been managed and thus represents a virgin forest. The bedrock consists of fine- to medium-grain porphyritic and biotite granite. Annual average rainfall is 866 mm, and annual average temperature is 6.2°C (42). The living tree volume, which is calculated to be 690 m³ ha⁻¹ (43), is dominated by *Fagus sylvatica* (51.5% of total living wood volume), followed by *Picea abies* (42.8%) and *Abies alba* (4.8%). Other tree species (*Ulmus glabra*, *Acer pseudoplatanus*, *Acer platanoides*, and *Sorbus aucuparia*) represent 1% of living wood volume. The dead coarse wood debris is calculated to be on average 208 m³ ha⁻¹ (44) and is more evenly represented by *F. sylvatica*, *P. abies*, and *A. alba*, with 23.6%, 43.7%, and 31.4% of the volume, respectively (43).

The log sampling scheme was detailed in previous publications (33, 36), but here follows a brief description. For the study area, detailed information is available about every living and dead tree with diameter at breast height (DBH) of ≥10 cm (including spatial location, DBH, tree species, tree status, live/dead, standing/lying, snag, breakage, windthrow, stump, etc.): all the variables were repeatedly recorded in 1975, 1997, 2008, and 2013 (45). Using this information, all trees belonging to *F. sylvatica*, *P. abies*, and *A. alba*, with a DBH between 30 cm and 100 cm, and first recorded as dead and lying in 1975, 1997, 2008, or 2013 were identified. Trees decomposing as standing before they were downed were omitted to exclude logs with unclear decay lengths. Hence, a tree species (beech, spruce, and fir), decay length (<5, 5 to 15, 16 to 38, or >38 years), and DBH was assigned to each log. Then, within each tree species and decay length class, logs were selected randomly. The final data set was composed of 118 trees: 39 beech logs (of which 9 had a decay length of <5 years, 13 of 5 to 15 years, 12 of 16 to 38 years, and 5 of >38 years), 36 fir logs (2 of <5 years, 14 of 5 to 15 years, 13 of 16 to 38 years, and 7 of >38 years), and 43 spruce logs (10 of <5 years, 12 of 5 to 15 years, 11 of 16 to 38 years, and 10 of >38 years) (see Table S2 in the supplemental material).

To obtain representative samples, four subsamples were obtained from each log in October 2013 using an electric drill with a bit diameter of 8 mm. The length of each log (or the sum of the lengths of its fragments) was measured, and subsamples were collected at one-fifth, two-fifths, three-fifths, and four-fifths of the log length. The four subsamples of each log were pooled to yield one composite sample per log. Drilling was performed vertically from the middle of the upper surface to a depth of 40 cm. The drill bit was sterilized between drillings.

Sample processing, chemical analysis, and DNA extraction and amplification. Details of sample processing and analysis were given in previous publications (33, 36). Briefly, the sawdust material was weighed, freeze-dried, and milled using an Ultra Centrifugal Mill ZM 200 (Retsch, Germany). Dry mass content was measured as a loss of mass during freeze-drying, and the pH was measured in distilled water (1:10). The wood C and N contents were measured in an external laboratory (Research Institute for Soil and Water Conservation, Prague, Czech Republic) as described previously (46). Klason lignin content was measured as dry weight of solids after hydrolysis with 72% (wt/wt) H₂SO₄ (47).

Total genomic DNA was extracted from 2 × 200 mg of material of each sample using the NucleoSpin Soil kit (Macherey-Nagel, Germany) according to the manufacturer's instructions. Then, PCR amplifications were performed in three PCRs per sample as described previously (33, 36) using barcoded gITS7 and ITS4 primers targeting fungal ITS2 (48) and barcoded 515F and 806R primers targeting the V4 region of the bacterial 16S rRNA gene (49). Amplicons were purified, pooled, and sequenced on the Illumina MiSeq to obtain pair-end sequences of 2 × 250 bp.

Sequence data processing. The sequencing data were processed using SEED v 2.0.3 (50) as described in references 33 and 36. For bacteria, pair-end reads were merged using fastq-join (51). For fungi, only forward read sequences beginning with the primer gITS7 were considered, since for certain highly abundant wood-decomposing fungi (e.g., *Armillaria* spp.), ITS2 is longer than 550 bases and these sequences would be missed during pair-end joining. The whole or partial ITS2 was extracted from fungal amplicons using ITS Extractor 1.0.8 (52). Sequences of inferior quality (mean Phred score of <30, all sequences with ambiguous bases) or length (<40 bases) were removed. Chimeric sequences were detected and deleted using UCHIME implementation in USEARCH 7.0.1090 (53). Sequences were clustered using UPARSE implemented in USEARCH (54) at a 97% similarity level. Consensus sequences were constructed for each cluster, and the closest hits at the species level were identified using BLASTn against UNITE (55) and GenBank for fungi and Ribosomal Database Project (56) and GenBank for bacteria. The minimum and maximum read counts were 1,598 and 21,375 for fungi, and 1,606 and 15,113 for bacteria, respectively. This resulted in 4,519 fungal and 21,260 bacterial OTUs, of which 263 and 11,601 were global singletons and were removed. Therefore, the final data consisted of 4,256 fungal and 9,659 bacterial OTUs.

Statistical analyses. We analyzed the data with a hierarchical modeling of species communities (HMSC) framework (57, 58), which belongs to the class of JSJM (5). In HMSC, community data are analyzed by constructing a hierarchical model in the generalized linear model (GLM) framework and using Bayesian inference.

The response data consisted of abundances (sequence counts) of bacterial and fungal OTUs in the $n = 118$ logs (i.e., sampling units). As the data were zero inflated (i.e., dominated by species' absences), we applied a hurdle model. A hurdle model consists of two parts, one modeling the presence-absence and the other modeling abundance conditional on presence. To fit the first model, we first truncated the data to presence-absence, keeping all zeros as zeros and setting the nonzeros to one, and we fitted a binomial model with probit link function to each column (i.e., OTU). Then, to fit the second model, we generated a second data set by setting all zeros to missing values (i.e., ignoring them) and keeping all nonzeros in their original values. To model these abundances conditional on presence (scaled to zero mean and unit variance), we used the lognormal model. We included both of the presence-absence and the abundance models in the same model, so that the response matrix \mathbf{Y} (for notation, see reference 58) included each fungal and bacterial OTU twice. See reference 3 for more details about HMSC models, including how hurdle models can be used to model zero-inflated data.

As data on rare species are not sufficiently informative to enable fitting species-specific models (see, e.g., reference 3), we included in the analyses only those OTUs with a prevalence of >10% among the sampling units and which had at least 0.5% relative abundance in one of the sampling units. These choices resulted in 452 fungal OTUs and 570 bacterial OTUs. To test the robustness of the results against these choices, we also ran an alternative analysis, where we used 20% as the prevalence threshold and 5% as the maximal relative abundance threshold, resulting in 103 fungal and 51 bacterial OTUs. Additionally, to assess how the filtering criteria affected fungal and bacterial community structure, we carried out NMDS ordination plots separately for (i) the whole community (4,256 fungal and 9,659 bacterial OTUs); (ii) the data obtained with the filter generating a bigger data set (452 fungal and 570 bacterial OTUs); and (iii) the data obtained with filter generating the smaller data set (103 fungal and 51 bacterial OTUs). NMDS was performed using metaMDS() function from vegan (59). Because fungal communities were too complex to obtain reliable NMDS ordinations in two dimensions, we conducted the ordinations in three dimensions by setting the argument $k = 3$ in the metaMDS() function. The first two axes are shown in results, since interpreting three-dimensional plots is very difficult. Significant explanatory variables were added to the ordinations as arrow vectors using envfit() function from vegan (59). Significance of each explanatory variable was tested independently using 999 permutations.

As fixed explanatory variables in the matrix \mathbf{X} of HMSC, we included variables related to wood chemistry and physical characteristics. The continuous variables describing wood chemistry were (i) percent water content, (ii) pH, (iii) percent C content, (iv) log-transformed percent N content, and (v) percent lignin content. Variables related to log physical characteristics were (vi) tree species (categorical with beech, spruce, and fir levels), (vii) decay time (categorical with <5, 5 to 15, 16 to 38, or >38 years levels), and (viii) DBH in centimeters (continuous). To control for variation in sequencing depth, we also included the (ix) log-transformed number of reads as a continuous variable. To identify association networks within fungi and within bacteria, as well as among these two groups, we included a community-level random effect (implemented with the help of latent variables [see reference 58]) at the sampling unit (i.e., the log) level. The community-level random effect models covariation among the species that cannot be attributed to the environmental variables, including the effects of species interactions, or to the responses of the

species to environmental covariates not included in the model (3). In the following, we refer to such unexplained covariation among the species as species associations, irrespective of what is the causal reason behind it. In an exploratory analysis prior to model fitting, we excluded C/N ratio as an explanatory variable, since it almost perfectly correlated with wood N content. We then partitioned the explained variance into fixed effects (i.e., explanatory covariates) and log-level random effects (i.e., residual association matrix). Fixed effects were further grouped as log chemical characteristics (pooling water, pH, C, N, and lignin) and log physical characteristics (pooling tree species identity, decay time, and DBH).

We built species-to-species association matrices using the correlation matrix \mathbf{R} both for a model including the explanatory variables described above (called the full model) and a model which otherwise had the same structure but did not include explanatory variables (called the null model). The association matrix derived from the null model showed a combination of co-occurrence patterns created by shared habitat use as well as the patterns resulting from interactive reciprocal effects. In contrast, association matrices derived from the full model showed the co-occurrence patterns once the environmental effects were taken into account and thus were more likely to result from interactive associations.

Explanatory and predictive powers of the models were assessed by calculating AUC for presence-absence data and the standard R^2 for the abundance data. When computing explanatory power, models were fitted to all data, i.e., the same data were used to fit the models and make the predictions. When computing predictive power, we applied a 2-fold cross-validation approach across the sampling units. In cross-validation, sampling units are randomly divided into two folds, and to make predictions in one fold (i.e., the testing set), the models are fitted to the data from the other fold (i.e., the training set). First, we computed unconditional predictive power where community data Y is assumed to be known in only those sampling units that belong to the training set. Hence, the unconditional predictive power only uses the information on the environmental predictors and ignores the information in the species association matrix. Then, to examine the link between fungi and bacteria, we asked how much improvement the JSDM was able to make for predictions on bacterial communities when knowing the fungal composition, and, vice versa, how much improvement the JSDM was able to make for predictions on fungal communities when knowing the bacterial composition. To do so, we computed conditional predictive power, where the occurrences and abundances of bacteria were assumed to be known in the testing set when predicting fungi and where occurrences and abundances of fungi were assumed to be known when predicting bacteria. In contrast to unconditional predictive power, in conditional predictive power, the information in the species association matrix is used to make the predictions in addition to the information on environmental predictors (see reference 3 for technical details). We quantified the information value of fungi for predicting bacteria (and vice versa, the information value of bacteria for predicting fungi) as the difference between conditional and unconditional predictive power, i.e., the predictive power that did versus the power that did not utilize information about the occurrences and abundances of the non-focal species group.

We fitted the model with the R-package (60) Hmisc (57) assuming the default prior distributions. We sampled the posterior distribution with four Markov Chain Monte Carlo (MCMC) chains, each of which was run for 150,000 iterations, of which the first 50,000 were removed as burn-in. The iterations were thinned by 100 to yield 1,000 posterior samples per chain and thus 4,000 posterior samples in total. We assessed MCMC convergence by computing the effective number of samples and the potential scale reduction factor (57) for the parameters measuring species responses to environmental covariates and species-to-species associations (Fig. S5).

Data availability. Raw sequence data for fungi and bacteria are available in the MG RAST public database with data set numbers [mvp18370](#) and [mvp82275](#), respectively. Processed OTU and metadata tables as well as R scripts supporting the results have been archived in the Dryad repository (<https://doi.org/10.5061/dryad.sxksn030s>).

SUPPLEMENTAL MATERIAL

Supplemental material is available online only.

FIG S1, TIF file, 0.1 MB.

FIG S2, TIF file, 0.4 MB.

FIG S3, TIF file, 0.8 MB.

FIG S4, TIF file, 0.2 MB.

FIG S5, TIF file, 0.1 MB.

TABLE S1, DOCX file, 0.1 MB.

TABLE S2, DOCX file, 0.1 MB.

ACKNOWLEDGMENTS

This work was supported by the Czech Science Foundation (17-20110S). I.O. was supported by the Ministry of Education, Youth and Sports of the Czech Republic and ESIF (CZ.02.2.69/0.0/0.0/16_027/0007990).

REFERENCES

- Deveau A, Bonito G, Uehling J, Paoletti M, Becker M, Bindschedler S, Hacquard S, Hervé V, Labbé J, Lastovetsky OA, Mieszkin S, Millet LJ, Vajna B, Junier P, Bonfante P, Krom BP, Olsson S, van Elsas JD, Wick LY. 2018. Bacterial–fungal interactions: ecology, mechanisms and challenges. *FEMS Microbiol Rev* 42:335–352. <https://doi.org/10.1093/femsre/fuy008>.
- Götzenberger L, de Bello F, Bräthen KA, Davison J, Dubuis A, Guisan A, Lepš J, Lindborg R, Moora M, Pärtel M, Pellissier L, Pottier J, Vittoz P, Zobel K, Zobel M. 2012. Ecological assembly rules in plant communities—approaches, patterns and prospects. *Biol Rev Camb Philos Soc* 87:111–127. <https://doi.org/10.1111/j.1469-185X.2011.00187.x>.
- Ovaskainen O, Abrego N. 2020. Joint species distribution modelling: with applications in R. Cambridge University Press, Cambridge, United Kingdom.
- García-Baquero G, Crujeiras RM. 2015. Can environmental constraints determine random patterns of plant species co-occurrence? *Ecol Evol* 5:1088–1099. <https://doi.org/10.1002/ece3.1349>.
- Warton DI, Blanchet FG, O'Hara RB, Ovaskainen O, Taskinen S, Walker SC, Hui FK. 2015. So many variables: joint modeling in community ecology. *Trends Ecol Evol* 30:766–779. <https://doi.org/10.1016/j.tree.2015.09.007>.
- Zurell D, Pollock LJ, Thuiller W. 2018. Do joint species distribution models reliably detect interspecific interactions from co-occurrence data in homogenous environments? *Ecography* 41:1812–1819. <https://doi.org/10.1111/ecog.03315>.
- Ovaskainen O, Hottola J, Siitonen J. 2010. Modeling species co-occurrence by multivariate logistic regression generates new hypotheses on fungal interactions. *Ecology* 91:2514–2521. <https://doi.org/10.1890/10-0173.1>.
- Baldrian P. 2017. Forest microbiome: diversity, complexity and dynamics. *FEMS Microbiol Rev* 41:109–130. <https://doi.org/10.1093/femsre/fuw040>.
- Lladó S, López-Mondéjar R, Baldrian P. 2017. Forest soil bacteria: diversity, involvement in ecosystem processes, and response to global change. *Microbiol Mol Biol Rev* 81:e00063-16. <https://doi.org/10.1128/MMBR.00063-16>.
- Gómez-Brandón M, Probst M, Siles JA, Peintner U, Bardelli T, Egli M, Insam H, Ascher-Jenuil J. 2020. Fungal communities and their association with nitrogen-fixing bacteria affect early decomposition of Norway spruce deadwood. *Sci Rep* 10:8025. <https://doi.org/10.1038/s41598-020-64808-5>.
- Johnston SR, Boddy L, Weightman AJ. 2016. Bacteria in decomposing wood and their interactions with wood-decay fungi. *FEMS Microbiol Ecol* 92:fiw179. <https://doi.org/10.1093/femsec/fiw179>.
- Watkinson S, Bebbler D, Darrah P, Fricker M, Tlalka M, Boddy L. 2006. The role of wood decay fungi in the carbon and nitrogen dynamics of the forest floor, p 151–181. In Gadd GM (ed), *Fungi in biogeochemical cycles*. Cambridge University Press, Cambridge, United Kingdom.
- de Boer W, Folman LB, Klein Gunnewiek PJA, Svensson T, Bastviken D, Öberg G, del Rio JC, Boddy L. 2010. Mechanism of antibacterial activity of the white-rot fungus *Hypholoma fasciculare* colonizing wood. *Can J Microbiol* 56:380–388. <https://doi.org/10.1139/w10-023>.
- Folman LB, Klein Gunnewiek PJA, Boddy L, De Boer W. 2008. Impact of white-rot fungi on numbers and community composition of bacteria colonizing beech wood from forest soil. *FEMS Microbiol Ecol* 63:181–191. <https://doi.org/10.1111/j.1574-6941.2007.00425.x>.
- Valášková V, de Boer W, Klein Gunnewiek PJA, Pospíšek M, Baldrian P. 2009. Phylogenetic composition and properties of bacteria coexisting with the fungus *Hypholoma fasciculare* in decaying wood. *ISME J* 3:1218–1221. <https://doi.org/10.1038/ismej.2009.64>.
- Rinne KT, Rajala T, Peltoniemi K, Chen J, Smolander A, Mäkipää R. 2017. Accumulation rates and sources of external nitrogen in decaying wood in a Norway spruce dominated forest. *Funct Ecol* 31:530–541. <https://doi.org/10.1111/1365-2435.12734>.
- Murray AC, Woodward S. 2003. *In vitro* interactions between bacteria isolated from Sitka spruce stumps and Heterobasidion annosum. *Forest Pathol* 33:53–67. <https://doi.org/10.1046/j.1439-0329.2003.00307.x>.
- De Boer W, Wagenaar A-M, Klein Gunnewiek PJA, Van Veen JA. 2007. *In vitro* suppression of fungi caused by combinations of apparently non-antagonistic soil bacteria. *FEMS Microbiol Ecol* 59:177–185. <https://doi.org/10.1111/j.1574-6941.2006.00197.x>.
- Caldeira AT, Feio SS, Arreiro JMS, Coelho AV, Roseiro JC. 2008. Environmental dynamics of *Bacillus amyloliquefaciens* CCM1 1051 antifungal activity under different nitrogen patterns. *J Appl Microbiol* 104:808–816. <https://doi.org/10.1111/j.1365-2672.2007.03601.x>.
- Brabcová V, Nováková M, Davidová A, Baldrian P. 2016. Dead fungal mycelium in forest soil represents a decomposition hotspot and a habitat for a specific microbial community. *New Phytol* 210:1369–1381. <https://doi.org/10.1111/nph.13849>.
- Hervé V, Ketter E, Pierrat J-C, Gelhaye E, Frey-Klett P. 2016. Impact of *Phanerochaete chrysosporium* on the functional diversity of bacterial communities associated with decaying wood. *PLoS One* 11:e0147100. <https://doi.org/10.1371/journal.pone.0147100>.
- Hervé V, Junier T, Bindschedler S, Verrecchia E, Junier P. 2016. Diversity and ecology of oxalotrophic bacteria. *World J Microbiol Biotechnol* 32:28. <https://doi.org/10.1007/s11274-015-1982-3>.
- Nazir R, Tazetdinova DI, van Elsas JD. 2014. *Burkholderia terrae* B5001 migrates proficiently with diverse fungal hosts through soil and provides protection from antifungal agents. *Front Microbiol* 5:598. <https://doi.org/10.3389/fmicb.2014.00598>.
- Tecon R, Or D. 2017. Biophysical processes supporting the diversity of microbial life in soil. *FEMS Microbiol Rev* 41:599–623. <https://doi.org/10.1093/femsre/fux039>.
- Kohlmeier S, Smits THM, Ford RM, Keel C, Harms H, Wick LY. 2005. Taking the fungal highway: mobilization of pollutant-degrading bacteria by fungi. *Environ Sci Technol* 39:4640–4646. <https://doi.org/10.1021/es047979z>.
- Johnston SR, Hiscox J, Savoury M, Boddy L, Weightman AJ. 2019. Highly competitive fungi manipulate bacterial communities in decomposing beech wood (*Fagus sylvatica*). *FEMS Microbiol Ecol* 95:fy225. <https://doi.org/10.1093/femsec/fy225>.
- Christofides SR, Hiscox J, Savoury M, Boddy L, Weightman AJ. 2019. Fungal control of early-stage bacterial community development in decomposing wood. *Fungal Ecol* 42:100868. <https://doi.org/10.1016/j.funeco.2019.100868>.
- Hoppe B, Kahl T, Karasch P, Wubet T, Bauhus J, Buscot F, Krüger D. 2014. Network analysis reveals ecological links between N-fixing bacteria and wood-decaying fungi. *PLoS One* 9:e88141. <https://doi.org/10.1371/journal.pone.0088141>.
- Kielak AM, Scheublin TR, Mendes LW, van Veen JA, Kuramae EE. 2016. Bacterial community succession in pine-wood decomposition. *Front Microbiol* 7:231. <https://doi.org/10.3389/fmicb.2016.00231>.
- Rinta-Kanto JM, Sinkko H, Rajala T, Al-Soud WA, Sørensen SJ, Tamminen MV, Timonen S. 2016. Natural decay process affects the abundance and community structure of *Bacteria* and *Archaea* in *Picea abies* logs. *FEMS Microbiol Ecol* 92:fiw087. <https://doi.org/10.1093/femsec/fiw087>.
- Purahong W, Wubet T, Krüger D, Buscot F. 2018. Molecular evidence strongly supports deadwood-inhabiting fungi exhibiting unexpected tree species preferences in temperate forests. *ISME J* 12:289–295. <https://doi.org/10.1038/ismej.2017.177>.
- Küffer N, Gillet F, Senn-Irlet B, Job D, Aragno M. 2008. Ecological determinants of fungal diversity on dead wood in European forests. *Fungal Divers* 30:83–95.
- Baldrian P, Zrůstová P, Tláškal V, Davidová A, Merhautová V, Vrška T. 2016. Fungi associated with decomposing deadwood in a natural beech-dominated forest. *Fungal Ecol* 23:109–122. <https://doi.org/10.1016/j.funeco.2016.07.001>.
- Hoppe B, Krüger D, Kahl T, Arnstadt T, Buscot F, Bauhus J, Wubet T. 2015. A pyrosequencing insight into sprawling bacterial diversity and community dynamics in decaying deadwood logs of *Fagus sylvatica* and *Picea abies*. *Sci Rep* 5:9456. <https://doi.org/10.1038/srep09456>.
- Moll J, Kellner H, Leonhardt S, Stengel E, Dahl A, Bässler C, Buscot F, Hofrichter M, Hoppe B. 2018. Bacteria inhabiting deadwood of 13 tree species are heterogeneously distributed between sapwood and heartwood. *Environ Microbiol* 20:3744–3756. <https://doi.org/10.1111/1462-2920.14376>.
- Tláškal V, Zrůstová P, Vrška T, Baldrian P. 2017. Bacteria associated with decomposing dead wood in a natural temperate forest. *FEMS Microbiol Ecol* 93:fix157. <https://doi.org/10.1093/femsec/fix157>.
- Leibold MA, Chase JM. 2017. *Metacommunity ecology*. Princeton University Press, Princeton, NY.
- Purahong W, Wubet T, Lentendu G, Schlotter M, Pecyna MJ, Kapturska D, Hofrichter M, Krüger D, Buscot F. 2016. Life in leaf litter: novel insights into community dynamics of bacteria and fungi during litter decomposition. *Mol Ecol* 25:4059–4074. <https://doi.org/10.1111/mec.13739>.
- Worrhich A, König S, Miltner A, Banitz T, Centler F, Frank K, Thullner M, Harms H, Kästner M, Wick LY. 2016. Mycelium-like networks increase bacterial dispersal, growth, and biodegradation in a model ecosystem at various water potentials. *Appl Environ Microbiol* 82:2902–2908. <https://doi.org/10.1128/AEM.03901-15>.
- Tecon R, Or D. 2016. Bacterial flagellar motility on hydrated rough surfaces controlled by aqueous film thickness and connectedness. *Sci Rep* 6:19409. <https://doi.org/10.1038/srep19409>.
- Banitz T, Fetzer I, Johst K, Wick LY, Harms H, Frank K. 2011. Assessing

- biodegradation benefits from dispersal networks. *Ecol Modell* 222:2552–2560. <https://doi.org/10.1016/j.ecolmodel.2010.07.005>.
42. Anderson-Teixeira KJ, Davies SJ, Bennett AC, Gonzalez-Akre EB, Muller-Landau HC, Wright SJ, Abu Salim K, Almeyda Zambrano AM, Alonso A, Baltzer JL, Basset Y, Bourg NA, Broadbent EN, Brockelman WY, Bunyavejchewin S, Burslem DFRP, Butt N, Cao M, Cardenas D, Chuyong GB, Clay K, Cordell S, Dattaraja HS, Deng X, Detto M, Du X, Duque A, Erikson DL, Ewango CEN, Fischer GA, Fletcher C, Foster RB, Giardina CP, Gilbert GS, Gunatilleke N, Gunatilleke S, Hao Z, Hargrove WW, Hart TB, Hau BCH, He F, Hoffman FM, Howe RW, Hubbell SP, Inman-Narahari FM, Jansen PA, Jiang M, Johnson DJ, Kanzaki M, Kassim AR, et al. 2015. CTF5-ForestGEO: a worldwide network monitoring forests in an era of global change. *Glob Chang Biol* 21:528–549. <https://doi.org/10.1111/gcb.12712>.
 43. Král K, Valtera M, Janík D, Šamonil P, Vrška T. 2014. Spatial variability of general stand characteristics in central European beech-dominated natural stands – effects of scale. *For Ecol Manage* 328:353–364. <https://doi.org/10.1016/j.foreco.2014.05.046>.
 44. Král K, Janík D, Vrška T, Adam D, Hort L, Unar P, Šamonil P. 2010. Local variability of stand structural features in beech dominated natural forests of Central Europe: implications for sampling. *For Ecol Manage* 260:2196–2203. <https://doi.org/10.1016/j.foreco.2010.09.020>.
 45. Privětivý T, Janík D, Unar P, Adam D, Král K, Vrška T. 2016. How do environmental conditions affect the deadwood decomposition of European beech (*Fagus sylvatica* L.)? *For Ecol Manage* 381:177–187. <https://doi.org/10.1016/j.foreco.2016.09.033>.
 46. Větrovský T, Baldrian P. 2015. An in-depth analysis of actinobacterial communities shows their high diversity in grassland soils along a gradient of mixed heavy metal contamination. *Biol Fertil Soils* 51:827–837. <https://doi.org/10.1007/s00374-015-1029-9>.
 47. Kirk TK, Obst JR. 1988. Lignin determination. *Methods Enzymol* 161:87–101. [https://doi.org/10.1016/0076-6879\(88\)61014-7](https://doi.org/10.1016/0076-6879(88)61014-7).
 48. Ihrmark K, Bodeker ITM, Cruz-Martinez K, Friberg H, Kubartova A, Schenck J, Strid Y, Stenlid J, Brandström-Durling M, Clemmensen KE, Lindahl BD. 2012. New primers to amplify the fungal ITS2 region - evaluation by 454-sequencing of artificial and natural communities. *FEMS Microbiol Ecol* 82:666–677. <https://doi.org/10.1111/j.1574-6941.2012.01437.x>.
 49. Caporaso JG, Lauber CL, Walters WA, Berg-Lyons D, Lozupone CA, Turnbaugh PJ, Fierer N, Knight R. 2011. Global patterns of 16S rRNA diversity at a depth of millions of sequences per sample. *Proc Natl Acad Sci U S A* 108:4516–4522. <https://doi.org/10.1073/pnas.1000080107>.
 50. Větrovský T, Baldrian P, Morais D. 2018. SEED 2: a user-friendly platform for amplicon high-throughput sequencing data analyses. *Bioinformatics* 34:2292–2294. <https://doi.org/10.1093/bioinformatics/bty071>.
 51. Aronesty E. 2013. Comparison of sequencing utility programs. *Open Bioinform J* 7:1–8. <https://doi.org/10.2174/1875036201307010001>.
 52. Nilsson RH, Veldre V, Hartmann M, Unterseher M, Amend A, Bergsten J, Kristiansson E, Ryberg M, Jumpponen A, Abarenkov K. 2010. An open source software package for automated extraction of ITS1 and ITS2 from fungal ITS sequences for use in high-throughput community assays and molecular ecology. *Fungal Ecol* 3:284–287. <https://doi.org/10.1016/j.funeco.2010.05.002>.
 53. Edgar RC, Haas BJ, Clemente JC, Quince C, Knight R. 2011. UCHIME improves sensitivity and speed of chimera detection. *Bioinformatics* 27:2194–2200. <https://doi.org/10.1093/bioinformatics/btr381>.
 54. Edgar RC. 2013. UPARSE: highly accurate OTU sequences from microbial amplicon reads. *Nat Methods* 10:996–998. <https://doi.org/10.1038/nmeth.2604>.
 55. Kõljalg U, Nilsson RH, Abarenkov K, Tedersoo L, Taylor AFS, Bahram M, Bates ST, Bruns TD, Bengtsson-Palme J, Callaghan TM, Douglas B, Drenkhan T, Eberhardt U, Dueñas M, Grebenc T, Griffith GW, Hartmann M, Kirk PM, Kohout P, Larsson E, Lindahl BD, Lücking R, Martín MP, Matheny PB, Nguyen NH, Niskanen T, Oja J, Peay KG, Peintner U, Peterson M, Pöldmaa K, Saag L, Saar I, Schübler A, Scott JA, Senés C, Smith ME, Suija A, Taylor DL, Telleria MT, Weiss M, Larsson K-H. 2013. Towards a unified paradigm for sequence-based identification of fungi. *Mol Ecol* 22:5271–5277. <https://doi.org/10.1111/mec.12481>.
 56. Cole JR, Wang Q, Fish JA, Chai B, McGarrell DM, Sun Y, Brown CT, Porras-Alfaro A, Kuske CR, Tiedje JM. 2014. Ribosomal Database Project: data and tools for high throughput rRNA analysis. *Nucleic Acids Res* 42:D633–D642. <https://doi.org/10.1093/nar/gkt1244>.
 57. Tikhonov G, Opedal ØH, Abrego N, Lehtikoinen A, Jonge MMJ, Oksanen J, Oksanen O. 2020. Joint species distribution modelling with the r-package Hmsc. *Methods Ecol Evol* 11:442–447. <https://doi.org/10.1111/2041-210X.13345>.
 58. Ovaskainen O, Tikhonov G, Norberg A, Guillaume Blanchet F, Duan L, Dunson D, Roslin T, Abrego N. 2017. How to make more out of community data? A conceptual framework and its implementation as models and software. *Ecol Lett* 20:561–576. <https://doi.org/10.1111/ele.12757>.
 59. Oksanen J, Blanchet FG, Friendly M, Kindt R, Legendre P, McGlenn D, Minchin PR, O'Hara RB, Simpson GL, Solymos P, Stevens MHH, Szoecs E, Wagner H. 2019. vegan: community ecology package. R package version 2.5–6.
 60. R Core Team. 2017. R: a language and environment for statistical computing. R Foundation for Statistical Computing, Vienna, Austria.



Complementary Roles of Wood-Inhabiting Fungi and Bacteria Facilitate Deadwood Decomposition

Vojtěch Tláškal,^{a,b} Vendula Brabcová,^a Tomáš Větrovský,^a Mayuko Jomura,^c Rubén López-Mondéjar,^a Lummy Maria Oliveira Monteiro,^d João Pedro Saraiva,^d Zander Rainier Human,^a Tomáš Cajthaml,^a Ulisses Nunes da Rocha,^d  Petr Baldrian^a

^aInstitute of Microbiology of the Czech Academy of Sciences, Prague, Czech Republic

^bFaculty of Science, Charles University, Prague, Czech Republic

^cDepartment of Forest Science and Resources, College of Bioresource Sciences, Nihon University, Fujisawa, Kanagawa, Japan

^dDepartment of Environmental Microbiology, UFZ-Helmholtz Centre for Environmental Research, Leipzig, Germany

ABSTRACT Forests accumulate and store large amounts of carbon (C), and a substantial fraction of this stock is contained in deadwood. This transient pool is subject to decomposition by deadwood-associated organisms, and in this process it contributes to CO₂ emissions. Although fungi and bacteria are known to colonize deadwood, little is known about the microbial processes that mediate carbon and nitrogen (N) cycling in deadwood. In this study, using a combination of metagenomics, metatranscriptomics, and nutrient flux measurements, we demonstrate that the decomposition of deadwood reflects the complementary roles played by fungi and bacteria. Fungi were found to dominate the decomposition of deadwood and particularly its recalcitrant fractions, while several bacterial taxa participate in N accumulation in deadwood through N fixation, being dependent on fungal activity with respect to deadwood colonization and C supply. Conversely, bacterial N fixation helps to decrease the constraints of deadwood decomposition for fungi. Both the CO₂ efflux and N accumulation that are a result of a joint action of deadwood bacteria and fungi may be significant for nutrient cycling at ecosystem levels. Especially in boreal forests with low N stocks, deadwood retention may help to improve the nutritional status and fertility of soils.

IMPORTANCE Wood represents a globally important stock of C, and its mineralization importantly contributes to the global C cycle. Microorganisms play a key role in deadwood decomposition, since they possess enzymatic tools for the degradation of recalcitrant plant polymers. The present paradigm is that fungi accomplish degradation while commensalist bacteria exploit the products of fungal extracellular enzymatic cleavage, but this assumption was never backed by the analysis of microbial roles in deadwood. This study clearly identifies the roles of fungi and bacteria in the microbiome and demonstrates the importance of bacteria and their N fixation for the nutrient balance in deadwood as well as fluxes at the ecosystem level. Deadwood decomposition is shown as a process where fungi and bacteria play defined, complementary roles.

KEYWORDS bacteria, deadwood, decomposition, forest ecosystems, fungi, metatranscriptomics, microbiome, nitrogen fixation, nutrient cycling

Forests play a crucial role in making the Earth habitable by maintaining biodiversity and serving as an important part of biogeochemical cycles (1, 2). Forests, especially unmanaged natural forests, accumulate and store large amounts of carbon (3). A substantial fraction of this C stock, 73 ± 6 Pg, or 8% of the total global forest C stock (2), is contained within deadwood. This C pool is transient, because during its transformation by saprotrophic organisms, most C is liberated as CO₂ into the atmosphere, while the

Citation Tláškal V, Brabcová V, Větrovský T, Jomura M, López-Mondéjar R, Oliveira Monteiro LM, Saraiva JP, Human ZR, Cajthaml T, Nunes da Rocha U, Baldrian P. 2021.

Complementary roles of wood-inhabiting fungi and bacteria facilitate deadwood decomposition. *mSystems* 6:e01078-20. <https://doi.org/10.1128/mSystems.01078-20>.


Editor Karoline Faust, KU Leuven

Ad Hoc Peer Reviewers Yahya Kooch, Tarbiat Modares University; Maraike Probst, University of Innsbruck

The review history of this article can be read [here](#).

Copyright © 2021 Tláškal et al. This is an open-access article distributed under the terms of the [Creative Commons Attribution 4.0 International license](#).

Address correspondence to Petr Baldrian, baldrian@biomed.cas.cz.

 Fungi and bacteria play complementary roles in deadwood transformation where fungi dominate in decomposition while bacteria and their N₂ fixation are important for the nutrient balance in deadwood as well as fluxes at the ecosystem level.

Received 16 October 2020

Accepted 13 December 2020

Published 12 January 2021

rest is sequestered in soils as dissolved organic C or within microbial biomass along with other nutrients. Recent reports estimate the annual deadwood C efflux through respiration from temperate and boreal stands to be 0.5 to 3.6 Mg C ha⁻¹ year⁻¹ (4, 5). Thus, the C efflux originating in deadwood decomposition is comparable to that of forest soil respiration of 7.8 and 5.0 Mg C ha⁻¹ year⁻¹ in temperate and boreal forests, respectively (6).

Deadwood is a specific substrate that is rich in C but highly recalcitrant and physically impermeable. Deadwood hosts a wide range of fungi and bacteria (7, 8), and the cord-forming basidiomycetes are considered major wood decomposers due to their strong enzymatic production. This feature makes them able to degrade all important components of wood and to rapidly penetrate it (9, 10). Furthermore, fresh deadwood of most temperate and boreal trees has a low nitrogen content, ranging between 0.03 and 0.19% of dry mass (11), which represents a major limitation for decomposition (12). During decomposition, the N content in deadwood typically increases (13, 14) as a consequence of C loss by respiration. In addition, bacterial fixation of atmospheric N₂ was shown to substantially contribute to the N increase in deadwood during decomposition (15, 16). N fixation is highly energy-demanding, and young deadwood with available C sources represents a potentially ideal setting for this process (17). In specific situations, N content in deadwood also may be increased through translocation by ectomycorrhizal or certain other fungi (9, 16). We ask how C utilization and N cycling in deadwood are coupled and what the roles are of the individual members of deadwood microbiome. The answers to these questions are especially important for the understanding of the ecology of high-latitude forests that are typically N limited and both symbiotic and asymbiotic soil N fixation is low (18, 19). Under these conditions, N fixation in deadwood may represent a process of ecosystem-level importance.

In this study, we utilized the combination of metagenomics, metatranscriptomics, and gas flux measurements to analyze the participation of the deadwood-associated microbiome of a European beech (*Fagus sylvatica*)-dominated temperate natural forest in the cycling of C and N. Our findings suggest that deadwood in the ecosystem of temperate forests is a hot spot of bacterial N fixation and fungal degradation. We demonstrate that decomposition of deadwood is done through complementing traits of fungi and bacteria playing specific roles in C and N cycling.

RESULTS AND DISCUSSION

None of the parameters of wood chemistry were significantly different between old and young deadwood (Fig. 1). In particular, the wood density, indicating the progress of decomposition, showed high variation, ranging from 290 to 470 kg m⁻³. This is not surprising, since individual deadwood logs are under the complex influence of the individual history of the microbial community assembly and microclimate conditions, including sun exposure and soil contact (20, 21). Both CO₂ production from deadwood and N fixation showed a significant correlation with pH ($r = -0.720$, $P = 0.016$ and $r = -0.832$, $P = 0.003$, respectively). The young and old deadwood had similar levels of respiration of 1.43 ± 0.31 and 1.21 ± 0.38 g CO₂ kg⁻¹ day⁻¹ (Fig. 1), comparable to estimates from other temperate forests (4, 5). Considering that the average deadwood stock in the studied natural forest is 208 m³ ha⁻¹ (22), the CO₂ flux from deadwood would be in a similar range of CO₂ flux from soils in temperate and boreal forests, 7.8 ± 10.4 and 5.0 ± 18.0 Mg ha⁻¹ year⁻¹, respectively (6). This confirms previous reports of deadwood decomposition as an important CO₂ source (5).

The rates of N fixation were significantly higher in young deadwood than in old deadwood (297 ± 103 and 37 ± 20 ng N g⁻¹ day⁻¹, $P = 0.031$) (Fig. 1). These results reflect that the N content is very low in fresh *Fagus sylvatica* deadwood, while it is high in labile C sources that are required to fuel this highly energy-consuming process (17). As decomposition proceeds, N accumulation relieves N limitation in deadwood and, thus, affects microbial composition at the end of the deadwood life cycle. The accumulated N represents an input into forest soils with a potentially high impact, especially in

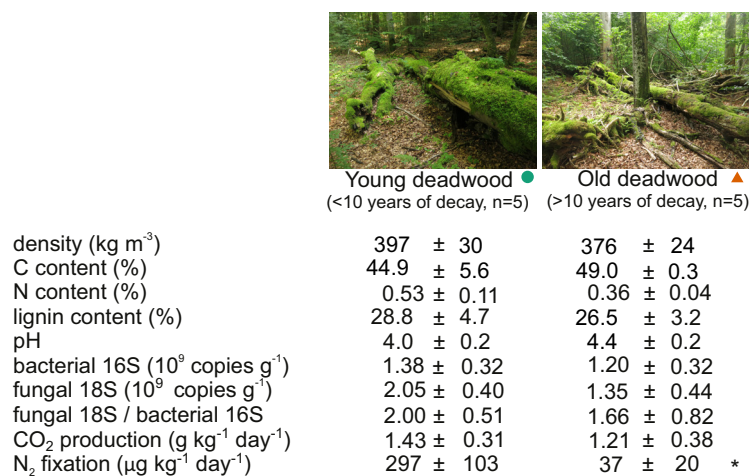


FIG 1 Comparison of properties of young and old deadwood. Chemical properties and microbial biomass across samples of old and young deadwood and the rates of CO₂ production and N fixation. Due to high variation, none of the measured parameters was significantly different among young and old deadwood, except for the N fixation rate, which was significantly higher in young deadwood (*). The values indicate means and standard errors ($n=5$); N fixation was estimated in an acetylene reduction assay.

N-limited high-latitude forests (18). The area-approximated N fixation of 0.49 g N₂ m⁻² year⁻¹ for the studied forest at the optimal temperature of 25°C is comparable to reports from boreal forests (15, 16). These values are typically higher than those reported for asymbiotic N fixation in soils of temperate and boreal forests (23, 24), which underlines the importance of N fixation in deadwood as the source of new N input (25).

Decomposing deadwood appeared to be rich in microbial biomass irrespective of deadwood age, with the number of copies of bacterial and fungal ribosomal DNA being approximately 10⁹ copies per g dry mass, and the counts of fungi were slightly higher than those of bacteria (Fig. 1). The composition of total biomass based on the small subunit rRNA, representing the pool of ribosomes, identified fungi and bacteria as the dominant components of the deadwood microbiome, with Arthropoda and Nematoda representing the most abundant nonmicrobial organisms. This finding also confirmed the dominance of Eukaryota, which represented 50 to 94% of the rRNA pool (Fig. 2a). Identified transcripts were again mostly assigned to Eukaryota (58 to 94%), with most of them being affiliated with the Basidiomycota and Ascomycota fungi; on average, the share of fungal transcripts was 85% and that of bacteria was 13% (Fig. 2b). When looking at the expression of ribosomal proteins that may represent a proxy of growth (26), the share of bacteria was slightly higher (Fig. 2c).

Importantly, the fungal community and transcriptional activity in all but three decomposing logs were dominated by Basidiomycota, where they were responsible for 72.5% ± 1.0% of transcription (Fig. 2b). In three logs, Ascomycota showed the highest share of transcription (38.6% ± 2.1%), and in this instance, the share of bacterial transcription was also higher (27.7% ± 3.5%), being approximately 4-fold higher than that of logs dominated by Basidiomycota (Fig. 2b). This distinction in microbiome composition is likely due to the colonization history of the substrate (20) but may also reflect the antagonism of Basidiomycota toward bacteria (7).

Deadwood is theoretically an unlimited stock of organic carbon, and its utilization is the main source of energy and biomass for deadwood-associated organisms. The share of genes with a known role in the decomposition of plant, fungal, and bacterial biomass ranged between 0.11% and 0.61% of the total transcription. This value did not differ among old and young deadwood but was significantly lower in the Ascomycota-dominated logs than in the Basidiomycota-dominated logs (0.12 ± 0.01 and 0.42 ± 0.06%,

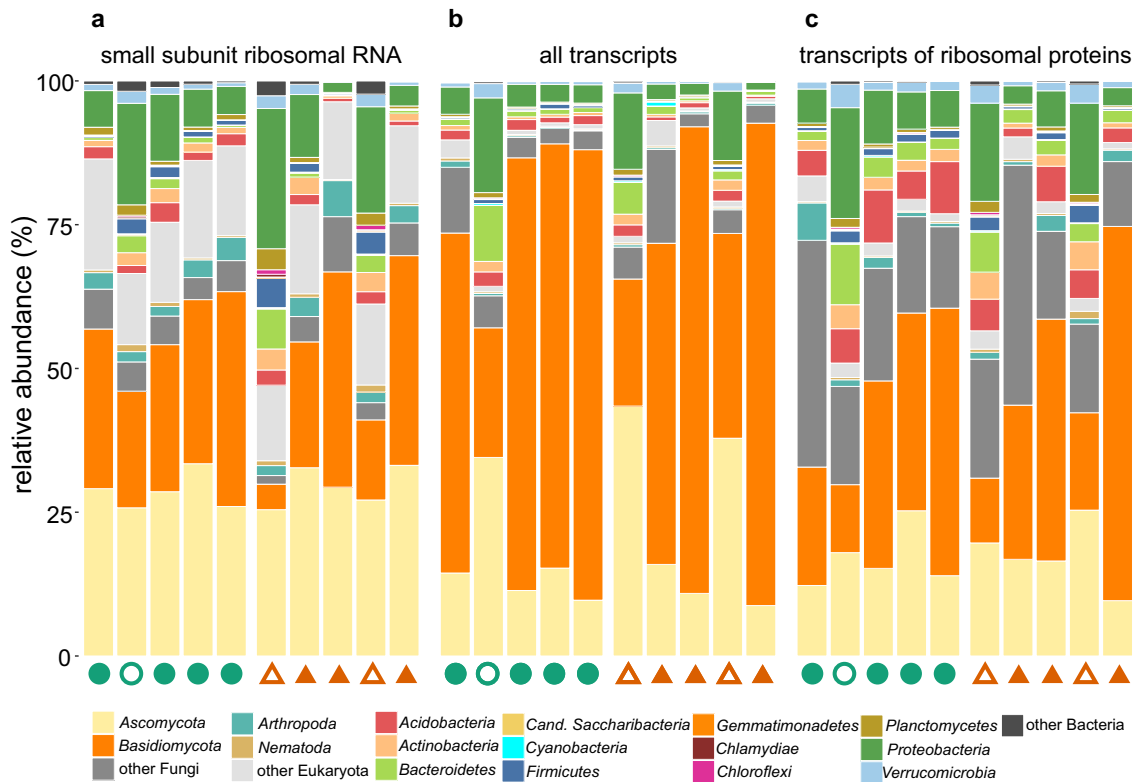


FIG 2 Taxonomic composition and activity of deadwood-associated organisms. Composition of the community of deadwood-associated organisms based on the relative abundance of small ribosomal subunit RNA, corresponding to ribosome counts (a), their activity based on the relative abundance of all mRNA transcripts (b), and their growth based on the relative abundance of mRNA of genes encoding ribosomal proteins (c). Filled symbols indicate samples dominated by Basidiomycota, and open symbols indicate those rich in Ascomycota and bacteria.

respectively, $P = 0.018$) (Fig. 3a). Enzyme expression also significantly decreased with pH ($r = -0.927$, $P < 0.001$). The pool of carbohydrate-active enzymes (CAZymes) was mostly composed of those targeting cellulose (0.17% of all transcripts), cellobiose and xylobiose (0.042%), fungal glucans (0.031%), lignin (0.020%), and chitin (0.015%) (Fig. 3a). The CAZyme families participating in the degradation of cellulose (AA9, GH5, and GH7), lignin (AA2), and chitin (GH18) were among the most abundant in both the metagenome and metatranscriptome (see Fig. S1 in the supplemental material), indicating that plant and fungal biomass are the most important C sources (Fig. 3a). Ordination of samples based on the CAZyme composition showed separation of Basidiomycota- and Ascomycota-dominated logs as well as clustering by deadwood age (Fig. 3b).

As much as 91% of transcripts of CAZymes decomposing biopolymers in deadwood were assigned to fungi with a share of bacteria of only 7% (Fig. 3c). Although fungi are also major producers of CAZymes in other environments, contributing, for instance, 78% and 42% in forest litter and soil (27, 28), the extent of fungal dominance in CAZyme transcription in deadwood is unprecedented (Fig. S1). For the two most recalcitrant wood biopolymers, lignin and cellulose, the ratio of fungal to bacterial transcripts was as high as 642:1. While 29.8% of CAZymes produced by fungi targeted lignin or cellulose, only 1.4% of CAZymes produced by bacteria targeted these substrates. Since the degradation of these structural biopolymers is required for wood colonization, fungi appear to play a decisive role in opening the physically recalcitrant substrate for utilization by deadwood-associated biota. In this context, the role of Basidiomycota should be stressed, since they represent the only microbial phylum to degrade lignin (Fig. S1). The bacterial contribution to C utilization was higher in the cases of starch/glycogen and peptidoglycan (Fig. 3c and Fig. S1). Methylophily was

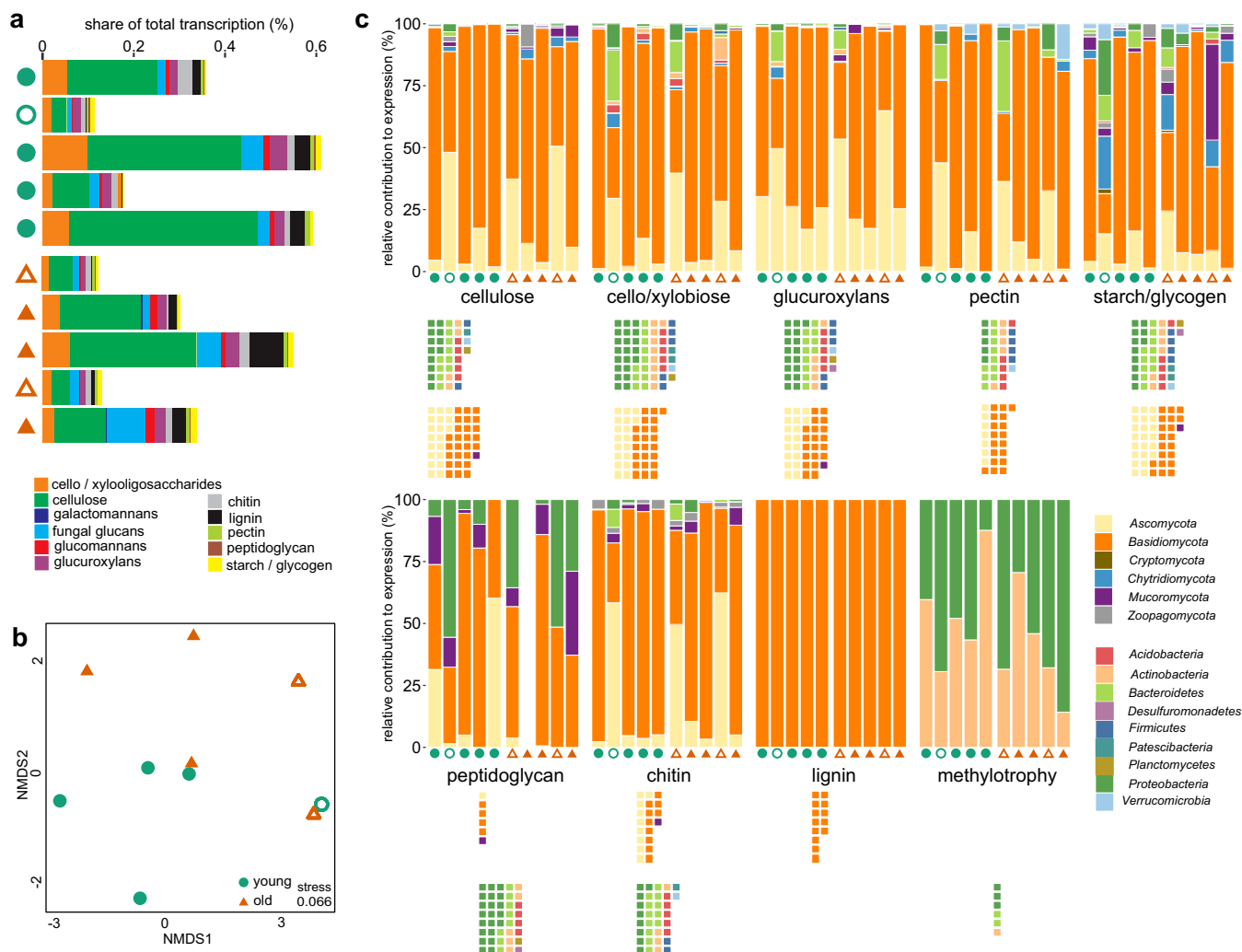


FIG 3 Functional diversity of enzymes targeting sources of carbon. The functional and taxonomic breakdown of CAZymes and methylotrophy genes is shown. The relative rate of transcription of CAZymes (GH and AA families) targeting relevant wood substrates across samples (a) and two-dimensional NMDS based on Euclidean distance of the transcription rates of individual CAZy families (b). (c) Relative contribution of fungi and bacteria to the expression of CAZymes and methylotrophy genes by target. Squares indicate the diversity and taxonomic assignment of fungal genera and bacterial MAGs with the potential to utilize a given substrate. Each square corresponds to one bacterial MAG or one fungal genus.

present in *Proteobacteria* and *Actinobacteria*, although its contribution to C utilization was relatively small, with 24 ± 3 reads per million reads being observed (Fig. 3c). In this bacterium-specific pathway, methylotrophs utilize C from methane and methanol, the by-products of fungal wood decomposition (29).

N-cycling genes accounted for an average of 0.06% of transcripts. Of these transcripts, genes involved in ammonia incorporation into organic molecules represented 85.8% and were transcribed by all microbial taxa (Fig. 4), catalyzing the recycling of N liberated from organic compounds. In agreement with the high rates of potential N fixation, N fixation was the dominant process of the transformation of inorganic N with a share of 7.4% of all N-cycling genes (Fig. 4). Excluding ammonia assimilation, the nitrogenase *nifD* was the most transcribed gene overall in the N cycle. N fixation was mostly performed by *Proteobacteria* but also by *Firmicutes*, *Chlorobi*, *Verrucomicrobia*, and *Bacteroidetes*. Nitrate and nitrite reduction were represented by 3.5% and 2.8% of N-cycling transcripts, with dissimilatory steps in the N cycle being represented by only 1.0% (Fig. 4). Compared to soils (30), the respiratory pathways utilizing nitrate or nitrite seem to be considerably less important in deadwood. Importantly, missing nitrification steps and high rates of ammonia assimilation underscore that almost all available N is

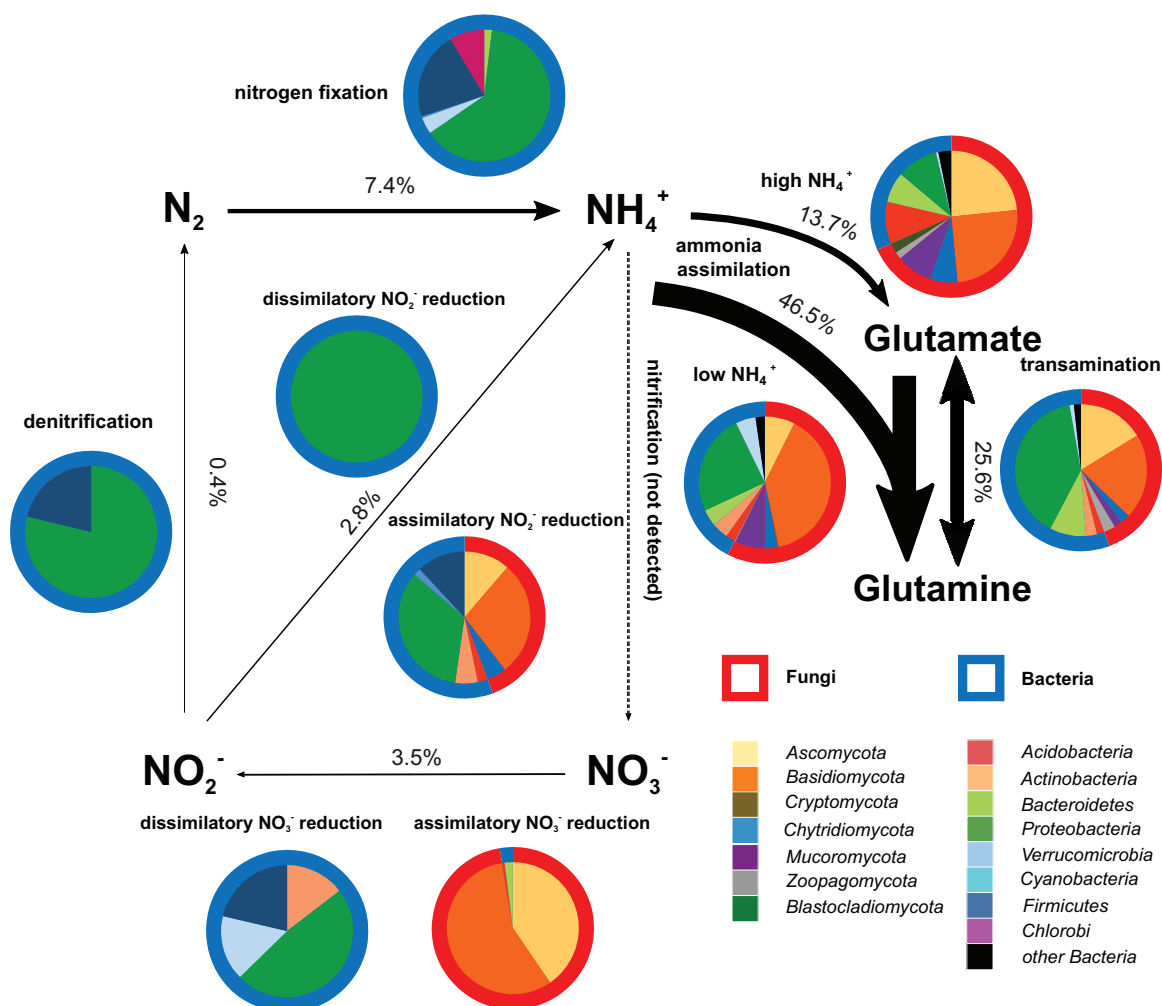


FIG 4 Nitrogen cycle and ammonia assimilation pathways occurring in deadwood. N-cycling intensity is expressed as the relative share of expression of each function across all N-cycling genes. Pie charts indicate the relative shares of bacterial and fungal transcription in each process. Nitrification was not detected.

incorporated into living systems. This finding is, again, in contrast with soils where large parts of N are oxidized by nitrification of bacteria to gain energy (27, 31).

The assignment of genes and transcripts to 58 high-quality metagenome-assembled genomes (MAGs) of bacteria or to fungal taxa makes it possible to find adaptations of microorganisms to life on decomposing deadwood (Fig. S2 and S4). The ability of bacteria to utilize a more or less wide range of C compounds showed phylogenetic clustering, with the MAGs classified as *Actinobacteria* and *Proteobacteria* containing 36 ± 5 and 46 ± 5 CAZymes per genome compared to 101 ± 15 and 122 ± 16 in the most versatile *Acidobacteria* and *Bacteroidetes* (Fig. S3). Several bacterial genomes (members of *Acidobacteria*, *Bacteroidetes*, *Firmicutes*, *Proteobacteria*, and *Planctomycetes*) combined the potential to fix N and to produce CAZymes targeting dominant plant biopolymers, such as cellulose, which makes them independent in C and N utilization (Fig. S2). Other N-fixing taxa within *Actinobacteria* and *Proteobacteria* lack the ability to decompose complex biopolymers and have to rely on the utilization of cello- and xylooligosaccharides provided by other decomposers. As the last option, the members of the order *Rhizobiales* combine N fixation with methylotrophy (Fig. S2), being dependent on the supply of C by fungal wood decomposers (32).

The classification of fungal transcripts indicates that within Basidiomycota, white-

rot fungi capable of lignin degradation, such as *Armillaria*, *Ganoderma*, or *Phlebia*, play important roles in deadwood decomposition. The dominant members of Ascomycota, such as *Xylaria* and *Anthostoma*, belong to soft-rot fungi that preferentially utilize cellulose and hemicelluloses in deadwood. The spectra of utilized C biopolymers across fungi are relatively wide, and cellulose is decomposed by most of the dominant taxa (Fig. S4). Fungal involvement in the N cycle is often constrained to the incorporation of ammonia into biomass, with assimilatory pathways on nitrate and nitrite reduction playing a much more limited role (Fig. S4). The fungal component of the deadwood microbiome is relatively diverse and includes, among others, plant pathogens and ectomycorrhizal fungi associated with tree seedlings that germinate on deadwood (Fig. S4). Among nutritional guilds, white-rot fungi display the most diverse enzyme sets, being able to utilize various carbon sources, while members of other guilds are less versatile. Only one of three dominant ectomycorrhizal fungi expressed polysaccharide-targeting enzyme-degrading fungal glucans (Fig. S5), which is not surprising, considering the low occurrence of biopolymer-degrading genes in their genomes (33). The versatility of white-rot basidiomycetes, enabling them to rapidly colonize wood by degrading both lignin and cellulose, is the likely reason for their high abundance and functional dominance in the majority of decomposing logs. Moreover, rapid hyphal growth was found to be a key predictor of overall deadwood decomposition rate, showing that versatile groups have direct influence on this process (34).

While deadwood potentially represents an exclusive stock of C and fungi often behave antagonistically toward competitors to capture as much of the deadwood resources as possible (7, 35), their activity in deadwood also opens a window of opportunity for selected bacteria (36). The colonization of deadwood by fungal hyphae promotes the spread of bacteria that can slide along hyphae (37) or benefit from nutrient redistribution (38). Moreover, the high share of expression of cello- and xylooligosaccharide-degrading enzymes by bacteria, such as β -glucosidases, indicates their utilization of cellulose and xylan fragments, the products of (almost exclusively) fungal degradation of the recalcitrant biopolymers. Previous analyses of deadwood microbiomes suggested cooperation between N-fixers and fungi (39, 40). While some bacterial N-fixers may be independent in C acquisition, methylotrophic and commensalist N-fixers depend on products of biopolymer decomposition by fungi. On the fungal side, N accumulation in deadwood due to bacterial fixation promotes the succession of decomposers. The white-rot fungi parasitic on living trees and primary colonizers of deadwood are adapted to N-limited conditions, such as *Fomitopsis*, with only 0.8% N in mycelia (41). These fungi, however, are not able to completely utilize deadwood resources. Many later colonizers have larger N requirements, with N content in mycelia of up to 6.4% as in the case of *Lycoperdon* (41). Although some N can be scavenged from dead mycelia of primary colonizers (42), bacterial N fixation alleviates N limitation and allows the complete recycling of organic matter by late decomposers and ultimately the incorporation of residual material into soil. Thus, the role partitioning between bacteria and fungi seems to be important for complete deadwood decomposition. In specific situations, such as in *Picea abies* forests where young trees establish on decomposing deadwood, N may be translocated to deadwood from soil by ectomycorrhizal or soil-foraging fungi (16). However, the *Fagus sylvatica* deadwood studied here was devoid of tree seedlings and ectomycorrhizal fungi (Fig. S4), and no overlap of cord-forming fungi was found between deadwood and the soil beneath it (43).

While the partitioning of roles between fungi and bacteria appears to be important for the individual fates of decomposing deadwood logs, the whole process also has ecosystem-level consequences. CO₂ fluxes from deadwood appear to be quantitatively important in forests where deadwood stocks are large. Although more research is still needed, it seems that the amount of fixed N₂ during deadwood decomposition may represent an important source of N entering the soil environment at the end of the deadwood life cycle. Especially in boreal forests with low N stocks, deadwood retention may help to improve the nutritional status and fertility of forest soils.

MATERIALS AND METHODS

Study site. The study was performed in the Žofínský Prales National Nature Reserve, an unmanaged forest in the south of the Czech Republic (48°39'57"N, 14°42'24"E). The core zone of the forest reserve (42 ha) had never been managed and any human intervention stopped in 1838, when it was declared as a reserve. Thus, it represents a rare fragment of European temperate virgin forest with deadwood left to spontaneous decomposition. The reserve is situated at 730 to 830 m above sea level, and the bedrock is almost homogeneous and consists of fine to medium-grained porphyritic and biotite granite. Annual average rainfall is 866 mm, and annual average temperature is 6.2°C (44). At present, the reserve is covered by a mixed forest where *Fagus sylvatica* predominates in all diameter classes (51.5% of total living wood volume), followed by *Picea abies* (42.8%) and *Abies alba* (4.8%). The mean living tree volume is 690 m³ h⁻¹, and the volume of coarse woody debris (logs, represented by tree trunks and their fragments, from 102 to 310 m³ h⁻¹ with an average of 208 m³ h⁻¹) (22, 45). Logs are repeatedly surveyed, and an approximate age of each log, the cause of death (e.g., stem breakage, windthrow, etc.), and status before downing (fresh or decomposed) is known (13).

Study design and sampling. Previous analysis indicated that deadwood age (time of decomposition) significantly affects both wood chemistry and the composition of microbial communities (13, 46). Thus, we randomly selected dead tree trunks that represented young deadwood (<10 years of decomposition, $n = 5$) and old deadwood (>10 years of decomposition, $n = 5$); only trees that were not alive and not decomposed before downing were considered. Selection was enabled by a database of deadwood with data from historical surveys. For metagenome (MG) analysis, to obtain a more comprehensive annotation source, 15 additional logs were sampled, giving a total 25 metagenomic samples. Sampling was performed in November 2016. The length of each selected log (or the sum of the lengths of its fragments) was measured, and four samples were collected evenly along the log length by drilling vertically from the middle of the upper surface through the whole diameter using an electric drill with an auger diameter of 10 mm. The sawdust from all four samples from each log was pooled and immediately frozen using liquid nitrogen, transported to the laboratory on dry ice, and stored at -80°C until further processing. For the measurement of CO₂ production and N fixation, compact pieces of deadwood of an approximate volume of 4 cm³ (three replicates per log) were collected and brought to the laboratory under refrigeration to be used for immediate analysis.

Deadwood chemistry, CO₂ production, and N fixation. For pH measurement, approximately 0.5 g of subsampled wood material was mixed with 5 ml of deionized water, left overnight at 4°C, and shaken for 60 min on an orbital shaker before assessment. The C and N contents were measured in an external laboratory: a freeze-dried subsample was milled (<0.1 mm particle size), and 10 to 30 mg of material was burned in 100% O₂ at 1,000°C. The amounts of oxidized C and N were recorded by Flash 2000 (Thermo Scientific) and analyzed with Eager Xperience software (Thermo Scientific) to obtain their relative contents. Deadwood density was estimated as a ratio of its dry mass after freeze-drying and volume.

Three independent samples of compact wood material per log, each of an approximate volume of 10 cm³, were collected for the estimation of CO₂ production and N fixation rates according to reference 5. For CO₂ production estimation, samples were incubated for 10 min in an acrylic chamber (volume, 2.2 liters). CO₂ concentration and humidity in the chamber were monitored with an infrared gas analyzer GMP 343 (Vaisala Inc.) and hydrometer RTR 503 (T and D Inc.). Per-second data were recorded by a data logger GL200A (Graphtec Inc.). The temperature of the surface of the samples was measured using a Fluke 561 infrared thermometer (Fluke Inc.). The last 5 min of incubation were used to calculate the respiration rate to avoid the effect of moisture change. To adjust for mean temperature at the site (6.2°C), the model $R_{CWD} = a \times e^{bT}$ was used to transform respiration data (4). For N fixation, an acetylene reduction assay was performed by following reference 47. Ten percent of the headspace of the 4-ml vial with wood block was replaced with acetylene gas and incubated at the temperature of maximal nitrogenase activity, 25.2°C, for 24 h (18). The concentration of ethylene in the headspace was analyzed by a gas chromatograph (436-Scion; Bruker). Head space (100 μ l) of the samples was used for injection, and the analytes were separated isothermally at 30°C using a Restek Rt U-Bond 30-m column (inner diameter, 0.25 mm; film thickness, 8 μ m), equipped with a PLOT column particle trap (2.5 m). The injector temperature was set to 240°C with a 1:20 splitter, and the carrier gas was helium (5.0; 2 ml min⁻¹). A conversion factor from acetylene reduction to N fixation of 4 was used (15). For retrieval of global records of soil CO₂ efflux, the SRDB database was accessed in February 2020 (git version 8ab37bf, temperate forest records $n = 1,310$, boreal forests records $n = 198$) [6].

Nucleic acid extraction. Wood samples (approximately 10 g of material) were homogenized using a mortar and pestle under liquid nitrogen prior to nucleic acid extraction and thoroughly mixed. Total DNA was extracted in triplicate from 200-mg batches of finely ground wood powder using a NucleoSpin soil kit (Macherey-Nagel).

Total RNA was extracted in triplicate from 200-mg batches of sample using a NucleoSpin RNA plant kit (Macherey-Nagel) according to the manufacturer's protocol after mixing with 900 μ l of the RA1 buffer and shaking on FastPrep-24 (MP Biomedicals) at 6.5 ms⁻¹ twice for 20 s. Triplicates were pooled and treated with a OneStep PCR inhibitor removal kit (Zymo Research). DNA was removed using a DNA-free DNA removal kit (Thermo Fisher Scientific). The efficiency of DNA removal was confirmed by the negative PCR results with the bacterial primers 515F and 806R (48). RNA quality was assessed using a 2100 Bioanalyzer (Agilent Technologies).

Analysis of deadwood-associated organisms. To estimate the relative representation of bacteria, fungi, and other organisms in deadwood, reads of small subunit rRNA, representing the ribosome counts, were identified and classified from total RNA. Libraries for high-throughput sequencing of total

RNA were prepared using a TruSeq RNA sample prep kit v2 (Illumina) according to the manufacturer's instructions, omitting the initial capture of poly(A) tails to enable total RNA to be ligated. Samples were pooled in equimolar volumes and sequenced on an Illumina HiSeq 2500 with a rapid run 2 × 250 option at Brigham Young University Sequencing Centre, USA. Raw FASTQ files were processed using Trimmomatic 0.36 (49) and FASTX-Toolkit (http://hannonlab.cshl.edu/fastx_toolkit/) to filter out adaptor contamination, trim low-quality ends of reads, and omit reads with overall low quality (<30). Sequences shorter than 40 bp were omitted. Non-rRNA reads were filtered out from the files using the `bbduk.sh` 38.26 program in BBTools (<https://sourceforge.net/projects/bbmap/>). BLASTn 2.7.1+ was used against the manually curated database SilvaMod, derived from Silva nr SSU Ref v128 (50, 51), to infer the best 50 hits with output as full-alignment XML file for all reads in each sample. Furthermore, the LCAClassifier script from CREST software (50) was used to construct alignments to find the best possible classification of each read with the lowest common ancestor approach.

Bacterial and fungal rRNA gene copies in DNA samples were quantified by quantitative PCR (qPCR) using the 1108f and 1132r primers for bacteria (52, 53) and FR1 and FF390 primers for fungi (54) as described previously (55). The fungal/bacterial rRNA gene ratio was calculated by dividing rRNA gene copy numbers.

Metagenomics and metatranscriptomics. For metatranscriptome (MT) analysis, the content of rRNA in RNA samples was reduced as described previously (55) using a combination of Ribo-Zero rRNA removal kit human/mouse/rat and Ribo-Zero rRNA removal kit bacteria (Illumina). Oligonucleotide probes annealed to rRNA from both types of kits were mixed together and added to each sample. The efficiency of the removal was checked using a 2100 Bioanalyzer, and removal was repeated when necessary. Reverse transcription was performed with SuperScript III (Thermo Fisher Scientific). Libraries for high-throughput sequencing were prepared using the ScriptSeq v2 RNA-Seq library preparation kit (Illumina) according to the manufacturer's instructions with a final 14 cycles of amplification by FailSafe PCR enzyme (Lucigen).

The NEBNext Ultra II DNA library prep kit for Illumina (New England BioLabs) was used to generate metagenome libraries according to the manufacturer's instructions. Samples of the metagenome and metatranscriptome were pooled in equimolar volumes and sequenced on an Illumina HiSeq 2500 with a rapid-run 2 × 250 option at Brigham Young University Sequencing Centre, USA.

MG assembly and annotation were performed as described previously (27). Briefly, Trimmomatic 0.36 (49) and FASTX-Toolkit (http://hannonlab.cshl.edu/fastx_toolkit/) were used to remove adaptor contamination, trim low-quality ends of reads, and omit reads with overall low quality (<30); sequences shorter than 50 bp were omitted. The combined assembly of all 25 samples was performed using MEGAHIT 1.1.3 (56). Metagenome sequencing yielded on average 22.5 ± 7.2 million reads per sample that were assembled into 17,936,557 contigs over 200 bp in length.

MT assembly and annotation were performed as described previously (55). Trimmomatic 0.36 (49) and FASTX-Toolkit (http://hannonlab.cshl.edu/fastx_toolkit/) were used to remove adaptor contamination, trim low-quality ends of reads, and omit reads with overall low quality (<30); sequences shorter than 50 bp were omitted. mRNA reads were filtered from the files using the `bbduk.sh` 38.26 program in BBTools (<https://sourceforge.net/projects/bbmap/>). Combined assembly was performed using MEGAHIT 1.1.3 (56). Metatranscriptome sequencing yielded, on average, 31.3 ± 9.1 million reads per sample that were assembled into 1,332,519 contigs over 200 bp in length.

Gene calling was performed using MG-RAST (57) and yielded a total of 22,171,460 and 1,404,953 predicted coding regions for MG and MT, respectively. Taxonomic identification was performed in MG-RAST as well as using BLAST against all published fungal genomes available in January 2018 (58). Of these two, taxonomic identification with a higher bit score was used as the best hit. Functions of predicted genes were annotated with the `hmmsearch` function in HMMER 3.2.1 (59) using the FOAM database as a source of HMMs for relevant genes (60). Genes encoding the carbohydrate-active enzymes (CAZymes) were annotated using the dbCAN HMM database V6 (61). CAZymes were grouped based on their participation in the utilization of distinct C sources based on their classification into known CAZyme families (62). Genes active in methylophony and N cycling were assigned to individual processes based on their KEGG classification (Tables S1, S2, and S3).

Taxonomic and functional annotations with E values higher than $10E^{-30}$ were disregarded. The contribution of various organisms to total transcription was based on the relative abundances of all reads (Fig. 2b) and reads of genes encoding ribosomal proteins (Fig. 2c). Since ribosomes are produced during cell division, these values should correspond to the growth of the organisms (26). Metatranscriptomic reads with the best hit to fungi were classified to fungal genera. Fungal genera were classified into the following ecophysiological groups: white rot, brown rot, soft rot, other saprotrophs, plant pathogens, animal parasites, mycoparasites, and ectomycorrhizal fungi based on published literature, with the definitions of the groups being the same as those in reference 63.

Identification and analysis of metagenome-assembled genomes. The creation and analysis of metagenome-assembled genomes make it possible to analyze the traits of individual prokaryotic taxa without the need of their isolation and, thus, are more representative for the study of ecosystem processes (64). Bins that represent prokaryotic taxa present in the metagenome were constructed using MetaBAT2 (65) with default settings, except for the minimal length of contigs set to 2,000 bp, which produced bins with overall better statistics than the minimal 2,500-bp size. CheckM 1.0.11 (66) served for assigning taxonomy and statistics to bins with the `lineage_wf` pipeline. Bins with a completeness score greater than 50% were selected for quality improvement using RefineM according to the instructions of the developers (67). Briefly, scaffolds with genomic properties (GC content, coverage profiles, and tetranucleotide signatures) whose values were different from those expected in each bin were excluded.

These values were calculated based on the mean absolute error and correlation criteria. Next, the refined bins were further processed to identify and remove scaffolds with taxonomic assignments different from those assigned to the bin. Lastly, the scaffolds that possessed 16S rRNA genes divergent from the taxonomic affiliation of the refined bins were removed. The taxonomy of the bins was inferred by GTDB-TK (68). Fifty-eight bins with quality scores of >50 (CheckM completeness value minus $5 \times$ contamination value) were considered metagenome-assembled genomes (MAGs) as defined by reference 67 and retained for analysis.

Metagenomic and metatranscriptomic reads were mapped to MAGs as described previously (26) using bowtie 2.2.4 (69) to infer the abundance of bins across samples and the expression of bin-specific genes. Relative abundances of mapped reads were obtained by dividing the number of mapped reads by the number of all reads in a given sample.

Statistical analyses. Statistical analysis was performed in the R environment (70). Two-dimensional nonmetric multidimensional scaling (NMDS) was used to plot the variation in the relative abundance of reads of the glycoside hydrolase and auxiliary enzyme families of the CAZymes using the function *metaMDS* from the *vegan* package (71) and Euclidean distance of the Hellinger-transformed CAZy abundance. Analysis of variance (ANOVA) was used to test for the differences in environmental variables. Spearman correlation coefficients were used as a measure of relationships between variables, and Monte Carlo permutation tests were used to determine the *P* values for correlations. Figures were generated using custom Java and R scripts (70), Rstudio (72), Tidyverse (73), and Inkscape (<https://inkscape.org/>).

Data availability. The code for reproducing sequence processing is provided at <https://github.com/TlaskalV/Deadwood-microbiome>. Data described in the manuscript, including raw sequences (total RNA, metatranscriptome, and metagenome), assembly files, and resolved MAGs, have been deposited in NCBI under BioProject accession number [PRJNA603240](https://www.ncbi.nlm.nih.gov/bioproject/PRJNA603240). Properties of dead *Fagus sylvatica* logs analyzed in this paper are provided in Table S4 in the supplemental material.

SUPPLEMENTAL MATERIAL

Supplemental material is available online only.

FIG S1, PDF file, 1.3 MB.

FIG S2, PDF file, 1.3 MB.

FIG S3, PDF file, 0.3 MB.

FIG S4, PDF file, 1.3 MB.

FIG S5, PDF file, 1.3 MB.

TABLE S1, DOCX file, 0.02 MB.

TABLE S2, DOCX file, 0.01 MB.

TABLE S3, DOCX file, 0.02 MB.

TABLE S4, DOCX file, 0.01 MB.

ACKNOWLEDGMENTS

This work was supported by the Czech Science Foundation (17-20110S), by the Ministry of Education, Youth and Sports of the Czech Republic (LTT17022), and by Charles University (GAUK 950217). Computational resources were supplied by the project “e-Infrastruktura CZ” (e-INFRA LM2018140), provided within the program Projects of Large Research, Development and Innovations Infrastructures.

We have no competing interests to declare.

REFERENCES

- Crowther TW, Glick HB, Covey KR, Bettigole C, Maynard DS, Thomas SM, Smith JR, Hintler G, Duguid MC, Amatulli G, Tuanmu MN, Jetz W, Salas C, Stam C, Piotto D, Tavano R, Green S, Bruce G, Williams SJ, Wisser SK, Huber MO, Hengeveld GM, Nabuurs GJ, Tikhonova E, Borchardt P, Li CF, Powrie LW, Fischer M, Hemp A, Homeier J, Cho P, Vibrans AC, Umunay PM, Piao SL, Rowe CW, Ashton MS, Crane PR, Bradford MA. 2015. Mapping tree density at a global scale. *Nature* 525:201–205. <https://doi.org/10.1038/nature14967>.
- Pan YD, Birdsey RA, Fang JY, Houghton R, Kauppi PE, Kurz WA, Phillips OL, Shvidenko A, Lewis SL, Canadell JG, Ciais P, Jackson RB, Pacala SW, McGuire AD, Piao SL, Rautiainen A, Sitch S, Hayes D. 2011. A large and persistent carbon sink in the world's forests. *Science* 333:988–993. <https://doi.org/10.1126/science.1201609>.
- Luyssaert S, Schulze ED, Börner A, Knohl A, Hessenmoller D, Law BE, Ciais P, Grace J. 2008. Old-growth forests as global carbon sinks. *Nature* 455:213–215. <https://doi.org/10.1038/nature07276>.
- Forrester JA, Mladenoff DJ, Gower ST, Stoffel JL. 2012. Interactions of temperature and moisture with respiration from coarse woody debris in experimental forest canopy gaps. *Forest Ecol Manag* 265:124–132. <https://doi.org/10.1016/j.foreco.2011.10.038>.
- Rinne-Garmston KT, Peltoniemi K, Chen J, Peltoniemi M, Fritze H, Makipaa R. 2019. Carbon flux from decomposing wood and its dependency on temperature, wood N₂ fixation rate, moisture and fungal composition in a Norway spruce forest. *Glob Chang Biol* 25:1852–1867. <https://doi.org/10.1111/gcb.14594>.
- Bond-Lamberty B, Thomson A. 2010. A global database of soil respiration data. *Biogeosciences* 7:1915–1926. <https://doi.org/10.5194/bg-7-1915-2010>.
- Johnston SR, Boddy L, Weightman AJ. 2016. Bacteria in decomposing wood and their interactions with wood-decay fungi. *FEMS Microbiol Ecol* 92:fw179. <https://doi.org/10.1093/femsec/fw179>.
- Větrovský T, Morais D, Kohout P, Lepinay C, Algora C, Awokunle Hollá S, Bahnmann BD, Bílohnědá K, Brabcová V, D'Alò F, Human ZR, Jomura M, Kolařík M, Kvasničková J, Lladó S, López-Mondéjar R, Martinović T, Mašinová T, Meszárosová L, Michalčíková L, Michalová T, Munda S,

- Navrátilová D, Odriozola I, Piché-Choquette S, Štursová M, Švec K, Tláskal V, Urbanová M, Vlček L, Voříšková J, Žifčáková L, Baldrian P. 2020. Global Fungi, a global database of fungal occurrences from high-throughput sequencing metabarcoding studies. *Sci Data* 7:228. <https://doi.org/10.1038/s41597-020-0567-7>.
9. Rayner ADM, Boddy L. 1988. Fungal decomposition of wood: its biology and ecology. Wiley, Chichester, NY.
 10. Eastwood DC, Floudas D, Binder M, Majcherczyk A, Schneider P, Aerts A, Asiegbu FO, Baker SE, Barry K, Bendixby M, Blumentritt M, Coutinho PM, Cullen D, de Vries RP, Gathman A, Goodell B, Henrissat B, Ihrmark K, Kauterud H, Kohler A, LaButti K, Lapidus A, Lavin JL, Lee YH, Lindquist E, Lilly W, Lucas S, Morin E, Murat C, Oguiza JA, Park J, Pisabarro AG, Riley R, Rosling A, Salamov A, Schmidt O, Schmutz J, Skrede I, Stenlid J, Wiebenga A, Xie XF, Kues U, Hibbett DS, Hoffmeister D, Hogberg N, Martin F, Grigoriev IV, Watkinson SC. 2011. The plant cell wall-decomposing machinery underlies the functional diversity of forest fungi. *Science* 333:762–765. <https://doi.org/10.1126/science.1205411>.
 11. Kahl T, Arnstadt T, Baber K, Bässler C, Bauhus J, Borcken W, Buscot F, Floren A, Heibl C, Hessenmöller D, Hofrichter M, Hoppe B, Kellner H, Krüger D, Linsenmair KE, Matzner E, Otto P, Purahong W, Seilwinder C, Schulze E-D, Wende B, Weisser WW, Gossner MM. 2017. Wood decay rates of 13 temperate tree species in relation to wood properties, enzyme activities and organismic diversities. *Forest Ecol Manag* 391:86–95. <https://doi.org/10.1016/j.foreco.2017.02.012>.
 12. Weedon JT, Cornwell WK, Cornelissen JH, Zanne AE, Wirth C, Coomes DA. 2009. Global meta-analysis of wood decomposition rates: a role for trait variation among tree species? *Ecol Lett* 12:45–56. <https://doi.org/10.1111/j.1461-0248.2008.01259.x>.
 13. Baldrian P, Zrůstová P, Tláskal V, Davidová A, Merhautová V, Vrška T. 2016. Fungi associated with decomposing deadwood in a natural beech-dominated forest. *Fungal Ecology* 23:109–122. <https://doi.org/10.1016/j.funeco.2016.07.001>.
 14. Smyth CE, Titus B, Trofymow JA, Moore TR, Preston CM, Prescott CE, Grp CW, the CIDET Working Group. 2016. Patterns of carbon, nitrogen and phosphorus dynamics in decomposing wood blocks in Canadian forests. *Plant Soil* 409:459–477. <https://doi.org/10.1007/s11104-016-2972-4>.
 15. Brunner A, Kimmins JP. 2003. Nitrogen fixation in coarse woody debris of *Thuja plicata* and *Tsuga heterophylla* forests on northern Vancouver Island. *Can J for Res* 33:1670–1682. <https://doi.org/10.1139/x03-085>.
 16. Rinne KT, Rajala T, Peltoniemi K, Chen J, Smolander A, Mäkipää R, Treseder K. 2017. Accumulation rates and sources of external nitrogen in decaying wood in a Norway spruce dominated forest. *Funct Ecol* 31:530–541. <https://doi.org/10.1111/1365-2435.12734>.
 17. Bentzon-Tilia M, Severin I, Hansen LH, Riemann L. 2015. Genomics and ecophysiology of heterotrophic nitrogen-fixing bacteria isolated from estuarine surface water. *mBio* 6:e00929-15. <https://doi.org/10.1128/mBio.00929-15>.
 18. Houlton BZ, Wang YP, Vitousek PM, Field CB. 2008. A unifying framework for dinitrogen fixation in the terrestrial biosphere. *Nature* 454:327–330. <https://doi.org/10.1038/nature07028>.
 19. Steidinger BS, Crowther TW, Liang J, Van Nuland ME, Werner GDA, Reich PB, Nabuurs GJ, de-Miguel S, Zhou M, Picard N, Herault B, Zhao X, Zhang C, Routh D, Peay KG, Consortium G, Gfbi Consortium. 2019. Climatic controls of decomposition drive the global biogeography of forest-tree symbioses. *Nature* 569:404–408. <https://doi.org/10.1038/s41586-019-1128-0>.
 20. Fukami T, Dickie IA, Wilkie JP, Paulus BC, Park D, Roberts A, Buchanan PK, Allen RB. 2010. Assembly history dictates ecosystem functioning: evidence from wood decomposer communities. *Ecology Lett* 13:675–684. <https://doi.org/10.1111/j.1461-0248.2010.01465.x>.
 21. Probst M, Gomez-Brandon M, Bardelli T, Egli M, Insam H, Ascher-Jenull J. 2018. Bacterial communities of decaying Norway spruce follow distinct slope exposure and time-dependent trajectories. *Environ Microbiol* 20:3657–3670. <https://doi.org/10.1111/1462-2920.14359>.
 22. Král K, Janík D, Vrška T, Adam D, Hort L, Unar P, Šamonil P. 2010. Local variability of stand structural features in beech dominated natural forests of Central Europe: implications for sampling. *Forest Ecology and Management* 260:2196–2203. <https://doi.org/10.1016/j.foreco.2010.09.020>.
 23. Cleveland CC, Townsend AR, Schimel DS, Fisher H, Howarth RW, Hedin LO, Perakis SS, Latty EF, Von Fischer JC, Elseroad A, Wasson MF. 1999. Global patterns of terrestrial biological nitrogen (N-2) fixation in natural ecosystems. *Global Biogeochem Cycles* 13:623–645. <https://doi.org/10.1029/1999GB900014>.
 24. Zheng MH, Chen H, Li DJ, Luo YQ, Mo JM. 2020. Substrate stoichiometry determines nitrogen fixation throughout succession in southern Chinese forests. *Ecol Lett* 23:336–347. <https://doi.org/10.1111/ele.13437>.
 25. Cleveland CC, Houlton BZ, Smith WK, Marklein AR, Reed SC, Parton W, Del Grosso SJ, Running SW. 2013. Patterns of new versus recycled primary production in the terrestrial biosphere. *Proc Natl Acad Sci U S A* 110:12733–12737. <https://doi.org/10.1073/pnas.1302768110>.
 26. Lladó S, Větrovský T, Baldrian P. 2019. Tracking of the activity of individual bacteria in temperate forest soils shows guild-specific responses to seasonality. *Soil Biol Biochem* 135:275–282. <https://doi.org/10.1016/j.soilbio.2019.05.010>.
 27. Žifčáková L, Větrovský T, Lombard V, Henrissat B, Howe A, Baldrian P. 2017. Feed in summer, rest in winter: microbial carbon utilization in forest topsoil. *Microbiome* 5:122. <https://doi.org/10.1186/s40168-017-0340-0>.
 28. Hesse CN, Mueller RC, Vuylsich M, Gallegos-Graves LV, Gleasner CD, Zak DR, Kuske CR. 2015. Forest floor community metatranscriptomes identify fungal and bacterial responses to N deposition in two maple forests. *Front Microbiol* 6:337. <https://doi.org/10.3389/fmicb.2015.00337>.
 29. Lenhart K, Bunge M, Ratering S, Neu TR, Schüttmann I, Greule M, Kammann C, Schnell S, Müller C, Zorn H, Keppler F. 2012. Evidence for methane production by saprotrophic fungi. *Nat Commun* 3:1046–1046. <https://doi.org/10.1038/ncomms2049>.
 30. Nelson MB, Martiny AC, Martiny JBH. 2016. Global biogeography of microbial nitrogen-cycling traits in soil. *Proc Natl Acad Sci U S A* 113:8033–8040. <https://doi.org/10.1073/pnas.1601070113>.
 31. Mackelprang R, Grube AM, Lamendella R, Jesus EC, Copeland A, Liang C, Jackson RD, Rice CW, Kapucija S, Parsa B, Tringe SG, Tiedje JM, Jansson JK. 2018. Microbial community structure and functional potential in cultivated and native tallgrass prairie soils of the midwestern United States. *Front Microbiol* 9:1775. <https://doi.org/10.3389/fmicb.2018.01775>.
 32. Mäkipää R, Leppänen SM, Sanz Munoz S, Smolander A, Tirola M, Tuomivirta T, Fritze H. 2018. Methanotrophs are core members of the diazotroph community in decaying Norway spruce logs. *Soil Biol Biochem* 120:230–232. <https://doi.org/10.1016/j.soilbio.2018.02.012>.
 33. Miyauchi S, Kiss E, Kuo A, Drula E, Kohler A, Sánchez-García M, Morin E, Andreopoulos B, Barry KW, Bonito G, Buée M, Carver A, Chen C, Cichocki N, Clum A, Culley D, Crous PW, Fauchery L, Girlanda M, Hayes RD, Kéri Z, LaButti K, Lipzen A, Lombard V, Magnuson J, Maillard F, Murat C, Nolan M, Ohm RA, Pangilinan J, Pereira MdF, Perotto S, Peter M, Pfister S, Riley R, Sitrit Y, Stielow JB, Szöllösi G, Žifčáková L, Štursová M, Spatafora JW, Tedersoo L, Vaario L-M, Yamada A, Yan M, Wang P, Xu J, Bruns T, Baldrian P, Vilgalys R, et al. 2020. Large-scale genome sequencing of mycorrhizal fungi provides insights into the early evolution of symbiotic traits. *Nat Commun* 11:5125. <https://doi.org/10.1038/s41467-020-18795-w>.
 34. Lustenhouwer N, Maynard DS, Bradford MA, Lindner DL, Oberle B, Zanne AE, Crowther TW. 2020. A trait-based understanding of wood decomposition by fungi. *Proc Natl Acad Sci U S A* 117:11551–11558. <https://doi.org/10.1073/pnas.1909166117>.
 35. Hiscox J, O'Leary J, Boddy L. 2018. Fungus wars: basidiomycete battles in wood decay. *Stud Mycol* 89:117–124. <https://doi.org/10.1016/j.simyco.2018.02.003>.
 36. Valášková V, De Boer W, Klein Gunnewiek PJA, Pospíšek M, Baldrian P. 2009. Phylogenetic composition and properties of bacteria coexisting with the fungus *Hypholoma fasciculare* in decaying wood. *ISME J* 3:1218–1221. <https://doi.org/10.1038/ismej.2009.64>.
 37. Kohlmeier S, Smits THM, Ford RM, Keel C, Harms H, Wick LY. 2005. Taking the fungal highway: mobilization of pollutant-degrading bacteria by fungi. *Environ Sci Technol* 39:4640–4646. <https://doi.org/10.1021/es047979z>.
 38. Worrich A, Stryhanyuk H, Musat N, König S, Banitz T, Centler F, Frank K, Thullner M, Harms H, Richnow H-H, Miltner A, Kastner M, Wick LY. 2017. Mycelium-mediated transfer of water and nutrients stimulates bacterial activity in dry and oligotrophic environments. *Nat Commun* 8:15472–15472. <https://doi.org/10.1038/ncomms15472>.
 39. Hoppe B, Kahl T, Karasch P, Wubet T, Bauhus J, Buscot F, Krüger D. 2014. Network analysis reveals ecological links between N-fixing bacteria and wood-decaying fungi. *PLoS One* 9:e88141. <https://doi.org/10.1371/journal.pone.0088141>.
 40. Gomez-Brandon M, Probst M, Siles JA, Peintner U, Bardelli T, Egli M, Insam H, Ascher-Jenull J. 2020. Fungal communities and their association with nitrogen-fixing bacteria affect early decomposition of Norway spruce deadwood. *Sci Rep* 10:8025. <https://doi.org/10.1038/s41598-020-64808-5>.
 41. Chen J, Heikkinen J, Hobbie EA, Rinne-Garmston KT, Penttilä R, Mäkipää R. 2019. Strategies of carbon and nitrogen acquisition by saprotrophic and ectomycorrhizal fungi in Finnish boreal *Picea abies*-dominated forests. *Fungal Biol* 123:456–464. <https://doi.org/10.1016/j.funbio.2019.03.005>.

42. Lindahl BD, Finlay RD. 2006. Activities of chitinolytic enzymes during primary and secondary colonization of wood by basidiomycetous fungi. *New Phytol* 169:389–397. <https://doi.org/10.1111/j.1469-8137.2005.01581.x>.
43. Šamonil P, Daněk P, Baldrian P, Tláškal V, Tejnecký V, Drábek O. 2020. Convergence, divergence or chaos? Consequences of tree trunk decay for pedogenesis and the soil microbiome in a temperate natural forest. *Geoderma* 376:114499. <https://doi.org/10.1016/j.geoderma.2020.114499>.
44. Anderson-Teixeira KJ, Davies SJ, Bennett AC, Gonzalez-Akre EB, Muller-Landau HC, Wright SJ, Abu Salim K, Almeyda Zambrano AM, Alonso A, Baltzer JL, Basset Y, Bourg NA, Broadbent EN, Brockelman WY, Bunyavejchewin S, Burslem DFRP, Butt N, Cao M, Cardenas D, Chuyong GB, Clay K, Cordell S, Dattaraja HS, Deng X, Detto M, Du X, Duque A, Erikson DL, Ewango CEN, Fischer GA, Fletcher C, Foster RB, Giardina CP, Gilbert GS, Gunatilleke N, Gunatilleke S, Hao Z, Hargrove WW, Hart TB, Hau BCH, He F, Hoffman FM, Howe RW, Hubbell SP, Inman-Narahari FM, Jansen PA, Jiang M, Johnson DJ, Kanzaki M, Kassim AR, et al. 2015. CTF5-ForestGEO: a worldwide network monitoring forests in an era of global change. *Glob Chang Biol* 21:528–549. <https://doi.org/10.1111/gcb.12712>.
45. Samonil P, Schaeztl RJ, Valtera M, Golias V, Baldrian P, Vasickova I, Adam D, Janik D, Hort L. 2013. Crossdating of disturbances by tree uprooting: can treethrow microtopography persist for 6000 years? *Forest Ecol Manag* 307:123–135. <https://doi.org/10.1016/j.foreco.2013.06.045>.
46. Tláškal V, Zrůstová P, Vrška T, Baldrian P. 2017. Bacteria associated with decomposing dead wood in a natural temperate forest. *FEMS Microbiol Ecol* 93:fx157. <https://doi.org/10.1093/femsec/fix157>.
47. Leppänen SM, Salemaa M, Smolander A, Mäkipää R, Tirola M. 2013. Nitrogen fixation and methanotrophy in forest mosses along a N deposition gradient. *Environ Exp Bot* 90:62–69. <https://doi.org/10.1016/j.envexpbot.2012.12.006>.
48. Caporaso JG, Lauber CL, Walters WA, Berg-Lyons D, Huntley J, Fierer N, Owens SM, Betley J, Fraser J, Bauer M, Gormley N, Gilbert JA, Smith G, Knight R. 2012. Ultra-high-throughput microbial community analysis on the Illumina HiSeq and MiSeq platforms. *ISME J* 6:1621–1624. <https://doi.org/10.1038/ismej.2012.8>.
49. Bolger AM, Lohse M, Usadel B. 2014. Trimmomatic: a flexible trimmer for Illumina sequence data. *Bioinformatics* 30:2114–2120. <https://doi.org/10.1093/bioinformatics/btu170>.
50. Lanzen A, Jorgensen SL, Huson DH, Gorfer M, Grindhaug SH, Jonassen I, Ovreas L, Urich T. 2012. CREST—classification resources for environmental sequence tags. *PLoS One* 7:e49334. <https://doi.org/10.1371/journal.pone.0049334>.
51. Quast C, Pruesse E, Yilmaz P, Gerken J, Schweer T, Yarza P, Peplies J, Glockner FO. 2013. The SILVA ribosomal RNA gene database project: improved data processing and web-based tools. *Nucleic Acids Res* 41: D590–D596. <https://doi.org/10.1093/nar/gks1219>.
52. Amann RI, Ludwig W, Schleifer KH. 1995. Phylogenetic identification and in-situ detection of individual microbial-cells without cultivation. *Microbiol Rev* 59:143–169. <https://doi.org/10.1128/MR.59.1.143-169.1995>.
53. Wilmotte A, Van der Auwera G, De Wachter R. 1993. Structure of the 16 S ribosomal RNA of the thermophilic cyanobacterium chlorogloeopsis HTF (mastigocladus laminosus HTF) strain PCC7518, and phylogenetic analysis. *FEBS Lett* 317:96–100. [https://doi.org/10.1016/0014-5793\(93\)81499-P](https://doi.org/10.1016/0014-5793(93)81499-P).
54. Prévost-Bouré NC, Christen R, Dequiedt S, Mougél C, Lelievre M, Jolivet C, Shahbazkia HR, Guillou L, Arrouays D, Ranjard L. 2011. Validation and application of a PCR primer set to quantify fungal communities in the soil environment by real-time quantitative PCR. *PLoS One* 6:e24166. <https://doi.org/10.1371/journal.pone.0024166>.
55. Žifčáková L, Větrovský T, Howe A, Baldrian P. 2016. Microbial activity in forest soil reflects the changes in ecosystem properties between summer and winter. *Environ Microbiol* 18:288–301. <https://doi.org/10.1111/1462-2920.13026>.
56. Li DH, Liu CM, Luo RB, Sadakane K, Lam TW. 2015. MEGAHIT: an ultra-fast single-node solution for large and complex metagenomics assembly via succinct de Bruijn graph. *Bioinformatics* 31:1674–1676. <https://doi.org/10.1093/bioinformatics/btv033>.
57. Meyer F, Paarmann D, D'Souza M, Olson R, Glass EM, Kubal M, Paczian T, Rodriguez A, Stevens R, Wilke A, Wilkening J, Edwards RA. 2008. The metagenomics RAST server—a public resource for the automatic phylogenetic and functional analysis of metagenomes. *BMC Bioinformatics* 9:386. <https://doi.org/10.1186/1471-2105-9-386>.
58. Grigoriev IV, Nikitin R, Haridas S, Kuo A, Ohm R, Otiillar R, Riley R, Salamov A, Zhao XL, Korzeniewski F, Smirnova T, Nordberg H, Dubchak I, Shabalov I. 2014. MycoCosm portal: gearing up for 1000 fungal genomes. *Nucleic Acids Res* 42:D699–D704. <https://doi.org/10.1093/nar/gkt1183>.
59. Eddy SR. 2011. Accelerated profile HMM searches. *PLoS Comput Biol* 7:e1002195. <https://doi.org/10.1371/journal.pcbi.1002195>.
60. Prestat E, David MM, Hultman J, Taş N, Lamendella R, Dvornik J, Mackelprang R, Myrold DD, Jumpponen A, Tringe SG, Holman E, Mavromatis K, Jansson JK. 2014. FOAM (Functional Ontology Assignments for Metagenomes): a Hidden Markov Model (HMM) database with environmental focus. *Nucleic Acids Res* 42:e145. <https://doi.org/10.1093/nar/gku702>.
61. Huang L, Zhang H, Wu PZ, Entwistle S, Li XQ, Yohe T, Yi HD, Yang ZL, Yin YB. 2018. dbCAN-seq: a database of carbohydrate-active enzyme (CAZyme) sequence and annotation. *Nucleic Acids Res* 46:D516–D521. <https://doi.org/10.1093/nar/gkx894>.
62. Lombard V, Ramulu HG, Drula E, Coutinho PM, Henrissat B. 2014. The carbohydrate-active enzymes database (CAZy) in 2013. *Nucleic Acids Res* 42: D490–D495. <https://doi.org/10.1093/nar/gkt1178>.
63. Tederloo L, Bahram M, Póme S, Kõljalg U, Yorou NS, Wijesundera R, Villarreal Ruiz L, Vasco-Palacios AM, Thu PQ, Suija A, Smith ME, Sharp C, Saluveer E, Saitta A, Rosas M, Riit T, Ratkowsky D, Pritsch K, Põldmaa K, Piepenbringer M, Phosri C, Peterson M, Parts K, Pärtel K, Ötsing E, Nouhra E, Njouonkou AL, Nilsson RH, Morgado LN, Mayor J, May TW, Majuakim L, Lodge DJ, Lee SS, Larsson K-H, Kohout P, Hosaka K, Hiiesalu I, Henkel TW, Harend H, Guo L-d, Greslebin A, Grelet G, Geml J, Gates G, Dunstan W, Dunk C, Drenkhan R, Dearnaley J, De Kesel A, et al. 2014. Global diversity and geography of soil fungi. *Science* 346:1256688. <https://doi.org/10.1126/science.1256688>.
64. Nayfach S, Roux S, Seshadri R, Udworthy D, Varghese N, Schulz F, Wu D, Paez-Espino D, Chen IM, Huntemann M, Palaniappan K, Ladau J, Mukherjee S, Reddy TBK, Nielsen T, Kirton E, Faria JP, Edirisinghe JN, Henry CS, Jungbluth SP, Chivian D, Dehal P, Wood-Charlson EM, Arkin AP, Tringe SG, Visel A, Abreu H, Acinas SG, Allen E, Allen MA, Andersen G, Anesio AM, Attwood G, Avila-Magaña V, Badis Y, Bailey J, Baker B, Baldrian P, Barton HA, Beck DAC, Becraft ED, Beller HR, Beman JM, Bernier-Latmani R, Berry TD, Bertagnolli A, Bertilsson S, Bhatnagar JM, Bird JT, Blumer-Schuette SE. 9 Nov 2020. A genomic catalog of Earth's microbiomes. *Nat Biotechnol* <https://doi.org/10.1038/s41587-020-0718-6>.
65. Kang DWD, Froula J, Egan R, Wang Z. 2015. MetaBAT, an efficient tool for accurately reconstructing single genomes from complex microbial communities. *PeerJ* 3:e1165. <https://doi.org/10.7717/peerj.1165>.
66. Parks DH, Imelfort M, Skennerton CT, Hugenholtz P, Tyson GW. 2015. CheckM: assessing the quality of microbial genomes recovered from isolates, single cells, and metagenomes. *Genome Res* 25:1043–1055. <https://doi.org/10.1101/gr.186072.114>.
67. Parks DH, Rinke C, Chuvochina M, Chaumeil PA, Woodcroft BJ, Evans PN, Hugenholtz P, Tyson GW. 2017. Recovery of nearly 8,000 metagenome-assembled genomes substantially expands the tree of life. *Nat Microbiol* 2:1533–1542. <https://doi.org/10.1038/s41564-017-0012-7>.
68. Parks DH, Chuvochina M, Waite DW, Rinke C, Skarshewski A, Chaumeil PA, Hugenholtz P. 2018. A standardized bacterial taxonomy based on genome phylogeny substantially revises the tree of life. *Nat Biotechnol* 36:996–1004. <https://doi.org/10.1038/nbt.4229>.
69. Langmead B, Trapnell C, Pop M, Salzberg SL. 2009. Ultrafast and memory-efficient alignment of short DNA sequences to the human genome. *Genome Biol* 10:R25. <https://doi.org/10.1186/gb-2009-10-3-r25>.
70. R Core Team. 2016. R: a language and environment for statistical computing. Version 3.3.1. R Foundation for Statistical Computing, Vienna, Austria.
71. Oksanen J, Blanchet FG, Friendly P, Kindt R, Legendre P, McGinn D, Minchin PR, O'Hara RB, Simpson GL, Solymos P, Stevens MHH, Szöcs E, Wagner H. 2018. vegan: community ecology package. R package version 2.5–2. <https://cran.r-project.org/web/packages/vegan/index.html>.
72. Racine JS. 2012. RStudio: a platform-independent IDE for R and Sweave. *J Appl Econ* 27:167–172. <https://doi.org/10.1002/jae.1278>.
73. Wickham H, Averick M, Bryan J, Chang W, McGowan L, François R, Grolemund G, Hayes A, Henry L, Hester J, Kuhn M, Pedersen T, Miller E, Bache S, Müller K, Ooms J, Robinson D, Seidel D, Spinu V, Takahashi K, Vaughan D, Wilke C, Woo K, Yutani H. 2019. Welcome to the Tidyverse. *Joss* 4:1686. <https://doi.org/10.21105/joss.01686>.

FIG S1: Contribution of deadwood organisms to expression and the gene pool of enzymes degrading biopolymers. The most abundant families of glycoside hydrolases (GH) and auxiliary enzymes (AA) in the metatranscriptome of deadwood and their representation in the metagenome are shown. The expressed genes are largely of fungal origin. Cellulose-degrading enzymes, such as AA9, GH7, and certain subfamilies of GH5, are highly expressed, indicating the importance of this deadwood component as a nutrient and energy source. The importance of lignin decomposition is exemplified by high class II peroxidase expression (AA2) as well as the production of hydrogen peroxide by AA3, AA4, and AA5 that support its activity; oxidation of phenols performed by laccases (AA1) is also important.

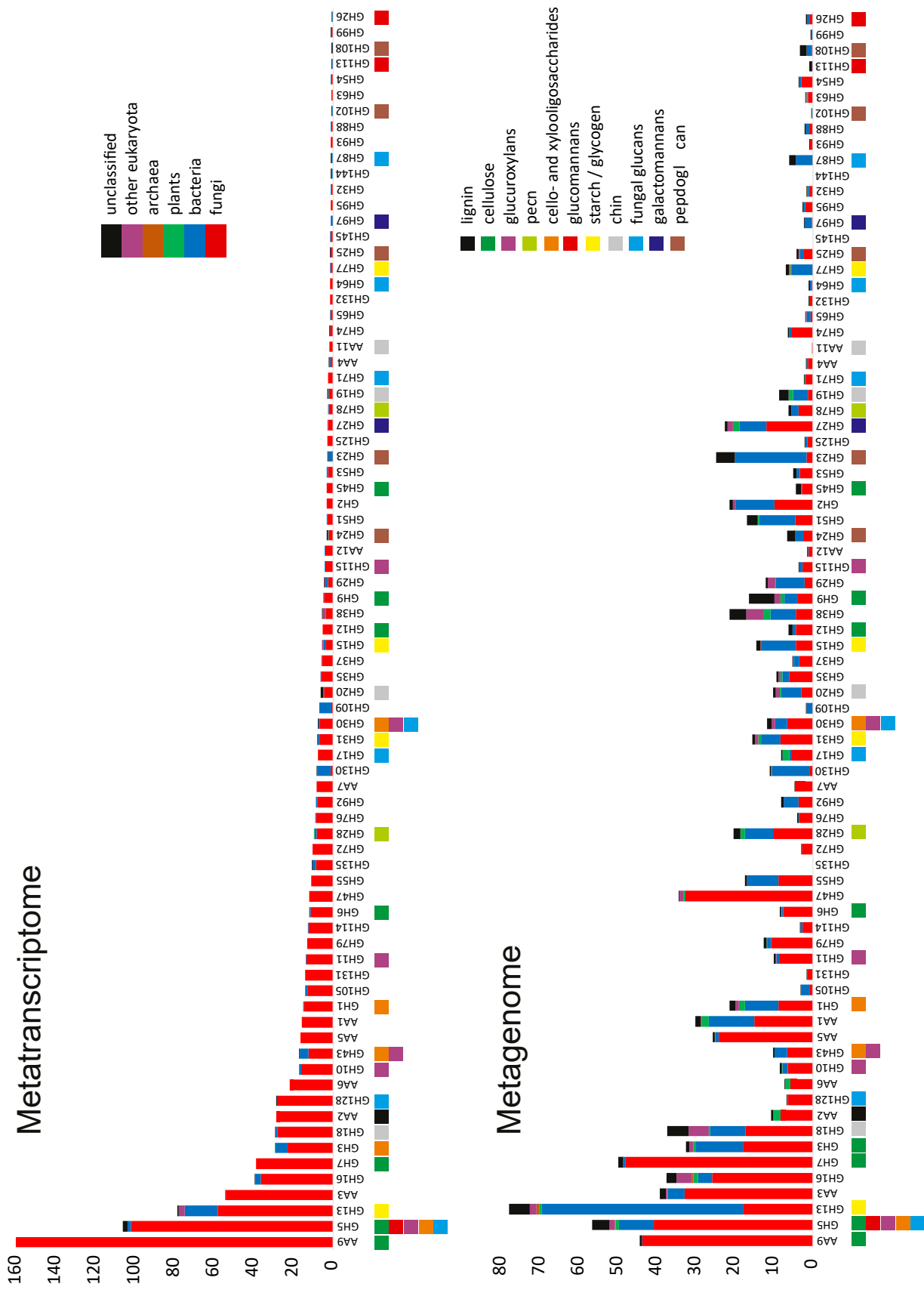
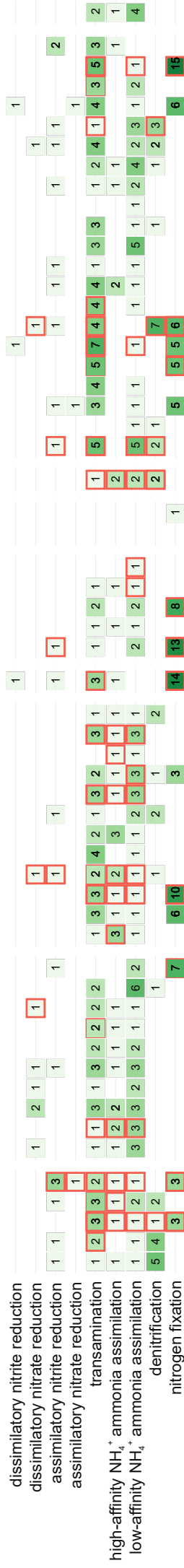
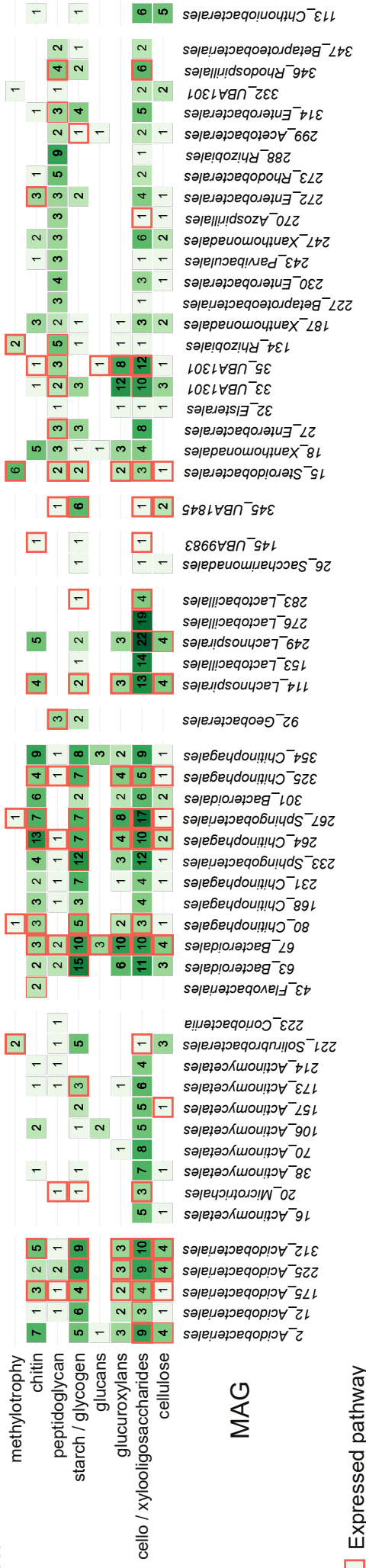


FIG S2: Genomic potential and transcription of genes involved in N-cycling and utilization of C sources in deadwood bacteria. Heatmap of the distribution of genes involved in particular processes across bacterial metagenome-assembled genomes. Color intensity and numbers in blocks represent the number of genes for each function, and expressed gene families identified by mapping metatranscriptome reads to the metagenome-assembled genomes are indicated by red outline. Some bacteria combine recalcitrant C utilization with N fixation, while others rely on C input from other decomposers.

N-cycling



C utilization



MAG

□ Expressed pathway

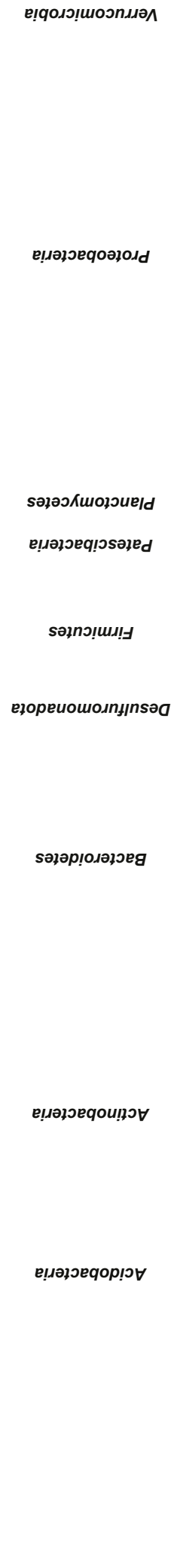


FIG S3: Total counts of carbohydrate-active enzymes in the genomes of deadwood bacteria. Bar plots indicate the range, upper and lower quartiles, and median of CAZy gene counts for genomes belonging to each bacterial phylum. While *Bacteroidetes* and *Acidobacteria* genomes typically harbor more than 50 CAZy genes, the genomes of other major phyla, including *Proteobacteria* and *Actinobacteria*, typically contain considerably fewer carbohydrate-active enzymes.

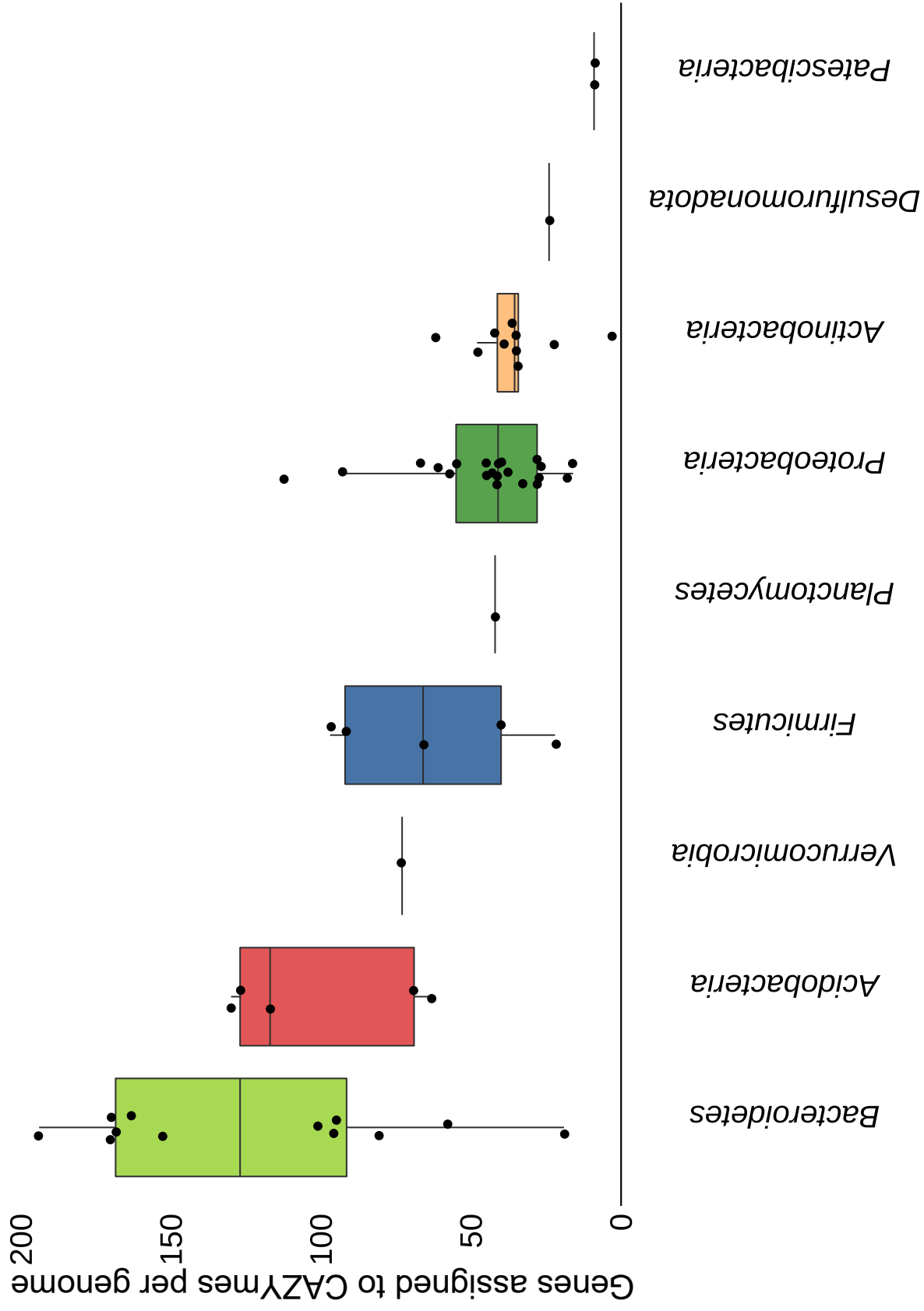
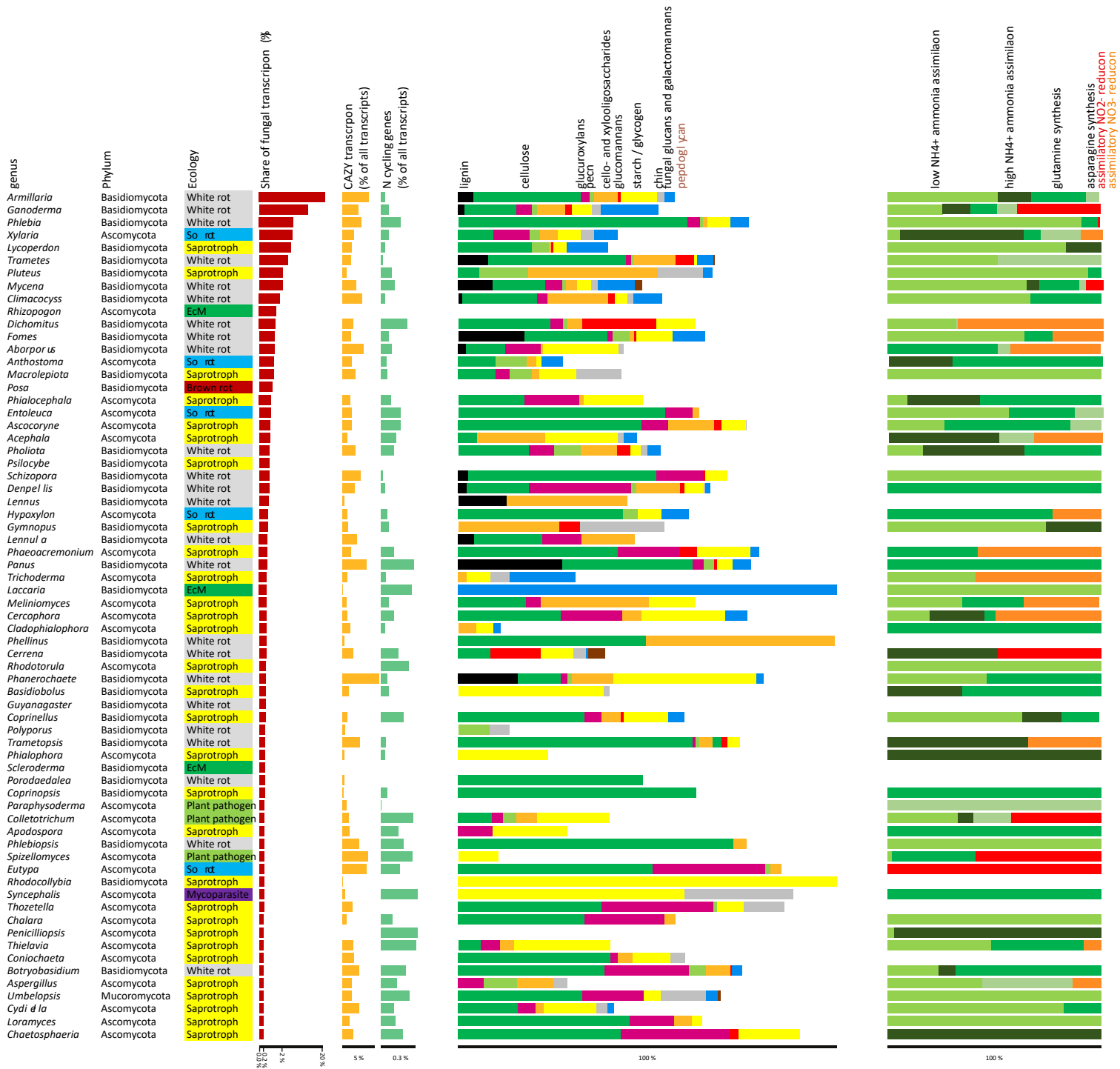


FIG S4: Expression of C- and N-cycling genes by fungi. Transcripts of deadwood fungi with the best hits for genera with assigned ecological guilds are shown. Bar plots indicate the contribution of each genus to total fungal transcription across all samples, share of CAZymes and N-cycling genes of all transcripts of each genus, and the assignment of CAZymes to target carbohydrates (share of total CAZyme expression) and of N-cycling genes to processes (share of total N-cycling gene expression).



V



OPEN

DATA DESCRIPTOR

Metagenomes, metatranscriptomes and microbiomes of naturally decomposing deadwood

Vojtěch Tláška¹✉, Vendula Brabcová¹, Tomáš Větrovský¹, Rubén López-Mondéjar¹, Lumy Maria Oliveira Monteiro², João Pedro Saraiva², Ulisses Nunes da Rocha² & Petr Baldrian¹

Deadwood represents significant carbon (C) stock in a temperate forests. Its decomposition and C mobilization is accomplished by decomposer microorganisms – fungi and bacteria – who also supply the foodweb of commensalist microbes. Due to the ecosystem-level importance of deadwood habitat as a C and nutrient stock with significant nitrogen fixation, the deadwood microbiome composition and function are critical to understanding the microbial processes related to its decomposition. We present a comprehensive suite of data packages obtained through environmental DNA and RNA sequencing from natural deadwood. Data provide a complex picture of the composition and function of microbiome on decomposing trunks of European beech (*Fagus sylvatica* L.) in a natural forest. Packages include deadwood metagenomes, metatranscriptomes, sequences of total RNA, bacterial genomes resolved from metagenomic data and the 16S rRNA gene and ITS2 metabarcoding markers to characterize the bacterial and fungal communities. This project will be of use to microbiologists, environmental biologists and biogeochemists interested in the microbial processes associated with the transformation of recalcitrant plant biomass.

Background & Summary

Forests, and especially unmanaged natural forests, accumulate and store large amounts of carbon (C)¹. A substantial fraction of this C stock – 73 ± 6 Pg or 8% of the total global forest C stock is contained within deadwood². This C pool is transient because during its transformation by saprotrophic organisms most C is liberated as CO₂ into the atmosphere³, while the rest is sequestered in soils as dissolved organic C, within microbial biomass or as a part of the soil organic matter – along with other nutrients⁴. Fungi in deadwood appear to be major decomposers using extracellular enzymes for the decomposition of recalcitrant plant biopolymers as shown in associated study⁵. Fungi also determine the bacterial community composition^{6,7}. Bacterial fixation of atmospheric N₂ was shown to substantially contribute to the nitrogen (N) increase in deadwood during decomposition^{5,8,9}. In addition to bacteria and fungi, deadwood also hosts a suite of other organisms including archaea, viruses, protists, nematodes and insects, whose roles in deadwood are so far unknown. In order to understand the deadwood as a dynamic habitat, it is necessary to describe the composition of associated microorganisms with an emphasis on the major groups – fungi and bacteria – whose ecologies are often genus-specific¹⁰. Further, it is important to link deadwood-associated organisms to processes occurring at different stages of decomposition either by characterization of isolates^{7,11} or by cultivation-independent techniques.

In this Data Descriptor we present the comprehensive datasets of DNA and RNA-derived data and sample metadata to characterize deadwood organisms and their activity at various stages of decomposition (Table 1, Supplementary Table 1). The data derived from DNA representing the community composition and genomic potential, include 16S rRNA gene sequences and ITS2 sequences, metagenomics reads, metagenome assembly and bacterial metagenome-assembled genomes (MAGs¹²). The data derived from RNA are represented by the total RNA reads whose majority originates from ribosomal RNA and which are taxonomically assignable and thus can be used as a proxy for the PCR-unbiased view of community composition. Further, data contain metatranscriptome raw reads and assembly that represent the processes occurring in deadwood. The dataset characterizes

¹Laboratory of Environmental Microbiology, Institute of Microbiology of the Czech Academy of Sciences, Videnska 1083, 14220, Praha 4, Czech Republic. ²Department of Environmental Microbiology, Helmholtz Centre for Environmental Research – UFZ, Permoserstraße 15, 04318, Leipzig, Germany. ✉e-mail: tlaskal@biomed.cas.cz

Sample	BioSample	Location	time since death (years)	diameter (cm)	length (m)	pH	N content (%)	C content (%)	water content (%)	nucleic acids extraction
sample_130	SAMN13925149	48.666701 N 14.704277 E	<4	50	29.4	5.4	0.28	49.09	40.9	DNA
sample_131	SAMN13925150	48.666134 N 14.707596 E	<4	70	24.3	5.46	0.19	50.06	37.4	DNA
sample_132	SAMN13925151	48.667505 N 14.707659 E	<4	94	37.1	4.65	0.27	49.7	36.1	DNA
sample_133	SAMN13925152	48.664471 N 14.709305 E	<4	62	22.8	5.33	0.19	49.88	42.5	DNA
sample_134	SAMN13925153	48.66419 N 14.705787 E	<4	60	18.6	4.96	0.42	48.55	49.3	DNA
sample_006	SAMN13925154	48.666377 N 14.709879 E	4–7	60	8.4	3.95	0.71	50.65	83.1	DNA, RNA
sample_007	SAMN13762420	48.666311 N 14.709489 E	4–7	42	9.8	4.76	0.12	22.45	47.5	DNA, RNA
sample_044	SAMN13925156	48.66597 N 14.706626 E	4–7	55	9.7	3.87	0.43	50.29	49.0	DNA, RNA
sample_110	SAMN13925157	48.665322 N 14.708804 E	4–7	65	7.7	4.12	0.68	49.62	75.2	DNA, RNA
sample_116	SAMN13925158	48.666959 N 14.704827 E	4–7	85	18.1	3.32	0.69	51.25	76.3	DNA, RNA
sample_031	SAMN13925159	48.666891 N 14.703544 E	8–19	95	37.1	4.87	0.34	48.7	52.8	DNA, RNA
sample_049	SAMN13925160	48.665518 N 14.706881 E	8–19	34	20.6	4.44	0.23	49.25	51.8	DNA, RNA
sample_055	SAMN13925161	48.665975 N 14.709225 E	8–19	70	4.0	3.99	0.33	49.93	63.7	DNA, RNA
sample_069	SAMN13925162	48.664308 N 14.704474 E	8–19	75	34.7	4.78	0.5	48.16	82.1	DNA, RNA
sample_106	SAMN13925163	48.664703 N 14.708727 E	8–19	30	22.0	4.07	0.4	49.19	78.1	DNA, RNA
sample_003	SAMN13925164	48.666874 N 14.709428 E	20–41	30	10.8	3.53	0.61	50.23	71.8	DNA
sample_028	SAMN13925165	48.667629 N 14.703671 E	20–41	70	11.5	3.75	2.11	50.83	69.2	DNA
sample_039	SAMN13925166	48.665832 N 14.705361 E	20–41	50	18.6	3.73	1.47	49.96	88.1	DNA
sample_057	SAMN13925167	48.664869 N 14.709048 E	20–41	100	26.2	3.79	0.83	51.07	69.9	DNA
sample_084	SAMN13925168	48.663645 N 14.70741 E	20–41	80	10.9	3.05	1.13	51.31	75.3	DNA
sample_058	SAMN13925169	48.664099 N 14.709529 E	>41	70	11.1	4.15	1.31	56.11	66.2	DNA
sample_101	SAMN13925170	48.66386 N 14.705644 E	>41	70	7.8	3.34	1.95	51.7	83.9	DNA
sample_111	SAMN13925171	48.667297 N 14.704368 E	>41	48	17.5	4.35	0.51	54.92	72.2	DNA
sample_113	SAMN13925172	48.666702 N 14.707763 E	>41	80	8.5	3.61	1.47	52.2	75.4	DNA
sample_115	SAMN13925173	48.667087 N 14.705332 E	>41	60	10.7	3.33	0.67	50.9	64.6	DNA

Table 1. Sample metadata for 25 samples used for sequencing.

decomposing trunks of the European beech (*Fagus sylvatica* L.) in a beech-dominated natural forest in the temperate Europe (Fig. 1). The metagenome was assembled from 25 DNA samples of deadwood with decomposition time ranging from young wood (<4 years since tree death) to almost completely decomposed wood (>41 years of decomposition). It was possible to perform the resolving of 58 high-quality metagenome assembled genomes (MAGs) with a total of 19.5×10^3 contigs spanning 10 bacterial phyla including those that are difficult to culture, such as *Acidobacteria*, *Patescibacteria*, *Verrucomicrobia* and *Planctomycetes* (Fig. 2, Supplementary Table 2). 16S rRNA gene and ITS2 amplicon data contribute to comparison of microbial diversity and occurrence patterns at the global scale using public databases GlobalFungi¹³ or Earth Microbiome¹⁴ (Supplementary Fig. 1). Deadwood metatranscriptome was assembled from 10 RNA samples spanning two age classes of decomposing deadwood (between 4 and 19 years old). The amount of raw and assembled data in individual data packages is summarized in the Table 2. Overview of data previously used to describe complementarity of fungal and bacterial roles in deadwood is specified in Data Records summary⁵.

The previous studies devoted to deadwood have not seen such a comprehensive set of information about the associated biota. These data significantly improve the width and resolution and thus the understanding of the biodiversity of deadwood associated biota and its function. Given that natural forests represent an essential ecosystem concerning C storage and nutrient cycling, the data within this Data Descriptor make it possible to fully appreciate the ecosystem-level roles that deadwood plays in forest ecosystems.

Methods

Study area and sampling. Deadwood was sampled in the core zone of the Žofínský prales National Nature Reserve, an unmanaged forest in the south of the Czech Republic (48°39'57"N, 14°42'24"E) as described earlier in the associated study⁵. The core zone had never been managed and any human intervention stopped in 1838 when it was declared as reserve. It thus represents a rare fragment of European temperate virgin forest left to spontaneous development. The reserve is situated at 730–830 m a.s.l., bedrock is almost homogeneous and consists of finely to medium-grained porphyritic and biotite granite. Annual average rainfall is 866 mm and annual average temperature is 6.2 °C¹⁵.

Previous analysis indicated that deadwood age (time of decomposition) significantly affects both wood chemistry and the composition of microbial communities^{16,17}. We thus randomly selected dead tree trunks that represented age classes 1–5 assigned based on the decomposition length¹⁸. Each age class was represented by five logs of 30–100 cm diameter (Table 1). The age class 1 was <4 years since tree death, class 2 4–7 years, class 3 8–19 years, class 4 20–41 years and class 5 > 41 years (n = 5 per age class); only trees that were not alive and not decomposed before downing were considered. DNA was extracted from all logs. Due to sample-specific RNA extraction yields, RNA of sufficient amount and quality was extracted from the subset of logs (age classes 2 and 3). Sampling was performed in November 2016. The length of each selected log (or the sum of the lengths of its fragments)

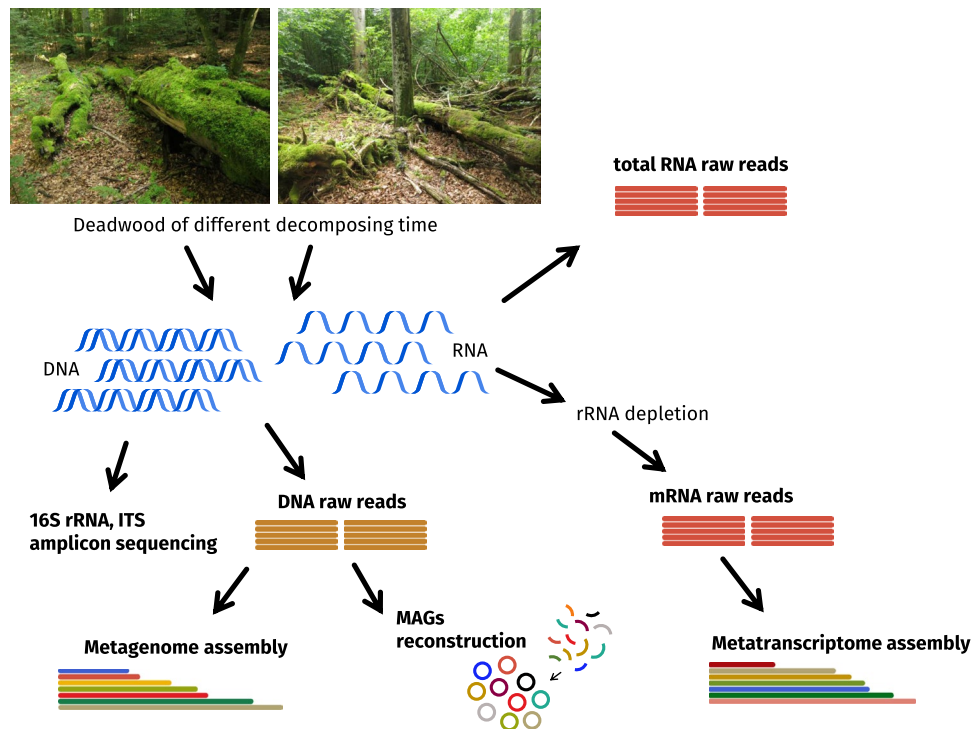


Fig. 1 Study workflow and sequencing data sources. Available data packages are in bold. The age class 1 was <4 years since tree death, class 2 4–7 years, class 3 8–19 years, class 4 20–41 years and class 5 >41 years ($n = 5$ per age class).

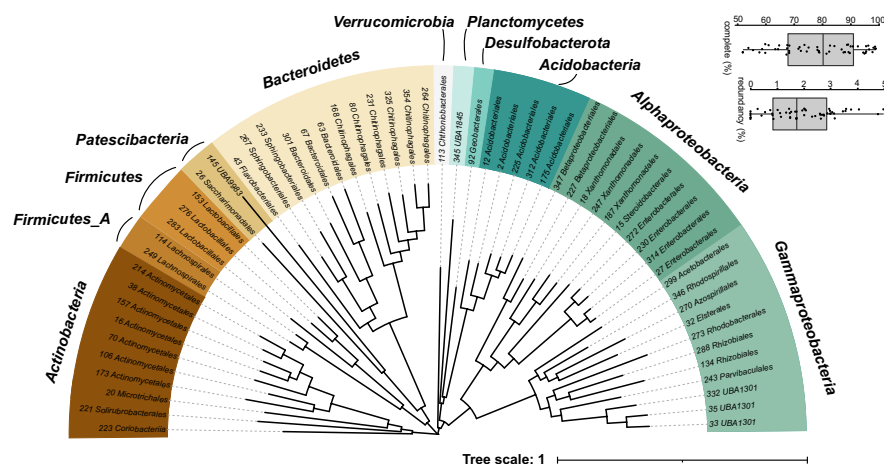


Fig. 2 Phylogenetic tree of 58 high-quality MAGs based on set of bacterial single copy genes. Phyla (or classes of *Proteobacteria*) are color-coded, tree tips are labelled with order taxonomy obtained from GTDB database. Boxplots represent completeness and redundancy values of MAGs.

was measured and four samples were collected at the positions of 20%, 40%, 60% and 80% of the log length by drilling. This was performed vertically from the middle of the upper surface through the whole diameter using an electric drill with an auger diameter of 10 mm. The sawdust from all four drill holes from each log was pooled and immediately frozen using liquid nitrogen, transported to the laboratory on dry ice and stored at -80°C until further processing.

Sample processing, DNA and RNA extraction. Sample characteristics as pH, C, N and water content were measured as described in the associated study⁵. Similarly, workflow of nucleic acid preparation, ligation and sequencing was described previously. Briefly, wood samples (approximately 10 g of material) were homogenized using a mortar and pestle under liquid nitrogen prior to nucleic acid extraction and thoroughly mixed. Total DNA was extracted in triplicate from 200 mg batches of finely ground wood powder using a NucleoSpin Soil kit (Macherey-Nagel).

data type	N samples	raw reads	common assembly [contigs]	L50 [contigs]
metagenome	25	$22.5 \pm 7.2 \times 10^6$	17.9×10^6	4.5×10^6
metatranscriptome	10	$31.3 \pm 9.1 \times 10^6$	1.3×10^6	0.5×10^6
total RNA	10	$15.1 \pm 1.8 \times 10^6$		
ITS2 marker	25	$18.3 \pm 1.4 \times 10^3$		
16S rRNA marker	25	$21.7 \pm 1.6 \times 10^3$		

Table 2. Raw read counts in individual data packages (mean \pm SE) and statistics of metagenome and metatranscriptome assembly.

Total RNA was extracted in triplicate from 200 mg batches of sample using NucleoSpin RNA Plant kit (Macherey-Nagel) according to manufacturer's protocol after mixing with 900 μ l of the RA1 buffer and shaking on FastPrep-24 (MP Biomedicals) at 6.5 ms^{-1} twice for 20 s. Triplicates were pooled and treated with OneStep PCR Inhibitor Removal kit (Zymo Research), DNA was removed using DNA-free DNA Removal Kit (Thermo Fisher Scientific). The efficiency of DNA removal was confirmed by the negative PCR results with the bacterial primers 515F and 806R¹⁹. RNA quality was assessed using a 2100 Bioanalyzer (Agilent Technologies).

Analysis of deadwood-associated organisms. To estimate the relative representation of deadwood-associated organisms in deadwood, total RNA was sequenced since the majority of the RNA represents either small subunit ribosomal RNA or large subunits ribosomal RNA that allows the identification of organisms by BLASTing against the curated databases from SILVA^{20,21}. Read abundances represent the abundances of ribosomes of each taxon and thus reflect the abundance of each taxon. Libraries for high-throughput sequencing of total RNA were prepared using TruSeq RNA Sample Prep Kit v2 (Illumina) according to the manufacturer's instructions, omitting the initial capture of polyA tails to enable total RNA to be ligated. Samples were pooled in equimolar volumes and sequenced on an Illumina HiSeq 2500 (2 \times 250 bases) at Brigham Young University Sequencing Centre, USA.

Metatranscriptomics and metagenomics. For metatranscriptome analysis, the content of rRNA in RNA samples was reduced as described previously^{5,22} using a combination of Ribo-Zero rRNA Removal Kit Human/Mouse/Rat and Ribo-Zero rRNA Removal Kit Bacteria (Illumina). Oligonucleotide probes from both types of Ribo-Zero kits were mixed together and added to each sample which allowed their annealing to rRNA and subsequent rRNA removal. The efficiency of the removal was checked using a 2100 Bioanalyzer and removal was repeated when necessary. Reverse transcription was performed with SuperScript III (Thermo Fisher Scientific). Libraries for high throughput sequencing were prepared using the ScriptSeq v2 RNA-Seq Library Preparation Kit (Illumina) according to the manufacturer's instructions with a final 14 cycles of amplification by FailSafe PCR Enzyme (Lucigen).

The NEBNext Ultra II DNA Library Prep Kit for Illumina (New England BioLabs) was used to generate metagenome libraries according to the manufacturer's instructions. Samples of the metagenome and metatranscriptome were pooled in equimolar volumes and sequenced on an Illumina HiSeq 2500 (2 \times 250 bases) at Brigham Young University Sequencing Centre, USA.

Metagenome assembly and annotation were performed as described previously⁵. Briefly, Trimmomatic 0.36²³ and FASTX-Toolkit (http://hannonlab.cshl.edu/fastx_toolkit/) were used to remove adaptor contamination, trim low-quality ends of reads and omit reads with overall low quality (<30), sequences shorter than 50 bp were omitted. Combined assembly of all 25 samples was performed using MEGAHIT 1.1.3²⁴. Metagenome sequencing yielded on average 22.5 ± 7.2 million reads per sample that were assembled into 17,936,557 contigs over 200 bp in length.

Metatranscriptome (MT) assembly and annotation were performed as described previously⁵. Trimmomatic 0.36²³ and FASTX-Toolkit (http://hannonlab.cshl.edu/fastx_toolkit/) were used to remove adaptor contamination, trim low-quality ends of reads and omit reads with overall low quality (<30), sequences shorter than 50 bp were omitted. mRNA reads were filtered from the files using the bbdutk.sh 38.26 program in BBTools (<https://sourceforge.net/projects/bbmap/>). Combined assembly was performed using MEGAHIT 1.1.3²⁴. Metatranscriptome sequencing yielded on average 31.3 ± 9.1 million reads per sample that were assembled into 1,332,519 contigs over 200 bp in length.

Identification and analysis of metagenome-assembled genomes. Bins that represent prokaryotic taxa present in the metagenome were constructed using MetaBAT2²⁵ as described previously⁵ with default settings except for the minimal length of contigs set to 2000 bp, which produced bins with overall better statistics than the minimal 2500 bp size. CheckM 1.0.11²⁶ served for assigning taxonomy and statistics to bins with *lineage_wf* pipeline. Bins with a completeness score greater than 50% were selected for quality improvement using RefineM according to the instructions of the developers²⁷. Briefly, scaffolds with genomic properties (GC content, coverage profiles and tetranucleotide signatures) whose values were different from those expected in each bin were excluded. These values were calculated based on the mean absolute error and correlation criteria. Next, the refined bins were further processed to identify and remove scaffolds with taxonomic assignments different from those assigned to the bin. Lastly, the scaffolds that possessed 16S rRNA genes divergent from the taxonomic affiliation of the refined bins were removed. The taxonomy of the bins was inferred by GTDB-Tk²⁸. 58 bins with quality scores >50 (CheckM completeness value - 5 \times redundancy value) were considered metagenome-assembled genomes (MAGs) as defined by²⁷ and deposited in the NCBI database.

GToTree v1.5.39²⁹ together with Prodigal³⁰, HMMER3³¹, Muscle³², trimAl³³, FastTree2³⁴ were used to infer phylogeny of MAGs based on set of 74 bacterial single-copy gene HMM profiles with minimal marker share >25%.

ITS2 and 16S rRNA gene amplicon sequencing and analysis. Subsamples of DNA were used to amplify the fungal ITS2 region using barcoded gITS7 and ITS4 primers³⁵ and the hypervariable region V4 of the bacterial 16S rRNA gene using the barcoded primers 515F and 806R¹⁹ in three PCR reactions per sample. PCR premix for ITS2 or 16S rRNA gene metabarcoding contained 5 µl of 5 × Q5 Reaction Buffer, 5 µl of 5 × Q5 High GC Enhancer and 0.25 µl Q5 High-Fidelity DNA Polymerase (New England Biolabs), 1.5 µl of BSA (10 mg ml⁻¹), 0.5 µl of dNTPs Nucleotide Mix 10 mM (Bioline), 1 µl of each primer, 9.75 µl of H₂O and 1 µl of template DNA. PCR conditions of fungal amplification were 5 min at 94 °C, 30 cycles of (30 s at 94 °C, 30 s at 56 °C and 30 s 72 °C) and 7 min at 72 °C. PCR conditions of bacterial amplification were 4 min at 94 °C, 25 cycles of (45 s at 94 °C, 60 s at 50 °C and 75 s 72 °C) and 10 min at 72 °C.

Three PCR reactions were pooled together, purified by MinElute PCR Purification Kit (Qiagen) and mixed in equimolar amount according to concentration measured on the Qubit 2.0 Fluorometer (Thermo Fisher Scientific). Sequencing libraries were prepared using the TruSeq PCR-Free Kit (Illumina) according to manufacturer's instructions and sequencing was performed in-house on Illumina MiSeq (2 × 250 bases).

The amplicon sequencing data were processed using the pipeline SEED 2.1.05³⁶. Briefly, paired-end reads were merged using fastq-join³⁷. Sequences with ambiguous bases and those with a mean quality score below 30 were omitted. The fungal ITS2 region was extracted using ITS Extractor 1.0.11³⁸ before processing. Chimeric sequences were detected using USEARCH 8.1.1861³⁹ and deleted, and sequences were clustered using UPARSE implemented within USEARCH⁴⁰ at a 97% similarity level. The most abundant sequences were taken as representative for each OTU. The closest fungal hits at the species level were identified using BLASTn 2.5.0 against UNITE 8.1⁴¹. Where the best fungal hit showed lower similarity than 97% with 95% coverage, the best genus-level hit was identified. The closest bacterial hit from SILVA SSU database r138²¹ was found by DECIPHER 2.18.1 package⁴² using IDTAXA algorithm with threshold 60⁴³. Sequences identified as nonfungal and nonbacterial were discarded.

Data Records

Data described in this study are summarized in the Supplementary Tables 1 and 2 together with the NCBI accession numbers. Raw sequencing reads (total RNA, metatranscriptomics and metagenomics), assembly files and resolved MAGs have been deposited under NCBI BioProject accession number PRJNA603240⁴⁴. In the associated study⁵ metatranscriptome assembly together with raw reads mapping was used for annotation of microbial functions, total RNA raw reads were used to infer mainly fungal and bacterial taxonomic composition, metagenome assembly and raw reads mapping served solely for MAGs identification. Amplicon data of bacterial 16S rRNA gene and fungal ITS2 that were not published previously, have been deposited under NCBI BioProject accession number PRJNA672674⁴⁵.

Technical Validation

Deadwood samples were taken aseptically by using sterilized equipment and sterile RNase and DNase-free tubes. RNA and DNA were extracted in an RNase free environment. During the library preparation quantity and quality of the nucleic acids were measured with a Qubit 2.0 Fluorometer and 2100 Bioanalyzer, respectively. PCR with bacterial primers 515F and 806R, negative control containing PCR-grade water and positive control containing extracted bacterial DNA was used to confirm the success of the DNase degradation of RNA samples. 2100 Bioanalyzer measurement was used to confirm successful rRNA depletion. No positive or negative sequencing controls were used to obtain metagenomic and metatranscriptomic data. For 16S rRNA gene amplification, negative and positive controls in the form of PCR-grade water and bacterial DNA, respectively were included. The concentration of the 16S rRNA gene amplicons and controls was measured with a Qubit 2.0 Fluorometer and their quality were analysed using agarose gel electrophoresis. Equimolar pooling of all barcoded sequencing libraries was done according to the quantification using KAPA Library Quantification Kit (Roche).

Usage Notes

The metagenome and metatranscriptome data described in this Data Descriptor were used to demonstrate the complementarity of fungal and bacterial functions in the carbon and nitrogen cycling in decomposing deadwood and linked them to corresponding biogeochemical processes⁵. However, the analysis on the deposited data packages in the associated study⁵ focused solely on fungi and bacteria despite the presence of other groups of organisms in the studied deadwood. The present deposition of the metagenome assembly and total RNA sequencing data opens the opportunity for biologists interested in virus ecology⁴⁶, bacterial metagenomics^{47,48} and ecology of eukaryota^{49,50} to explore the functional potential of the deadwood-associated biota through the analysis of the metagenome as well as to obtain taxonomic overview of all deadwood-associated organisms using total RNA that allows reliable taxonomic classification of taxa across the whole tree of life^{51,52}. Amplicon data described here for the first time offer intra-comparison with metagenomes and metatranscriptomes as well as inter-comparison with further deadwood studies^{16,53,54} and analysis of cross-domain interactions^{6,55}. Efforts to collect data and generalize microbial diversity patterns^{13,14,56} profit from fully annotated, accessible and metadata-rich sequences which we present here. The Data Descriptor further provides information for ecologists, biogeochemists and conservation biologists interested in the role of deadwood in ecosystem processes and deadwood associated biodiversity, an important topic of the present research in forest ecology⁵⁷.

Code availability

The above methods indicate the programs used for analysis within the relevant sections. The code used to analyse individual data packages is deposited at <https://github.com/TlaskalV/Deadwood-microbiome>.

Received: 25 January 2021; Accepted: 1 July 2021;

Published online: 03 August 2021

References

- Luyssaert, S. *et al.* Old-growth forests as global carbon sinks. *Nature* **455**, 213–215 (2008).
- Pan, Y. *et al.* A large and persistent carbon sink in the world's forests. *Science* **333**, 988–993 (2011).
- Rinne-Garmston, K. T. *et al.* Carbon flux from decomposing wood and its dependency on temperature, wood N₂ fixation rate, moisture and fungal composition in a Norway spruce forest. *Glob. Chang. Biol.* **25**, 1852–1867 (2019).
- Šamonil, P. *et al.* Convergence, divergence or chaos? Consequences of tree trunk decay for pedogenesis and the soil microbiome in a temperate natural forest. *Geoderma* **376**, 114499 (2020).
- Tláškal, V. *et al.* Complementary roles of wood-inhabiting fungi and bacteria facilitate deadwood decomposition. *mSystems* **6**, e01078–20 (2021).
- Odrizola, I. *et al.* Fungal communities are important determinants of bacterial community composition in deadwood. *mSystems* **6**, e01017–20 (2021).
- Valášková, V., de Boer, W., Gunnewiek, P. J. A. K., Pospíšek, M. & Baldrian, P. Phylogenetic composition and properties of bacteria coexisting with the fungus *Hypholoma fasciculare* in decaying wood. *ISME J.* **3**, 1218–1221 (2009).
- Brunner, A. & Kimmins, J. P. Nitrogen fixation in coarse woody debris of *Thuja plicata* and *Tsuga heterophylla* forests on northern Vancouver Island. *Can. J. For. Res.* **33**, 1670–1682 (2003).
- Rinne, K. T. *et al.* Accumulation rates and sources of external nitrogen in decaying wood in a Norway spruce dominated forest. *Funct. Ecol.* **31**, 530–541 (2016).
- Pölme, S. *et al.* FungalTraits: a user-friendly traits database of fungi and fungus-like stramenopiles. *Fungal Divers.* **105**, 1–16 (2020).
- Tláškal, V. & Baldrian, P. Deadwood-inhabiting bacteria show adaptations to changing carbon and nitrogen availability during decomposition. *Front. Microbiol.* **12**, 685303 (2021).
- Lemos, L. N., Mendes, L. W., Baldrian, P. & Pylro, V. S. Genome-resolved metagenomics is essential for unlocking the microbial black box of the soil. *Trends Microbiol.* **29**, 279–282 (2021).
- Větrovský, T. *et al.* GlobalFungi, a global database of fungal occurrences from high-throughput-sequencing metabarcoding studies. *Sci. Data* **7**, 228 (2020).
- Thompson, L. R. *et al.* A communal catalogue reveals Earth's multiscale microbial diversity. *Nature* **551**, 457–463 (2017).
- Anderson-Teixeira, K. J., Davies, S. J., Bennett, A. C., Muller-landau, H. C. & Wright, S. J. CTFIS-ForestGEO: a worldwide network monitoring forests in an era of global change. *Glob. Chang. Biol.* **21**, 528–549 (2015).
- Baldrian, P. *et al.* Fungi associated with decomposing deadwood in a natural beech-dominated forest. *Fungal Ecol.* **23**, 109–122 (2016).
- Smyth, C. E. *et al.* Patterns of carbon, nitrogen and phosphorus dynamics in decomposing wood blocks in Canadian forests. *Plant Soil* **9**, 46–62 (2016).
- Král, K. *et al.* Local variability of stand structural features in beech dominated natural forests of Central Europe: Implications for sampling. *For. Ecol. Manage.* **260**, 2196–2203 (2010).
- Caporaso, J. G. *et al.* Ultra-high-throughput microbial community analysis on the Illumina HiSeq and MiSeq platforms. *ISME J.* **6**, 1621–1624 (2012).
- Lanzén, A. *et al.* CREST – Classification resources for environmental sequence tags. *PLoS One* **7**, e49334 (2012).
- Quast, C. *et al.* The SILVA ribosomal RNA gene database project: improved data processing and web-based tools. *Nucleic Acids Res.* **41**, D590–D596 (2013).
- Žifčáková, L., Větrovský, T., Howe, A. & Baldrian, P. Microbial activity in forest soil reflects the changes in ecosystem properties between summer and winter. *Environ. Microbiol.* **18**, 288–301 (2016).
- Bolger, A. M., Lohse, M. & Usadel, B. Trimmomatic: A flexible trimmer for Illumina sequence data. *Bioinformatics* **30**, 2114–2120 (2014).
- Li, D., Liu, C. M., Luo, R., Sadakane, K. & Lam, T. W. MEGAHIT: An ultra-fast single-node solution for large and complex metagenomics assembly via succinct de Bruijn graph. *Bioinformatics* **31**, 1674–1676 (2015).
- Kang, D. D., Froula, J., Egan, R. & Wang, Z. MetaBAT, an efficient tool for accurately reconstructing single genomes from complex microbial communities. *PeerJ* **3**, e1165 (2015).
- Parks, D. H., Imelfort, M., Skennerton, C. T., Hugenholtz, P. & Tyson, G. W. CheckM: assessing the quality of microbial genomes recovered from isolates, single cells, and metagenomes. *Genome Res.* **25**, 1043–1055 (2015).
- Parks, D. H. *et al.* Recovery of nearly 8,000 metagenome-assembled genomes substantially expands the tree of life. *Nat. Microbiol.* **2**, 1533–1542 (2017).
- Parks, D. H. *et al.* A standardized bacterial taxonomy based on genome phylogeny substantially revises the tree of life. *Nat. Biotechnol.* **36**, 996–1004 (2018).
- Lee, M. D. GToTree: A user-friendly workflow for phylogenomics. *Bioinformatics* **35**, 4162–4164 (2019).
- Hyatt, D. *et al.* Prodigal: prokaryotic gene recognition and translation initiation site identification. *BMC Bioinformatics* **11**, 119 (2010).
- Eddy, S. R. Accelerated profile HMM searches. *PLoS Comput. Biol.* **7**, e1002195 (2011).
- Edgar, R. C. MUSCLE: Multiple sequence alignment with high accuracy and high throughput. *Nucleic Acids Res.* **32**, 1792–1797 (2004).
- Capella-Gutiérrez, S., Silla-Martínez, J. M. & Gabaldón, T. trimAl: A tool for automated alignment trimming in large-scale phylogenetic analyses. *Bioinformatics* **25**, 1972–1973 (2009).
- Price, M. N., Dehal, P. S. & Arkin, A. P. FastTree 2 – approximately maximum-likelihood trees for large alignments. *PLoS One* **5**, e9490 (2010).
- Ihrmark, K. *et al.* New primers to amplify the fungal ITS2 region – evaluation by 454-sequencing of artificial and natural communities. *FEMS Microbiol. Ecol.* **82**, 666–677 (2012).
- Větrovský, T., Baldrian, P. & Morais, D. SEED 2: A user-friendly platform for amplicon high-throughput sequencing data analyses. *Bioinformatics* **34**, 2292–2294 (2018).
- Aronesty, E. Comparison of sequencing utility programs. *Open Bioinforma. J.* **7**, 1–8 (2013).
- Nilsson, R. H. *et al.* An open source software package for automated extraction of ITS1 and ITS2 from fungal ITS sequences for use in high-throughput community assays and molecular ecology. *Fungal Ecol.* **3**, 284–287 (2010).
- Edgar, R. C. Search and clustering orders of magnitude faster than BLAST. *Bioinformatics* **26**, 2460–2461 (2010).
- Edgar, R. C. UPARSE: highly accurate OTU sequences from microbial amplicon reads. *Nat. Methods* **10**, 996–998 (2013).
- Nilsson, R. H. *et al.* The UNITE database for molecular identification of fungi: handling dark taxa and parallel taxonomic classification. *Nucleic Acids Res.* **47**, D259–D264 (2018).
- Wright, E. S. Using DECIPHER v2.0 to analyze big biological sequence data in R. *R J.* **8**, 352–359 (2016).
- Murali, A., Bhargava, A. & Wright, E. S. IDTAXA: A novel approach for accurate taxonomic classification of microbiome sequences. *Microbiome* **6**, 140 (2018).
- NCBI BioProject <https://identifiers.org/ncbi/bioproject:PRJNA603240> (2020).

45. NCBI Sequence Read Archive, <https://identifiers.org/ncbi/bioproject:PRJNA672674> (2020).
46. Sutela, S., Poimala, A. & Vainio, E. J. Viruses of fungi and oomycetes in the soil environment. *FEMS Microbiol. Ecol.* **95**, fiz119 (2019).
47. Woodcroft, B. J. *et al.* Genome-centric view of carbon processing in thawing permafrost. *Nature* **560**, 49–54 (2018).
48. Mackelprang, R. *et al.* Microbial community structure and functional potential in cultivated and native tallgrass prairie soils of the Midwestern United States. *Front. Microbiol.* **9**, 1775 (2018).
49. Hervé, V. *et al.* Phylogenomic analysis of 589 metagenome-assembled genomes encompassing all major prokaryotic lineages from the gut of higher termites. *PeerJ* **8**, e8614 (2020).
50. Clissmann, F. *et al.* First insight into dead wood protistan diversity: a molecular sampling of bright-spored Myxomycetes (Amoebozoa, slime-moulds) in decaying beech logs. *FEMS Microbiol. Ecol.* **91**, fiv050 (2015).
51. Urich, T. *et al.* Simultaneous assessment of soil microbial community structure and function through analysis of the metatranscriptome. *PLoS One* **3**, e2527 (2008).
52. Geisen, S. *et al.* Metatranscriptomic census of active protists in soils. *ISME J.* **9**, 2178–2190 (2015).
53. Tláskal, V., Zrůstová, P., Vrška, T. & Baldrian, P. Bacteria associated with decomposing dead wood in a natural temperate forest. *FEMS Microbiol. Ecol.* **93**, fix157 (2017).
54. Moll, J. *et al.* Bacteria inhabiting deadwood of 13 tree species reveal great heterogeneous distribution between sapwood and heartwood. *Environ. Microbiol.* **20**, 3744–3756 (2018).
55. Christofides, S. R., Hiscox, J., Savoury, M., Boddy, L. & Weightman, A. J. Fungal control of early-stage bacterial community development in decomposing wood. *Fungal Ecol.* **42**, 100868 (2019).
56. Nayfach, S. *et al.* A genomic catalog of Earth's microbiomes. *Nat. Biotechnol.* **39**, 499–509 (2021).
57. Seibold, S. *et al.* Experimental studies of dead-wood biodiversity — A review identifying global gaps in knowledge. *Biol. Conserv.* **191**, 139–149 (2015).

Acknowledgements

This work was supported by the Czech Science Foundation (21-09334 J). Computational resources were supplied by the project “e-Infrastruktura CZ” (e-INFRA LM2018140) provided within the program Projects of Large Research, Development and Innovations Infrastructures.

Author contributions

The study was conceived by V.T., V.B. and P.B. Sample processing and sequencing library preparation were performed by V.T. Metagenome and metatranscriptome data processing was performed by T.V. and V.T. U.N.R., L.M.O.M., J.P.S. and R.L.M. resolved, curated and annotated bacterial MAGs. V.T. deposited sequencing data. The original version of the manuscript was written by V.T. and P.B. All authors contributed to the final version of the manuscript.

Competing interests

The authors declare no competing interests.

Additional information

Supplementary information The online version contains supplementary material available at <https://doi.org/10.1038/s41597-021-00987-8>.

Correspondence and requests for materials should be addressed to V.T.

Reprints and permissions information is available at www.nature.com/reprints.

Publisher's note Springer Nature remains neutral with regard to jurisdictional claims in published maps and institutional affiliations.

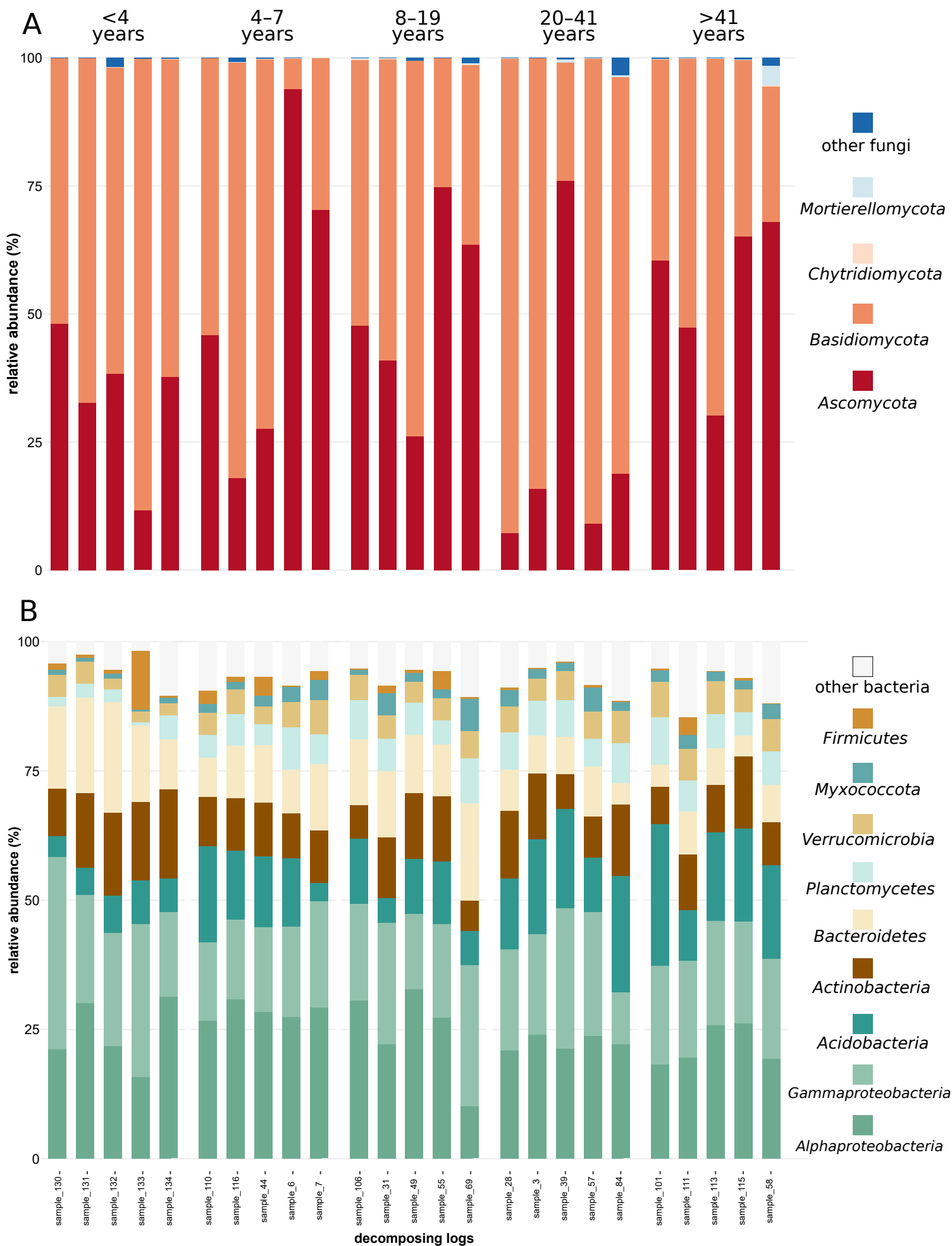


Open Access This article is licensed under a Creative Commons Attribution 4.0 International License, which permits use, sharing, adaptation, distribution and reproduction in any medium or format, as long as you give appropriate credit to the original author(s) and the source, provide a link to the Creative Commons license, and indicate if changes were made. The images or other third party material in this article are included in the article's Creative Commons license, unless indicated otherwise in a credit line to the material. If material is not included in the article's Creative Commons license and your intended use is not permitted by statutory regulation or exceeds the permitted use, you will need to obtain permission directly from the copyright holder. To view a copy of this license, visit <http://creativecommons.org/licenses/by/4.0/>.

The Creative Commons Public Domain Dedication waiver <http://creativecommons.org/publicdomain/zero/1.0/> applies to the metadata files associated with this article.

© The Author(s) 2021

Supplementary Figure 1: Relative abundance of microbial taxa represented by A) ITS2 region and B) 16S rRNA gene in 25 samples of *F. sylvatica*. Samples are grouped based on the decomposition length in years. Only the most abundant phyla (or classes of *Proteobacteria*) are shown.





Deadwood-Inhabiting Bacteria Show Adaptations to Changing Carbon and Nitrogen Availability During Decomposition

Vojtěch Tláškal* and Petr Baldrian

Laboratory of Environmental Microbiology, Institute of Microbiology of the Czech Academy of Sciences, Praha, Czechia

OPEN ACCESS

Edited by:

Svetlana N. Dedysh,
Winogradsky Institute of Microbiology,
Russian Academy of Sciences
(RAS), Russia

Reviewed by:

Miha Humar,
University of Ljubljana, Slovenia
Sarah Christofides,
Cardiff University, United Kingdom

*Correspondence:

Vojtěch Tláškal
tlaskal@biomed.cas.cz

Specialty section:

This article was submitted to
Terrestrial Microbiology,
a section of the journal
Frontiers in Microbiology

Received: 24 March 2021

Accepted: 04 May 2021

Published: 17 June 2021

Citation:

Tláškal V and Baldrian P (2021)
Deadwood-Inhabiting Bacteria Show
Adaptations to Changing Carbon and
Nitrogen Availability During
Decomposition.
Front. Microbiol. 12:685303.
doi: 10.3389/fmicb.2021.685303

Deadwood decomposition is responsible for a significant amount of carbon (C) turnover in natural forests. While fresh deadwood contains mainly plant compounds and is extremely low in nitrogen (N), fungal biomass and N content increase during decomposition. Here, we examined 18 genome-sequenced bacterial strains representing the dominant deadwood taxa to assess their adaptations to C and N utilization in deadwood. Diverse gene sets for the efficient decomposition of plant and fungal cell wall biopolymers were found in *Acidobacteria*, *Bacteroidetes*, and *Actinobacteria*. In contrast to these groups, *Alphaproteobacteria* and *Gammaproteobacteria* contained fewer carbohydrate-active enzymes and depended either on low-molecular-mass C sources or on mycophagy. This group, however, showed rich gene complements for N₂ fixation and nitrate/nitrite reduction—key assimilatory and dissimilatory steps in the deadwood N cycle. We show that N₂ fixers can obtain C independently from either plant biopolymers or fungal biomass. The succession of bacteria on decomposing deadwood reflects their ability to cope with the changing quality of C-containing compounds and increasing N content.

Keywords: deadwood, bacterial genomes, cellulose, mycophagy, nitrogen fixation

INTRODUCTION

The decomposition of deadwood in forests is a complex process during which plant polymers such as cellulose, hemicellulose, and lignin are exploited by members of the microbial community. Since the deadwood microbiome is dominated by fungi, their cell wall constituents represent another important resource, especially in the late phases of decomposition. Deadwood is estimated to contain 8% of the total global forest carbon (C) stock (Pan et al., 2011; Martin et al., 2021), making it an important source of carbon. However, the degree of the recalcitrance of C in deadwood components varies considerably and changes over time with the progress of decomposition. Fungi and bacteria produce a wide array of enzymes to access complex C sources, typically termed carbohydrate-active enzymes (CAZymes, Berlemont and Martiny, 2015). C-source niche partitioning in the utilization of C compounds is observed among microbial taxa (Gallardo et al., 2021), as well as various levels of opportunism in C acquisition (Lladó et al., 2019), where released degradation products may be utilized by microbes incapable of decomposition without the need to invest in enzyme production (Berlemont and Martiny, 2013). In contrast to C, the initial nitrogen (N) content in deadwood is extremely low (typically <1%), which leads to strong N limitation of microbial growth and substrate colonization (Tláškal et al., 2017). N accumulates in

deadwood during decomposition either due to transport via the mycelium of ectomycorrhizal and soil foraging fungi (Philpott et al., 2014) or via the activity of the diazotrophic bacterial community (Rinne et al., 2016; Tláškal et al., 2021a). Such an increase gradually alleviates N limitation, leading to a more favorable C:N ratio of the whole habitat (Weedon et al., 2009).

A previous study analyzing the decomposition of *Fagus sylvatica* deadwood through metatranscriptome analysis showed the major role of fungi in C release, as demonstrated by their dominance in CAZyme production (Tláškal et al., 2021a). Notably, even the composition of the bacterial community in deadwood is heavily affected by fungi due to their primary access to C resources (Odrizola et al., 2021). The effect of fungi on bacteria might be direct (such as through antibiosis) or indirect through substrate acidification, allowing for the selection of acid-tolerant bacterial taxa (Valášková et al., 2009; Christofides et al., 2019; Johnston et al., 2019). Fungal biomass formation also represents a nutritional basis for several bacteria (Brabcová et al., 2016; López-Mondéjar et al., 2018). Such mycophagous bacteria developed enzymes for chitin degradation to overcome N limitation by feeding on fungal biomass containing N-rich chitin and chitosan (Uroz et al., 2013; Brabcová et al., 2016; Starke et al., 2020). As a result of fungal modulation and changing conditions in the substrate, the composition and abundance of the bacterial community in deadwood change over time showing an increase of bacterial biomass and taxa succession toward community similar to that in soil (Rinta-Kanto et al., 2016; Tláškal et al., 2017). Among the factors influencing bacterial community composition in deadwood, the most often reported are pH, the C:N ratio, and water content (Folman et al., 2008; Hoppe et al., 2015; Tláškal et al., 2017; Moll et al., 2018; Mieszkin et al., 2021), but the biopolymer composition and fungal abundance are also important (Rinta-Kanto et al., 2016; Odrizola et al., 2021). Due to limited knowledge of the functional traits of deadwood bacteria, it is unclear how exactly these factors influence the members of the bacterial community or vice versa and which adaptations make bacterial species successful at various stages of deadwood decomposition.

While culture-independent methods may provide the best picture of bacterial community composition and gene expression, the characterization of isolates of dominant bacteria represents the best approach for the characterization of their phenotypes and traits (Lladó et al., 2016). The genome sequencing of bacterial isolates has helped distinguish the functional guilds of decomposers and opportunists within soil bacteria (Lladó et al., 2019). While metagenome analysis may help predict bacterial traits based on the construction of metagenome-assembled genomes (MAGs, Tláškal et al., 2021a), this approach has multiple limitations. MAGs are mostly incomplete, subject to potential contamination by non-target sequences, and often difficult to link to existing 16S rRNA gene sequences and, as such, exact bacterial identities (Bowers et al., 2017). Furthermore, the ability to recover dominant bacteria as MAGs is also variable (Nayfach et al., 2020). All of these limitations can be overcome by isolate characterization, which also offers the opportunity for phenotype screening in cultures (Madin et al., 2020).

The present study isolated the dominant bacteria from decomposing deadwood to describe their functional traits through genome sequencing and phenotype analysis and used this information to explain the preference of specific bacterial taxa for certain stages of deadwood decomposition. We focused on the bacterial ability to release C from plant and fungal polymers and bacterial assimilatory and dissimilatory N cycling pathways. We expect dominant bacteria to show differing occurrences throughout deadwood decomposition stages, driven by substrate availability and their metabolic ability to be constrained by taxonomic identity.

MATERIALS AND METHODS

Strain Isolation

This study was conducted in the Žofínský Prales National Nature Reserve, a temperate unmanaged forest in the south of the Czech Republic (48°39'57"N, 14°42'24"E). The core zone of the forest reserve (42 ha) has never been managed, and any human intervention ceased in 1838 when it was declared a reserve. This reserve thus represents a rare fragment of European temperate virgin forest with deadwood left to spontaneously decompose. The reserve is situated at 730–830 m above sea level and the bedrock is almost homogeneous and consists of finely to medium-grained porphyritic and biotite granite. The annual average rainfall is 866 mm, and the annual average temperature is 6.2°C (Anderson-Teixeira et al., 2015). At present, the reserve is covered by a mixed forest where *Fagus sylvatica* predominates in all diameter classes (51.5% of the total living wood volume), followed by *Picea abies* (42.8%) and *Abies alba* (4.8%). The mean living tree volume is 690 m³ h⁻¹, and the volume of coarse woody debris (logs, represented by tree trunks and their fragments) ranges from 102 to 310 m³ h⁻¹ with an average of 208 m³ h⁻¹ (Král et al., 2010; Šamonil et al., 2013). Logs are repeatedly surveyed, and the approximate age of each log, the cause of death (stem breakage, windthrow, etc.), and status before downing (fresh, decomposed) is known.

Decomposing wood samples were collected as described previously (Tláškal et al., 2017). Briefly, dead tree trunks (coarse woody debris; CWD) of *F. sylvatica*, *P. abies*, and *A. alba* with breast height diameters between 30 and 100 cm at the time of downing were chosen to evenly represent all decay lengths (age classes) of deadwood and the span of the diameter range. Trees decomposing as standing snags were omitted to exclude CWD with unclear decay lengths. The CWD decay length ranged from <5 to >38 years. In October 2013, four samples were obtained by drilling with an electrical drill vertically covering sapwood and heartwood along the whole decomposing stem. Part of the material was used for the description of fungal and bacterial communities and wood chemistry (Baldrian et al., 2016; Tláškal et al., 2017), while another part was used for the isolation of bacteria. For this latter category of subsamples, wood chips from each stem were pooled together and transported to the laboratory, where they were cooled until the next day. Approximately 2 g of wood material were shaken with 15 mL of Ringer solution for 2 h and this suspension was diluted 10⁴–10⁶×. Five hundred microlitres of each dilution were plated

on nutrient-limited NB medium (0.26 g L⁻¹ nutrient broth, 15 g L⁻¹ agar, pH 5) and WYA4 medium (0.1 g L⁻¹ yeast extract, 15 g L⁻¹ agar, pH 5, Valášková et al., 2009) with cycloheximide (50 mg L⁻¹). Occurrences of bacterial colonies were recorded on Petri dishes incubated at 24°C for 8 weeks and marked with a marker indicating the week of the first appearance. Colony PCR was used to infer the taxonomy of the selected strains that appeared during the course of incubation. PCR premix and cycling conditions were as follows: 2.5 µL of 10× buffer for DyNAzyme DNA Polymerase; 0.75 µL of DyNAzyme II DNA polymerase (2 u µL⁻¹); 0.75 µL of BSA (20 mg mL⁻¹); 0.5 µL of PCR Nucleotide Mix (10 mM); 1 µL of primer eub530f (10 µM, 5'-GTG CCA GCM GCN GCG G); 1 µL of primer eub1100br (10 µM, 5'-GGG TTN CGN TCG TTG, Lane, 1991) and sterile ddH₂O up to 25 µL, with amplification started at 94°C for 5 min followed by 35 cycles of 94°C for 1 min, 62°C for 1 min, 72°C for 1 min and a final setting of 72°C for 10 min. Sanger sequencing was performed from the reverse primer as an external service. The obtained sequences were compared by BLASTn with bacterial 16S rRNA-based community data from the same deadwood objects that were used for isolation (Tláškal et al., 2017). Bacterial strains with high similarity (>97%) and coverage (>90%) relative to the most abundant deadwood OTUs were selected for further cultivation. The strains that were cultivable on laboratory media in subsequent passages and those that exhibited sufficient growth and biomass production were used for genome sequencing and culturing tests. By this approach, we were able to select 18 bacterial strains with high similarity to highly abundant bacterial OTUs from the studied deadwood.

Cultivation Tests

The activity of the cell wall-associated fraction of enzymes was measured in cells after 2 weeks of incubation in triplicate in 50 mL of liquid GY-VL55 medium as described previously (Lasa et al., 2019). To assess the ability to grow on cellulose, carboxymethyl cellulose medium (CMC) was prepared (5 g L⁻¹ CMC, 2 g L⁻¹ yeast extract, 15 g L⁻¹ agar, pH 5). Plates were incubated at 24°C for 2 weeks. After incubation, 12 mL of 1% Congo Red was poured onto each plate, staining was performed for 30 min, the Congo Red was replaced with 12 mL of 1 M NaCl, the NaCl was left for 30 min, the NaCl was replaced with 12 mL of H₂O, and the H₂O was left overnight. The presence of a halo around the colonies indicated CMC utilization.

DNA Extraction, Sequencing, Genome Assembly, and Annotation

Selected bacterial strains were cultivated in 50 mL of GY-VL55 liquid medium shaken in Erlenmeyer flasks (Lladó et al., 2019) for 2 weeks at 23°C. Cells were collected by centrifugation, and DNA was extracted by an ArchivePure DNA Yeast and Gram+ Kit (5 Prime, Germany) according to the manufacturer's instructions. DNA was sheared by a Bioruptor Pico sonication device (Diagenode, Belgium) to an average length of 550 bp, and sequencing adapters were ligated by the TruSeq DNA PCR-Free Library Prep Kit (Illumina Inc., USA). Ligated libraries were sequenced in-house on the Illumina MiSeq platform.

Genome assembly of each isolate was performed using a Unicycler 0.4.7 (Wick et al., 2017) in normal mode with the following programs: SPAdes 3.13.0 (Bankevich et al., 2012), BLAST 2.7.1+ (Altschul et al., 1997), Bowtie 2.2.4 (Langmead et al., 2009), SAMtools 1.9 (Li et al., 2009), and Pilon 1.22 (Walker et al., 2014). Prokka 1.13.3 (Seemann, 2014) with RNAmmer (Lagesen et al., 2007) was used for gene calling, annotation, and rRNA gene identification. The taxonomy of the closest complete genome in the NCBI database with >97% similarity of 16S rRNA gene sequences were used to assign strains at the genus level. GToTree v1.5.39 (Lee, 2019) together with Prodigal (Hyatt et al., 2010), HMMER3 (Eddy, 2011), Muscle (Edgar, 2004), trimAI (Capella-Gutiérrez et al., 2009), FastTree2 (Price et al., 2010), and GNU Parallel (Tange, 2018) was used to construct a phylogenetic tree of the genomes based on a set of HMM profiles for 74 bacterial single-copy genes.

For CAZyme annotation, Prokka gene prediction was used to obtain the sequences of genes. Amino acid sequences were compared with the dbCAN database version 07312018 using the run-dbcAN.py script (Zhang et al., 2018) and HMMER 3.2.1 (Eddy, 2011). CAZymes with an e-value ≤ 1E⁻³⁰ were considered for further annotation and their most probable target substrates were identified based on the genes with characterized functions in the CAZy database (<http://www.cazy.org>; Lombard et al., 2014). Functions of predicted genes were annotated with the hmsearch function in HMMER 3.2.1, using the FOAM database as a source of HMMs for relevant genes (Prestat et al., 2014). FOAM functions with an e-value ≤ 1E⁻³⁰ were considered for further annotation. In the case of genes with more than one hit in the dbCAN and the FOAM databases, the function with the lowest e-value was selected.

Metagenome Mapping

The metagenomes of naturally decomposing *F. sylvatica* deadwood were obtained in a previous study (Tláškal et al., 2021a, Tláškal et al., under review) and used to quantify genome coverage in deadwood of various decay lengths. This metagenome study included 25 CWD samples of *F. sylvatica*. The CWD samples were classified into five decay length classes of <4, 4–7, 8–19, 20–41, and > 41 years. Metagenomic reads were mapped to genomes as described previously (Lladó et al., 2019) using Bowtie v2.3.4.1 (Langmead and Salzberg, 2013). Metagenomic reads from sample with NCBI accession SRR10968255 were omitted from mapping due to under-sampling. The number of mapped reads was normalized to the sequencing depth of each sample, divided by the genome length of individual strains, and multiplied by the average genome size of sequenced bacteria. Differences among groups were tested by the Kruskal-Wallis test using the agricolae package (de Mendiburu, 2017) and considered to be statistically significant at the level $P < 0.05$.

16S rRNA Gene-Based Phylogeny of OTUs and Strains

Dereplicated 16S rRNA genes of strains with sequenced genomes were merged with representative OTU sequences (most frequent sequences from each OTU, Tláškal et al., 2017). Only the globally

most abundant OTUs represented by an abundance >0.5% in >10 samples were selected ($n = 86$ OTUs). Sequences were aligned by the MAFFT online tool (Katoh et al., 2018) with default settings. A phylogenetic tree was constructed using FastTree2 (Price et al., 2010) with default settings. The taxonomy of the tree tips was assigned with DECIPHER v2.0 (Wright, 2016) using SILVA SSU database release 138 (Quast et al., 2013). A phylogenetic tree of 16S rRNA sequences from all 959 obtained isolates was constructed by the same approach. The diversity of the whole isolated collection was inferred by clustering using VSEARCH 2.4.3 (Rognes et al., 2016). Tables were processed using R 4.0.2 (R Core Team, 2020) and tidyverse 1.3.0 (Wickham et al., 2019). The resulting images were processed with Inkscape 1.0 (<https://inkscape.org/>).

RESULTS

Isolation yielded 959 isolates, with *Gammaproteobacteria* being the most represented class, followed by the class *Alphaproteobacteria* and the phyla *Actinobacteria*, *Bacteroidetes*, *Acidobacteria*, and *Firmicutes* (**Supplementary Figure 1A**). The largest share of isolates was represented by the *Burkholderia-Caballeronia-Paraburkholderia* complex (17%), followed by the genera *Mucilaginibacter* (7%) and *Pseudomonas* (7%, **Supplementary Figure 1B**). Isolates clustered into 467 OTUs (>99% similarity) and were binned to 4.5% of OTUs from the 16S rRNA amplicon study from the same CWD samples published previously (Tláškal et al., 2017). The isolates represented on average $33.5 \pm 1.3\%$ of bacteria in a CWD sample. The youngest age class of deadwood, comprising CWD samples with a decay length <5 years, was most represented by the isolates ($38.8 \pm 2.6\%$).

The selected sequenced strains binned to 0.7% of bacterial OTUs, representing $15.3 \pm 0.8\%$ of bacteria in CWD samples (**Supplementary Figure 2**; **Table 1**). The phylogeny of 86 dominant OTUs in the whole amplicon dataset, i.e., those representing >0.5% sequences in >10 CWD samples, showed that we retrieved members of the top five deadwood bacterial phyla and classes of *Proteobacteria*. These were *Acidobacteria*, *Alphaproteobacteria*, *Gammaproteobacteria*, *Actinobacteria*, and *Bacteroidetes* (**Figure 1**; **Table 1**). Members of other phyla that represented only a small minority among the dominant OTUs—*Firmicutes* ($n = 1$), class *Polyangia* ($n = 1$), *Planctomycetes* ($n = 2$), *Verrucomicrobia* ($n = 5$), and WPS-2 ($n = 1$)—either were not isolated or failed to grow in subsequent cultures. Except for the strains of *Bradyrhizobium* (1.5%), each genome represented on average <1% of bacteria across all CWD samples. Up to 26.7% of bacteria were represented in the best-covered CWD samples (**Table 1**).

CAZy analysis showed a considerable level of variation in the carbon utilization traits among strains (**Figure 2**). Four strains were distinct in terms of high CAZyme counts and diversity: two *Acidobacteria* (*Edaphobacter* strain 441 and *Granulicella* strain 53), *Mucilaginibacter* strain 454, and *Sphingomonas* strain 22. The *Granulicella* strain showed the most CAZymes ($n = 187$

in 72 CAZy families), representing 3.7% of its total genes. In contrast, six members of the genera *Variovorax*, *Pseudomonas*, and *Bradyrhizobium* contained only 62–75 CAZymes in 28–35 CAZy families, representing 1% of their total genes (**Figure 2**).

Functional analysis of the identified CAZymes showed the specific C sources targeted by the strains (**Figure 2**). Genes for cellulose degradation were present in three copies of cellulase GH6 in the genome of *Glaciihabitans* strain 435. *Mucilaginibacter* strain 454 and *Sphingomonas* strain 22 each contained two copies of cellulases. Other strains with a single copy of a cellulase gene included both *Acidobacteria* strains, both *Caballeronia* strains, both *Sodalis* strains, and *Mesorhizobium* strain 380. An increased number of chitinase genes were present in *Granulicella* strain 53 and *Edaphobacter* strain 441 ($n = 7$ and 5, respectively). *Mucilaginibacter* strain 454 contained three genes for enzymes involved in chitin degradation, and *Luteibacter* strain 328 contained two chitinases. Both *Pseudomonas* strains encoded a single chitinase gene, and genes encoding enzymes targeting chitin were present in both *Variovorax* strains, *Caballeronia* strain 276 and *Sphingomonas* strain 22. An increased number of hemicellulases were present in two *Acidobacteria* strains, *Sphingomonas* strain 22, *Mucilaginibacter* strain 454, and *Luteibacter* strain 328. CAZymes for the labile substrates cellobiose and xylobiose and α -glucanases were present throughout the isolated strains without evident differences. CAZymes for other labile substrates, pectinases, β -glucanases, and glycoconjugate-degrading enzymes, were preferentially found in high-CAZy-containing *Acidobacteria* strains, *Mucilaginibacter* strain 454, *Glaciihabitans* strain 435, and *Sphingomonas* strain 22. Two *Pseudomonas* strains contained lytic polysaccharide monoxygenase genes from CAZy family AA10 for the oxidation of a broad range of polysaccharides. Some of the low-CAZy genomes contained genes for C uptake from alternative sources: the *mxoF* gene for methanol dehydrogenase, which oxidizes methanol, was present in *Variovorax* and *Caballeronia* (both *Burkholderiales*), and four copies of this gene were present in *Bradyrhizobium* strain 411. *Mesorhizobium* together with *Caballeronia* contained genes for soluble diiron monoxygenases.

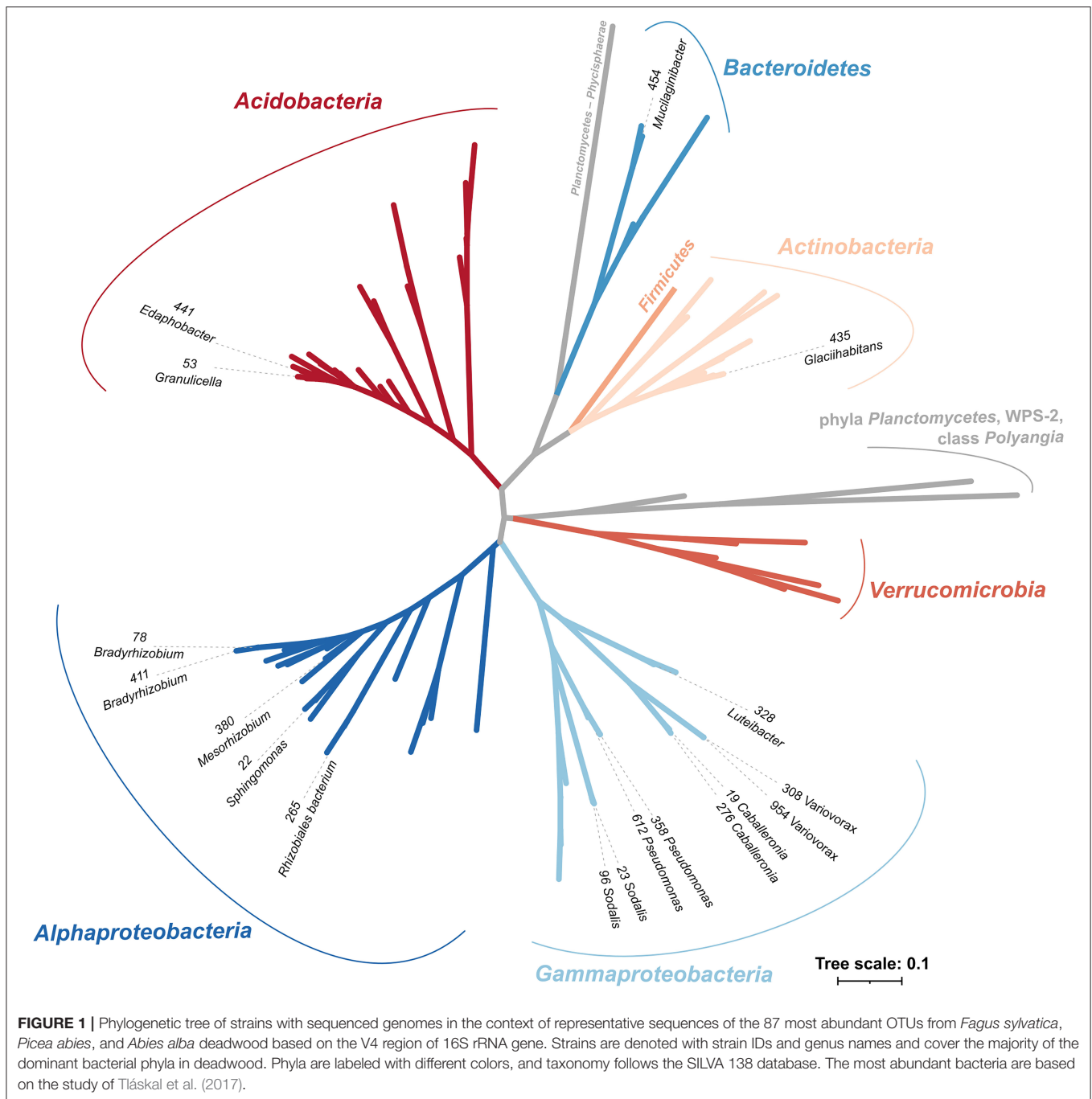
Luteibacter strain 328 showed by far the most active cell wall-associated enzymatic fraction. Except for *Luteibacter*, chitinase activity was highest in *Bradyrhizobium* strains, *Variovorax* strains, and *Pseudomonas* strains. Strains of *Pseudomonas*, *Variovorax*, and *Luteibacter* were not able to grow on CMC medium but displayed cellobiohydrolase and β -glucosidase activities suitable for the degradation of cellulose-derived oligosaccharides (**Table 1**; **Supplementary Figure 3**).

Nitrogen cycling-related genes showed a higher occurrence in the genomes of *Alphaproteobacteria* and *Gammaproteobacteria* (**Figure 2**). *Bradyrhizobium* strain 78, *Mesorhizobium* strain 380, and the two *Sodalis* strains contained the nitrogenase operon *nifHDK*, which enables nitrogen fixation. Genomes of both *Sodalis* strains and *Mesorhizobium* strain 380 showed a combination of nitrogenase genes and cellulase genes. The two *Caballeronia* and the two *Sodalis* strains contained an increased number of genes for dissimilatory nitrate to nitrite reduction. Assimilatory nitrate reduction genes seem to be limited only

TABLE 1 | Genomic traits of dominant bacteria associated with decomposing deadwood.

Strain ID	Taxonomy	Source medium	CMC growth	Mean abundance in 16S rRNA data (%)	Max abundance in 16S rRNA data (%)	Assembly size (Mbp)	GC content (%)	Gene number	Accession	SRA
435	<i>Glacihabitans; Actinobacteria</i>	WY		0.60 ± 0.09	10.80	3.7	65.9	3600	PRJNA613978	SRR11413040
454	<i>Mucilaginibacter; Bacteroidetes</i>	WY		0.16 ± 0.05	18.38	4.7	43.2	4112	PRJNA613980	SRR11413148
53	<i>Granulicella; Acidobacteria</i>	NB		0.65 ± 0.05	11.69	6.1	57.7	5062	PRJNA613883	SRR11396417
441	<i>Edaphobacter; Acidobacteria</i>	WY		0.73 ± 0.08	10.32	4.9	58.8	4133	PRJNA613979	SRR11413017
22	<i>Sphingomonas; Alphaproteobacteria</i>	NB		0.35 ± 0.07	16.74	4.4	66.8	3947	PRJNA613993	SRR11396416
265	<i>Rhizobiales b.; Alphaproteobacteria</i>	WY		0.31 ± 0.02	2.95	4.2	64.1	3934	PRJNA613888	SRR11412665
380	<i>Mesorhizobium; Alphaproteobacteria</i>	WY		0.09 ± 0.02	0.42	6.9	62.6	6578	PRJNA701764	SRR13706190
78	<i>Bradyrhizobium; Alphaproteobacteria</i>	NB	yes	1.51 ± 0.12	10.01	6.0	62.1	5585	PRJNA613884	SRR11412340
411	<i>Bradyrhizobium; Alphaproteobacteria</i>	WY	yes	1.51 ± 0.12	10.01	7.3	61.1	6712	PRJNA613977	SRR11413018
276	<i>Caballeronia; Gammaproteobacteria</i>	WY		0.46 ± 0.06	6.68	6.8	59.7	6165	PRJNA613889	SRR11413014
19	<i>Variovorax; Gammaproteobacteria</i>	NB	yes	0.46 ± 0.06	6.68	9.1	60.0	8229	PRJNA613879	SRR11392425
954	<i>Variovorax; Gammaproteobacteria</i>	NB		0.16 ± 0.02	2.76	8.1	66.1	7409	PRJNA613983	SRR11413163
308	<i>Luteibacter; Gammaproteobacteria</i>	WY		0.16 ± 0.02	2.76	7.9	66.0	7144	PRJNA615766	SRR11432075
328	<i>Luteibacter; Gammaproteobacteria</i>	WY		0.77 ± 0.28	19.95	5.1	64.2	4532	PRJNA613890	SRR11413015
612	<i>Pseudomonas; Gammaproteobacteria</i>	WY		0.32 ± 0.12	26.70	7.4	59.7	6455	PRJNA613981	SRR11413149
358	<i>Pseudomonas; Gammaproteobacteria</i>	WY	yes	0.48 ± 0.18	13.88	5.5	62.0	5049	PRJNA613975	SRR11413016
96	<i>Sodalis; Gammaproteobacteria</i>	NB	yes	0.30 ± 0.08	10.61	5.9	54.0	5307	PRJNA613885	SRR11431239
23	<i>Sodalis; Gammaproteobacteria</i>	NB	yes	0.30 ± 0.08	10.61	6.4	55.0	5770	PRJNA599932	SRR10875134

The average and maximal representations in the CWD are based on the 16S rRNA gene community data (Tláškal et al., 2017).



to the presence of the *nasB* gene in a restricted number of taxa. In contrast, the assimilatory nitrite reduction genes *nirAB* were present in almost all isolated strains. Denitrification steps leading to the production of N_2 —reduction of nitric oxide and nitrous oxide—were not detected in any genome. However, several genomes (especially those in the genus *Sodalis*) contained genes for dissimilatory nitrite reduction (*nrfC* or *nrfD*), directing N flow into dissimilatory nitrate reduction to the ammonia pathway (DNRA). Similar to denitrification genes, nitrification genes, including those that allow the oxidation of ammonia, were missing in the bacterial genomes examined.

Genome-sequenced bacterial strains differed in their tendency to associate with deadwood of a certain decay length, as demonstrated by the mapping of metagenome reads from decomposing *F. sylvatica*. Mapping showed that several strains were restricted to very fresh deadwood (<4 years of decomposition), while others tended to increase in abundance at later decomposition stages (Figure 3). The isolates *Glaciihabitans* strain 435, *Pseudomonas* strain 358, *Sodalis* strains 23, and 96 and *Sphingomonas* strain 22 were significantly more abundant in the fresh CWD, while several other strains also showed high abundances in the fresh

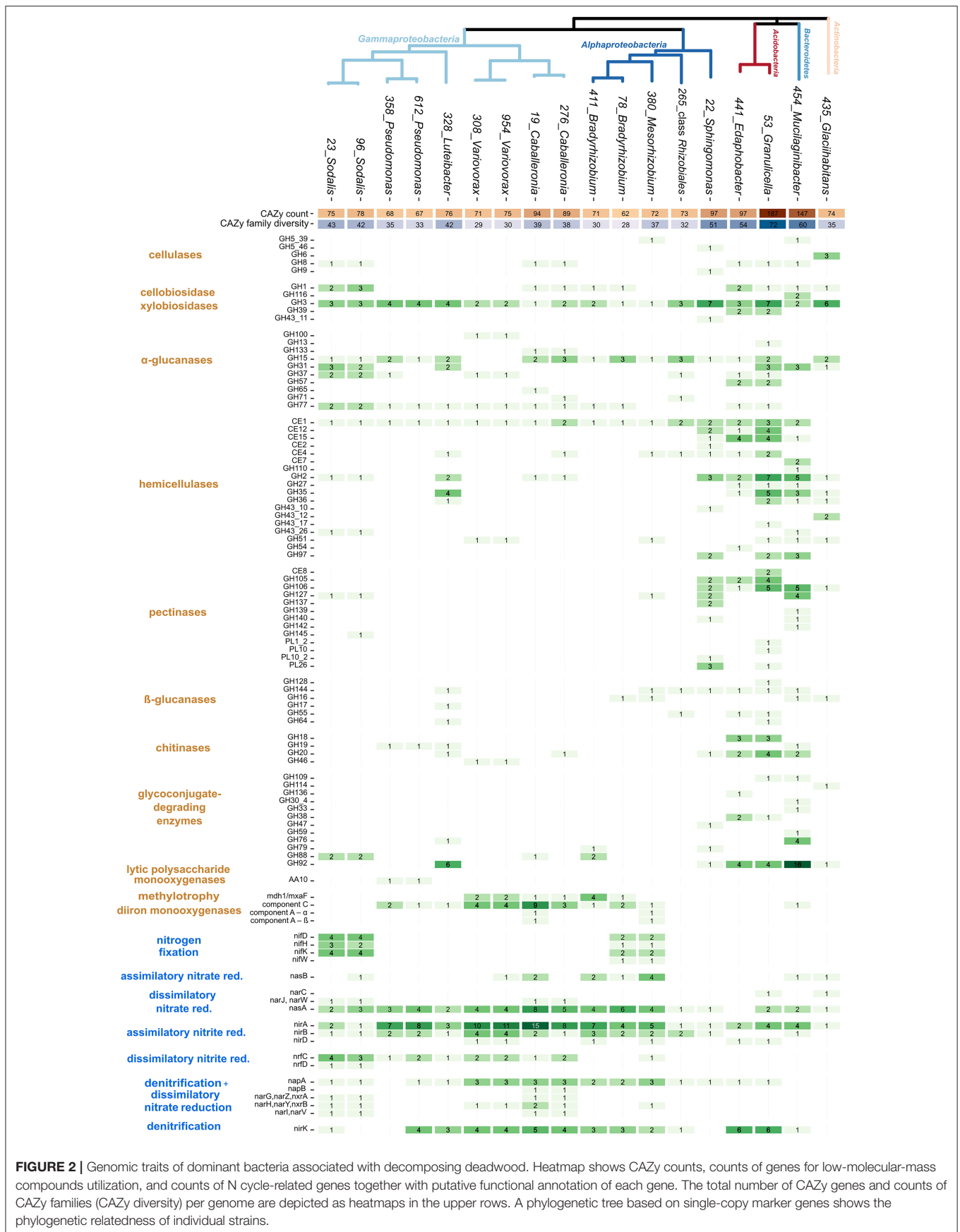


FIGURE 2 | Genomic traits of dominant bacteria associated with decomposing deadwood. Heatmap shows CAZy counts, counts of genes for low-molecular-mass compounds utilization, and counts of N cycle-related genes together with putative functional annotation of each gene. The total number of CAZy genes and counts of CAZy families (CAZy diversity) per genome are depicted as heatmaps in the upper rows. A phylogenetic tree based on single-copy marker genes shows the phylogenetic relatedness of individual strains.

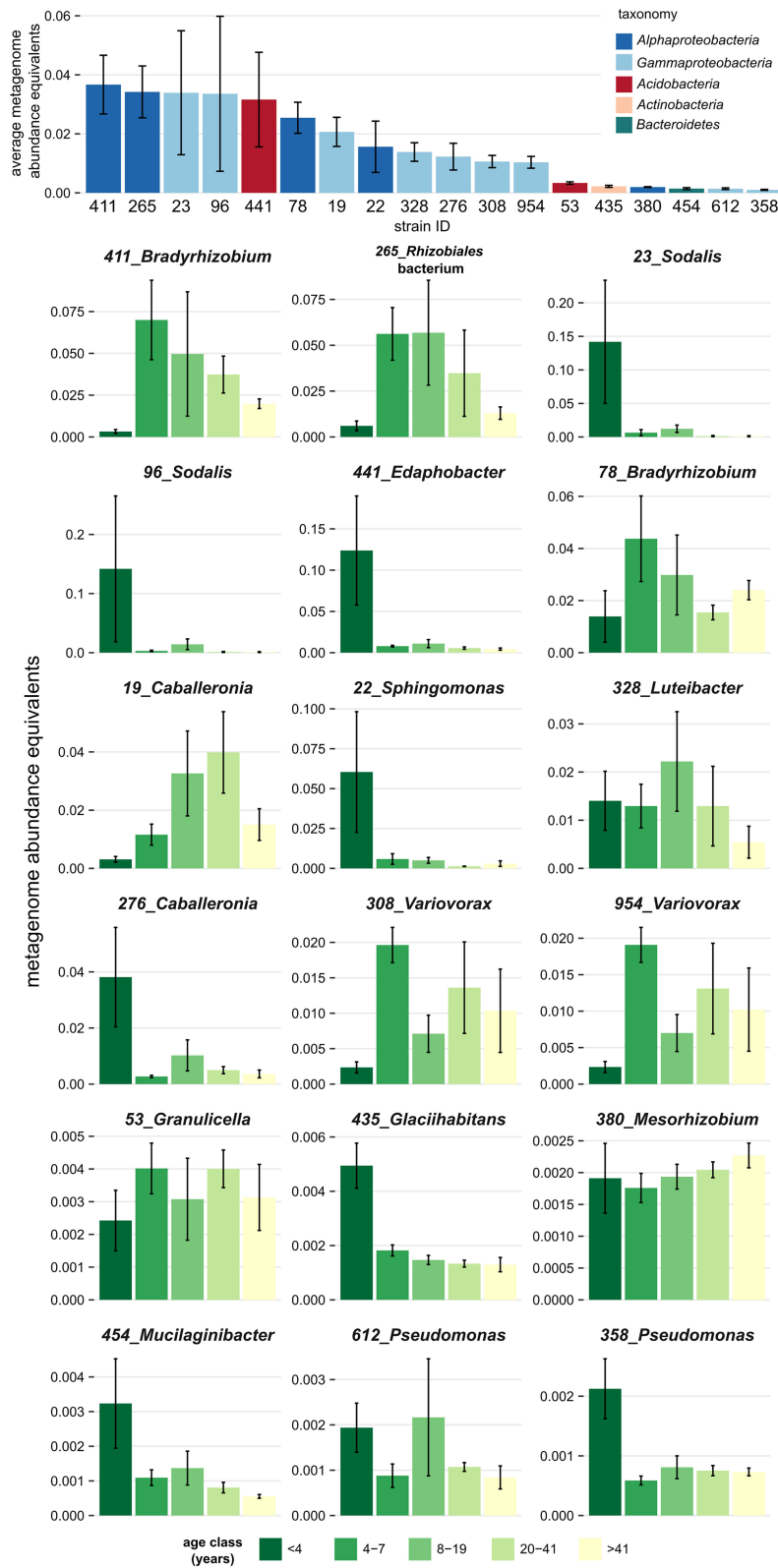


FIGURE 3 | Association of dominant bacteria isolated from decomposing *Fagus sylvatica* deadwood with a certain age of deadwood. Mapping of the deadwood metagenome reads (Tláškal et al., under review) to genomes of strains shows a distinct overall abundance of these bacteria in metagenomes and distinct occurrence in individual deadwood age classes. Strains are sorted based on the total average metagenome abundance. The height of the bar plots corresponds to abundance equivalents—relative share of mapped reads corrected to the genome size of each strain. Error bars represent standard errors.

deadwood (*Edaphobacter* strain 441, *Caballeronia* strain 276 and *Mucilaginibacter* strain 454) but only inhabited certain CWD samples from the youngest age class. The abundance of other strains, including two *Bradyrhizobium* strains and *Rhizobiales* strain 265, peaked later during decomposition. Notably, the aforementioned *Alphaproteobacteria* represent bacteria with the highest abundance in the examined metagenomes (Figure 3).

DISCUSSION

Using prolonged cultivation, it is possible to capture a wide diversity of bacteria, including slow-growing taxa, with potentially important ecological functions (Sait et al., 2002; Lladó et al., 2016). Our isolation, which resulted in 959 deadwood bacterial isolates, was partly redundant, with many taxa repeatedly captured (Supplementary Figure 1), yet due to the presence of several members of dominant deadwood OTUs, the collection represented a relatively large portion of the bacterial community—on average, approximately one-third of the bacteria present in CWD. In contrast to culture-independent genome resolving, isolation provides complete data about the genome content of a particular strain without the threat of chimeric genomes (Shaiber and Eren, 2019) and represents a suitable approach for fully describing the role of key members of the microbiome (Valášková et al., 2009).

We characterized members of the most abundant deadwood bacterial taxa *Acidobacteria*, *Alphaproteobacteria*, *Gammaproteobacteria*, *Actinobacteria*, and *Bacteroidetes*. These dominant phyla appear to be generally occurring in deadwood (Johnston et al., 2016). Although our functional assignment of genes was done as accurately as possible, it should be noted that, in some cases, one CAZy family of enzymes can target different substrates (e.g., GH6; such genes found in *Glaciihabitans* displayed the highest similarity to known endo- β -1,4-glucanases). Therefore, we show the most probable functions of the CAZymes. Among cultivated bacteria, we identified strains with an increased potential for the utilization of complex carbohydrates, including cellulose, chitin, hemicelluloses, and pectin. These strains belong to the phyla *Acidobacteria*, *Bacteroidetes*, *Actinobacteria*, and the genus *Sphingomonas* from the *Alphaproteobacteria*. The strong hydrolytic capabilities of these taxa have been reported previously for some of the soil-inhabiting groups (Uroz et al., 2013; Větrovský et al., 2014; López-Mondéjar et al., 2019). Specifically, *Acidobacteria* and *Bacteroidetes* were identified as efficient decomposers of carbohydrate biopolymers (Lladó et al., 2019). This also corresponds to the identified chitinase activity (Lladó et al., 2016) and degradation of fungal mycelium by *Acidobacteria* including genus *Granulicella* (López-Mondéjar et al., 2018). This trait was supported by an increased number of chitinase genes in the cultivated *Acidobacteria* in our study.

In contrast to general degraders, deadwood *Gammaproteobacteria* and most *Alphaproteobacteria* harbored lower numbers of CAZymes, indicating a narrow spectrum of potential C sources. The least CAZy-equipped strains were those assigned to the genera *Variovorax*, *Pseudomonas*, and

Bradyrhizobium. Despite the lack of CAZymes for plant-derived compound degradation, such as cellulose or hemicellulose, these low-CAZy strains have the potential to compensate for this narrow range by decomposition of fungal biomass. Adherence to fungal hyphae or enrichment in the presence of fungi were repeatedly described for *Burkholderiales*, suggesting a mycophagous lifestyle for these strains (Valášková et al., 2009; Hervé et al., 2016; Brabcová et al., 2018; Starke et al., 2020). Our *Variovorax* and *Caballeronia* strains from *Burkholderiales* indeed contained chitinase and *N*-acetylglucosaminidase genes, respectively, which are involved in the degradation of the main fungal structural biopolymers chitin and chitosan. The genus *Pseudomonas* showed a similar chitinase gene presence to strains of the same genus involved in the decomposition of fungal biomass (Starke et al., 2020). The chitinolytic activity of the membrane-bound enzymes was measured for the *Bradyrhizobium* strains and the *Luteibacter* strain. *Luteibacter* displayed the highest chitinase activity in this study, and its mycolytic and cellulolytic activity was described previously (López-Mondéjar et al., 2016; Mieszkin et al., 2021); *Luteibacter* additionally showed a generally high activity of membrane-bound enzymes (Lasa et al., 2019).

The bacteria from the classes *Alphaproteobacteria* and *Gammaproteobacteria*, which are low in carbohydrate-active enzymes, showed the presence of genes for putative methanol oxidation. Genes for soluble diiron monooxygenases in *Caballeronia* and *Mesorhizobium* point to oxidation of other low-molecular-mass C sources rather than performing methanotrophy which was not described for these taxa (Leahy et al., 2003). Altogether, the presence of these genes suggests that *Alphaproteobacteria* and *Gammaproteobacteria* utilize simple C compounds generated during lignin decomposition by fungi (Fillee et al., 2002; Lenhart et al., 2012). Methylo-trophy of *Alphaproteobacteria* is sometimes accompanied by diazotrophic activity (Vorob'ev et al., 2009). Changes in bacterial deadwood community composition are tightly linked with changes in the pH, water content, and C:N ratio of the substrate (Hoppe et al., 2015; Tláškal et al., 2017). The C:N ratio of fresh deadwood is very high and decreases during decomposition, which is a result of N accumulation partially through fungal translocation and mainly through bacterial N_2 fixation (Rayner and Boddy, 1988; Rinne et al., 2016; Tláškal et al., 2021a).

The ability to fix N_2 might explain the association of *Alphaproteobacteria* with low-N conditions and their positive correlation with the C:N ratio (Rinta-Kanto et al., 2016; Mieszkin et al., 2021). Previous studies detected the order *Rhizobiales* (*Alphaproteobacteria*) as one of the abundant members in the deadwood community (Hervé et al., 2013) and showed the presence of nitrogenase genes assigned to this group (Hoppe et al., 2015). In line with this, we cultivated two *Rhizobiales* strains containing the nitrogenase *nifHDK* operon. The other two nitrogen fixers are enterobacteria from the genus *Sodalis*, and both are closely related to *Sodalis* insect endosymbionts that lack nitrogenase genes (Tláškal et al., 2021b). After almost 40 years, non-symbiotic N_2 -fixing *Sodalis* and *Rhizobiales* strains widen a small group of cultivated deadwood diazotrophic bacteria successfully retrieved from naturally decomposing CWD (Seidler

et al., 1972; Spano et al., 1982). *Sodalis* strains were most abundant in early decomposition when the N limitation was most severe, and the abundance of *Rhizobiales* peaked later. Deadwood seems to be a hotspot of non-symbiotic N₂ fixation, and these abundant taxa contribute to the N enrichment of the substrate (Brunner and Kimmins, 2003; Tláškal et al., 2021a). Notably, three out of four nitrogen-fixing strains (the two *Sodalis* and *Mesorhizobium* strains) also contained a single cellulase gene, which suggests that these strains might be independent in recalcitrant substrates utilization. Examination of other N cycle pathways shows that genes encoding dissimilatory steps are less common than those encoding assimilatory steps. Specifically, *Sodalis* strains (and partly *Caballeronia* strains) contain genes for DNRA, enabling the transformation of oxidized forms of N into ammonium. The balance between DNRA and denitrification is crucial for the soil N budget (Nelson et al., 2016), and a similar mechanism might exist in deadwood. The absence of complete denitrification and the preferred DNRA pathway thus prevents the loss of scarce nitrogen (Tláškal et al., 2021a).

Bacterial community composition was shown to undergo a significant change between the early and late decomposition stages at a deadwood age of ~15 years (Tláškal et al., 2017). Here, several strains showed a preference for very young and almost intact deadwood (though there was a high variation among individual fresh stems), while the same strains were less abundant in the subsequent decomposition stages. Conversely, strains that reached the highest abundance in the late decomposition phase were considerably less abundant in fresh deadwood. Bacteria involved in N₂ fixation occur in fresh deadwood as well as in the following decomposition phases, showing the importance of this activity throughout decomposition. As the most readily available plant biopolymers are gradually depleted during decomposition, bacteria with genes for chitin degradation might switch to utilizing C from fungal biomass. Mycophagous bacteria such as *Granulicella*, *Luteibacter*, and *Burkholderiales* indeed tended to be more abundant in the later decomposition stages when fungal biomass in deadwood increases and starts to represent a relatively easily accessible source of both C and N.

Different C utilization strategies were described for soil habitats in which *Acidobacteria* and *Bacteroidetes* served as decomposers with a high number of expressed CAZymes, while *Proteobacteria* were recognized as opportunists relying on C

uptake from other labile sources (Lladó et al., 2019). With the high taxonomic and functional overlap in these soil groups, we can identify two distinct strategies of abundant deadwood bacterial taxa: degraders with high decomposition potential and less generalist bacteria filling their C needs by alternative source utilization and mycophagy. Moreover, the latter are active in N cycling, and their presence might be beneficial for the total microbial community due to N₂ fixation. Metabolically diverse bacteria thus show specific adaptations to challenging deadwood habitats and complement deadwood decomposition driven by fungi through N enrichment.

CODE AVAILABILITY

The above methods indicate the programs used for analysis within the relevant sections. The code for reproducing the sequence processing is provided at <https://github.com/TlaskalV/Deadwood-bacterial-isolates>

DATA AVAILABILITY STATEMENT

Data described in this manuscript, including raw sequences from short read sequencing and genome assembly files have been deposited in NCBI under BioProject accession numbers summarized in the **Table 1**.

AUTHOR CONTRIBUTIONS

VT and PB conceived the study and wrote the manuscript. VT performed strain isolation, genome processing, and strain growth characterization. All authors contributed to the article and approved the submitted version.

FUNDING

This work was supported by the Czech Science Foundation (21-09334J).

SUPPLEMENTARY MATERIAL

The Supplementary Material for this article can be found online at: <https://www.frontiersin.org/articles/10.3389/fmicb.2021.685303/full#supplementary-material>

REFERENCES

- Altschul, S. F., Madden, T. L., Schäffer, A. A., Zhang, J., Zhang, Z., Miller, W., et al. (1997). Gapped BLAST and PSI-BLAST: a new generation of protein database search programs. *Nucleic Acids Res.* 25, 3389–3402. doi: 10.1093/nar/25.17.3389
- Anderson-Teixeira, K. J., Davies, S. J., Bennett, A. C., Muller-landau, H. C., and Wright, S. J. (2015). CTFs-ForestGEO: a worldwide network monitoring forests in an era of global change. *Glob. Change Biol.* 21, 528–549. doi: 10.1111/gcb.12712
- Baldrian, P., Zrůstová, P., Tláškal, V., Davidová, A., Merhautová, V., and Vrška, T. (2016). Fungi associated with decomposing deadwood in a natural beech-dominated forest. *Fungal Ecol.* 23, 109–122. doi: 10.1016/j.funeco.2016.07.001
- Bankevich, A., Nurk, S., Antipov, D., Gurevich, A. A., Dvorkin, M., Alexander S. Kulikov A. S., et al. (2012). SPAdes: a new genome assembly algorithm and its applications to single-cell sequencing. *J. Comput. Biol.* 19, 455–477. doi: 10.1089/cmb.2012.0021
- Berlemont, R., and Martiny, A. C. (2013). Phylogenetic distribution of potential cellulases in bacteria. *Appl. Environ. Microbiol.* 79, 1545–1554. doi: 10.1128/AEM.03305-12
- Berlemont, R., and Martiny, A. C. (2015). Genomic potential for polysaccharide deconstruction in Bacteria. *Appl. Environ. Microbiol.* 81, 1513–1519. doi: 10.1128/AEM.03718-14
- Bowers, R. M., Kyrpides, N. C., Stepanauskas, R., Harmon-Smith, M., Doud, D., Reddy, T. B. K., et al. (2017). Minimum information about a single amplified genome (MISAG) and a metagenome-assembled genome (MIMAG) of bacteria and archaea. *Nat. Biotechnol.* 35, 725–731. doi: 10.1038/nbt.3893

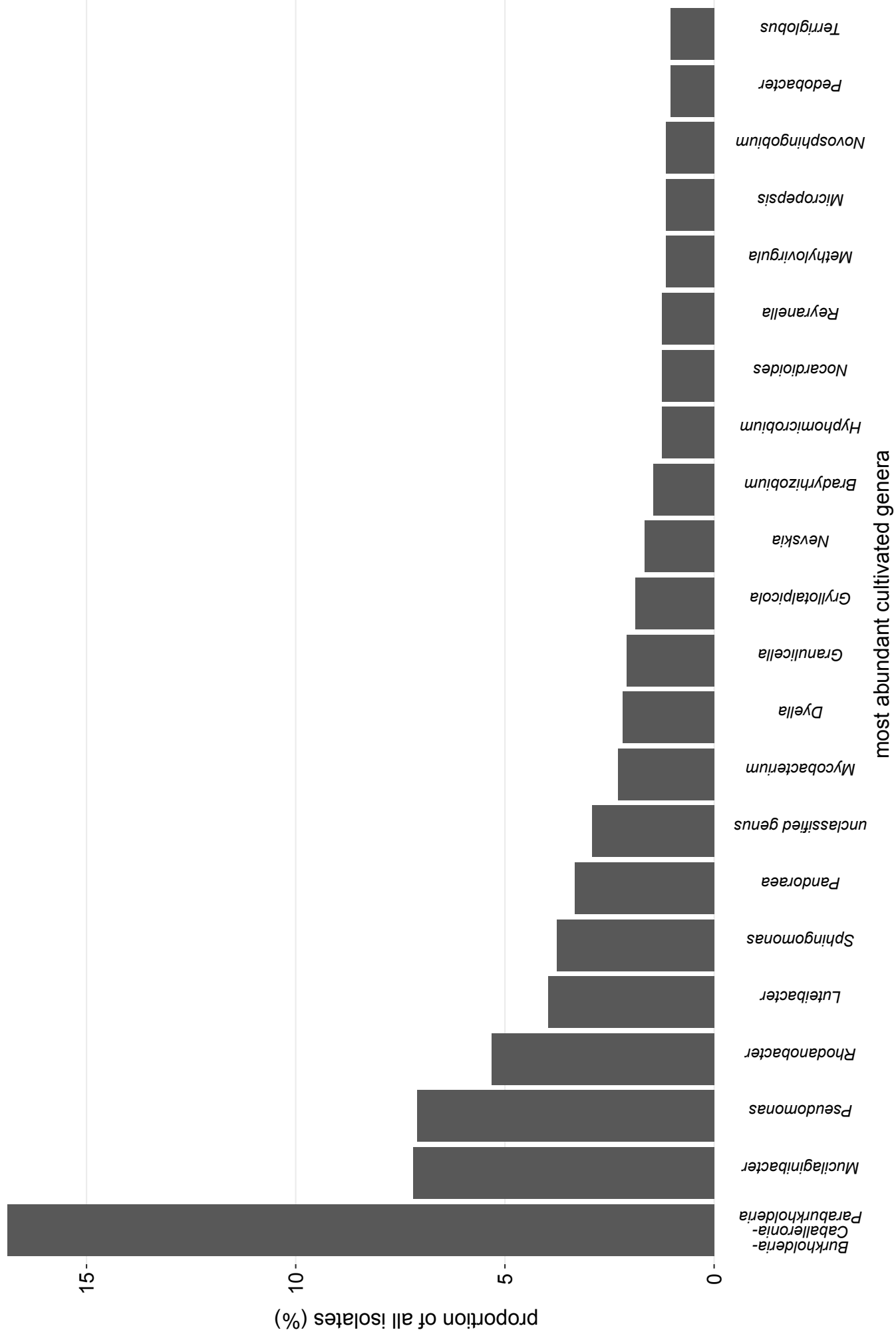
- Brabcová, V., Nováková, M., Davidová, A., and Baldrian, P. (2016). Dead fungal mycelium in forest soil represents a decomposition hotspot and a habitat for a specific microbial community. *New Phytol.* 210, 1369–1381. doi: 10.1111/nph.13849
- Brabcová, V., Štursová, M., and Baldrian, P. (2018). Nutrient content affects the turnover of fungal biomass in forest topsoil and the composition of associated microbial communities. *Soil Biol. Biochem.* 118, 187–198. doi: 10.1016/j.soilbio.2017.12.012
- Brunner, A., and Kimmins, J. P. (2003). Nitrogen fixation in coarse woody debris of *Thuja plicata* and *Tsuga heterophylla* forests on northern Vancouver Island. *Can. J. For. Res.* 33, 1670–1682. doi: 10.1139/x03-085
- Capella-Gutiérrez, S., Silla-Martínez, J. M., and Gabaldón, T. (2009). trimAl: a tool for automated alignment trimming in large-scale phylogenetic analyses. *Bioinformatics* 25, 1972–1973. doi: 10.1093/bioinformatics/btp348
- Christofides, S. R., Hiscox, J., Savoury, M., Boddy, L., and Weightman, A. J. (2019). Fungal control of early-stage bacterial community development in decomposing wood. *Fungal Ecol.* 42:100868. doi: 10.1016/j.funeco.2019.100868
- de Mendiburu, F. (2017). *Agricolae: Statistical Procedures for Agricultural Research. R package version 1.2–4.*
- Eddy, S. R. (2011). Accelerated profile HMM searches. *PLoS Comput. Biol.* 7:e1002195. doi: 10.1371/journal.pcbi.1002195
- Edgar, R. C. (2004). MUSCLE: multiple sequence alignment with high accuracy and high throughput. *Nucleic Acids Res.* 32, 1792–1797. doi: 10.1093/nar/gkh340
- Filley, T. R., Cody, G. D., Goodell, B., Jellison, J., Noser, C., and Ostrofsky, A. (2002). Lignin demethylation and polysaccharide decomposition in spruce sapwood degraded by brown rot fungi. *Org. Geochem.* 33, 111–124. doi: 10.1016/S0146-6380(01)00144-9
- Folman, L. B., Gunnewiek, P. J. A. K., Boddy, L., and de Boer, W. (2008). Impact of white-rot fungi on numbers and community composition of bacteria colonizing beech wood from forest soil. *FEMS Microbiol. Ecol.* 63, 181–191. doi: 10.1111/j.1574-6941.2007.00425.x
- Gallardo, C. A., Baldrian, P., and López-mondéjar, R. (2021). Litter-inhabiting fungi show high level of specialization towards biopolymers composing plant and fungal biomass. *Biol. Fertil. Soils* 57, 77–88. doi: 10.1007/s00374-020-01507-3
- Hervé, V., Ketter, E., Pierrat, J.-C., Gelhaye, E., and Frey-Klett, P. (2016). Impact of *Phanerochaete chrysosporium* on the functional diversity of bacterial communities associated with decaying wood. *PLoS ONE* 11:e0147100. doi: 10.1371/journal.pone.0147100
- Hervé, V., Le Roux, X., Uroz, S., Gelhaye, E., and Frey-Klett, P. (2013). Diversity and structure of bacterial communities associated with *Phanerochaete chrysosporium* during wood decay. *Environ. Microbiol.* 16, 2238–2252. doi: 10.1111/1462-2920.12347
- Hoppe, B., Krüger, D., Kahl, T., Arnstadt, T., Buscot, F., Bauhus, J., et al. (2015). A pyrosequencing insight into sprawling bacterial diversity and community dynamics in decaying deadwood logs of *Fagus sylvatica* and *Picea abies*. *Sci. Rep.* 5:9456. doi: 10.1038/srep09456
- Hyatt, D., Chen, G. L., LoCascio, P. F., Land, M. L., Larimer, F. W., and Hauser, L. J. (2010). Prodigal: prokaryotic gene recognition and translation initiation site identification. *BMC Bioinformatics* 11:119. doi: 10.1186/1471-2105-11-119
- Johnston, S. R., Boddy, L., and Weightman, A. J. (2016). Bacteria in decomposing wood and their interactions with wood-decay fungi. *FEMS Microbiol. Ecol.* 92:fiw179. doi: 10.1093/femsec/fiw179
- Johnston, S. R., Hiscox, J., Savoury, M., Boddy, L., and Weightman, A. J. (2019). Highly competitive fungi manipulate bacterial communities in decomposing beech wood (*Fagus sylvatica*). *FEMS Microbiol. Ecol.* 95:fiy225. doi: 10.1093/femsec/fiy225
- Katoh, K., Rozewicki, J., and Yamada, K. D. (2018). MAFFT online service: multiple sequence alignment, interactive sequence choice, and visualization. *Brief. Bioinform.* 20, 1160–1166. doi: 10.1093/bib/bbx108
- Král, K., Janík, D., Vrška, T., Adam, D., Hort, L., Unar, P., et al. (2010). Local variability of stand structural features in beech dominated natural forests of Central Europe: Implications for sampling. *For. Ecol. Manage.* 260, 2196–2203. doi: 10.1016/j.foreco.2010.09.020
- Lagesen, K., Hallin, P., Rødland, E. A., Sterfeldt, H. H., Rognes, T., and Ussery, D. W. (2007). RNAmmer: consistent and rapid annotation of ribosomal RNA genes. *Nucleic Acids Res.* 35, 3100–3108. doi: 10.1093/nar/gkm160
- Lane, D. J. (1991). “16S/23S rRNA sequencing,” in *Nucleic Acid Techniques in Bacterial Systematics*, eds E. Stackebrandt and M. Goodfellow (New York, NY: Wiley), 115–175.
- Langmead, B., and Salzberg, S. L. (2013). Fast gapped-read alignment with Bowtie 2. *Nat. Methods* 9, 357–359. doi: 10.1038/nmeth.1923
- Langmead, B., Trapnell, C., Pop, M., and Salzberg, S. L. (2009). Ultrafast and memory-efficient alignment of short DNA sequences to the human genome. *Genome Biol.* 10:R25. doi: 10.1186/gb-2009-10-3-r25
- Lasa, A. V., Mašínová, T., Baldrian, P., and Fernández-López, M. (2019). Bacteria from the endosphere and rhizosphere of *Quercus* spp. use mainly cell wall-associated enzymes to decompose organic matter. *PLoS ONE* 14:e0214422. doi: 10.1371/journal.pone.0214422
- Leahy, J. G., Batchelor, P. J., and Morcomb, S. M. (2003). Evolution of the soluble diiron monooxygenases. *FEMS Microbiol. Rev.* 27, 449–479. doi: 10.1016/S0168-6445(03)00023-8
- Lee, M. D. (2019). GToTree: a user-friendly workflow for phylogenomics. *Bioinformatics* 35, 4162–4164. doi: 10.1093/bioinformatics/btz188
- Lenhart, K., Bunge, M., Ratering, S., Neu, T. R., Schüttmann, I., Greule, M., et al. (2012). Evidence for methane production by saprotrophic fungi. *Nat. Commun.* 3:1046. doi: 10.1038/ncomms2049
- Li, H., Handsaker, B., Wysoker, A., Fennell, T., Ruan, J., Homer, N., et al. (2009). The sequence alignment/map format and SAMtools. *Bioinformatics* 25, 2078–2079. doi: 10.1093/bioinformatics/btp352
- Lladó, S. F., Větrovský, T., and Baldrian, P. (2019). Tracking of the activity of individual bacteria in temperate forest soils shows guild-specific responses to seasonality. *Soil Biol. Biochem.* 135, 275–282. doi: 10.1016/j.soilbio.2019.05.010
- Lladó, S. F., Žifčáková, L., Větrovský, T., Eichlerová, I., and Baldrian, P. (2016). Functional screening of abundant bacteria from acidic forest soil indicates the metabolic potential of Acidobacteria subdivision 1 for polysaccharide decomposition. *Biol. Fertil. Soils* 52, 251–260. doi: 10.1007/s00374-015-1072-6
- Lombard, V., Golaconda Ramulu, H., Drula, E., Coutinho, P. M., and Henrissat, B. (2014). The carbohydrate-active enzymes database (CAZy) in 2013. *Nucleic Acids Res.* 42, D490–D495. doi: 10.1093/nar/gkt1178
- López-Mondéjar, R., Algorta, C., and Baldrian, P. (2019). Lignocellulolytic systems of soil bacteria: a vast and diverse toolbox for biotechnological conversion processes. *Biotechnol. Adv.* 37, 399–404. doi: 10.1016/j.biotechadv.2019.03.013
- López-Mondéjar, R., Brabcová, V., Štursová, M., Davidová, A., and Jansa, J., Cajthaml, T., et al. (2018). Decomposer food web in a deciduous forest shows high share of generalist microorganisms and importance of microbial biomass recycling. *ISME J.* 12, 1768–1778. doi: 10.1038/s41396-018-0084-2
- López-Mondéjar, R., Zühlke, D., Becher, D., Riedel, K., and Baldrian, P. (2016). Cellulose and hemicellulose decomposition by forest soil bacteria proceeds by the action of structurally variable enzymatic systems. *Sci. Rep.* 6:25279. doi: 10.1038/srep25279
- Madin, J. S., Nielsen, D. A., Brbic, M., Corkrey, R., Danko, D., Edwards, K., et al. (2020). A synthesis of bacterial and archaeal phenotypic trait data. *Sci. Data* 7:170. doi: 10.1038/s41597-020-0497-4
- Martin, A. R., Domke, G. M., Doraisami, M., and Thomas, S. C. (2021). Carbon fractions in the world's dead wood. *Nat. Commun.* 12:889. doi: 10.1038/s41467-021-21149-9
- Mieszkin, S., Richet, P., Bach, C., Lambrot, C., Augusto, L., Buée, M., et al. (2021). Oak decaying wood harbors taxonomically and functionally different bacterial communities in sapwood and heartwood. *Soil Biol. Biochem.* 155:108160. doi: 10.1016/j.soilbio.2021.108160
- Moll, J., Kellner, H., Leonhardt, S., Stengel, E., Dahl, A., Buscot, F., et al. (2018). Bacteria inhabiting deadwood of 13 tree species reveal great heterogeneous distribution between sapwood and heartwood. *Environ. Microbiol.* 20, 3744–3756. doi: 10.1111/1462-2920.14376
- Nayfach, S., Roux, S., Seshadri, R., Udvarny, D., Varghese, N., Schulz, F., et al. (2020). A genomic catalog of Earth's microbiomes. *Nat. Biotechnol.* 39:520. doi: 10.1038/s41587-020-00769-4
- Nelson, M. B., Martiny, A. C., and Martiny, J. B. H. (2016). Global biogeography of microbial nitrogen-cycling traits in soil. *Proc. Natl. Acad. Sci. U.S.A.* 113, 8033–8040. doi: 10.1073/pnas.1601070113
- Odriozola, I., Abrego, N., Tláškal, V., Zrůstová, P., Morais, D., Větrovský, T., et al. (2021). Fungal communities are important determinants of bacterial community composition in deadwood. *mSystems* 6, e01017–e01020. doi: 10.1128/mSystems.01017-20

- Pan, Y., Birdsey, R. A., Fang, J., Houghton, R., Kauppi, P. E., Kurz, W. A., et al. (2011). A large and persistent carbon sink in the world's forests. *Science* 333, 988–993. doi: 10.1126/science.1201609
- Philpott, T. J., Prescott, C. E., Chapman, W. K., and Grayston, S. J. (2014). Nitrogen translocation and accumulation by a cord-forming fungus (*Hypholoma fasciculare*) into simulated woody debris. *For. Ecol. Manage.* 315, 121–128. doi: 10.1016/j.foreco.2013.12.034
- Prestat, E., David, M. M., Hultman, J., Taş, N., Lamendella, R., Dvornik, J., et al. (2014). FOAM (Functional Ontology Assignments for Metagenomes): a Hidden Markov Model (HMM) database with environmental focus. *Nucleic Acids Res.* 42:e145. doi: 10.1093/nar/gku702
- Price, M. N., Dehal, P. S., and Arkin, A. P. (2010). FastTree 2—approximately maximum-likelihood trees for large alignments. *PLoS ONE* 5:e9490. doi: 10.1371/journal.pone.0009490
- Quast, C., Pruesse, E., Yilmaz, P., Gerken, J., Schweer, T., Yarza, P., et al. (2013). The SILVA ribosomal RNA gene database project: improved data processing and web-based tools. *Nucleic Acids Res.* 41, D590–D596. doi: 10.1093/nar/gks1219
- R Core Team (2020). *R: A Language and Environment for Statistical Computing*. Available online at: <http://www.r-project.org/> (accessed June 22, 2020).
- Rayner, A. D., and Boddy, L. (1988). *Fungal Decomposition of Wood. Its Biology and Ecology*. Hoboken, NJ: John Wiley and Sons Ltd.
- Rinne, K. T., Rajala, T., Peltoniemi, K., Chen, J., Smolander, A., and Mäkipää, R. (2016). Accumulation rates and sources of external nitrogen in decaying wood in a Norway spruce dominated forest. *Funct. Ecol.* 31, 530–541. doi: 10.1111/1365-2435.12734
- Rinta-Kanto, J. M., Sinkko, H., Rajala, T., Al-Soud, W. A., Sørensen, S. J., Tamminen, M. V., et al. (2016). Natural decay process affects the abundance and community structure of Bacteria and Archaea in *Picea abies* logs. *FEMS Microbiol. Ecol.* 92:fiw087. doi: 10.1093/femsec/fiw087
- Rognes, T., Flouri, T., Nichols, B., Quince, C., and Mahé, F. (2016). VSEARCH: a versatile open source tool for metagenomics. *PeerJ*. 4:e2584. doi: 10.7717/peerj.2584
- Sait, M., Hugenholtz, P., and Janssen, P. H. (2002). Cultivation of globally distributed soil bacteria from phylogenetic lineages previously only detected in cultivation-independent surveys. *Environ. Microbiol.* 4, 654–666. doi: 10.1046/j.1462-2920.2002.00352.x
- Šamonil, P., Schaezel, R. J., Valtera, M., Goliáš, V., Baldrian, P., Vašíčková, I., et al. (2013). Crossdating of disturbances by tree uprooting: can treethrow microtopography persist for 6000 years? *For. Ecol. Manage.* 307, 123–135. doi: 10.1016/j.foreco.2013.06.045
- Seemann, T. (2014). Prokka: rapid prokaryotic genome annotation. *Bioinformatics* 30, 2068–2069. doi: 10.1093/bioinformatics/btu153
- Seidler, R. J., Aho, P. E., Raju, P. N., and Evans, H. J. (1972). Nitrogen fixation by bacterial isolates from decay in living white fir trees [*Abies concolor* (Gord. and Glend.) Lindl.]. *J. Gen. Microbiol.* 73, 413–416. doi: 10.1099/00221287-73-2-413
- Shaiber, A., and Eren, A. M. (2019). Composite metagenome-assembled genomes reduce the quality of public genome repositories. *mBio* 10, e00725–e00719. doi: 10.1128/mBio.00725-19
- Spano, S. D., Jurgensen, M. F., Larsen, M. J., and Harvey, A. E. (1982). Nitrogen-fixing bacteria in Douglas-fir residue decayed by *Fomitopsis pinicola*. *Plant Soil* 68, 117–123. doi: 10.1007/BF02374731
- Starke, R., Morais, D., Větrovský, T., Mondéjar, R. L., Baldrian, P., and Brabcová, V. (2020). Feeding on fungi: genomic and proteomic analysis of the enzymatic machinery of bacteria decomposing fungal biomass. *Environ. Microbiol.* 22, 4604–4619. doi: 10.1111/1462-2920.15183
- Tange, O. (2018). *GNU Parallel*. Frederiksberg: The USENIX Magazine.
- Tláškal, V., Brabcová, V., Větrovský, T., Jomura, M., López-Mondéjar, R., Monteiro, M. O. L., et al. (2021a). Complementary roles of wood-inhabiting fungi and bacteria facilitate deadwood decomposition. *mSystems* 6, e01078–e01020. doi: 10.1128/mSystems.01078-20
- Tláškal, V., Žižňáková, L., Pylro, V. S., and Baldrian, P. (2021b). Ecological divergence within the enterobacterial genus *Sodalis*: from insect symbionts to inhabitants of decomposing deadwood. *Front. Microbiol.* 12:668644. doi: 10.3389/fmicb.2021.668644
- Tláškal, V., Zrůstová, P., Vrška, T., and Baldrian, P. (2017). Bacteria associated with decomposing dead wood in a natural temperate forest. *FEMS Microbiol. Ecol.* 93:fix157. doi: 10.1093/femsec/fix157
- Uroz, S., Courty, P. E., Pierrat, J. C., Peter, M., Buée, M., Turpault, M. P., et al. (2013). Functional profiling and distribution of the forest soil bacterial communities along the soil mycorrhizosphere continuum. *Microb. Ecol.* 66, 404–415. doi: 10.1007/s00248-013-0199-y
- Valášková, V., de Boer, W., Gunnewiek, P. J. A. K., Pospíšek, M., and Baldrian, P. (2009). Phylogenetic composition and properties of bacteria coexisting with the fungus *Hypholoma fasciculare* in decaying wood. *ISME J.* 3, 1218–1221. doi: 10.1038/ismej.2009.64
- Větrovský, T., Steffen, K. T., and Baldrian, P. (2014). Potential of cometabolic transformation of polysaccharides and lignin in lignocellulose by soil *Actinobacteria*. *PLoS ONE* 9:e89108. doi: 10.1371/journal.pone.0089108
- Vorob'ev, A. V., de Boer, W., Folman, L. B., Bodelier, P. L. E., Doronina, N. V., Suzina, N. E., et al. (2009). *Methylovirgula ligni* gen. nov., sp. nov., an obligately acidophilic, facultatively methylotrophic bacterium with a highly divergent *mxoF* gene. *Int. J. Syst. Evol. Microbiol.* 59, 2538–2545. doi: 10.1099/ijs.0.010074-0
- Walker, B. J., Abeel, T., Shea, T., Priest, M., Boueilliel, A., Sakthikumar, S., et al. (2014). Pilon: an integrated tool for comprehensive microbial variant detection and genome assembly improvement. *PLoS ONE* 9:e112963. doi: 10.1371/journal.pone.0112963
- Weedon, J. T., Cornwell, W. K., Cornelissen, J. H. C., Zanne, A. E., Wirth, C., and Coomes, D. A. (2009). Global meta-analysis of wood decomposition rates: a role for trait variation among tree species? *Ecol. Lett.* 12, 45–56. doi: 10.1111/j.1461-0248.2008.01259.x
- Wick, R. R., Judd, L. M., Gorrie, C. L., and Holt, K. E. (2017). Unicycler: resolving bacterial genome assemblies from short and long sequencing reads. *PLoS Comput. Biol.* 13:e1005595. doi: 10.1371/journal.pcbi.1005595
- Wickham, H., Averick, M., Bryan, J., Chang, W., McGowan, L. D. A., François, R., et al. (2019). Welcome to the Tidyverse. *J. Open Source Softw.* 4:1686. doi: 10.21105/joss.01686
- Wright, E. S. (2016). Using DECIPHER v2.0 to analyze big biological sequence data in R. *R J.* 8, 352–359. doi: 10.32614/RJ-2016-025
- Zhang, H., Yohe, T., Huang, L., Entwistle, S., Wu, P., Yang, Z., et al. (2018). dbCAN2: a meta server for automated carbohydrate-active enzyme annotation. *Nucleic Acids Res.* 46, W95–W101. doi: 10.1093/nar/gky418

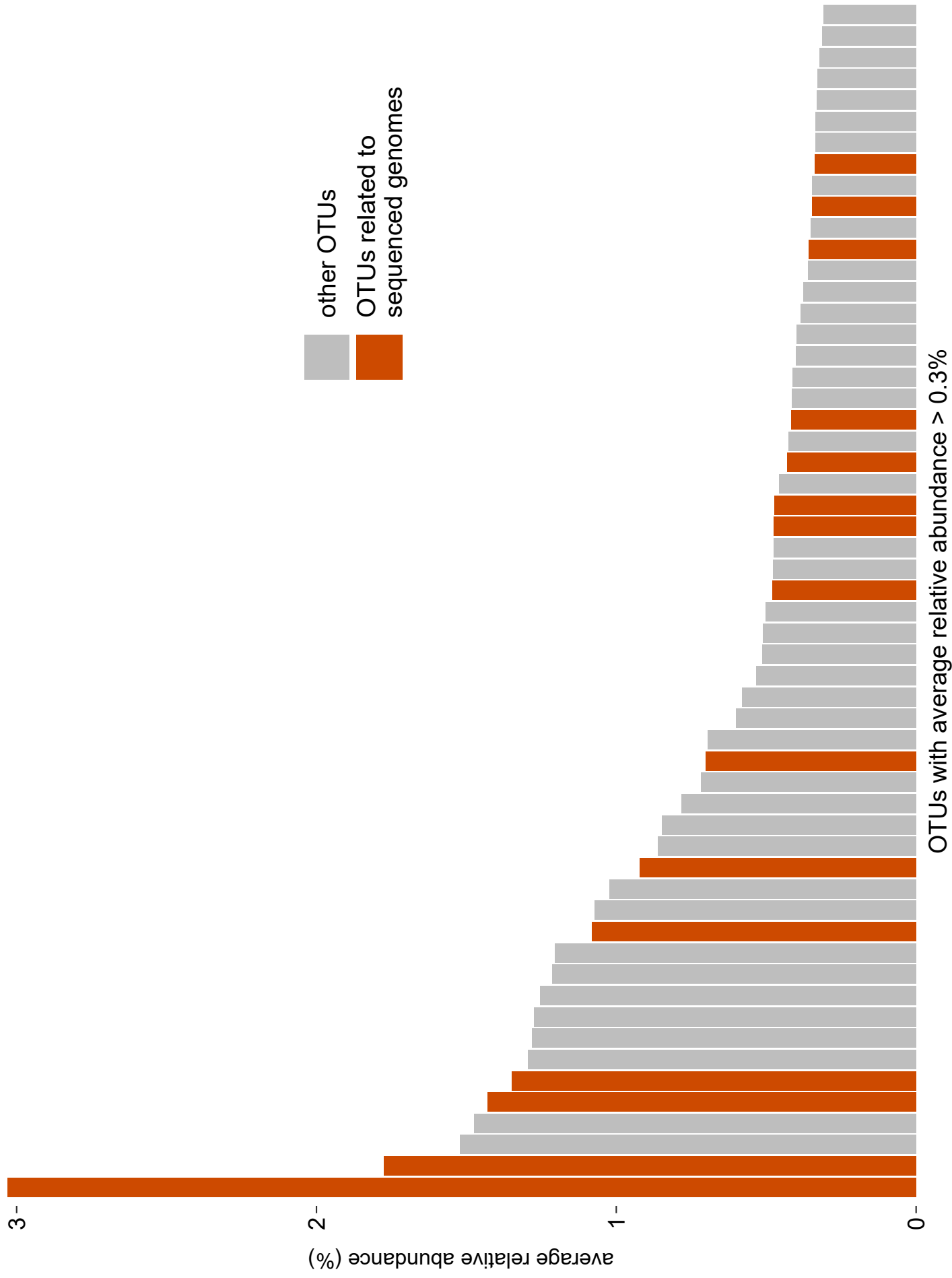
Conflict of Interest: The authors declare that the research was conducted in the absence of any commercial or financial relationships that could be construed as a potential conflict of interest.

Copyright © 2021 Tláškal and Baldrian. This is an open-access article distributed under the terms of the Creative Commons Attribution License (CC BY). The use, distribution or reproduction in other forums is permitted, provided the original author(s) and the copyright owner(s) are credited and that the original publication in this journal is cited, in accordance with accepted academic practice. No use, distribution or reproduction is permitted which does not comply with these terms.

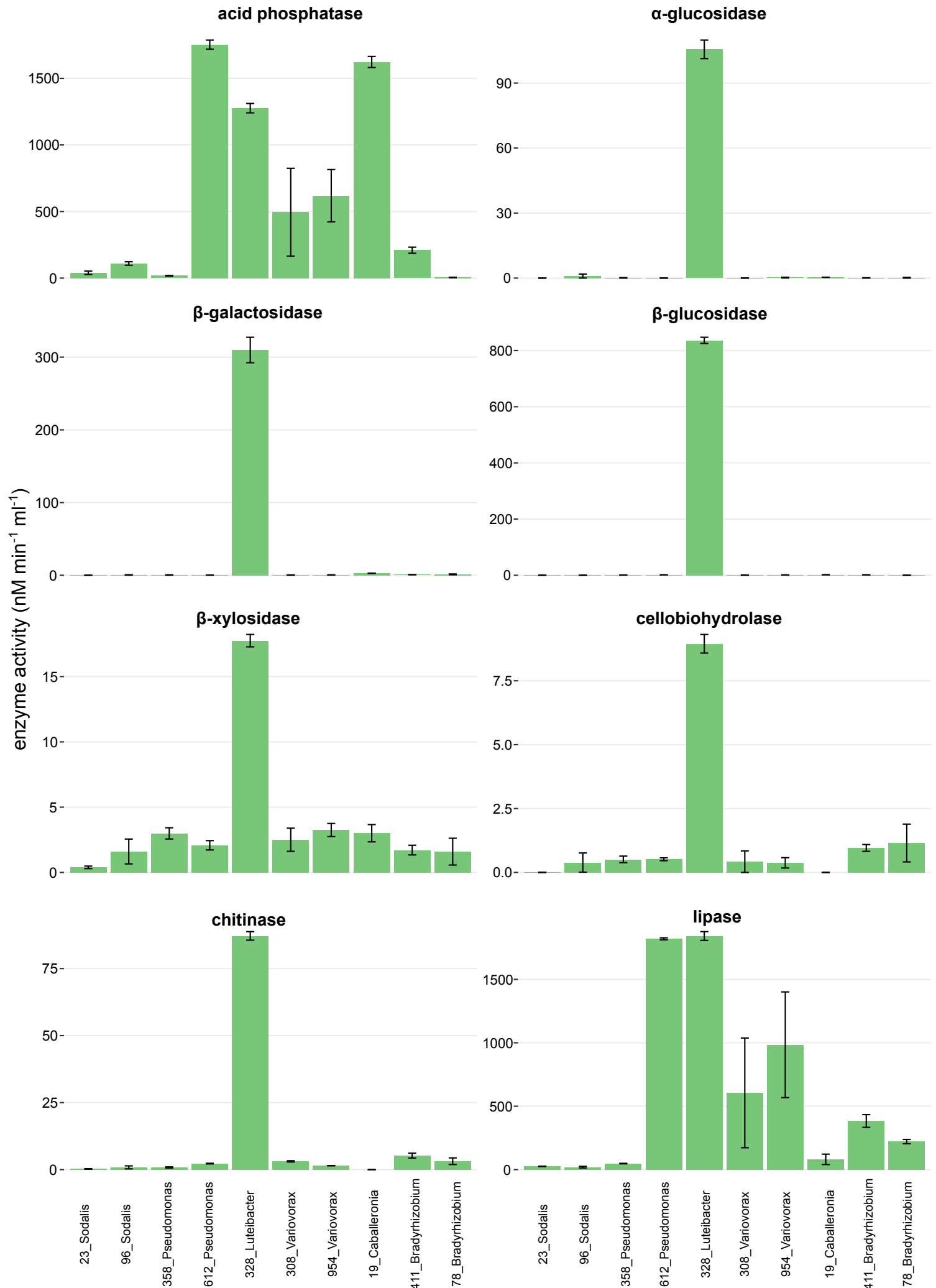
Supplementary Figure 1: Relative abundance of genera among the 959 bacterial isolates from decomposing deadwood. Genera with > 1% occurrence are displayed. Taxonomy follows the SILVA 138 database.



Supplementary Figure 2: Relative share of the most abundant OTUs from the study of Tláskal et al. (2017) with those matching to sequenced genomes in orange. OTUs with average relative abundance > 0.3% are displayed.



Supplementary Figure 3: Activity of cell-wall associated fraction of selected extracellular enzymes analyzed in bacterial isolates from decomposing deadwood.





Ecological Divergence Within the Enterobacterial Genus *Sodalis*: From Insect Symbionts to Inhabitants of Decomposing Deadwood

Vojtěch Tláškal^{1*}, Victor Satler Pylro^{1,2}, Lucia Žifčáková¹ and Petr Baldrian¹

¹ Laboratory of Environmental Microbiology, Institute of Microbiology of the Czech Academy of Sciences, Praha, Czechia,

² Microbial Ecology and Bioinformatics Laboratory, Department of Biology, Federal University of Lavras (UFLA), Lavras, Brazil

OPEN ACCESS

Edited by:

Paolina Garbeva,
Netherlands Institute of Ecology
(NIOO-KNAW), Netherlands

Reviewed by:

Eva Novakova,
University of South Bohemia in České
Budějovice, Czechia
Rosario Gil,
University of Valencia, Spain

*Correspondence:

Vojtěch Tláškal
tlaskal@biomed.cas.cz

Specialty section:

This article was submitted to
Terrestrial Microbiology,
a section of the journal
Frontiers in Microbiology

Received: 16 February 2021

Accepted: 17 May 2021

Published: 11 June 2021

Citation:

Tláškal V, Pylro VS, Žifčáková L
and Baldrian P (2021) Ecological
Divergence Within the Enterobacterial
Genus *Sodalis*: From Insect
Symbionts to Inhabitants
of Decomposing Deadwood.
Front. Microbiol. 12:668644.
doi: 10.3389/fmicb.2021.668644

The bacterial genus *Sodalis* is represented by insect endosymbionts as well as free-living species. While the former have been studied frequently, the distribution of the latter is not yet clear. Here, we present a description of a free-living strain, *Sodalis ligni* sp. nov., originating from decomposing deadwood. The favored occurrence of *S. ligni* in deadwood is confirmed by both 16S rRNA gene distribution and metagenome data. Pangenome analysis of available *Sodalis* genomes shows at least three groups within the *Sodalis* genus: deadwood-associated strains, tsetse fly endosymbionts and endosymbionts of other insects. This differentiation is consistent in terms of the gene frequency level, genome similarity and carbohydrate-active enzyme composition of the genomes. Deadwood-associated strains contain genes for active decomposition of biopolymers of plant and fungal origin and can utilize more diverse carbon sources than their symbiotic relatives. Deadwood-associated strains, but not other *Sodalis* strains, have the genetic potential to fix N₂, and the corresponding genes are expressed in deadwood. Nitrogenase genes are located within the genomes of *Sodalis*, including *S. ligni*, at multiple loci represented by more gene variants. We show decomposing wood to be a previously undescribed habitat of the genus *Sodalis* that appears to show striking ecological divergence.

Keywords: insect symbionts, *Sodalis*, deadwood, nitrogen fixation, free-living, non-symbiotic

INTRODUCTION

Bacterial insect endosymbionts that occupy tissues of their hosts are widespread in multiple insect taxa (reviewed in Perlmutter and Bordenstein, 2020). The nature of such symbiosis may take the form of parasitism, mutualism or commensalism depending on the ecology of the bacterial symbiont. Parasitic bacteria may manipulate reproduction of their hosts, while mutualistic bacteria may provide essential vitamins or participate in nitrogen (N) cycling (Akman et al., 2002; Behar et al., 2005; Sabree et al., 2009). Commensal bacteria can use insects at some part of their life cycle as vectors for transmission to their target host organism, e.g., plants for which they are parasitic (Nadarasah and Stavrinides, 2011). The life strategy of the symbiont depends on the evolutionary

history with the host and is driven by the length of its coexistence with the host (Toh et al., 2006). Different bacterial symbionts with distinct evolutionary histories have been described, e.g., in tsetse flies (*Glossina* sp.). *Wigglesworthia glossinidia* (*Enterobacteriales*) provides vitamins to the tsetse fly and to other symbionts (Hall et al., 2019) and represents an obligate mutualist with a long coevolutionary history (Chen et al., 1999). Another tsetse fly enterobacterium, *Sodalis glossinidius*, shows a more recent association with its host as suggested by its relatively large genome that contains a high number of pseudogenes, which remain actively transcribed in a cell-free culture (Toh et al., 2006; Goodhead et al., 2020; Hall et al., 2020). Further hinting at the recent establishment of the *Sodalis*-tsetse symbiosis was the successful establishment and vertical transmission of the non-native *Sodalis* population in tsetse flies cleared from their native symbionts. It indicates lack of host-symbiont extensive coevolution (Weiss et al., 2006).

Sodalis endosymbionts are present in other insects with nutritionally restricted diets, such as bloodsucking Diptera (Nováková and Hypša, 2007; Chrudimský et al., 2012), Phthiraptera (Fukatsu et al., 2007; Boyd et al., 2016), sapsucking Hemiptera (Kaiwa et al., 2010) and Coleoptera (Heddi et al., 1999). Multiple *Sodalis* species have thus been identified within their hosts and shown to supply essential vitamins to the host (Heddi et al., 1999; Boyd et al., 2016). In contrast, only one free-living member of this genus has been described despite the apparent recent establishment of the host-dependent life strategy of the endosymbionts. *Sodalis* sp. strain HS, later described as *S. praecaptivus* was isolated from a hand wound of a human impaled with a tree branch (Clayton et al., 2012; Chari et al., 2015). Incidental isolation of *Sodalis*-related strain from such source was unexpected and as a consequence *Sodalis* became a textbook example of microbial specialization processes (Yong, 2016).

The genome-wide sequence comparison of *Sodalis* species shows *S. glossinidius* and the cereal weevil symbiont *S. pierantonius* strain SOPE to be closely related to *S. praecaptivus*. In particular, the *S. pierantonius* strain SOPE shares high genome similarity with free-living *S. praecaptivus*, and its symbiosis with the weevil shows evidence of recent origin (Clayton et al., 2012). Despite the presence of numerous pseudogenes, genes of both symbionts represent a subset of the genes in the *S. praecaptivus* genome, showing that the *S. praecaptivus*-like ancestor might be the ancestor for symbionts as well (Clayton et al., 2012). The genome characteristics of *S. praecaptivus* correspond to host-independent life and stabilizing gene selection pressure; in comparison with symbiotic relatives, it has a larger genome, fewer pseudogenes and fewer IS elements (Oakeson et al., 2014). Consequently, due to its wide spectrum of genes and high coding density, *S. praecaptivus* is able to utilize several carbon (C) sources, including chitin and plant sugars (cellobiose, xylose, rhamnose) and N sources, such as ammonia and nitrate (Chari et al., 2015). While *S. praecaptivus* is host-independent, it is able to colonize weevils and tsetse flies through quorum sensing suppression of its virulence, which suggests a mechanism of insect symbiosis development in the *Sodalis* group (Enomoto et al., 2017; Munoz et al., 2020). Despite

the well-characterized phylogeny and genome properties of the *Sodalis* group, a systematic approach to assess the environmental distribution of free-living *Sodalis* strains has not been performed. It remains to be determined whether there are different levels of relatedness of non-symbiotic strains with symbionts in distinct insect taxa hosts.

Here, we present a *Sodalis* pangenome analysis that allowed us to characterize different guilds within this genus. Guilds differ in their gene composition as well as in their life strategy. Our results show that the *Sodalis* genus is functionally versatile with multiple ecological roles. We report novel free-living *Sodalis* species-level taxon associated in high abundances with decomposing wood, for which we propose the name *Sodalis ligni* sp. nov. This taxon is represented by the strain dw23^T and can utilize C-rich labile wood-derived compounds and fix atmospheric nitrogen. *Sodalis ligni* is a globally distributed species that is directly related to symbiotic *Sodalis* members with characterized genomes while maintaining a non-symbiotic lifestyle and preferring deadwood habitats.

MATERIALS AND METHODS

Sodalis Isolation

Wood samples for bacterial isolation were obtained in the Žofínský Prales National Nature Reserve, an unmanaged forest in the south of the Czech Republic (48°39'57''N, 14°42'24''E). The core zone of the forest reserve (42 ha) has never been managed, and human intervention stopped in 1838, when it was declared a reserve. This reserve thus represents a rare fragment of European temperate virgin forest with deadwood left to spontaneous decomposition. The reserve is situated at 730–830 m a.s.l., the bedrock is almost homogeneous and consists of fine to medium-grained porphyritic and biotite granite. The annual average rainfall is 866 mm, and the annual average temperature is 6.2°C (Anderson-Teixeira et al., 2015). At present, the reserve is covered by a mixed forest in which *Fagus sylvatica* predominates, followed by *Picea abies* and *Abies alba*. The mean living tree volume is 690 m³ h⁻¹, and the mean volume of coarse woody debris (logs, represented by tree trunks and their fragments) is 208 m³ h⁻¹ (Král et al., 2010; Šamonil et al., 2013). Logs are repeatedly surveyed, and the approximate age of each log, the cause of death (e.g., stem breakage, windthrow, etc.) and the status before downing (fresh, decomposed) is known. The area has been subjected to the characterization of bacterial and fungal succession on deadwood (Baldrian et al., 2016; Tláškal et al., 2017; Odriozola et al., 2021), and the functional roles of the members of the deadwood microbiome were determined (Tláškal et al., 2021).

Wood samples were obtained as described previously in Tláškal et al. (2017). Briefly, in October 2013, four samples from selected logs were obtained by drilling with an electrical drill vertically along the whole decomposing stem. Part of the material was used for bacterial community characterization (Tláškal et al., 2017) and part was treated as follows: wood chips from each stem were pooled together and transported to the laboratory, where they were kept at 4°C until the next day. Wood material

was shaken with 15 mL of Ringer solution for 2 h and diluted $10^4 \times$ to $10^6 \times$. Dilutions were plated on nutrient-limited NB medium (0.26 g L^{-1} Nutrient Broth, 15 g L^{-1} agar, pH 5). The growth of bacterial colonies was recorded on Petri dishes using a marker for 8 weeks. Colony PCR was used to infer the taxonomy of the slow-growing strains that appeared in the later phase of cultivation. The PCR premix and cycling conditions were as follows: $2.5 \mu\text{L}$ $10 \times$ buffer for DyNAzyme DNA Polymerase; $0.75 \mu\text{L}$ DyNAzyme II DNA polymerase ($2 \mu\text{L}^{-1}$); $0.75 \mu\text{L}$ of BSA (20 mg mL^{-1}); $0.5 \mu\text{L}$ of PCR Nucleotide Mix (10 mM); $1 \mu\text{L}$ of each primer eub530f ($10 \mu\text{M}$) and eub1100br ($10 \mu\text{M}$) (Lane, 1991) and sterile ddH_2O up to $25 \mu\text{L}$; amplification started at 94°C for 5 min, followed by 35 cycles of 94°C for 1 min, 62°C for 1 min, 72°C for 1 min and finished with a final setting of 72°C for 10 min. Sanger sequencing was performed using the reverse primer. The obtained sequences were compared by BLASTn with bacterial 16S rRNA gene-based community data from the same habitat (Tláškal et al., 2017). Bacterial strains with high similarity and coverage to the most abundant bacteria recovered by environmental DNA sequencing were selected for further cultivation and genome sequencing (Tláškal and Baldrian, 2021).

By this approach, we were able to select two bacterial strains (labeled *Sodalis* sp. strain dw23^T and strain dw96) with high similarity to the abundant cluster CL27 in community data (Tláškal et al., 2017), which is 100% similar to the 16S rRNA gene sequence with NCBI accession AJ011333.1, which is mislabeled as *Yersinia* sp. (Elo et al., 2000). The nearest relative with a complete genome sequence available was the *Sodalis praecaptivus* strain HS (CP006569.1, similarity 97.2%, Chari et al., 2015). Strains dw23^T and dw96 originated from two distinct *Fagus sylvatica* stems 9 m and 12 m long, respectively, that had been decomposing for less than 5 years.

DNA Extraction, Sequencing, and Genome Assembly

The two *Sodalis* strains were cultivated in 50 mL of GY-VL55 liquid medium (Lladó et al., 2019) with shaking for 2 weeks at 23°C . After cultivation, the cells were pelleted and DNA was extracted using the ArchivePure DNA Yeast + Gram- + Kit (5 Prime, Germany) according to the manufacturer's instructions. The DNA was quantified by a Qubit 2.0 Fluorometer (Life Technologies, United States), and sheared by Bioruptor Pico (Diagenode, Belgium) to an average length of 550 bp. Sequencing adapters were ligated by the TruSeq DNA PCR-Free Library Prep Kit (Illumina Inc., United States). The ligated library was sequenced on the Illumina MiSeq platform with 2×250 (strain dw23^T) and 2×300 (strain dw96) paired-end runs.

Sodalis ligni dw23^T was selected for further Nanopore MinION sequencing. DNA was extracted by mechanical cell lysis using vortex, followed by DNA binding and purification on AMPure XP magnetic beads (Beckman Coulter, United States) with 70% ethanol. The SQK-LSK108 ligation kit was used to prepare a long-read sequencing library according to the manufacturer's instructions. The library was loaded onto a Nanopore flow-cell version FLO-MIN106 for a 48 h sequencing run. The obtained FAST5 reads were basecalled into FASTQ with

local Albacore 2.1.7 (available via ONT community site¹) with a minimal quality threshold of 7. Passed reads were scanned for remaining adapters, which were trimmed with Porechop 0.2.3².

The *Sodalis* sp. strain dw96 genome assembly used short reads only, and *Sodalis ligni* dw23^T used a hybrid assembly of short and long reads. Assembly was performed with Unicycler 0.4.4 (Wick et al., 2017) in normal mode wrapping the following programs: SPAdes 3.11.1 (Bankevich et al., 2012), BLAST 2.2.28+ (Altschul et al., 1997), bowtie 2.2.4 (Langmead et al., 2009), samtools 1.6 (Li et al., 2009) and pilon 1.22 (Walker et al., 2014). Prokka 1.13 (Seemann, 2014) with RNAmmer (Lagesen et al., 2007) was used for gene calling, annotation and rRNA genes identification. Genome completeness and contamination were estimated using CheckM v1.1.3 (Parks et al., 2015). The genomes were compared with NCBI Prok database of complete prokaryotic genomes (release Dec-29-2020) using whole-genome based comparison in MiGA (Rodríguez-R et al., 2018).

Pangenome Analysis

The NCBI-genome-download 0.2.12 script³ was used to retrieve all sequenced genomes from the genus *Sodalis* (March, 2020). The two strains obtained from deadwood were added to the set of genomes. *Sodalis*-like endosymbionts and other related strains analyzed previously by Santos-García et al. (2017) were included to estimate size of the core gene set of *Sodalis*-allied group which takes into account significant genome reduction reported for some of these symbionts. Further analysis was focused on *Sodalis* strains with large genomes while those symbionts which are in the advanced reductive evolution process were excluded from the analysis because of their smaller genomes with significantly distinct gene compositions (Santos-García et al., 2017). Selected genomes are summarized in **Supplementary Table 1** and consist of *Sodalis* sensu stricto strains from unpublished as well as published studies (Toh et al., 2006; Chrudimský et al., 2012; Clayton et al., 2012; Oakeson et al., 2014; Rosas-Pérez et al., 2017; Rubin et al., 2018). Genomes were subsequently analyzed within pangenome analysis in anvio 6.2 (Eren et al., 2015, see the "Code Availability" section) to identify deadwood-associated genes and genes shared by all the genomes. ANI was calculated using pyANI 0.2.10 (Pritchard et al., 2015). The resulting image was processed with Inkscape⁴. For CAZyme annotation, prokka 1.13 gene prediction was used to obtain sequences of genes from 11 *Sodalis* genomes. The amino acid sequences were compared with the dbCAN database version 07312018 using run-dbcAN.py 2.0.11 script (Zhang et al., 2018) and hmmer 3.3 (Eddy, 2011). CAZymes with an e -value $\leq 1\text{E}-20$ were considered for further annotation. Ward's clustering was used to group genomes based on the Hellinger transformed counts of all the detected CAZymes and pheatmap 1.0.12 package was used to generate a CAZy heatmap (Kolde, 2019). Spearman correlation was used to calculate genome-related statistics.

¹<https://community.nanoporetech.com>

²<https://github.com/rrwick/Porechop>

³<https://github.com/kbclin/ncbi-genome-download>

⁴<https://inkscape.org/>

nifH Phylogenetics

The curated database of *nifH* sequences classified to the phylum level or below was retrieved (Moynihan, 2020). Genes from the phylum *Proteobacteria* and a random *nifH* representative for each taxonomic group were selected. Two *nifH* genes from *Sodalis* sp. strain dw96 and three from *Sodalis ligni* were aligned with the retrieved *nifH* collection using the online MAFFT v7.475 (Katoh et al., 2018). Maximum likelihood tree was constructed using IQ-TREE v1.6.12 (-alrt 1000 -bb 1000) (Nguyen et al., 2014) using best-fit model GTR + F + R10 identified by ModelFinder (Kalyaanamoorthy et al., 2017) with UFBoot ultrafast bootstrap (Hoang et al., 2017). Tree was further edited using iTOL (Letunic and Bork, 2011).

Habitat Context—Soil and Deadwood

To confirm the presence of *Sodalis* in deadwood 16S rRNA gene datasets from previous studies published by Hoppe et al. (2015), Moll et al. (2018), Probst et al. (2018), and Šamonil et al. (2020) were screened for similarity with the 16S rRNA genes of strain dw23^T and strain dw96 using BLAST 2.2.28+, and the relative abundance of the most abundant OTU within each study with >97% similarity to the cultivated strains was calculated.

Furthermore, three wood-associated *Sodalis* genomes together with genome of *Sodalis praecapticus* and genome of *Sodalis pierantonius* strain SOPE were used as a reference for the mapping of metagenomes of naturally decomposing wood obtained in the Žofinský prales Nature Reserve (Tláškal et al., 2021, unpublished). The metagenomic study included five age classes of differently decomposed deadwood of *Fagus sylvatica*, with the youngest age class decomposing for <5 years and the oldest age class decomposing for more than 41 years. *Sodalis ligni* dw23^T was recovered from the same decomposing tree as one of the metagenomic and metatranscriptomic sample (SRA BioSample SAMN13762420). Mapping procedure used BWA-MEM 0.7.17 (Li, 2013) with the default settings, samclip 0.4.0⁵ for the removal of mapped reads with hard- and soft-clipped flanking ends longer than 10 bp, samtools-1.9 (Li et al., 2009) for SAM/BAM format conversion and for filtering of mapped reads, and bedtools 2.29.2 (Quinlan and Hall, 2010) for the conversion of BAM into the BED format with the attached CIGAR string. Analysis was focused only on reads with mapping scores of 60, i.e., exact mapping to the unique position along the genome. The metagenomic sample SRR10968255 was omitted from mapping due to the low number of sequences.

The raw BWA-MEM 0.7.17 mapping files of the deadwood metagenomes to the *S. ligni* genome were used as inputs into the anvi'o 6.2 metagenomic pipeline to visualize the occurrence of *S. ligni* in individual deadwood age classes. No read filtering was applied to allow for single-nucleotide variants (SNVs) density calculation of *S. ligni* according to Reveillaud et al. (2019) (see “Code Availability” section). Similarly, metatranscriptomic reads from a previous study (Tláškal et al., 2021, unpublished) were mapped against the set of *S. ligni* genes to infer nitrogen fixation expression in decomposing wood. The data were summarized using R 4.0.0 (R Core Team, 2020) and tidyverse

⁵<https://github.com/tseemann/samclip>

1.3.0 package (Wickham et al., 2019). Significant differences were tested by the Kruskal-Wallis test using the agricolae package (de Mendiburu, 2017).

Insect Cell-Free Cultivation and Enzyme Activity

To assess growth on insect cell-free media containing wood and to exclude the possibility that the *Sodalis* isolates are obligatory symbionts of a deadwood-associated insect, wood pellets from fresh beech wood were milled using an Ultra Centrifugal Mill ZM 200 (Retsch, Germany); 0.3 g of fine wood dust was mixed with 30 mL of Ringer solution and autoclaved. Media were inoculated in duplicate with *S. ligni* colonies growing on plates. Inoculated liquid media containing wood as the only C source were left at 24°C on an orbital shaker for incubation. Aliquots of media were regularly sampled, and samples were immediately frozen. To quantify the increase in cell biomass, DNA from the aliquots was extracted using a DNeasy UltraClean Microbial Kit (Qiagen, Germany) according to the manufacturer's protocol with an additional initial spin for wood dust removal. The bacterial rRNA gene copies in DNA were quantified by qPCR using the 1108f and 1132r primers (Wilmotte et al., 1993; Amann et al., 1995). Sanger sequencing from the primer 1492r (Lane, 1991) was used to confirm the presence of *Sodalis*-only DNA in the final aliquots.

The activity of the cell wall-associated fraction of enzymes was measured in cell suspension after 2 weeks of incubation in 50 mL of liquid GY-VL55 medium as described previously (Lasa et al., 2019). For the catalase and oxidase tests, bacterial cells from a GY-VL55 agar plate were transferred into 3% H₂O₂ solution and 1% N, N, N', N'-tetramethyl-*p*-phenylenediamine dihydrochloride drops, respectively. The Biolog PM1 system was used according to the manufacturer's instructions to identify growth on different C sources.

RESULTS

S. ligni was able to grow on laboratory media in which beech wood was the only source of C, reaching a cell density up to 1.3×10^8 mL⁻¹ within 4 weeks of incubation. This growth excluded the possibility that it is an obligate symbiont of deadwood-associated insects. Hybrid assembly of the *Sodalis ligni* dw23^T provided 32 contigs (>200 bp, N50: 3.8 Mbp), a total genome size of 6.4 Mbp, GC content 54.96% and a mean coverage of 99×. Assembly of the *Sodalis* sp. strain dw96 provided 85 contigs (>200 bp, max 0.72 Mbp, N50: 0.25 Mbp), a total genome size of 5.9 Mbp, GC content 54.04% and a mean coverage of 52×. Genome completeness was 98.8 and 99.9% for the *Sodalis ligni* dw23^T and strain dw96, respectively. Contamination was not detected in the assembled genomes. *Sodalis ligni* dw23^T was placed within the genus *Sodalis* ($P = 0.211$) and belongs to a species not represented in the NCBI database of prokaryotic genomes ($P = 0.0025$).

We retrieved 11 *Sodalis* genomes from NCBI together with the strain metadata (Supplementary Table 1). Pangenome analysis divided the available *Sodalis* genomes into three distinct guilds based on gene frequency (Figure 1). One group consisted

of two genomes of *Sodalis glossinidius morsitans* (strains Sg and ASM), which are tsetse fly endosymbionts. The two *Sodalis ligni* dw23^T and strain dw96 isolated in this study from deadwood formed the second group together with the free-living *Sodalis* sp. strain 159R retrieved from NCBI as an anaerobic lignin degrader. The third group consisted of endosymbionts of hymenopteran, hemipteran, dipteran and coleopteran insects. The gene frequency, gene count and genome length of *S. praecaptivus* have high similarity with the third group of endosymbionts, thus placing this free-living strain distant from deadwood-associated *Sodalis* sp. strains dw23^T and dw96 despite their relatively high 16S rRNA gene similarity (97.2 and 97.8%, respectively). The ANI between strain dw23^T or strain dw96 and the rest of the analyzed genomes ranged from 76 to 78%, except for strain 159R (98 and 88%, respectively, **Figure 1** and **Supplementary Table 2**). The ANI between strains dw23^T and dw96 was 88%. The genome size of all *Sodalis* strains and their gene count were closely correlated ($\rho = 0.82$, $P = 0.004$), while the genome size and gene counts per Kbp were negatively correlated ($\rho = -0.63$, $P = 0.04$). Free-living strains exhibited the lowest coding density (0.87–0.90 genes per kbp) and longer genes than symbionts (947 ± 7 bp and 732 ± 39 bp, respectively, $P < 0.01$, **Supplementary Table 1**).

Pangenome analysis allowed us to identify clusters of orthologous genes (COGs) that were shared among strain guilds. Genes shared by all the genomes represent the core *Sodalis* pangenome (in average 1,747 genes per genome from 1,561 core gene clusters, 35.6% of genes from the average *Sodalis* genome, **Figure 1**). The core gene set shared with the *Sodalis*-like symbionts with extremely reduced genomes is represented by in average 130 genes from only 125 gene clusters. The COG categories with the highest share of classified core genes were translation, amino acid and carbohydrate metabolism, cell wall/membrane biosynthesis and replication categories (**Figures 1, 2**). Genes shared only among free-living strains were less frequent (in average 109 genes from 106 gene clusters; 2.0% per average free-living *Sodalis* genome) and were dominated by genes related to carbohydrate metabolism. Gene sharing among wood-associated strains was relatively common (in average 1,596 genes from 1,519 gene clusters, 28.4% per average wood-associated *Sodalis* genome), these genes were mostly classified in carbohydrate and amino acid utilization and transcription regulation COG categories. The nitrogenase gene *nifH* and genes encoding an ABC-type molybdate transport system were significantly enriched in the accessory genes of the wood-associated guild (adj. q -value = 0.01). *Sodalis ligni* dw23^T, *Sodalis* sp. strain dw96 and *Sodalis* sp. strain 159R each contained *nifHDK* operons, while nitrogen fixation genes were absent in other *Sodalis* genomes. Similar to symbionts, wood-associated strains contained type III secretion system components.

In total, 833 genes encoding carbohydrate-active enzymes from 66 CAZy families were identified across all the genomes. Free-living strains together with the symbiotic *Sodalis* sp. strain SAL2 contained the highest per-genome share of CAZy, with >1.62% of the total genes being identified as CAZymes (**Supplementary Tables 3, 4**). Wood-associated strains showed the highest diversity of CAZy, possessing >80% of the detected

CAZy families each. The lowest diversity of CAZy (43.9% of detected families) was recorded in tsetse fly-associated strains. CAZy richness in individual genomes was correlated with CAZy abundance ($\rho = 0.7$, $P = 0.02$). The distribution of detected CAZymes followed *Sodalis* guild differentiation, with distinct CAZy patterns for wood-associated strains, tsetse fly symbionts and other symbionts (**Figure 3A**). Additionally, the functional annotation of CAZy families showed to some extent their conservation within *Sodalis* guilds (**Figure 3B** and **Supplementary Table 4**). In comparison to symbionts, wood-associated strains had more genes for α -glucan, cellobiose, xylobiose and chitin utilization. Genes for cellulose, pectin and hemicelluloses degradation were also detected; however, the counts of these CAZymes were comparable with those in the genomes of symbionts. Glycoconjugate utilization CAZymes were enriched in wood dwellers as well as free-living *S. praecaptivus*. Lytic polysaccharide monoxygenases (LPMOs) were not detected in the genomes of wood-associated strains.

16S rRNA genes assigned to *Sodalis* were present in other published community studies from deadwood (see the “Data Availability” section) and typically exhibited high relative abundance. The mean abundance of one *Sodalis* OTU related to strains dw23^T and strain dw96 at 98.8% similarity was $2.79 \pm 0.86\%$ ($n = 155$, spruce deadwood in Finland, Schigel et al., unpublished data). Another *Sodalis* OTU (98% similarity to the presented genomes) was found on beech and spruce wood at 0.57–0.70% (Hoppe et al., 2015). When comparing deadwood of 13 tree species after 6 years of decomposition, the broadleaved species *Betula* sp., *Populus* spp., *Carpinus* sp. showed the highest abundance of *Sodalis* OTU (**Supplementary Table 5**; Moll et al., 2018). The abundance of other *Sodalis* OTU (99.6% similarity to the presented genomes) also differed in samples of spruce wood cubes ($0.23 \pm 0.16\%$, $n = 26$) and surrounding soil ($0.004 \pm 0.002\%$, $n = 30$, $P < 0.001$, Probst et al., 2018). Similarly, sequences assigned to *Sodalis* (100% similarity) were enriched in decomposing beech trees in Žofínský prales Nature Reserve ($0.93 \pm 0.48\%$, $n = 24$, $P < 0.001$), when compared to underlying soil ($0.0004 \pm 0.0002\%$, $n = 48$, Šamonil et al., 2020).

The exact mapping of the deadwood metagenomic data to the *Sodalis* genomes confirmed the higher abundances of the *S. ligni*, *Sodalis* sp. strain dw96 and *Sodalis* sp. strain 159R guild in a deadwood habitat than *S. praecaptivus* and *S. pierantonius* strain SOPE ($P < 0.001$, **Figure 4A**). For the three wood-associated strains, the average number of exactly mapped reads was 808 ± 220 reads per million reads (812 ± 397 reads per million for *S. ligni* only). *S. ligni* showed an even distribution throughout the gradient of deadwood decomposition stages when considering the proportion of mapped reads from the total reads available (**Figure 4B**). The rate of SNVs per one mapped read was 0.03 ± 0.01 ($n = 23$), and the density of SNVs against the *S. ligni* genome showed homogenous *Sodalis* populations in the deadwood metagenomes, with mean SNVs of $0.17 \pm 0.07\%$ except for the outlier population in one young deadwood metagenome (1.7% SNVs, **Figure 4B**). Most SNVs occurred in the third codon wobbling position (**Supplementary Figure 1**). Three distinct *nifHDK* operons were identified in the genome of *Sodalis ligni*. Two of these operons successfully called reads

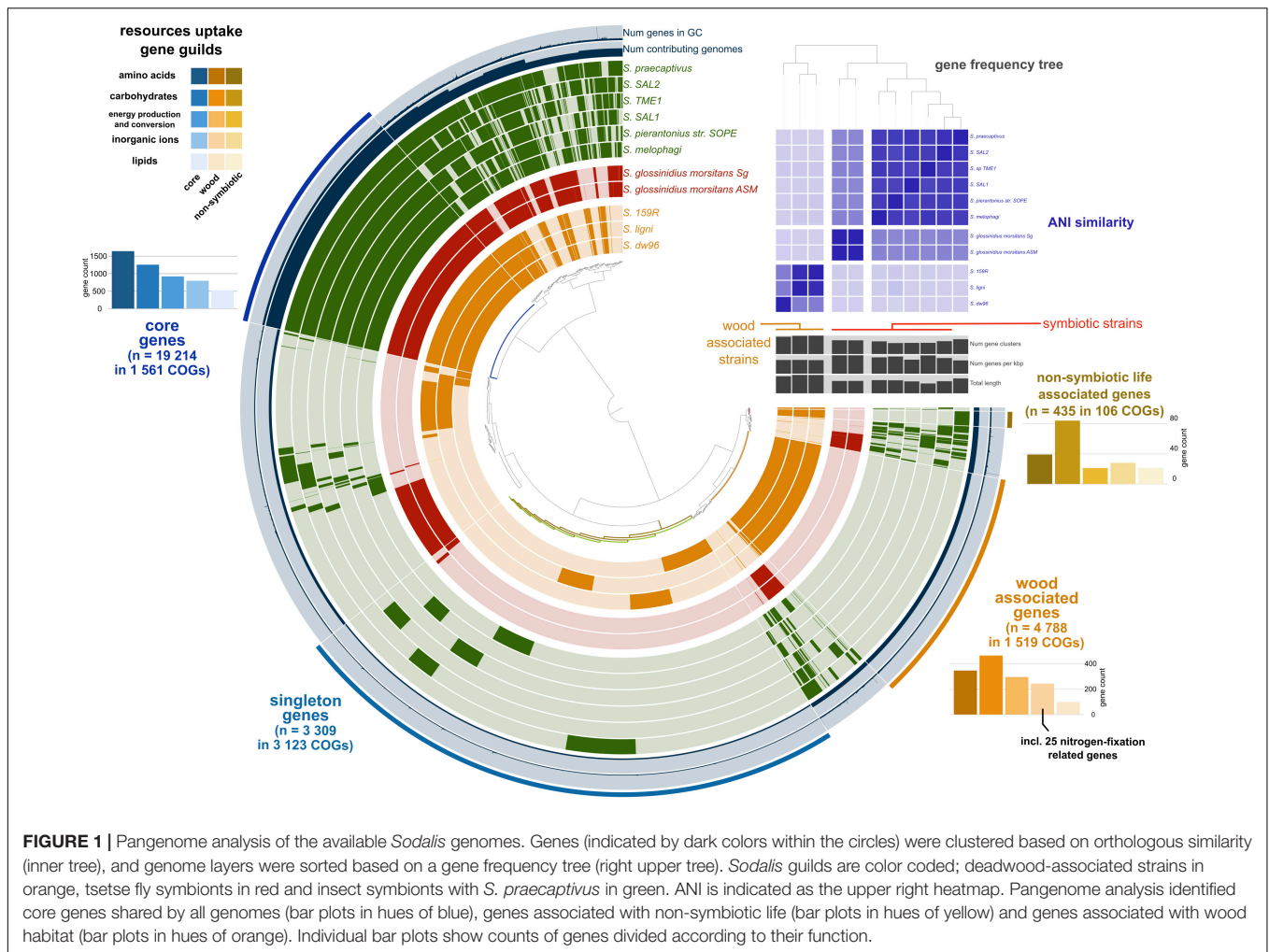


FIGURE 1 | Pangenome analysis of the available *Sodalis* genomes. Genes (indicated by dark colors within the circles) were clustered based on orthologous similarity (inner tree), and genome layers were sorted based on a gene frequency tree (right upper tree). *Sodalis* guilds are color coded; deadwood-associated strains in orange, tsetse fly symbionts in red and insect symbionts with *S. praecaptivus* in green. ANI is indicated as the upper right heatmap. Pangenome analysis identified core genes shared by all genomes (bar plots in hues of blue), genes associated with non-symbiotic life (bar plots in hues of yellow) and genes associated with wood habitat (bar plots in hues of orange). Individual bar plots show counts of genes divided according to their function.

from two deadwood metatranscriptome samples (SRA accessions SRR10968245, SRR10968250). Notably, the same decomposing tree (BioSample SAMN13762420) served as the source of RNA for the latter metatranscriptome, as well as for the cultivation of *S. ligni*. Phylogenetic analysis of the *nifH* gene across the phylum *Proteobacteria* showed placement of *Sodalis* nitrogenase genes into distinct clades common to other *Enterobacteriales*, with the exception of one *Sodalis ligni nifH* placed on a distant branch (Figure 5).

Description of *Sodalis ligni* sp. nov.

Sodalis ligni (lig'ni. L. gen. n. *ligni* of wood, referring to the isolation of the type strain from wood material).

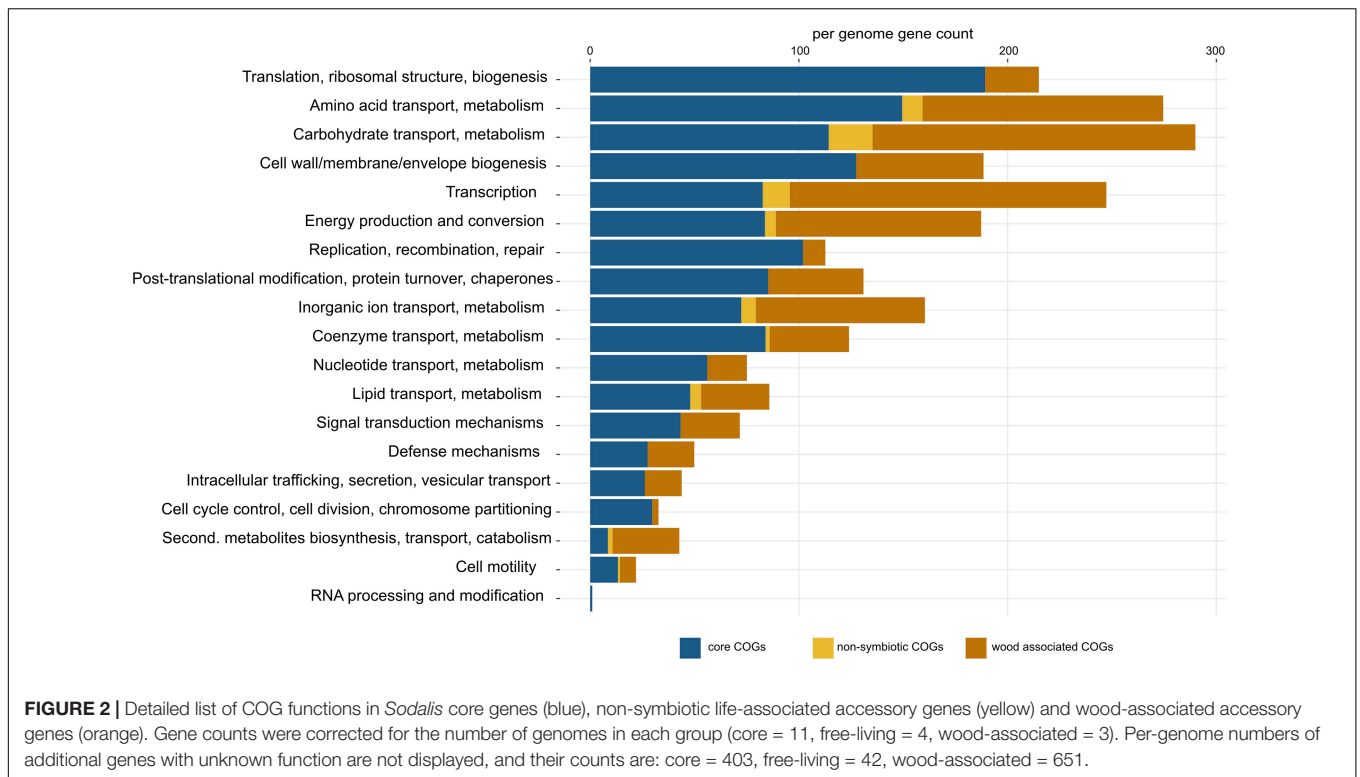
Cells are aerobic, Gram-negative, cocci (0.6 μm) or short rods (1.2 × 0.6 μm). They grow separately without forming groups. Colonies on solid medium are circular, regularly edged, smooth, mucoid and white. Catalase positive and oxidase negative. The enzymatic *in vitro* assays were positive for β-glucosidase, β-xylosidase, *N*-acetyl-glucosaminidase, phosphodiesterase, acid phosphatase and lipase. L-serine, D-saccharic acid, *N*-acetyl-beta-D-mannosamine, D-cellobiose, D-galactose, L-fucose, fumaric acid, L-lactic acid, β-methyl-D-glucoside, adonitol,

dulcitol, glycerol, L-galactonic acid-γ-lactone, and monomethyl succinate could be used as C sources. Optimal growth occurs on GY-VL55 medium (Lladó et al., 2019) and GY agar at pH 4.5–5.5 at 24°C.

The type strain is dw23^T (=CECT 30299^T = BCCM/LMG 32208^T), isolated from decomposing wood of *Fagus sylvatica* L. in a temperate mixed forest, Central Europe. The genomic G + C content of the type strain is 54.96%.

DISCUSSION

The genus *Sodalis* represents the model for the development of insect-associated lifestyle and host-symbiont interactions due to its evolutionarily young transition from a free-living to a symbiotic bacterium (Hall et al., 2020; Maire et al., 2020). Moreover, the tsetse fly symbiont *Sodalis glossinidius* is able to grow independently on its host under laboratory conditions, further pointing to the recent development of its non-facultative symbiosis (Goodhead et al., 2020). Until now, *S. praecaptivus* was the only free-living species described, which hints that there is a more diversified spectrum of life



strategies than only association with insects (Clayton et al., 2012; Chari et al., 2015). Here, we describe two other free-living isolates from the *Sodalis* genus, one of which, strain dw23^T, is suggested to represent the type strain for *Sodalis ligni* sp. nov. within the family *Enterobacteriales*. The genome-to-genome alignment of the available *Sodalis* genomes shows ~77% ANI with our strain, thus supporting the establishment of a new species within the *Sodalis* genus (Konstantinidis et al., 2006; Richter and Rosselló-Móra, 2009; Barco et al., 2020). This is supported also by comparison with NCBI database of prokaryotic genomes (Rodríguez-R et al., 2018). In contrast to *Sodalis* insect endosymbionts, *S. ligni* occupies deadwood and possesses genome characteristics connected with non-symbiotic life: a larger genome, a higher number of longer genes and a lower coding density (Toh et al., 2006; Oakeson et al., 2014). It refers to independent nutrient provisioning from more complex resources, the necessity for more sophisticated regulatory systems in fluctuating environments and a large effective population of free-living taxa in contrast to their symbiotic relatives (Giovannoni et al., 2014; Bobay and Ochman, 2018). We identified three ecological guilds within the genus *Sodalis*: tsetse endosymbionts, endosymbionts of other insect taxa and the wood-associated guild presented here. This differentiation is consistent based on ANI and on the functional genome content when considering either all genes or their subset CAZymes.

S. ligni appears in multiple 16S rRNA-based deadwood studies and is usually ranked among the most abundant taxa. Due to the multi-copy character of the 16S rRNA gene (Větrovský and Baldrian, 2013), amplicon studies might provide imperfect

abundance estimates. This is true especially for the family *Enterobacteriales*, as the mean number of 16S rRNA genes is 7 ± 0.5 ($n = 3,130$, Stoddard et al., 2015), which overestimates their abundance when comparing relative counts of 16S rRNA. Seven copies of 16S rRNA were also confirmed in the genome of *S. ligni*. Hybrid assembly using short and long reads helped to identify their individual copies, which are otherwise usually merged into one consensus copy by the assembler when assembling short reads only (Waters et al., 2018).

Despite the limitations of abundance estimates, amplicon studies showed clear habitat selection of *S. ligni*, which preferentially colonizes deadwood rather than the underlying soil (Probst et al., 2018; Šamonil et al., 2020). Moreover, *Sodalis*-related metagenome-assembled genomes are also absent in the recent large-scale cultivation-independent genome catalog, suggesting a low abundance of *S. ligni* in global soils (Nayfach et al., 2020). We therefore propose that *S. ligni* is a member of a wood-associated *Sodalis* guild. The independence of *S. ligni* from insect hosts is supported by its ability to grow solely on wood. The wood-associated guild further contains the other two isolates, *Sodalis* strain dw96 and *Sodalis* strain 159R, the former of which was identified in the present study and the latter was identified in an unpublished study. Other related *Sodalis* members, the previously described free-living *S. praecaptivus* and symbiont *Sodalis pierantonius* strain SOPE, do not show a deadwood preference (Oakeson et al., 2014). While for the symbiont this is not surprising, the main habitat and ecological functions of *S. praecaptivus* remain to be identified, considering its genome composition (which is closer to symbionts than to

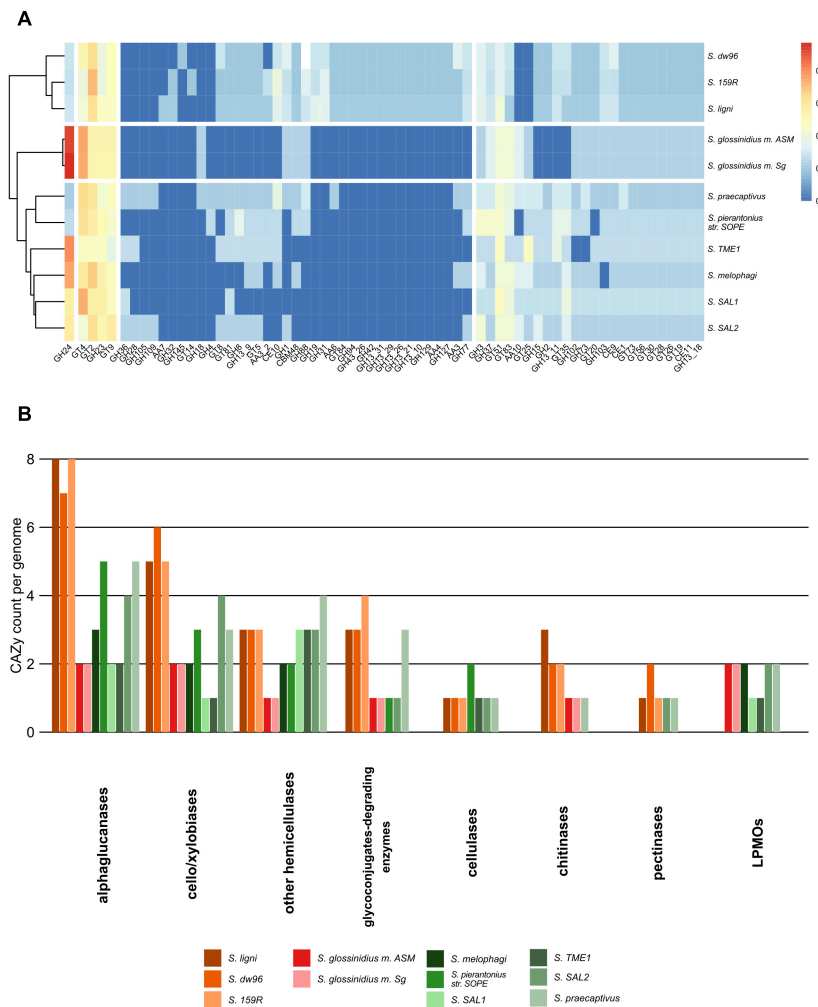


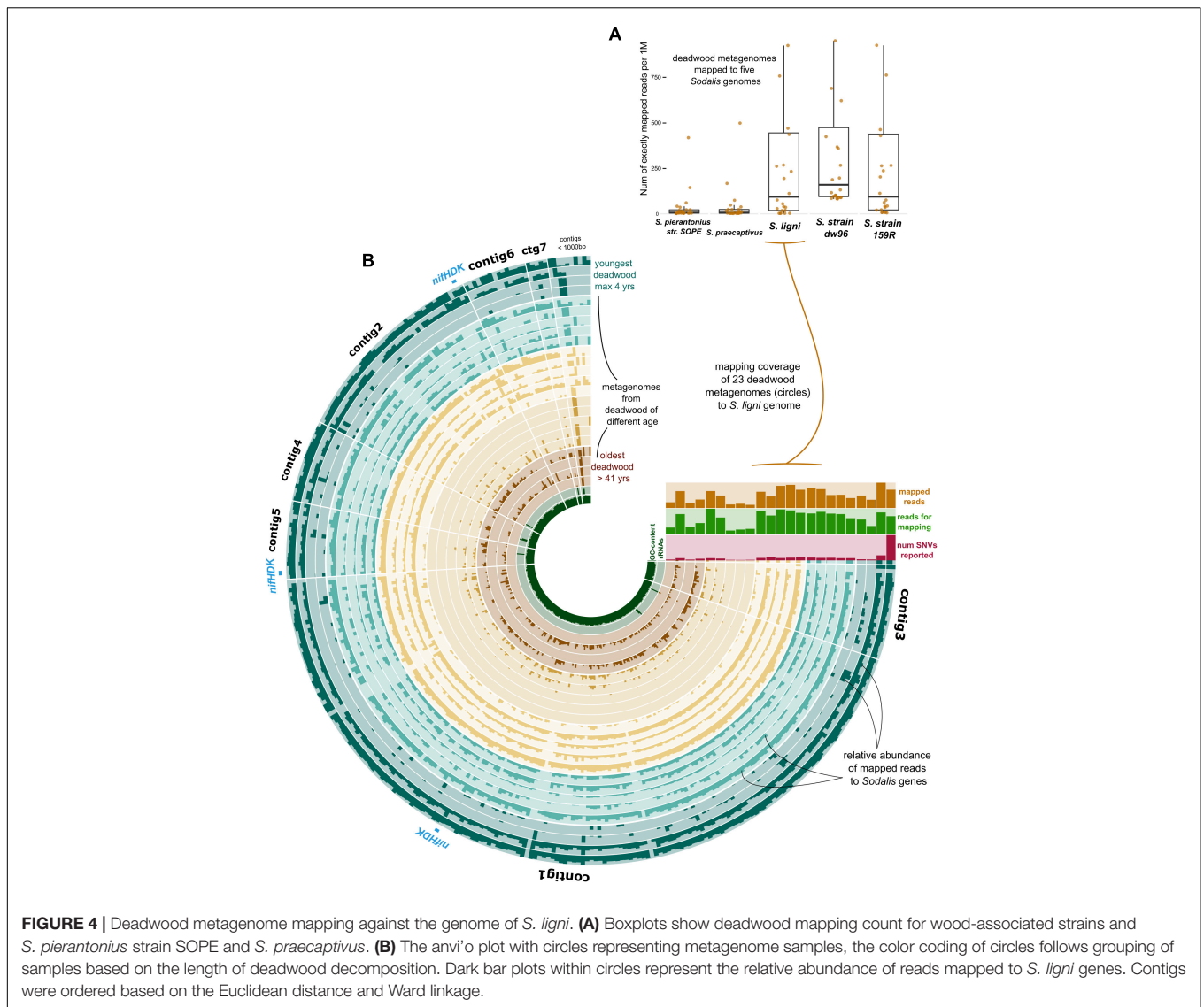
FIGURE 3 | CAZy presence in the *Sodalis* genomes. **(A)** CAZy heatmap with clustering analysis shows the CAZyme abundance pattern, which follows *Sodalis* guild differentiation into wood-associated strains, tsetse symbionts and other symbiotic strains. Legend shows transformed counts. **(B)** Functional annotation of the CAZymes found in the genomes of *Sodalis* genomes. Genes for labile substrate utilization, such as cello/xylobiose and α -glucan, are increased in deadwood-associated strains.

wood-associated strains), wood cultivation source and ability to grow in human and insect tissues (Clayton et al., 2012; Enomoto et al., 2017; Munoz et al., 2020). Based on the presence of virulence factors, *S. praecaptivus* may represent a plant pathogen transmitted by insects (Clayton et al., 2012) and thus may prefer living plants rather than decomposing wood.

Preferential colonization of wood of particular tree species by *S. ligni* might occur, as was observed in the data from conifers and broadleaved trees (Hoppe et al., 2015; Moll et al., 2018). However, further research across more deadwood types is needed to disentangle potential tree species selection. The abundance of *S. ligni* in decomposing wood does not seem to vary over tens of years, which is a typical lifetime for decomposing trees in temperate forests (Přívětivý et al., 2016), and the *S. ligni* population is homogenous with regard to SNVs density.

The core genes shared by all *Sodalis* strains contain genes for crucial cell functions, mainly translation, replication,

transcription, amino acid and carbohydrate metabolism and cell wall/membrane biosynthesis. Furthermore, pangenome analysis unveiled a relatively low number of genes specific for non-symbiotic life, while accessory genes specific for wood-associated guild represent a significant portion of the total identified genes and are involved in, e.g., amino acid and carbohydrate metabolism. Such gene-specific enrichment is connected with a more diverse set of nutrient resources in deadwood habitats. The presence of type III secretion system genes in wood-associated strains might serve as an evolutionary predisposition for host infection by related symbiotic *Sodalis* members (Maire et al., 2020). The composition of CAZymes of wood-associated strains differentiates them from symbionts as well. Substrates targeted by CAZymes show that wood-associated *Sodalis* members utilize rather labile plant polymers or chitin to obtain C and do not serve as important cellulose degraders. The broader degradation capabilities were



described for other deadwood-associated bacterial taxa such as those from the phyla *Acidobacteria* and *Bacteroidetes* (Tláškal and Baldrian, 2021). The ecological function of free-living *Sodalis* strains might be resolved based on the multiplied presence of *nifHDK* operons expressing nitrogenase, a key enzyme for nitrogen fixation which is dependent on the metal cofactors (e.g., molybdenum). The sequence difference between nitrogenase variants shows the importance of these genes for the bacterium. To reduce atmospheric nitrogen is energetically costly, and thus, there is probably a selection pressure in the *Sodalis* deadwood guild to not combine nitrogen fixation with resource-intensive degradation of recalcitrant plant polymers. Nitrogen fixation within the family *Enterobacterales* is known from taxa living in association with plants (Rosenblueth et al., 2004), with leaf-cutter ant fungus gardens (Pinto-Tomás et al., 2009) and with Diptera (Behar et al., 2005). Deadwood was previously described as a hotspot of nitrogen fixation by which bacteria enrich material with

a low nitrogen content and relieve the nitrogen limitation on microbial colonization (Tláškal et al., 2021). Deadwood-associated *S. ligni* thus represents a candidate for nitrogen fixation and one of the rarely described free-living nitrogen fixing *Enterobacterales* members.

To conclude, we identified *S. ligni* as a member of the wood-associated *Sodalis* guild, and we provide a comprehensive analysis of its genome potential, substrate utilization and ecological function in the context of other known isolated *Sodalis* sensu stricto strains. Members of the *Sodalis* genus show broad life strategies with distinct specialization, indicating all-rounder character of this genus, including free-living deadwood inhabitants, non-symbiotic strains with the ability to colonize internal insect and human tissues and recently established symbionts in several insect orders. Such an extensive niche differentiation is known from another enterobacterial species, *Escherichia coli* (Tenaillon et al., 2010; Luo et al., 2011), but has not been described

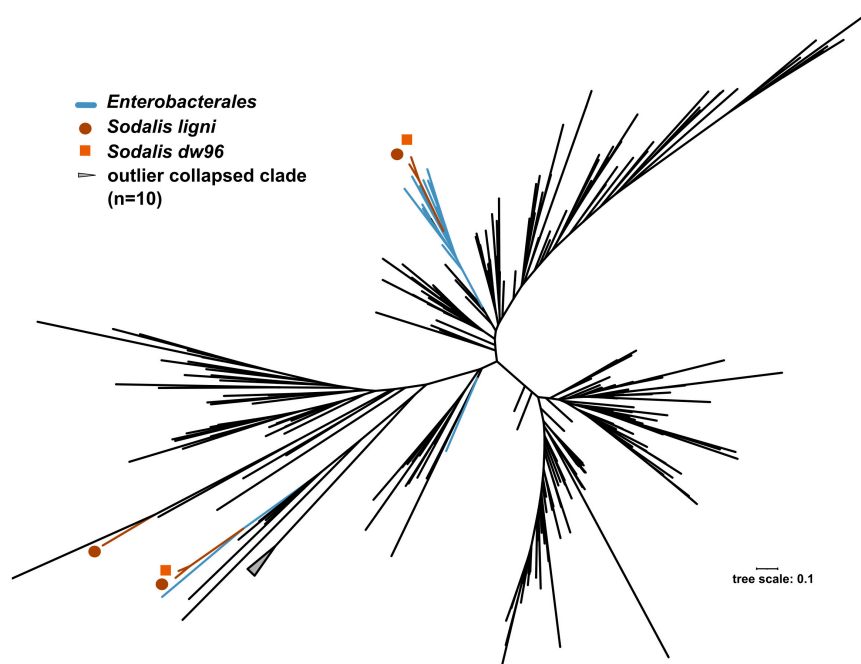


FIGURE 5 | Phylogenetic tree based on *nifH* genes described from members of the phylum *Proteobacteria*. Blue branches denote *Enterobacterales*. Positions of the three *nifH* sequences from *Sodalis ligni* are labeled with dark brown circles, two of which are placed together with other enterobacteria. Two *nifH* sequences from *Sodalis dw96* are labeled with bright brown squares, and both are placed together with other *nifH* from enterobacteria.

for *Sodalis*-related taxa. There is not enough evidence and more isolates from related sources are needed to determine whether deadwood served as a reservoir pool for symbiotic bacteria diversification via genome reduction or whether there was another common ancestor for both wood-associated and insect-associated guilds.

CODE AVAILABILITY

The above methods indicate the programs used for analysis within the relevant sections. The code for reproducing all sequence processing is provided at <https://github.com/TlaskalV/Deadwood-Sodalis>.

DATA AVAILABILITY STATEMENT

Data described in this manuscript, including raw sequences from short-read sequencing and genome assembly files, have been deposited in the NCBI under BioProject accession numbers PRJNA599932 (*Sodalis ligni* dw23^T) and PRJNA613885 (*Sodalis* sp. strain dw96). We further deposited MinION long-read sequencing data in ENA nucleotide archive (PRJEB43208), 16S rRNA sequences of *Sodalis* clustered in other deadwood studies (10.6084/m9.figshare.13227464), *anvi'o* pangenome databases (10.6084/m9.figshare.13221065), *anvi'o* deadwood metagenome mapping databases (10.6084/m9.figshare.13221074) and *nifH* tree in Newick format (10.6084/m9.figshare.14562279).

AUTHOR CONTRIBUTIONS

VT conceived the study with input from PB. VT performed the strain isolation, pangenome analysis, metagenomic mapping, and strain characterization. LŽ and VP performed the library preparation and sequencing, genome assembly, and annotation. VT and PB wrote the original version of the manuscript. All authors contributed to the final version of the manuscript.

FUNDING

This work was supported by the Czech Science Foundation (21-09334J).

SUPPLEMENTARY MATERIAL

The Supplementary Material for this article can be found online at: <https://www.frontiersin.org/articles/10.3389/fmicb.2021.668644/full#supplementary-material>

Supplementary Table 1 | List of available *Sodalis* genomes together with genome, life strategy metadata and description of referencing studies.

Supplementary Table 2 | ANI statistics calculated for 11 available *Sodalis* genomes.

Supplementary Table 3 | Total count, gene share and richness of CAZymes identified in *Sodalis* genomes. Deadwood-associated strains followed by *S. praecaptivus* contain the highest number of diverse CAZy.

Supplementary Table 4 | Per family counts of CAZymes and their assigned activities in individual genomes.

Supplementary Table 5 | Relative abundances of a *Sodalis* OTU with 99.6% similarity to *S. ligni* among deadwood of 13 tree species after 6 years of decomposition from the study Moll et al. (2018). Data represent means and standard errors.

Supplementary Figure 1 | Single-nucleotide variants (SNVs) detected after mapping deadwood metagenome reads to the *S. ligni* genome shown as boxplots of the occurrence of SNVs for each codon position. Each dot represents one metagenome sample.

REFERENCES

- Akman, L., Yamashita, A., Watanabe, H., Oshima, K., Shiba, T., Hattori, M., et al. (2002). Genome sequence of the endocellular obligate symbiont of tsetse flies, *Wigglesworthia glossinidia*. *Nat. Genet.* 32, 402–407. doi: 10.1038/ng986
- Altschul, S. F., Madden, T. L., Schäffer, A. A., Zhang, J., Zhang, Z., Miller, W., et al. (1997). Gapped BLAST and PSI-BLAST: a new generation of protein database search programs. *Nucleic Acids Res.* 25, 3389–3402. doi: 10.1093/nar/25.17.3389
- Amann, R. L., Ludwig, W., and Schleifer, K.-H. (1995). Phylogenetic identification and in situ detection of individual microbial cells without cultivation. *Microbiol. Rev.* 59, 143–169. doi: 10.1128/mr.59.1.143-169.1995
- Anderson-Teixeira, K. J., Davies, S. J., Bennett, A. C., Muller-landau, H. C., and Wright, S. J. (2015). CTFS-ForestGEO: a worldwide network monitoring forests in an era of global change. *Glob. Chang. Biol.* 21, 528–549. doi: 10.1111/gcb.12712
- Baldrian, P., Zrůstová, P., Tláškal, V., Davidová, A., Merhautová, V., and Vrška, T. (2016). Fungi associated with decomposing deadwood in a natural beech-dominated forest. *Fungal Ecol.* 23, 109–122. doi: 10.1016/j.funeco.2016.07.001
- Bankevich, A., Nurk, S., Antipov, D., Gurevich, A. A., Dvorkin, M., Kulikov, A. S., et al. (2012). SPAdes: a new genome assembly algorithm and its applications to single-cell sequencing. *J. Comput. Biol.* 19, 455–477. doi: 10.1089/cmb.2012.0021
- Barco, R. A., Garrity, G. M., Scott, J. J., Amend, J. P., Nealson, K. H., and Emerson, D. (2020). A genus definition for *Bacteria* and *Archaea* based on a standard genome relatedness index. *mBio* 11:e002475-19. doi: 10.1128/mBio.02475-19
- Behar, A., Yuval, B., and Jurkevitch, E. (2005). Enterobacteria-mediated nitrogen fixation in natural populations of the fruit fly *Ceratitidis capitata*. *Mol. Ecol.* 14, 2637–2643. doi: 10.1111/j.1365-294X.2005.02615.x
- Bobay, L.-M., and Ochman, H. (2018). Factors driving effective population size and pan-genome evolution in bacteria. *BMC Evol. Biol.* 18:153. doi: 10.1186/s12862-018-1272-4
- Boyd, B. M., Allen, J. M., Koga, R., Fukatsu, T., Sweet, A. D., Johnson, K. P., et al. (2016). Two bacterial genera, *Sodalis* and *Rickettsia*, associated with the Seal Louse *Proechinophthirus fluctus* (Phthiraptera: Anoplura). *Appl. Environ. Microbiol.* 82, 3185–3197. doi: 10.1128/AEM.00282-16
- Chari, A., Oakeson, K. F., Enomoto, S., Grant Jackson, D., Fisher, M. A., and Dale, C. (2015). Phenotypic characterization of *Sodalis praecaptivus* sp. nov., a close non-insect-associated member of the *Sodalis*-allied lineage of insect endosymbionts. *Int. J. Syst. Evol. Microbiol.* 65, 1400–1405. doi: 10.1099/ijso.0.000091
- Chen, X., Li, S., and Aksoy, S. (1999). Concordant evolution of a symbiont with its host insect species: molecular phylogeny of genus *Glossina* and its bacteriome-associated endosymbiont, *Wigglesworthia glossinidia*. *J. Mol. Evol.* 48, 49–58. doi: 10.1007/PL00006444
- Chrudimský, T., Husník, F., Nováková, E., and Hypša, V. (2012). *Candidatus Sodalis melophagi* sp. nov.: phylogenetically independent comparative model to the tsetse fly symbiont *Sodalis glossinidius*. *PLoS One* 7:e40354. doi: 10.1371/journal.pone.0040354
- Clayton, A. L., Oakeson, K. F., Gutin, M., Pontes, A., Dunn, D. M., von Niederhäusern, A. C., et al. (2012). A novel human-infection-derived bacterium provides insights into the evolutionary origins of mutualistic insect-bacterial symbioses. *PLoS Genet.* 8:e1002990. doi: 10.1371/journal.pgen.1002990
- de Mendiburu, F. (2017). *Agricolae: Statistical Procedures for Agricultural Research. R Package Version 1.2-4*.
- Eddy, S. R. (2011). Accelerated profile HMM searches. *PLoS Comput. Biol.* 7:e1002195. doi: 10.1371/journal.pcbi.1002195
- Elo, S., Maunukela, L., Salkinoja-Salonen, M., Smolander, A., and Haahtela, K. (2000). Humus bacteria of Norway spruce stands: plant growth promoting properties and birch, red fescue and alder colonizing capacity. *FEMS Microbiol. Ecol.* 31, 143–152. doi: 10.1111/j.1574-6941.2000.tb00679.x
- Enomoto, S., Chari, A., Clayton, A. L., and Dale, C. (2017). Quorum sensing attenuates virulence in *Sodalis praecaptivus*. *Cell Host Microb.* 21, 629–636. doi: 10.1016/j.chom.2017.04.003
- Eren, A. M., Esen, Ö.C., Quince, C., Vineis, J. H., Morrison, H. G., Sogin, M. L., et al. (2015). Anvi'o: an advanced analysis and visualization platform for 'Omics data. *PeerJ* 3:e1319. doi: 10.7717/peerj.1319
- Fukatsu, T., Koga, R., Smith, W. A., Tanaka, K., Nikoh, N., Sasaki-Fukatsu, K., et al. (2007). Bacterial endosymbiont of the slender pigeon louse, *Columbicola columbae*, allied to endosymbionts of grain weevils and tsetse flies. *Appl. Environ. Microbiol.* 73, 6660–6668. doi: 10.1128/AEM.01131-07
- Giovannoni, S. J., Cameron Thrash, J., and Temperton, B. (2014). Implications of streamlining theory for microbial ecology. *ISME J.* 8, 1553–1565. doi: 10.1038/ismej.2014.60
- Goodhead, I., Blow, F., Brownridge, P., Hughes, M., Kenny, J., Krishna, R., et al. (2020). Large-scale and significant expression from pseudogenes in *Sodalis glossinidius* - A facultative bacterial endosymbiont. *Microb. Genom.* 6:e000285. doi: 10.1099/mgen.0.000285
- Hall, R. J., Flanagan, L. A., Wood, A. J., Thomas, H., Springthorpe, V., Thorpe, S., et al. (2019). A tale of three species: adaptation of *Sodalis glossinidius* to tsetse biology, *Wigglesworthia* metabolism, and host diet. *mBio* 10:e002106-18. doi: 10.1128/mBio.02106-18
- Hall, R. J., Thorpe, S., Thomas, G. H., and Wood, A. J. (2020). Simulating the evolutionary trajectories of metabolic pathways for insect symbionts in the genus *Sodalis*. *Microb. Genomics* 6:mgen000378. doi: 10.1099/mgen.0.000378
- Heddi, A., Grenier, A. M., Khatchadourian, C., Charles, H., and Nardon, P. (1999). Four intracellular genomes direct weevil biology: nuclear, mitochondrial, principal endosymbiont, and *Wolbachia*. *Proc. Natl. Acad. Sci. U.S.A.* 96, 6814–6819. doi: 10.1073/pnas.96.12.6814
- Hoang, D. T., Chernomor, O., Haeseler, A., Von Minh, B. Q., and Vinh, L. S. (2017). UFBoot2: improving the ultrafast bootstrap approximation. *Mol. Biol. Evol.* 35, 518–522. doi: 10.1093/molbev/msx281
- Hoppe, B., Krüger, D., Kahl, T., Arnstadt, T., Buscot, F., Bauhus, J., et al. (2015). A pyrosequencing insight into sprawling bacterial diversity and community dynamics in decaying deadwood logs of *Fagus sylvatica* and *Picea abies*. *Sci. Rep.* 5:9456. doi: 10.1038/srep09456
- Kaiwa, N., Hosokawa, T., Kikuchi, Y., Nikoh, N., Meng, X. Y., Kimura, N., et al. (2010). Primary gut symbiont and secondary, *Sodalis*-allied symbiont of the scutellerid stinkbug *Cantao ocellatus*. *Appl. Environ. Microbiol.* 76, 3486–3494. doi: 10.1128/AEM.00421-10
- Kalyaanamoorthy, S., Minh, B. Q., Wong, T. K. F., Von, A., and Jermini, L. S. (2017). ModelFinder: fast model selection for accurate phylogenetic estimates. *Nat. Methods* 14, 587–589. doi: 10.1038/nmeth.4285
- Katoh, K., Rozewicki, J., and Yamada, K. D. (2018). MAFFT online service: multiple sequence alignment, interactive sequence choice and visualization. *Brief. Bioinform.* 20, 1160–1166. doi: 10.1093/bib/bbx108
- Kolde, R. (2019). *phatmap: Pretty Heatmaps. R Package Version 1.0.12*.
- Konstantinidis, K. T., Ramette, A., and Tiedje, J. M. (2006). The bacterial species definition in the genomic era. *Philos. Trans. R. Soc. Lond. B. Biol. Sci.* 361, 1929–1940. doi: 10.1098/rstb.2006.1920
- Král, K., Janík, D., Vrška, T., Adam, D., Hort, L., Unar, P., et al. (2010). Local variability of stand structural features in beech dominated natural forests of Central Europe: implications for sampling. *For. Ecol. Manag.* 260, 2196–2203. doi: 10.1016/j.foreco.2010.09.020
- Lagesen, K., Hallin, P., Rødland, E. A., Staerfeldt, H. H., Rognes, T., and Ussery, D. W. (2007). RNAmmer: consistent and rapid annotation of ribosomal RNA genes. *Nucleic Acids Res.* 35, 3100–3108. doi: 10.1093/nar/gkm160
- Lane, D. J. (1991). "16S/23S rRNA sequencing," in *Nucleic Acid Techniques in Bacterial Systematics*, eds E. Stackebrandt and M. Goodfellow (New York, NY: Wiley).
- Langmead, B., Trapnell, C., Pop, M., and Salzberg, S. L. (2009). Ultrafast and memory-efficient alignment of short DNA sequences to the human genome. *Genome Biol.* 10:R25. doi: 10.1186/gb-2009-10-3-r25

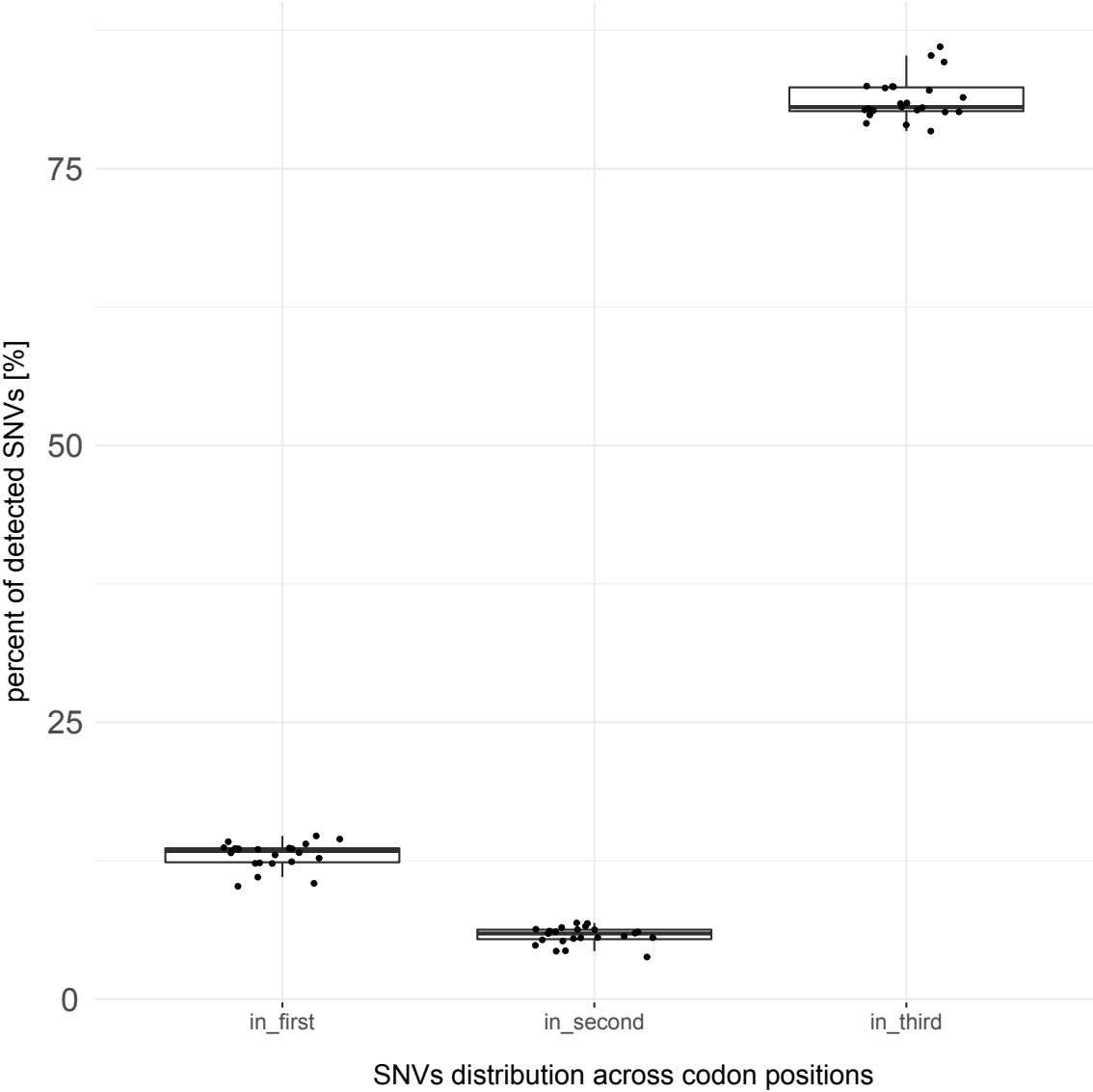
- Lasa, A. V., Mašínová, T., Baldrian, P., and Fernández-López, M. (2019). Bacteria from the endosphere and rhizosphere of *Quercus* spp. use mainly cell wall-associated enzymes to decompose organic matter. *PLoS One* 14:e0214422. doi: 10.1371/journal.pone.0214422
- Letunic, I., and Bork, P. (2011). Interactive Tree of Life v2: online annotation and display of phylogenetic trees made easy. *Nucleic Acids Res.* 39, W475–W478. doi: 10.1093/nar/gkr201
- Li, H. (2013). Aligning sequence reads, clone sequences and assembly contigs with BWA-MEM. *arXiv [Preprint]*. Available online at: <http://arxiv.org/abs/1303.3997>
- Li, H., Handsaker, B., Wysoker, A., Fennell, T., Ruan, J., Homer, N., et al. (2009). The sequence Alignment/Map format and SAMtools. *Bioinformatics* 25, 2078–2079. doi: 10.1093/bioinformatics/btp352 (accessed May 11, 2019).
- Lladó, S. F., Větrovský, T., and Baldrian, P. (2019). Tracking of the activity of individual bacteria in temperate forest soils shows guild-specific responses to seasonality. *Soil Biol. Biochem.* 135, 275–282. doi: 10.1016/j.soilbio.2019.05.010
- Luo, C., Walk, S. T., Gordon, D. M., Feldgarden, M., Tiedje, J. M., and Konstantinidis, K. T. (2011). Genome sequencing of environmental *Escherichia coli* expands understanding of the ecology and speciation of the model bacterial species. *Proc. Natl. Acad. Sci. U.S.A.* 108, 7200–7205. doi: 10.1073/pnas.1015622108
- Maire, J., Parisot, N., Ferrarini, M. G., Vallier, A., Gillet, B., Hughes, S., et al. (2020). Spatial and morphological reorganization of endosymbiosis during metamorphosis accommodates adult metabolic requirements in a weevil. *Proc. Natl. Acad. Sci. U.S.A.* 117, 19347–19358. doi: 10.1073/pnas.2007151117
- Moll, J., Kellner, H., Leonhardt, S., Stengel, E., Dahl, A., Buscot, F., et al. (2018). Bacteria inhabiting deadwood of 13 tree species reveal great heterogeneous distribution between sapwood and heartwood. *Environ. Microbiol.* 20, 3744–3756. doi: 10.1111/1462-2920.14376
- Moynihan, M. A. (2020). *nifH* data 2 *GitHub Repository*. Zenodo. Available online at: <https://zenodo.org/record/3958405/export/xm#.YKU5vbczIU> (accessed January 20, 2021).
- Munoz, M. M., Spencer, N., Enomoto, S., Dale, C., and Rio, R. V. M. (2020). Quorum sensing sets the stage for the establishment and vertical transmission of *Sodalis praecaptivus* in tsetse flies. *PLoS Genet.* 16:e1008992. doi: 10.1371/journal.pgen.1008992
- Nadarasah, G., and Stavrinides, J. (2011). Insects as alternative hosts for phytopathogenic bacteria. *FEMS Microbiol. Rev.* 35, 555–575. doi: 10.1111/j.1574-6976.2011.00264.x
- Nayfach, S., Roux, S., Seshadri, R., Udwy, D., Varghese, N., Schulz, F., et al. (2020). A genomic catalog of Earth's microbiomes. *Nat. Biotechnol.* 39, 499–509. doi: 10.1038/s41587-020-0718-6
- Nguyen, L., Schmidt, H. A., Haeseler, A., and Von Minh, B. Q. (2014). IQ-TREE: a fast and effective stochastic algorithm for estimating maximum-likelihood phylogenies. *Mol. Biol. Evol.* 32, 268–274. doi: 10.1093/molbev/msu300
- Nováková, E., and Hypša, V. (2007). A new *Sodalis* lineage from bloodsucking fly *Craterina melbae* (Diptera, Hippoboscidae) originated independently of the tsetse flies symbiont *Sodalis glossinidius*. *FEMS Microbiol. Lett.* 269, 131–135. doi: 10.1111/j.1574-6968.2006.00620.x
- Oakeson, K. F., Gil, R., Clayton, A. L., Dunn, D. M., Von Niederhausern, A. C., Hamil, C., et al. (2014). Genome degeneration and adaptation in a nascent stage of symbiosis. *Genome Biol. Evol.* 6, 76–93. doi: 10.1093/gbe/evt210
- Odriozola, I., Abrego, N., Tláškal, V., Zrůstová, P., Morais, D., Větrovský, T., et al. (2021). Fungal communities are important determinants of bacterial community composition in deadwood. *mSystems* 6:e01017-20. doi: 10.1128/mSystems.01017-20
- Parks, D. H., Imelfort, M., Skennerton, C. T., Hugenholtz, P., and Tyson, G. W. (2015). CheckM: assessing the quality of microbial genomes recovered from isolates, single cells, and metagenomes. *Genome Res.* 25, 1043–1055. doi: 10.1101/gr.186072.114
- Perlmutter, J. I., and Bordenstein, S. R. (2020). Microorganisms in the reproductive tissues of arthropods. *Nat. Rev. Microbiol.* 18, 97–111. doi: 10.1038/s41579-019-0309-z
- Pinto-Tomás, A. A., Anderson, M. A., Suen, G., Stevenson, D. M., Chu, F. S. T., Wallace Cleland, W., et al. (2009). Symbiotic nitrogen fixation in the fungus gardens of leaf-cutter ants. *Science* 326, 1120–1123. doi: 10.1126/science.1173036
- Pritchard, L., Glover, R. H., Humphris, S., Elphinstone, J. G., and Toth, I. K. (2015). Genomics and taxonomy in diagnostics for food security: soft-rotting enterobacterial plant pathogens. *Anal. Methods* 8, 12–24. doi: 10.1039/C5AY02550H
- Přivětivý, T., Janík, D., Unar, P., Adam, D., Král, K., and Vrška, T. (2016). How do environmental conditions affect the deadwood decomposition of European beech (*Fagus sylvatica* L.)? *For. Ecol. Manag.* 381, 177–187. doi: 10.1016/j.foreco.2016.09.033
- Probst, M., Gómez-Brandón, M., Bardelli, T., Egli, M., Insam, H., and Ascher-Jenull, J. (2018). Bacterial communities of decaying Norway spruce follow distinct slope exposure and time-dependent trajectories. *Environ. Microbiol.* 20, 3657–3670. doi: 10.1111/1462-2920.14359
- Quinlan, A. R., and Hall, I. M. (2010). BEDTools: a flexible suite of utilities for comparing genomic features. *Bioinformatics* 26, 841–842. doi: 10.1093/bioinformatics/btq033
- R Core Team (2020). *R: A Language and Environment for Statistical Computing*. Vienna: R Core Team.
- Reveillaud, J., Bordenstein, S. R., Cruaud, C., Shaiber, A., Esen, ÖC., Weill, M., et al. (2019). The *Wolbachia* mobilome in *Culex pipiens* includes a putative plasmid. *Nat. Commun.* 10:1051. doi: 10.1038/s41467-019-08973-w
- Richter, M., and Rosselló-Móra, R. (2009). Shifting the genomic gold standard for the prokaryotic species definition. *Proc. Natl. Acad. Sci. U.S.A.* 106, 19126–19131. doi: 10.1073/pnas.0906412106
- Rodriguez-R, L. M., Gunturu, S., Harvey, W. T., Rosselló-Mora, R., Tiedje, J. M., Cole, J. R., et al. (2018). The Microbial Genomes Atlas (MiGA) webserver: taxonomic and gene diversity analysis of *Archaea* and *Bacteria* at the whole genome level. *Nucleic Acids Res.* 46, W282–W288. doi: 10.1093/nar/gky467
- Rosas-Pérez, T., Vera-Ponce de León, A., Rosenblueth, M., Ramírez-Puebla, S. T., Rincón-Rosales, R., Martínez-Romero, J., et al. (2017). “The symbiome of *Llaveia cochineals* (Hemiptera: Coccoidea: Monophlebidae) includes a gammaproteobacterial cosymbiont *Sodalis* TME1 and the known *Candidatus* Walzuchella monophlebidarum,” in *Insect Physiology and Ecology*, ed. V. D. C. Shields (London: IntechOpen), 115–134. doi: 10.5772/66442
- Rosenblueth, M., Martínez, L., Silva, J., and Martínez-Romero, E. (2004). *Klebsiella variicola*, a novel species with clinical and plant-associated isolates. *Syst. Appl. Microbiol.* 27, 27–35. doi: 10.1078/0723-2020-00261
- Rubin, B. E. R., Sanders, J. G., Turner, K. M., Pierce, N. E., and Kocher, S. D. (2018). Social behaviour in bees influences the abundance of *Sodalis* (*Enterobacteriaceae*) symbionts. *R. Soc. Open Sci.* 5:180369. doi: 10.1098/rsos.180369
- Sabree, Z. L., Kambampati, S., and Moran, N. A. (2009). Nitrogen recycling and nutritional provisioning by *Blattabacterium*, the cockroach endosymbiont. *Proc. Natl. Acad. Sci. U.S.A.* 106, 19521–19526. doi: 10.1073/pnas.0907504106
- Šamonil, P., Daněk, P., Baldrian, P., Tláškal, V., Tejnecký, V., and Drábek, O. (2020). Convergence, divergence or chaos? Consequences of tree trunk decay for pedogenesis and the soil microbiome in a temperate natural forest. *Geoderma* 376:114499. doi: 10.1016/j.geoderma.2020.114499
- Šamonil, P., Schaeztl, R. J., Valtera, M., Goliáš, V., Baldrian, P., Vašíčková, I., et al. (2013). Crossdating of disturbances by tree uprooting: can treethrow microtopography persist for 6000 years? *For. Ecol. Manag.* 307, 123–135. doi: 10.1016/j.foreco.2013.06.045
- Santos-García, D., Silva, F. J., Morin, S., Dettner, K., and Kuechler, S. M. (2017). The all-rounder *Sodalis*: a new bacteriome-associated endosymbiont of the lygaeoid bug *Henestaris halophilus* (Heteroptera: Henestarinae) and a critical examination of its evolution. *Genome Biol. Evol.* 9, 2893–2910. doi: 10.1093/gbe/evx202
- Seemann, T. (2014). Prokka: rapid prokaryotic genome annotation. *Bioinformatics* 30, 2068–2069. doi: 10.1093/bioinformatics/btu153
- Stoddard, S. F., Smith, B. J., Hein, R., Roller, B. R. K., and Schmidt, T. M. (2015). *rrnDB*: improved tools for interpreting rRNA gene abundance in bacteria and archaea and a new foundation for future development. *Nucleic Acids Res.* 43, D593–D598. doi: 10.1093/nar/gku1201
- Tenaillon, O., Skurnik, D., Picard, B., and Denamur, E. (2010). The population genetics of commensal *Escherichia coli*. *Nat. Rev. Microbiol.* 8, 207–217. doi: 10.1038/nrmicro2298
- Tláškal, V., and Baldrian, P. (2021). Deadwood-inhabiting bacteria show adaptations to changing carbon and nitrogen availability during decomposition. *Front. Microbiol.* 12, 1353. doi: 10.3389/fmicb.2021.685303

- Tláškal, V., Brabcová, V., Větrovský, T., Jomura, M., López-Mondéjar, R., Monteiro, M. O. L., et al. (2021). Complementary roles of wood-inhabiting fungi and bacteria facilitate deadwood decomposition. *mSystems* 6:e001078-20. doi: 10.1128/mSystems.01078-20
- Tláškal, V., Zrůstová, P., Vrška, T., and Baldrian, P. (2017). Bacteria associated with decomposing dead wood in a natural temperate forest. *FEMS Microbiol. Ecol.* 93:fix157. doi: 10.1093/femsec/fix157
- Toh, H., Weiss, B. L., Perkin, S. A. H., Yamashita, A., Oshima, K., Hattori, M., et al. (2006). Massive genome erosion and functional adaptations provide insights into the symbiotic lifestyle of *Sodalis glossinidius* in the tsetse host. *Genome Res.* 16, 149–156. doi: 10.1101/gr.4106106
- Větrovský, T., and Baldrian, P. (2013). The variability of the 16S rRNA gene in bacterial genomes and its consequences for bacterial community analyses. *PLoS One* 8:e57923. doi: 10.1371/journal.pone.0057923
- Walker, B. J., Abeel, T., Shea, T., Priest, M., Abouelliel, A., Sakthikumar, S., et al. (2014). Pilon: an integrated tool for comprehensive microbial variant detection and genome assembly improvement. *PLoS One* 9:e112963. doi: 10.1371/journal.pone.0112963
- Waters, N. R., Abram, F., Brennan, F., Holmes, A., and Pritchard, L. (2018). riboSeed: leveraging prokaryotic genomic architecture to assemble across ribosomal regions. *Nucleic Acids Res.* 46:e68. doi: 10.1093/nar/gky212
- Weiss, B. L., Mouchotte, R., Rio, R. V. M., Wu, Y. N., Wu, Z., Heddi, A., et al. (2006). Interspecific transfer of bacterial endosymbionts between tsetse fly species: infection establishment and effect on host fitness. *Appl. Environ. Microbiol.* 72, 7013–7021. doi: 10.1128/AEM.01507-06
- Wick, R. R., Judd, L. M., Gorrie, C. L., and Holt, K. E. (2017). Unicycler: resolving bacterial genome assemblies from short and long sequencing reads. *PLoS Comput. Biol.* 13:e1005595. doi: 10.1371/journal.pcbi.1005595
- Wickham, H., Averick, M., Bryan, J., Chang, W., McGowan, L. D. A., François, R., et al. (2019). Welcome to the Tidyverse. *J. Open Source Softw.* 4:1686. doi: 10.21105/joss.01686
- Wilmotte, A., Van der Auwera, G., and De Wachter, R. (1993). Structure of the 16S ribosomal RNA of the thermophilic cyanobacterium *Chlorogloeopsis* HTF (*Mastigocladus laminosus* HTF) strain PCC7518, and phylogenetic analysis. *FEBS Lett.* 317, 96–100. doi: 10.1016/0014-5793(93)81499-P
- Yong, E. (2016). *I Contain Multitudes: The Microbes Within us and a Grand View of Life*. London: HarperCollins.
- Zhang, H., Yohe, T., Huang, L., Entwistle, S., Wu, P., Yang, Z., et al. (2018). dbCAN2: a meta server for automated carbohydrate-active enzyme annotation. *Nucleic Acids Res.* 46, W95–W101. doi: 10.1093/nar/gky418

Conflict of Interest: The authors declare that the research was conducted in the absence of any commercial or financial relationships that could be construed as a potential conflict of interest.

Copyright © 2021 Tláškal, Pylro, Žižňáková and Baldrian. This is an open-access article distributed under the terms of the Creative Commons Attribution License (CC BY). The use, distribution or reproduction in other forums is permitted, provided the original author(s) and the copyright owner(s) are credited and that the original publication in this journal is cited, in accordance with accepted academic practice. No use, distribution or reproduction is permitted which does not comply with these terms.

Supplementary Figure 1: SNVs detected after mapping deadwood metagenome reads to the *S. ligni* genome shown as boxplots of the occurrence of SNVs for each codon position. Each dot represents one metagenome sample.



Taxonomy assignment of bacterial genes in a metagenome: assessment of accuracy and recommendations for reporting

Martina Kyselková*, Vojtěch Tláškal, Daniel Morais, Lenka Michalčíková, Sandra Awokunle Hollá, Tomáš Větrovský, and Petr Baldrian

Authors' affiliation: Laboratory of Environmental Microbiology, Institute of Microbiology of the Czech Academy of Sciences, Vídeňská 1083, 142 20 Praha 4, Czech Republic

* Correspondence: martina.kyselkova@biomed.cas.cz

Abstract

Correct taxonomic assignments of metagenome and metatranscriptome sequences are indispensable for linking predicted functions to the responsible members of environmental microbiomes as well as for assessing the relative representation of microbial taxa. End-users of annotation tools can use alignment reliability scores such as the bit score or e-value to improve the accuracy of the taxonomic assignment of called genes, but the use of these scores is limited by the fact that their accuracy thresholds have not been reported to date. In this study, we tested the accuracy of taxonomic assignments using a mock soil metagenome consisting of 82 bacterial genomes to assess the accuracy of taxonomic classifications across various e-value cutoffs and to make recommendations for reporting taxonomic information for metagenomes and metatranscriptomes. The accuracy of the taxonomic assignments of the called genes from our mock soil metagenome was highly dependent on both the e-value threshold used for data filtering and the chosen taxonomic rank. We showed that the mean rate of more than 95% of correct annotations was achievable at all e-value cutoffs for all ranks up to family level, and at e-value cutoff of $1E-90$ (bit score 276) for genus level. Though, the accuracy of taxonomic assignments substantially varied among bacterial genomes of various taxonomic placements and more stringent criteria such as assignments to only family level with e-value cutoff of $1E-40$ (bit score 146) should be applied to reach the 95% accuracy with 75% of the present genomes. Concluding, reporting highly accurate results from metagenomes and metatranscriptomes at low bacterial ranks is currently possible, but necessitates applying stringent e-value/bit score thresholds.

Keywords: metagenome, metatranscriptome, annotation, bacterial taxonomy, taxonomic assignment, taxonomic rank, e-value, bit score

Introduction

Shotgun metagenomics and metatranscriptomics represent prominent approaches to analyze the functional potential and activity of microbiomes and to link them to microbial taxa. While the identification of microbial taxa from shotgun metagenomes and metatranscriptomes is not biased by PCR as in metabarcoding, correct taxonomic classification of large numbers of genes or gene fragments represents a challenge. A bunch of software tools for metagenomic data processing has been developed previously (e.g., Markowitz et al., 2007; Hunter et al., 2014; Meyer et al., 2008) and these tools generally infer the taxonomy of predicted genes from comparison to reference databases using alignments. The alignment quality and reliability can be mathematically estimated using terms such as the bit score (i.e., estimation of the database size needed to find an equally good alignment by chance) and expectancy value (e-value; i.e., how many times a queried sequence aligns with the same score to a given database by chance). Since these metrics report probability values, they can, in theory, be easily used to assess the accuracy of taxonomic classification. The application of quality thresholds to taxonomic assessments is rare (Jacquiod et al., 2018; Tláskal et al., 2021), although the accuracy of the taxonomic or functional assignment of sequences with low bit scores or high e-values is questionable. For example, from approximately 30 studies mentioning “soil” and “metagenome” that were published between 2018 and 2020 in Nature Microbiology, the ISME Journal, Microbiome, Soil Biology and Biochemistry, Environmental Microbiology and Science of the Total Environment that used the MG-RAST server (Meyer et al., 2008) for metagenome or metatranscriptome annotation, only one applied a more stringent e-value cutoff than the default value of $< 1E-5$, and almost half of the studies did not mention any e-value-based filtering at all (Table S1). On the other hand, due to missing information about annotation reliability, past papers often reported results only with a coarse taxonomic resolution, such as the phylum to order level (Žifčáková et al. 2017, Sun and Badgley 2019, Tláskal et al. 2021).

Previous works on soil bacterial communities have indicated that high taxonomic ranks, such as phyla, may have ecological relevance, e.g., by predicting the *r*- or *K*-strategy (Fierer et al., 2007). Nevertheless, lower taxonomic ranks (class and below) have been shown to be more important for community structuring (Ramirez et al., 2018), and the number of conserved traits, including the most important ones, increases with decreasing phylogenetic distance, i.e., at lower taxonomic levels (Martiny et al., 2013, Isobe et al., 2019). It is thus

tempting to report taxonomy assignments at low taxonomic levels, such as microbial families or genera, at which new findings can be linked to the existing knowledge of taxon traits. Indeed, almost half of the papers that did not apply hit quality filtering (Table S1) still reported taxonomy at the genus level, even though the accuracy of taxonomic assignments from metagenomes at this level has been questioned in previous benchmarking studies. Specifically, the benchmarking initiative of Sczyrba et al. (2017), which used a complex mock community comprising genomes of approximately 700 microbial isolates, indicated that both the sensitivity and precision of taxonomic assignments decreased with decreasing taxonomic rank, and the most remarkable drop in accuracy measures was observed between the family and genus levels for most tools. Similar results were reported from an ongoing study by Meyer et al. (2019). In contrast, in the work of Lindgreen et al. (2016), which was based on mock communities of approximately 1,000 bacterial genomes, sensitivity and precision were comparable between the phylum and genus levels across the benchmarked tools. Importantly, alignment reliability metrics, such as e-values or bit-scores, were not taken into account in any of the abovementioned studies. In fact, no guidance for choosing the most suitable taxonomic ranks or e-value/bit score thresholds for the interpretation of metagenomic and metatranscriptomic data exists.

To solve this problem, we utilized a mock community including sequenced genomes of 82 soil bacteria with known taxonomic assignments and assessed the quality of feature annotation (i.e., the frequency of correct and incorrect annotations) across different taxonomic ranks and e-value thresholds, using a custom pipeline and the RefSeq Protein database. We show that a satisfactory taxonomic resolution can be currently achieved when classifying bacterial sequences from metagenomes and metatranscriptomes and provide recommendations for the taxonomic classification of shotgun sequencing results.

Methods

Choice, sequencing and assembly of genomes

The genomes of 82 bacterial isolates from forest soils, litter and decaying wood obtained from temperate forests that represent typical soil bacteria were chosen for this study (Table S2). Most of the genome sequences were only recently obtained and deposited in public

repositories, and none of them were included in the database (NCBI Protein Reference Sequences, May 6, 2021) that was chosen for feature annotation. This mimics the situation of environmental metagenome or metatranscriptome sequence annotation, for which limited numbers of closely matching sequences are present in databases. The genomes of the isolates were sequenced on the Illumina platforms (Table S2). Illumina paired-end reads were assembled with Unicycler 0.4.8 (using the options `-min_fasta_length 200`; `-mode normal`; `-min_polish_size 1000`; Wick et al., 2017), including SPAdes 3.14.0 (Bankevich et al., 2012). The 16S rRNA sequences were extracted using Prokka 1.13 (Seemann et al., 2014) with the use of RNAmmer (Lagesen et al., 2007).

Taxonomic classification of isolates

We combined two approaches based on (i) 16S rRNA gene sequence classification and (ii) whole genome sequence classification to assign taxonomy to the isolates. The 16S rRNA sequences were assigned with RDP Classifier (<http://rdp.cme.msu.edu/classifier/classifier.jsp>; accessed 2020-08-13; Wang et al., 2007), while the assembled genome sequences were classified with MiGA based on the average nucleotide/amino acid identity calculated for orthologous genes (<http://microbial-genomes.org/>; accessed 2020-09-08; Rodriguez-R et al., 2018) using the NCBI Prok database. Although the RDP Classifier is the gold standard for bacterial classification based on 16S rRNA sequences (Lan et al., 2012), it uses a taxonomic classification that somewhat differs from that used by NCBI Taxonomy. Thus, genus-level assignments based on RDP were classified into higher taxonomic ranks using NCBI Taxonomy. The final assignment of the isolates to certain taxa was considered reliable when (i) MiGA classified the isolate to its respective taxonomic rank with a p-value < 0.05 and (ii) an agreement was reached between the RDP-based and MiGA-based assignments. Using this approach, all 82 genomes could be reliably assigned at the domain, phylum and class levels; 78 genomes at the order level; 66 at the family level; and 34 at the genus level (Table S3), and these classifications served as the gold standard to which 'metagenome'-based annotations were compared.

Mock community metagenome annotation

The assembled sequences from the 82 bacterial genomes were combined into one file, and putative genes (features) were identified with FragGeneScan version 1.31 (FragGeneScan `-w 1 -t complete`; Rho et al., 2010). For each feature, best hit was found in the RefSeq Protein database (NCBI Protein Reference Sequences, May 6, 2021, containing 195,513,818 sequences

and 74,872,953,201 total residues) using DIAMOND v2.0.8.146 (diamond blastp -f 6; Buchfink et al., 2015). The final dataset contained 329,982 identified features with their best hits, e-values and bit score values.

Data filtering and analysis

NCBI Taxonomy (genus, family, order, class, phylum and domain ranks) was appended to each feature annotation (i.e., to its best hit). Each feature also included taxonomic information from the corresponding isolate of origin (Table S3). The numbers of matches between the ‘metagenome’-based taxonomy and isolate-based ‘gold standard’ taxonomy were recorded for different e-value levels (as the numbers of matches \leq e-value threshold) and taxonomic ranks. As a measure of the accuracy of the taxonomic assignments, the proportions of correct assignments (i.e., those with matching ‘metagenome’-based and isolate-based taxonomies) and incorrect assignments were calculated either from the total number of identified features per isolate genome or from the number of identified features per isolate genome that could be assigned at a given e-value cutoff (Table S4). The proportions of features that could not be assigned at given e-value cutoffs, out of total numbers of features per genome, were calculated as well (Table S4).

Results

The mean (Fig. 1) and median (Fig. S1) proportions of both correctly and incorrectly assigned features gradually decreased with decreasing e-value cutoffs across all taxonomic ranks. High e-value cutoffs thus allowed for higher numbers of assigned hits but also for higher numbers of incorrectly assigned hits compared to more stringent, low e-value cutoffs; Fig. 1 and S1. The ratio of incorrectly assigned hits to the number of assigned hits was, therefore, the worst at high e-value cutoffs across all taxonomic ranks (Fig. 2 and S2). For example, 6.6% of features were on average incorrectly classified to genus level at the e-value cutoff of 1E-05, while 4.7% were incorrectly classified with the most stringent e-value cutoff applied (1E-120). Though applying low e-value cutoffs improved the accuracy of the taxonomic assignments, this increased accuracy was at the expense of features that were filtered out. The gradual increase in lost features along with decreasing e-value levels is shown in Fig. 1 and S1 (in gray), showing, for example, that at an e-value cutoff of 1E-120, only on average 73% of features were classified, compared to almost 100% of features that

could be classified at the e-value cutoff of 1E-5. The improvement of the average accuracy by some 2% by applying the most stringent e-value cutoff for genus thus led to the loss of about 27% information.

The accuracy of the taxonomic assignments was further affected by the choice of taxonomic rank, with mean proportions of incorrectly assigned features out of all features (Fig. 1) and out of all assigned features (Fig. 2) gradually increasing from the domain to the genus level. As an example, 6.5% of all features were on average incorrectly assigned at the genus level at an e-value cutoff of 1E-5, while only 0.8% of features were incorrectly classified at the phylum level using the same e-value cutoff (Fig. 1). The mean rate of less than 5% of incorrect annotations was achievable at all e-value cutoffs for all ranks up to family level, and at e-value cutoff of 1E-90 for genus level (Fig. 2). The proportions of incorrectly assigned features varied, however, substantially with the genome of origin (Fig. S2). For example, the genomes VOJ_276 (genus *Burkholderia*) and 39_4QA (*Stenotrophomonas*) had 38 and 26% incorrectly assigned features (at the highest e-value cutoffs) at genus level, respectively, while 1_2GA (*Paenibacillus*) had less than 1% incorrectly assigned features at the same rank and e-value cutoff (Fig. S3). To ensure that 75% (3rd quartile, Fig. S2) of the present genomes have less than 5% of incorrect assignments, the data should be interpreted at order level, or at family level with e-value cut-off of 1E-40. It should be noted that the genomes for which high proportions of incorrectly assigned hits occurred at higher taxonomic ranks, such as family (genome 32_4CA, Fig. S4), order (genome 11_3CAB, Fig. S5) and class (genome VOJ_265, Fig. S6), usually could not be reliably classified (and therefore analyzed) at the respective lower taxonomic ranks). Certain genomes also significantly deviated in the proportions of unassigned hits at low e-value levels (Fig. S1), with VOJ_265 (Fig. S6) and SAL_L154 (Fig. S7) having more than 50% features unassigned at e-value 1E-120. The two genomes could be reliably classified only to class level, indicating that they represented lineages for which sequenced genomes of closely related taxa are currently missing in databases.

We used e-value cutoffs for result filtering since these values are most frequently reported in the literature and are also available in metagenomic tools such as MG-RAST (Meyer et al., 2008). It should be noted, however, that e-values are dependent on the size of the searched

database, and e-value thresholds, therefore, vary across tools and databases used for metagenome annotation. To provide measures that are independent of database size, we report the bit scores that corresponded to the e-value cutoffs used in this study. The bit scores, as a database size-independent measure of alignment quality, are reported along with the e-values in Fig. S1 and S2, showing the same cutoff classes as in Fig. 1 and Fig. 2, respectively.

Discussion

The choice of alignment quality thresholds and taxonomic ranks at which metagenome data should be interpreted seems to represent a trade-off between assignment reliability and the share of features to be annotated. However, considering that inaccurate annotations will bias the interpretation of results even more than missing annotations, high accuracy should be a primary requirement. Our results show that achieving an average of 95% accuracy was possible even at genus level by applying stringent alignment quality evaluators such as e-value of $1E-90$ or bit score of 276. This level of accuracy was further achievable at above-genus levels even at highest e-value cutoffs, i.e., with no burden of data loss. In this study, we did not observe any remarkable drop in accuracy below family level, which was previously reported in two benchmarking studies (Sczyrba et al., 2017; Meyer et al., 2019). The reason may be the constantly increasing numbers of hits in databases (RefSeq Protein database was used in this study) that may nowadays allow for more reliable assignments even at low taxonomic ranks. Although this study did not aim to compare the accuracy of taxonomic assignments from different software programs, we expect similar rank and bit score dependencies of the accuracy of taxonomy assignments as presented here for other tools based on BLAST-like algorithms.

The results of this study should be interpreted in the context of an environmental metagenome, or more specifically, a soil metagenome, as our mock community represented bacteria that occur in forest soils. While some of the included bacteria are members of easily culturable genera with many relatives in databases, others, e.g., *Acidobacteria*, were members of groups less frequently sequenced, and some even represented recently found lineages (e.g., the genome SAL_L154 belonging to the novel actinobacterial family; Rapoport

et al., 2020). Such taxa were a subject of higher rates of incorrect assignments or higher rates of unassigned features at stringent e-value cutoffs, likely due to the low numbers of highly related genomes in the annotation database. It should be noted that rare or poorly sequenced bacterial groups whose members are difficult to culture, such as those from candidate phyla radiation, (Brown et al., 2015), were not included in this study, even though they are common in soils (Nayfach et al., 2021). Due to the absence of corresponding taxa in annotation databases, the accuracy of the taxonomic assignment of genes from real soil metagenomes or metatranscriptomes would thus probably be even lower than that reported here, or higher numbers of identified features would be lost when applying stringent e-value/bit score cutoffs. Furthermore, the identified features in our mock metagenome mostly represented whole genes, while typical metagenomes and metatranscriptomes contain majority of incomplete gene fragments. Taxonomic assignments based on shorter gene fragments result in either a higher number of incorrect taxonomic placements or a lower number of assigned features if stringent e-value/bit score cutoffs are applied. All of the above findings support the use of stringent thresholds for reporting results.

It is important to note that even the application of strict criteria, such as high taxonomic rank reporting and highly stringent alignment quality thresholds, cannot fully prevent incorrect taxonomic assignments. First, it is estimated that 1.6–33% of bacterial genomes have recently been horizontally acquired (Koonin et al., 2001; Garcia-Vallvé et al., 2000), and this event cannot be recognized at the level of individual genes or gene fragments. Second, even taxa belonging to the same species often have very different genomes (Lladó et al., 2019). Indispensable single-copy genes are more likely to be correctly assigned due to their universal presence in the core genome of bacterial taxa and lower frequency of horizontal gene transfer in comparison to accessory genes (Simao et al., 2015).

A real soil metagenome or metatranscriptome also contains sequences from fungi and other eukaryotes, which were not taken into consideration in this study. Considering the less advanced development of fungal genomics, including the generally low representation of fungal genomes in annotation pipelines (Grigoriev et al., 2014) and the fact that a large amount of fungal genes are species-specific (Miyachi et al., 2020), their annotation is likely even less reliable than that of bacteria. This is why reports of fungal taxa in metagenomes and metatranscriptomes need to be taken with caution and are limited to high taxonomic

ranks, such as phyla (Žifčáková et al., 2017, Tláskal et al., 2021). Obviously, interdomain misassignments are possible and occurred in the current study (Fig. S1).

Conclusions

Taxonomic rank and alignment quality metrics such as the e-value or bit score must be taken into consideration when interpreting data from environmental metagenomes and metatranscriptomes. This study suggests that reliable taxonomic inferences from metagenomes and metatranscriptomes at low taxonomic ranks such as genus or family are possible when using stringent thresholds for alignment quality. Further improvements in reliability of taxonomic inferences from metagenomes may be achieved in a close future by annotating long stretches of DNA, such as those obtained by long read-enabling platforms in which the context of neighboring genes originating from the same organism can be taken into consideration. The validation of such approaches and the development of corresponding tools remain, however, yet to be implemented.

Funding

This work was supported by the Czech Science Foundation (18-25706S) and by the Ministry of Education, Youth and Sports of the Czech Republic (LTC20073).

Authors' contributions

MK and PB designed the study and wrote the manuscript. MK performed the data analyses. VT, DM and TV contributed to the data analyses and to the concept of the study. SAH and LM performed the literature review. All the authors read and approved the final manuscript.

Acknowledgements

We thank Ruben López-Mondéjar for providing advice on MiGA software.

References

- Bankevich, A., Nurk, S., Antipov, D., Gurevich, A.A., Dvorkin, M., Kulikov, A.S., et al. (2012). SPAdes: A new genome assembly algorithm and its applications to single-cell sequencing. *J. Comput. Biol.* 19, 455–477.
- Brown, C.T., Hug, L.A., Thomas, B.C., Sharon, I., Castelle, C.J., Singh, A., et al. (2015). Unusual biology across a group comprising more than 15% of domain Bacteria. *Nature* 523, 208-211.
- Buchfink, B., Xie, C., Huson, D. H. (2015). Fast and sensitive protein alignment using DIAMOND. *Nat. Methodes* 12, 59-60.
- Fierer, N., Bradford, M.A., Jackson, R.B. (2007). Toward an ecological classification of soil bacteria. *Ecology* 88, 1354-1364.
- Garcia-Vallvé, S., Romeu, A., Palau, J. (2000). Horizontal gene transfer in bacterial and archaeal complete genomes. *Genome Res.* 10, 1719-1725.
- Gardner, P.P., Watson, R.J., Morgan, X.C., Draper, J.L., Finn, R.D., Morales, S.E., Stott, M.B. (2019). Identifying accurate metagenome and amplicon software via a meta-analysis of sequence to taxonomy benchmarking studies. *PeerJ* 7:e6160.
- Grigoriev, I.V., Nikitin, R., Haridas, S., Kuo, A., Ohm, R., Otilar, R., et al. (2014). MycoCosm portal: gearing up for 1000 fungal genomes. *Nucleic Acids Res.* 42, D699-704.
- Hunter, S., Corbett, M., Denise, H., Fraser, M., Gonzalez-Beltran, A., Hunter, C., et al. (2014). EBI metagenomics—a new resource for the analysis and archiving of metagenomic data. *Nucleic Acids Res.* 42, D600-606.
- Isobe, K., Allison, S.D., Khalili, B., Martiny, A.C., Martiny, J.B.H. (2019). Phylogenetic conservation of bacterial responses to soil nitrogen addition across continents. *Nat. Commun.* 10:2499.
- Jacquioid, S., Nunes, I., Brejnrod, A., Hansen, M.A., Holm, P.E., Johansen, A., et al. (2018). Long-term soil metal exposure impaired temporal variation in microbial metatranscriptomes and enriched active phages. *Microbiome* 6:223.
- Koonin, E.V., Makarova, K.S., Aravind, L. (2001). Horizontal gene transfer in prokaryotes: quantification and classification. *Annu. Rev. Microbiol.* 55, 709-742.

- Lagesen, K., Hallin, P., Rødland, E.A., Stærfeldt, H.H., Rognes, T., Ussery, D.W. (2007). RNAmmer: Consistent and rapid annotation of ribosomal RNA genes. *Nucleic Acids Res.* 35, 3100–3108.
- Lindgreen, S., Adair, K.L., Gardner, P.P. (2016). An evaluation of the accuracy and speed of metagenome analysis tools. *Sci. Rep.* 6:19233.
- Lladó, S., Větrovský, T., Baldrian, P. (2019). The concept of operational taxonomic units revisited: genomes of bacteria that are regarded as closely related are often highly dissimilar. *Folia Microbiologica* 64, 19-23.
- Markowitz, V.M., Ivanova, N.N., Szeto, E., Palaniappan, K., Chu, K., Dalevi, D., et al. (2007). IMG/M: a data management and analysis system for metagenomes. *Nucleic Acids Res.* 36 Suppl 1:D534-538.
- Martiny, A.C., Treseder, K., Pusch, G. (2013). Phylogenetic conservatism of functional traits in microorganisms. *ISME J.* 7, 830-838.
- Meyer, F., Bremges, A., Belmann, P., Janssen, S., McHardy, A.C., Koslicki, D. (2019). Assessing taxonomic metagenome profilers with OPAL. *Genome Biol.* 20:51.
- Meyer, F., Paarmann, D., D'Souza, M., Olson, R., Glass, E.M., Kubal, M., et al. (2008). The metagenomics RAST server—a public resource for the automatic phylogenetic and functional analysis of metagenomes. *BMC Bioinformatics* 9:386.
- Miyauchi, S., Kiss, E., Kuo, A., Drula, E., Kohler, A., Sánchez-García, M., et al. (2020). Large-scale genome sequencing of mycorrhizal fungi provides insights into the early evolution of symbiotic traits. *Nat. Commun.* 11:5125.
- Nayfach, S., Roux, S., Seshadri, R., Udworthy, D., Varghese, N., Schulz, F., et al. (2021). A genomic catalog of Earth's microbiomes. *Nat. Biotechnol.* 39, 499–509.
- Lan, Y., Wang, Q., Cole, J.R., Rosen, G.L. (2012). Using the RDP classifier to predict taxonomic novelty and reduce the search space for finding novel organisms. *PLoS ONE.* 7:e32491.
- Ramirez, K.S., Knight, C.G., De Hollander, M., Brearley, F.Q., Constantinides, B., Cotton, A., et al. (2018). Detecting macroecological patterns in bacterial communities across independent studies of global soils. *Nat. Microbiol.* 3, 189-196.
- Rapoport, D., Sagova-Mareckova, M., Sedláček, I., Provazník, J., Králová, S., Pavlinic, D., et al. (2020). *Trebonia kvetii* gen. nov., sp. nov., an acidophilic actinobacterium, and proposal of the new actinobacterial family *Treboniaceae* fam. nov. *Int. J. Syst. Evol. Microbiol.* 70, 5106-5114.

- Rho, M., Tang, H., Ye, Y. (2010) FragGeneScan: predicting genes in short and errorprone reads. *Nucleic Acids Res.* 38, e191-e191.
- Rodriguez-R, L.M., Gunturu, S., Harvey, W.T., Rosselló-Mora, R., Tiedje, J.M., Cole, J.R., et al. (2018). The Microbial Genomes Atlas (MiGA) webserver: taxonomic and gene diversity analysis of Archaea and Bacteria at the whole genome level. *Nucleic Acids Res.* 46, W282-288.
- Sczyrba, A., Hofmann, P., Belmann, P., Koslicki, D., Janssen, S., Dröge, J., et al. (2017). Critical assessment of metagenome interpretation—a benchmark of metagenomics software. *Nat. Methods* 14, 1063-1071.
- Simao, F.A., Waterhouse, R.M., Ioannidis, P., Kriventseva, E.V., Zdobnov, E.M. (2015). BUSCO: assessing genome assembly and annotation completeness with single-copy orthologs. *Bioinformatics* 31, 3210-3212.
- Sun, S., and Badgley, B. D. (2019). Changes in microbial functional genes within the soil metagenome during forest ecosystem restoration. *Soil Biol. Biochem.* 135, 163-172.
- Tláskal, V., Brabcová, V., Větrovský, T., Jomura, M., López-Mondéjar, R., Oliveira Monteiro, L.M., et al. (2021). Complementary roles of wood-inhabiting fungi and bacteria facilitate deadwood decomposition. *mSystems* 6:e01078-20.
- Seemann, T. (2014). Prokka: rapid prokaryotic genome annotation. *Bioinformatics* 30, 2068-2069.
- Wang, Q., Garrity, G.M., Tiedje, J.M., Cole, J.R. (2007). Naive Bayesian classifier for rapid assignment of rRNA sequences into the new bacterial taxonomy. *Appl. Environ. Microbiol.* 73, 5261-5267.
- Wick, R.R., Judd, L.M., Gorrie, C.L., Holt, K.E. (2017). Unicycler: resolving bacterial genome assemblies from short and long sequencing reads. *PLoS Comput. Biol.* 13:e1005595.
- Žifčáková, L., Větrovský, T., Lombard, V., Henrissat, B., Howe, A., Baldrian, P. (2017). Feed in summer, rest in winter: microbial carbon utilization in forest topsoil. *Microbiome* 5:122.

Figure 1: Mean proportions of correctly assigned features (yellow), incorrectly assigned features (red) and unassigned features (gray) across all genomes at different e-value thresholds and taxonomic ranks.

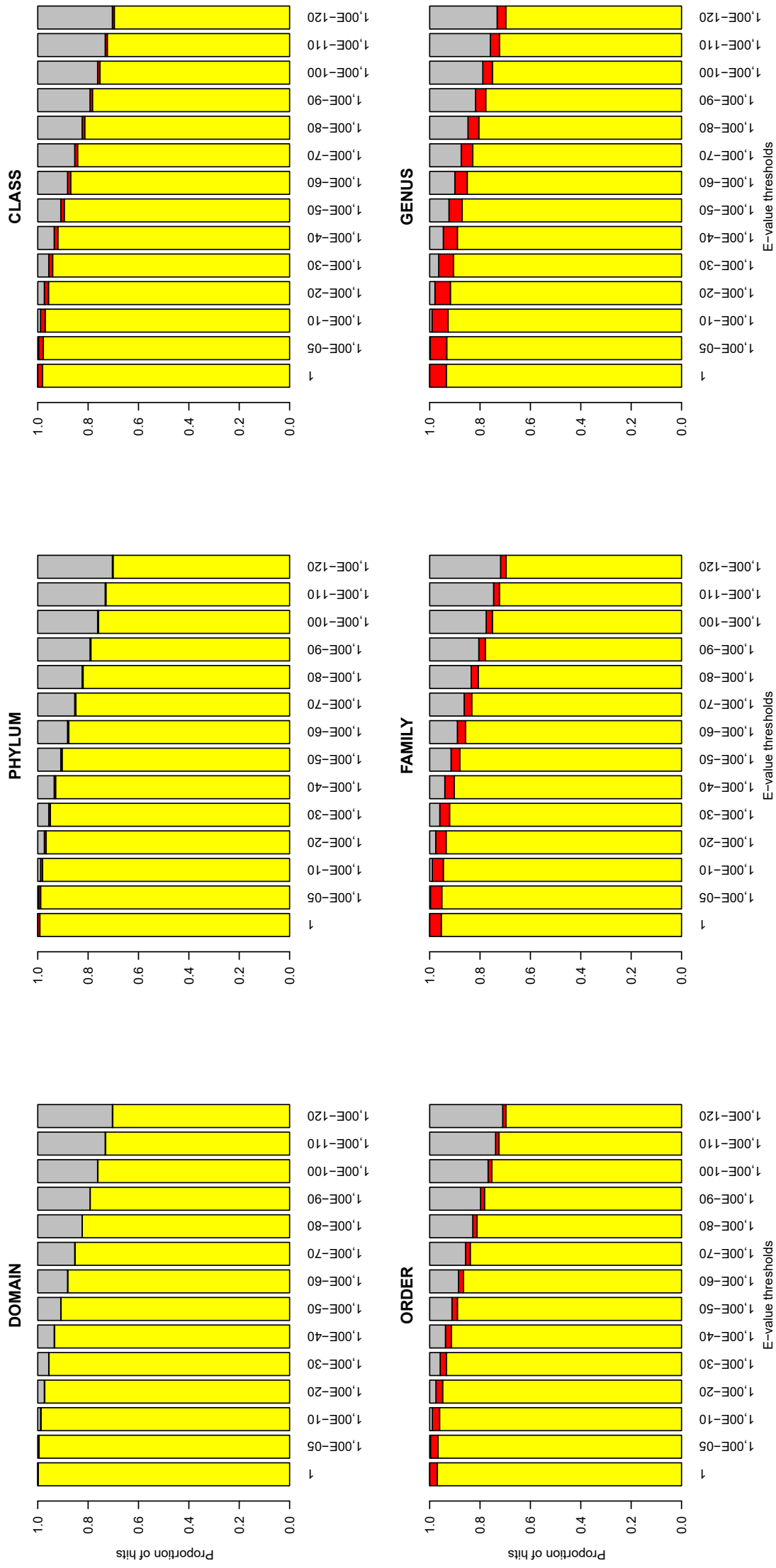


Figure 2: Mean ratio of incorrectly assigned hits to all assigned hits (i.e., correctly + incorrectly assigned hits) at different e-value thresholds and taxonomic ranks. The data are presented as means of values across all genomes. The red horizontal line indicates the ratio corresponding to 5% incorrectly assigned hits.

